



Università degli Studi di Cagliari

PHD DEGREE

Life, Environmental and Drug Sciences, Pharmaceutical Curriculum

Cycle XXXIII

TITLE OF THE PHD THESIS

**IDENTIFICATION AND DEVELOPMENT OF NEW
ANTITUMOR AGENTS WITH MULTI-TARGET ACTION**

Scientific Disciplinary Sector

CHIM/08

PhD Student:

Dott. Serenella Deplano

Supervisor

Prof. Elias Maccioni

Final exam. Academic Year 2019/2020

Thesis defence: January 2022 Session

Table of the content

TUMOR	5
1.1 Tumor: an overview	7
1.2 Cellular pathways involved in tumors	10
1.3 General mechanism of drugs	16
1.4 Tumors drugs	19
1.4.1 Resistance to chemotherapy	21
1.5 Multi target inhibitors	23
CARBONIC ANHYDRASE	27
2.1 Carbonic Anhydrase: overview	29
3.1.1 α-Carbonic Anhydrase	29
2.2 Carbonic Anhydrase IX E XII: physiological and pathological roles	35
2.3 Inhibitors and activators of Carbonic Anhydrase	37
CYCLOOXYGENASE	45
3.1 Cyclooxygenase: overview	47
3.2 Cyclooxygenase-2: physiological and pathological roles	52
3.3 Inhibitors and activators of Cyclooxygenase-2	54
KINASES	57
4.1 Kinases: overview	59
4.2 c-Src and Bcr-Abl: physiological and pathological roles	63
4.3 Inhibitors and activators of c-Src and Bcr-Abl	65
PROJECTS	69
5.1 Selective inhibition of carbonic anhydrase IX and XII by coumarin and psoralen derivatives	71
5.1.1 Background	71
5.1.2 Biological results and discussion	76
5.1.3 Conclusions	82
5.2 New 4-((4-oxo-2-phenylthiazolidin-3-yl)amino)benzenesulfonamide synthesis and inhibitory activity toward carbonic anhydrase I, II, IX, XII and the potential dual CA/COX-2 inhibition	83
5.2.1 Background	83
5.2.2 Biological results and discussion	85
5.2.3 Conclusions	87
5.3 Evaluation of drug like properties	88
5.3.1 Background	88

5.3.1 Biological results and discussion.....	91
5.4 Synthesis of new pyrazolo[3,4-<i>d</i>]pyrimidine compounds	111
5.4.1 Background	111
5.4.2 Biological results and discussion.....	116
5.4.3 Conclusions	116
EXPERIMENTAL SECTION	117
EMAC 10155 (a-m) and EMAC 10158 (a-m)	119
EMAC 10156 (a-m) and EMAC 10159 (a-m)	126
EMAC 10157 (a-m) and EMAC 10160 (a-m)	136
EMAC 10161 (a-m) and EMAC 10162 (a-m)	149
EMAC 10190 (b-l) and EMAC 10191 (b-l)	160
Pyrazolo[3,4- <i>d</i>]pyrimidine.....	176
BIBLIOGRAPHY	187
APPENDIX.....	203
Oral Communications in Scientific Meetings.....	203
Poster Communications in Scientific Meetings	203
Manuscripts in International Journals	204

TUMOR

1.1 Tumor: an overview

Cancer, according to the *World Health Organization* (WHO), is the second leading cause of death in the world, with 10 million deaths in 2020 and an estimated 19.3 million new cases.^{1,2}

Tumor is a disease that can affect any tissue and organ of the body, in which cells grow uncontrollably, cross the normal border to invade other parts of the body, and metastasizing: tumoral cells sever from adjacent cells and invade other tissue through extracellular matrix component and lymphatics.^{3, 4} Metastases are the major cause of cancer mortality.^{3,5}

The most common types of cancer that affect women are breast, colorectal, lung, cervical and thyroid cancer; the most common types of cancer that affect men are lung, prostate, colorectal, stomach and liver cancer.⁵

Normal cells can grow and differentiate under supervision of biochemical stimuli: the presence of growth stimuli allows cells to divide and proliferate, in absence of this type of stimuli, cells stop to grow and undergo programmed death, the apoptosis. In tumor cells these normal processes are deregulated: cells have uncontrolled growth, without external stimuli, lose their capacity to differentiate, resulting without their normal structure and functions; they also disactivate the capacity of apoptosis being immortal.^{6,7}

Tumorigenesis describes the process of tumor formation: the transformation of normal cells in tumor cells, with a multistep process that born with a precancerous lesion and continue with a malignant tumor. This process is conditioned by interaction between genetic factors and three external agents: biological carcinogens like infection from bacteria or virus, physical carcinogens, like UV radiation, and chemical carcinogens, such as arsenic and asbestos.⁵

Tumorigenesis is a 4-steps process showed in **Figure 1**:⁸

INITIATION

In the first phase alteration or mutation of a gene is observed, it can happen spontaneously or following an exposition with cancerogenic agent: in normal cells deregulation of biochemical pathways occurs, followed by cellular proliferation, differentiation and survival.⁸⁻¹⁰ These changes can be increased by mutation of other factors response of DNA repair function.⁸⁻¹⁰

PROMOTION

Different component, like environmental, interfere to promote preneoplastic cells proliferation and their accumulation; this phase is slow, and it can be reversible.⁸⁻¹⁰

PROGRESSION

In this stage proto-oncogene can convert themselves in oncogene, there are neoplastic transformations, with genetic and phenotypic mutations. Tumor dimensions increase, cells become invasive and promote the carcinogenesis.⁸⁻¹⁰

METASTASIS

With metastasis tumor cells can move in other districts of the body, using bloodstream, lymph system, and they can generate themselves new lymph system with angiogenesis.^{8,9}

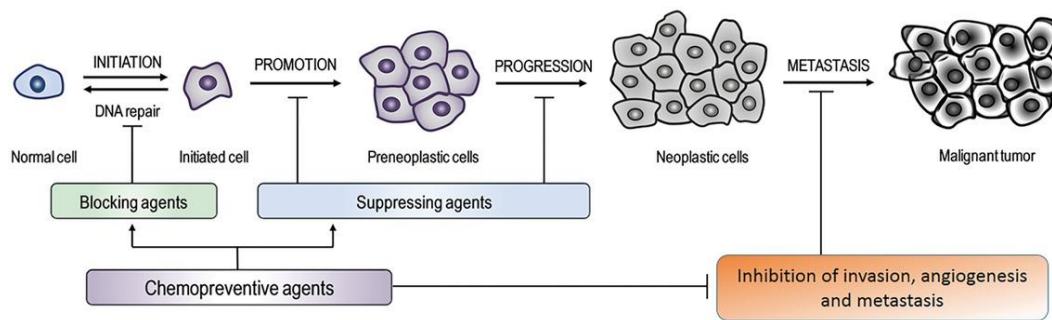


Figure 1 Tumorigenesis: Initiation, Promotion, Progression and Metastasis⁸

Cancer is also defined like an evolutionary process caused by somatic mutations in the progeny of a normal cell, that bring to uncontrolled replication and to a selective growth of mutated cells.¹¹ Different cellular and molecular events lead to malignant transformation of cells, like evasion of tumor suppression, inhibition of cell death, creation of a particular microenvironment containing blood vessels, acquisition of invasive and metastatic potential.¹²

The cancer stem cells (CSCs) can drive tumor initiation and can cause relapse, in fact they are also known as tumor-initialing cells (TICs): they are the principal controller of tumor growth for proliferation, resistance to chemotherapy and metastasis (**Figure 2**).¹¹ Both normal and neoplastic cell population include a subpopulation of stem cells that can self-renew and differentiate. The normal SC usually can support a genetic alteration but, if they are not able, they can generate altered SC; which can generate, in turn, a preneoplastic cell population.¹³

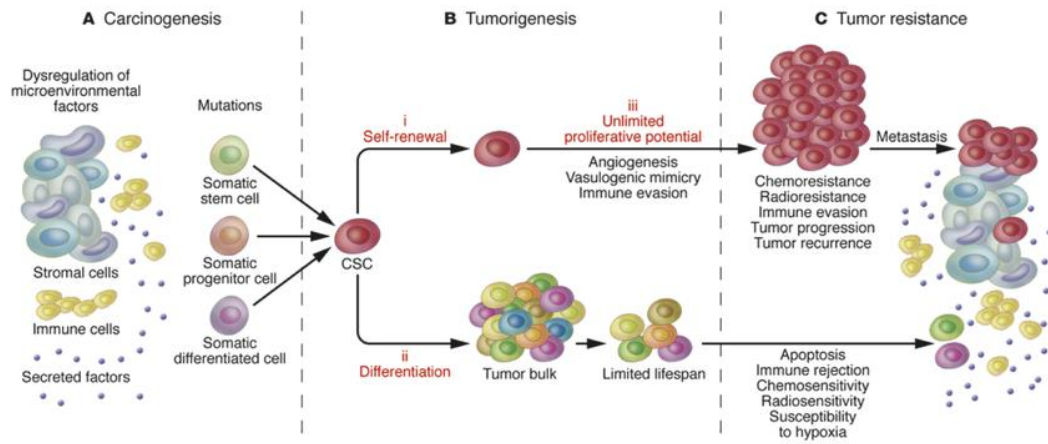


Figure 2 Carcinogenesis, tumorigenesis, and tumor resistance¹¹

1.2 Cellular pathways involved in tumors

Tumor cells present altered genetic, biochemical and histological mechanism, with respect to the normal cells; in particular they have altered energy metabolic activities, which promote the acquisition and maintenance of malignant properties.^{14, 15} The cells reprogram their activities through the metabolism, to have advantages for the tumorigenesis and for survival, growth and proliferation under stressful conditions; in particular they modify bioenergetics, enhanced biosynthesis and redox balance.¹⁴

Tumor cells can reprogram their metabolism: in conditions of nutrient-replete they prefer anabolic growth, otherwise, during nutrient-limitation conditions they can use catabolism and fortify the redox homeostatic systems to support the cell survival, and to resist to tumor suppressor.^{14, 16}

The most important feature of reprogrammed metabolic pathways is the aerobic glycolysis; this form of modified cellular metabolism is also known as the Warburg effect.^{14, 16}

Glycolysis supplies the necessary energy to the cells, in mitochondria, and its intermediates can be used for the synthesis of amino and fatty acid: one molecule of glucose is exploited to produce adenosine triphosphate (ATP), nicotinamide adenine dinucleotide hydrogen (NADHs) and pyruvate.¹⁷ The process occurs in absence or presence of oxygen: under aerobic conditions pyruvate is converted into acetyl coenzyme A (acetyl-CoA) which is oxidized to CO₂ and H₂O, through tricarboxylic acid (TCA) cycle and oxidative phosphorylation (OxPhos); in absence of oxygen, the pyruvate is reduced to lactate, necessary for the regeneration of NAD⁺, that can be used by the enzymes involved in glycolysis, in order to have an uninterrupted cycle.^{17, 18}

Healthy tissues usually prefer using oxidative phosphorylation to produce energy and use anaerobic glycolysis like a normal response to hypoxia. On the contrary, many tumor cells can exploit anaerobic glycolysis to produce lactate, regardless of the presence of oxygen: Warburg effect.¹⁴ Moreover, in cancer cells there is an increasing of glycolytic flux to respond to the rapid growth of tumor, causing condition of hypoxia in blood vessels, with an oxygen concentration in the range of 0-2% O₂.¹⁹ According to this, in tumor cells, anaerobic glycolysis prevails. With the Warburg effect, there is an increase of lactate secretion, that contribute to create an acid microenvironment, toxic both for the normal

cells and for the weakest cancer cells, but not for the strong aggressive cancer cells; furthermore, the extracellular environment acidosis promotes angiogenesis and increases the invasion ability of cancer cells, creating an environmental advantage for tumor progression.^{14, 20, 21}

Due to Warburg effect, the respiratory chain in mitochondria is downregulated, resulting in reduction of OxPhos and oxygen consumption: during the aerobic glycolysis a great amount of reactive oxygen species (ROS) were produced, they supports tumor cells to avoid apoptosis and increases their proliferation.²¹ The high rate of glycolysis in tumor cells is suggest by the increased transcription of genes of most enzymes and transporters involved in the pathway, that match with an increased synthesis of protein.¹⁵

In tumor cells there is a deregulation of signaling pathways such as over-regulation of pathways that support functions like anabolism, catabolism and redox balance, necessary for the cell survival (**Figure 3**).^{14, 22} Usually, in normal cells, growth factors stimulate and activate phosphatidylinositol 3-kinase (PI3K) and its pathways, protein kinase B (AKT) and mammalian target of rapamycin (mTOR), resulting in the activation of hypoxia-inducible factor-1 (HIF-1) and sterol regulatory element-binding protein (SREBP), that induce increase of glycolytic flux and fatty acid synthesis, respectively.^{14, 23} Tumor cells usually present mutations that interfere with the pathway of PI3K-AKT-mTOR, resulting in high levels of signaling, independent to the presence of growth factor.¹⁸ mTOR is a serine/threonine kinase, that after his activation by PI3K/Akt system, induce cell growth and inhibit the catabolic reactions.¹⁸ Aerobic glycolysis of tumor cells is also fundamental for the activation of oncogenes, loss of tumor suppressor and up-regulation of the PI3K pathway.¹⁴

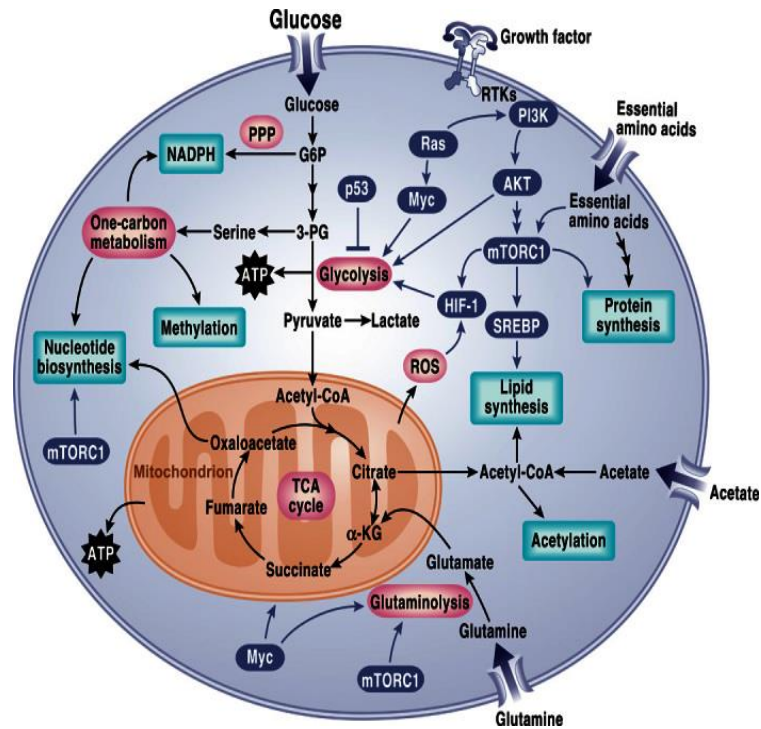


Figure 3 Signaling pathways that regulate cancer metabolism¹⁴

Hypoxia, induced by cellular changes, results necessary for tumor proliferation, metastasis, and resistance to therapy. Hypoxic and inflammatory stress, as well as metabolic and oxidative stress, can upregulate HIF-1, a transcription factor constituted by the subunits HIF-1 α and HIF-1 β .^{15, 18, 24} In normal and aerobic conditions, there is a program of HIF-1 α degradation when it is not necessary for the cells, otherwise, in anaerobiosis condition, the transcription factor became stable.^{15, 25} HIF-1 α can also be induced by cytokines, growth factors, reactive oxygen species, nitric oxide, and by energy-metabolism intermediates, like pyruvate (Pyr), lactate and oxaloacetate.¹⁵ The role of HIF-1 is to promote the expression of different enzymes involved in energetic metabolism, in order to stimulate the glycolytic flux; moreover, metastatic tumor cells line generally present overexpression of HIF-1, glycolytic enzymes and high glycolysis.^{15, 26} Two other targets of HIF-1 are vascular endothelial growth factor (VEGF) and carbonic anhydrases (CAs): the first promote angiogenesis, necessary for the reuptake of nutrient and oxygen; while CAs are necessary for the pH homeostasis in microenvironment.²⁴ Furthermore, HIF-1 transactivate cytochrome c oxidase (COX), to facilitate the adaptation of mitochondria to an hypoxic environment.¹⁸ HIF-1 work together with c-Myc, a proto-oncogene that code for transcription factors, to stimulate aerobic glycolysis through the induction of enzymes

involved in the cycle, like hexokinase 2 (HK2) and pyruvate dehydrogenase kinase 1 (PDK1).²⁷ HIF-1 with oncogenes and tumor suppressor genes are capable to reprogramming tumor cells metabolism in different step.

The protein p53 works as a tumor suppressor by regulating the replication cycle cell; it is involved in several stages of metabolism control and regulate proteins necessary to cellular response to cancer. This protein is also known as the “guardian of the genome”, because it is usually upregulated after a DNA damage to stop the cell cycle and to induce apoptosis.²¹ Also, the protein play an important role during viral infection, oxidative stress, altering cell metabolism. p53 acts inducing/inhibiting key metabolic genes involved in glycolytic pathway, OxPhos, lipid and amino acids metabolism and cell growth (**Figure 4**).²¹ In normal cells p53 usually promote OxPhos and suppress glycolysis.²¹ In many tumor cells a mutated p53 is present and overexpressed; mutated p53 have strong oncogenic activity, in fact it has a relevant role in inducing cell transformation. It is involved in several pathways such as modulating the mTOR pathway, repressing autophagy, and promoting drug resistance.

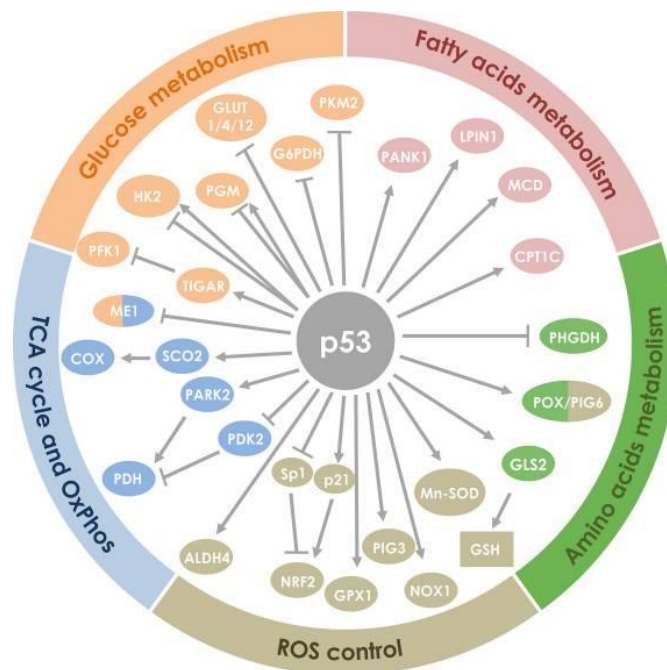


Figure 4 Regulation by p53 of proteins involved in cells metabolism²¹

Other important molecules involved in tumor cells metabolism are ROS, like hydroxyl radical, superoxide and hydrogen peroxide; they are by-products of metabolism of oxygen. Usually, in normal cells, they are present in a small quantity, while in tumor cells there is

an over-production; this situation leads to DNA damage, and consequently mutation and tumorigenesis: they activate apoptotic signaling and induce cell death.²¹ In normal cells, DNA damages induced by ROS, activate p53, that work to lower ROS levels. In tumor cells p53 is downregulated, and there is an enhanced of ROS, while cells with low amounts of p53, stimulate the expression of antioxidant genes like glutathione peroxidase (GPX1). The mutated p53 are present in tumor cells where they suppress the expression of genes involved in ROS inhibition.²¹

To respond at low oxygen levels in microenvironment, tumor cells apply changes, not only in metabolism and proliferation, but also in gene expression, genetic stability and survival.²⁸⁻³⁰ The high production of lactate and carbon dioxide by glycolysis, which are expelled in extracellular environment to preserve intracellular environment, concur to reducing extracellular pH. Tumoral cells can adapt their intracellular environment thanks to the activity of enzymes like carbonic anhydrase IX (CA IX).³¹ CAs are involved in the catalysis of carbon dioxide hydration to bicarbonate ions and protons. CA IX acidify extracellular environment, increasing carbon dioxide and protons level, and neutralize intracellular pH by the formation of bicarbonate ions.²⁸ HIF-1 is involved in regulation of CA IX transcription, so in tumor cells where HIF-1 is overexpressed, CAs are overexpressed too, especially the IX isoform.³²

Cyclooxygenase-2 (COX-2) is another enzyme involved in tumorigenesis, especially in colorectal cancer. Inflammation induce COX-2 expression; it is responsible of prostaglandins synthesis. His overexpression has been observed and investigated in several tumors, in association with his product, prostaglandin E₂ (PGE₂), that promote proliferation, evasion of apoptosis, angiogenesis and tissue invasion.³ PGE₂ has pleiotropic effects linked to the acquisition of cancer hallmarks and inflammation. Some tumor present a deregulation of COX-2 pathway caused by epigenetic alteration, like DNA methylation: **Figure 5** shows the hyper-methylated genes, evidenced in red boxes, and in which type of cancer they have been reported.³³

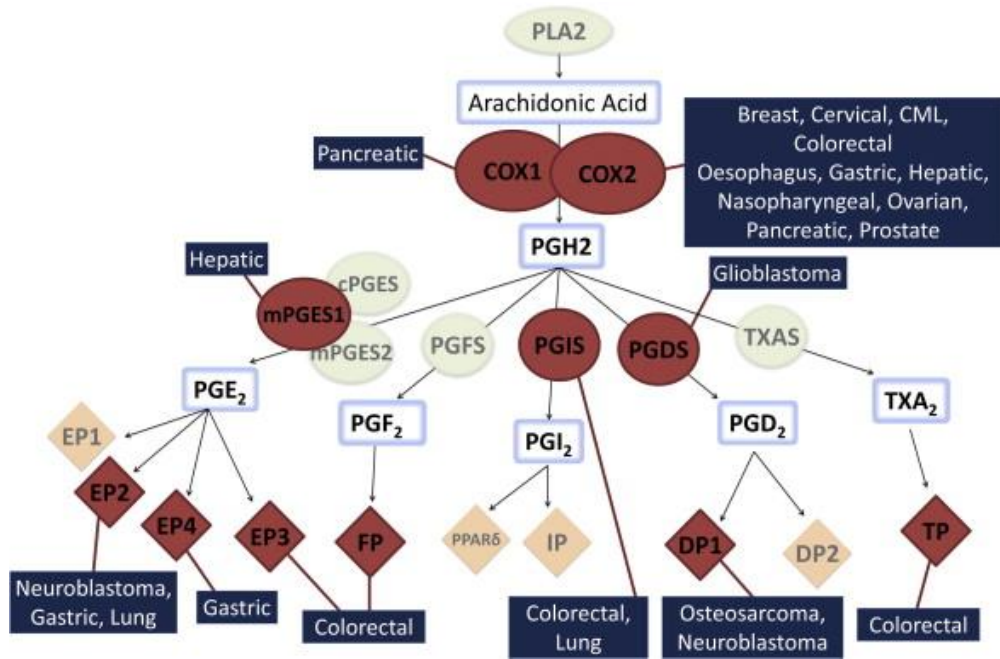


Figure 5 Deregulation of COX-2 pathway in different tumors³³

1.3 General mechanism of drugs

Drug effects depend by different factors: interactions between chemical component of molecule with proteins, nucleic acids and other macromolecules, as well as their degradation by enzymes in the organism; their transport through membrane, water solubility and, more generally, ADMET profile (absorption, distribution, metabolism, excretion, and toxicity).^{34, 35}

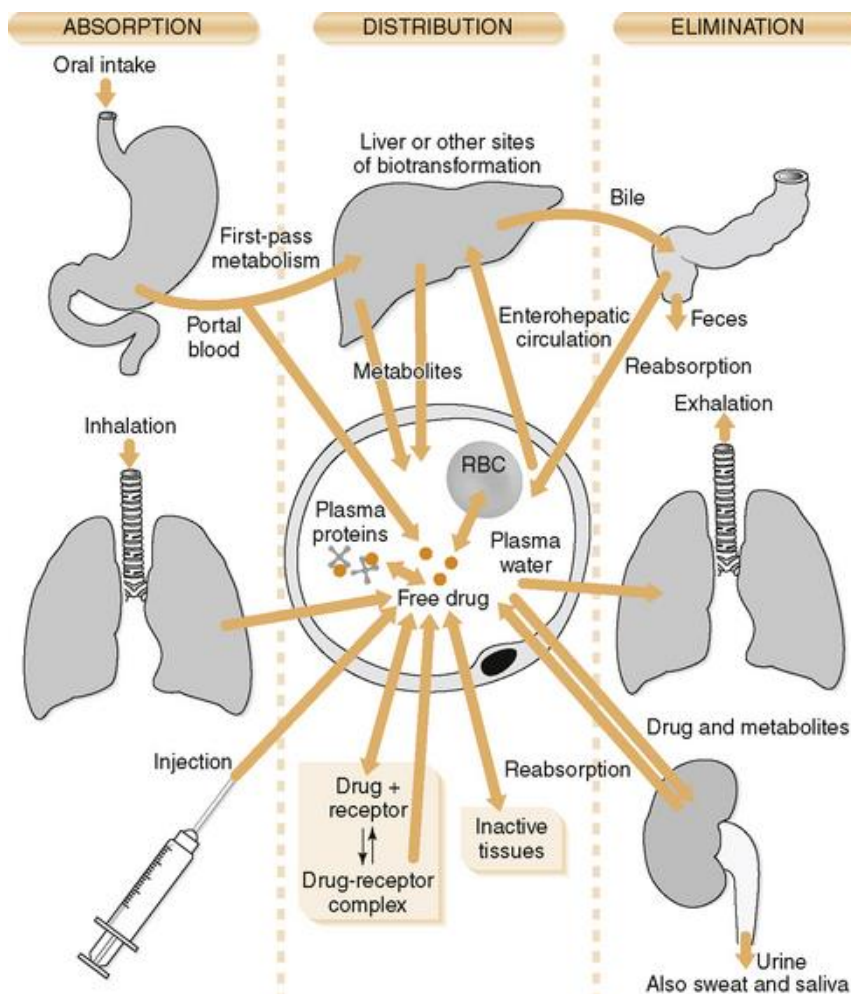


Figure 6 ADME³⁶

– SOLUBILITY

As a general rule, drugs must be polar enough to be water soluble: usually is necessary that the polar groups present in molecules exceed lipophile groups to achieve water solubility. In some cases, acid or basic groups are introduced to obtain ionizable species, more soluble in water.

– *MEMBRANE TRANSPORT*

Biological membrane wrap the cells and they are constituted by lipids. They represent the wall that must necessary overstepped by drugs to play their role; for this reason, drugs need to be water soluble and fat-soluble at the same time.

– *SYSTEM BIOLOGY INTERACTION*

Structure-activity relationship (SAR) is defined as the relationship between chemical structure of molecule with its biological activity; SAR helps to predict activity of a new molecule: similar molecules are supposed to act in a similar way and functional groups of a molecule usually contribute to its biological action and/or chemical-physic propriety. Molecular structure, its composition and the spatial orientation of the functional groups lead to the pharmacological effect of the molecule.³⁴

– *METABOLISM*

Metabolism is in most cases necessary to increase hydrophilicity of molecules as one of the main ways to facilitate excretion of the molecules.

– *ACTIVE TRANSPORT*

Active transports can bring a molecule across a physiological barrier, such as the membrane of gastrointestinal tract and the blood brain barrier. This process requires energy and can be divided in two different types: primary, that use ATP molecules and secondary, that use electrochemical gradient.³⁷

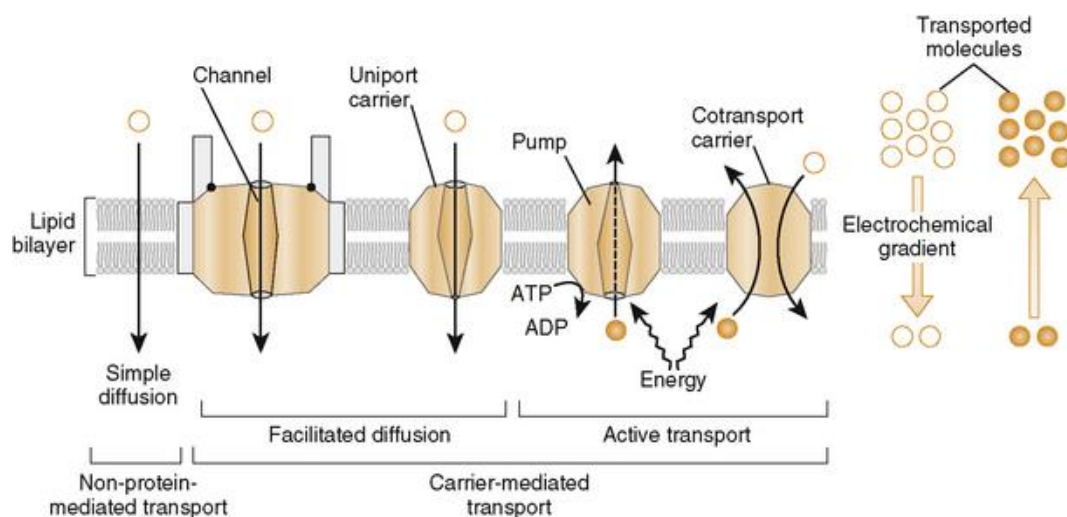


Figure 7 Example of active and passive transports³⁶

– *RECEPTORS*

Drugs interact with a target macromolecule generally leads to its activation or inactivation. As a general scheme, molecule can act as agonists if their binding to the receptor activate it, or antagonist if their binding block the receptor without activating it.

More generally, molecules need to interact with their biological target to express their activity, no matter if the target is a receptor, an enzyme, a nucleic acid, a membrane etc. In other words, the molecule needs to be complementary with its target or to be capable to achieve this complementarity according to conformational adaptations that involve both the ligand and the target. Thus, complementarity is a dynamic process strictly dependent on the molecule chemical-physic proprieties.

1.4 Tumors drugs

Current treatments for tumor, usually consist in chemotherapy, radiotherapy, surgery, targeted therapy, immunotherapy and endocrine therapy that can be used individually or in combination, depending on the stage and type of tumor and diagnosis.³⁸⁻⁴¹

Early detection of cancer is necessary to have a promising clinical prognosis and a successful treatment, but, unfortunately, most patients usually have a late-stage diagnosis, that, in combination with delayed therapies, lower the possibility of survival.⁴²

Following some approaches to cancer therapies.

Biomarkers

An interesting method for early tumor diagnosis can be the identification of tumor biomarkers. Biomarker is described by *U.S. National Institutes of Health* (NIH) as “a characteristic that is objectively measured and evaluated as an indication of normal biologic processes, pathogenic processes, or pharmacologic responses to a therapeutic intervention”.⁴²⁻⁴⁴ Cancer biomarkers found in tumor tissue or serum, can be molecules like proteins, enzymes, DNA, RNA, metabolites, transcription factors.⁴² By identifying cancer biomarkers, it is more easy to have an early cancer diagnosis, tumor classification and consequently, the appropriate therapy for the patient.

Precision oncology

Precision oncology is another approach to identify targetable genomic alterations, that characterize tumors in order to have a specific treatment for patients.⁴⁵⁻⁴⁷ The goal of precision oncology is to improve cancer therapy, lowering toxicity, by using drugs that are directed towards selective genes or proteins of tumor cells. From 2000 to 2014 almost the 79% of the newly approved tumor drugs are targeted therapeutic agents.⁴⁷

Treatments based on precision oncology:

PRODRUGS

Prodrugs are derivatives of drug molecules which need a bioconversion by human enzymes to perform their activity, and have the purpose to improve pharmacokinetics profile of the drug.^{48, 49} Some cancer prodrugs are activated in tumoral cells by specific enzymes, and need to have good activity at low pH values.⁵⁰

KINASE INHIBITORS

During the last twenty years an increasing number of small molecules directed toward tumor associated kinases, such as BCR-ABL, EGFR, VEGFR have been identified and introduced in therapy.⁵⁰⁻⁵² However, this therapeutic approach might lead to the expression of mutated resistant proteins to drugs.^{51, 53}

IMMUNOTHERAPY

Immunotherapy is based on the observation that immune cells are able to destroy tumor cells during the firsts stage of tumorigenesis.^{54, 55} During cells transformation from normal to cancer, cancer cells exhibit neo-antigens which can be recognize by the immune system provoking its activation and the destruction of the growing tumor. Unfortunately, tumor cells develop specific mechanisms to escape from immune cells: local immune evasion, induction of tolerance, systemic disorder of T cells signaling.^{54, 56} Among immunotherapy there are: cancer vaccines, oncolytic virus, adoptive transfer of ex vivo activated T and natural killer cells.⁵⁴

Gene therapy

With gene therapy, vectors take in tumoral cells exogenous nucleic acid, which modify gene expression to correct the abnormalities.⁵⁷

Nanocarriers

Nanocarriers are colloidal nano-scale system that transport in tumor cells, great concentration of antitumoral agents, like small molecules or macromolecules that result cytotoxic for cells.

Biosimilar

Biosimilars are synthetic macromolecules that have similar pharmacokinetic and pharmacodynamic properties to a license biological product, without differences for safety, purity and potency.^{58, 59} They were approved in EU in 2005.⁵⁸

Epigenetic therapy

This therapy is based on studies of genic pathways, which cause deregulation in gene expression, without modify DNA sequence.⁶⁰ Histone proteins are involved in modification of gene expression: they may undergo different post-translational changes and methylation that imprint on transcription.⁶⁰

1.4.1 Resistance to chemotherapy

The major problem in cancer treatments is the resistance to chemotherapy agents and to novel targeted drugs; it is responsible for the majority of therapy failures and patients deaths.³⁸ There are two type of resistance: acquired and intrinsic.^{38, 61, 62}

INTRINSIC RESISTANCE

Drug resistance can be present before therapy and it is called intrinsic; it affects almost 50% of patients.^{38, 61, 62} Three important factors cause innate resistance:

- Inherent genetic mutation
- Tumor heterogeneity, in which exist different type of cancer cells with distinct phenotypic profile, gene expression, metabolism, metastatic potential; in this case is very high the possibility of relapse after treatment
- Intrinsic pathway for defense against external toxins.³⁸

Therapeutic effects of tumoral drugs decrease with intrinsic resistance.

ACQUIRED RESISTANCE

Acquired resistance is induced after treatment and affects most of patient; it causes the reduction of efficacy of cancer drug during the therapy.^{38, 61, 62} Tumoral cells show defense mechanisms against external molecules, in this way the tumor acquire resistance thanks to different pathway:

- Activation of second proto-oncogene
- Genetic and epigenetic mutation that lead to modification in level of drug target expression
- Modification in tumor microenvironment (TME) after therapy.^{38, 61}

Some factors involved in resistance: members of the adenosine triphosphate (ATP)-binding cassette transporter gene family, glutathione-dependent enzymes, topoisomerase, metallothionein, O6-methylguanine-DNA-methyltransferase, thymidylate synthetase, dihydrofolate reductase, heat shock proteins, growth factors, proliferative, apoptotic and angiogenetic factors, protooncogenes and suppressor genes.⁶³ Cancer cells can also acquire resistance to targeted drugs, thanks to develop of new mutation in target protein genes; in this way there is a secondary mutation, such as BCR-ABL kinase domain.^{38, 64}

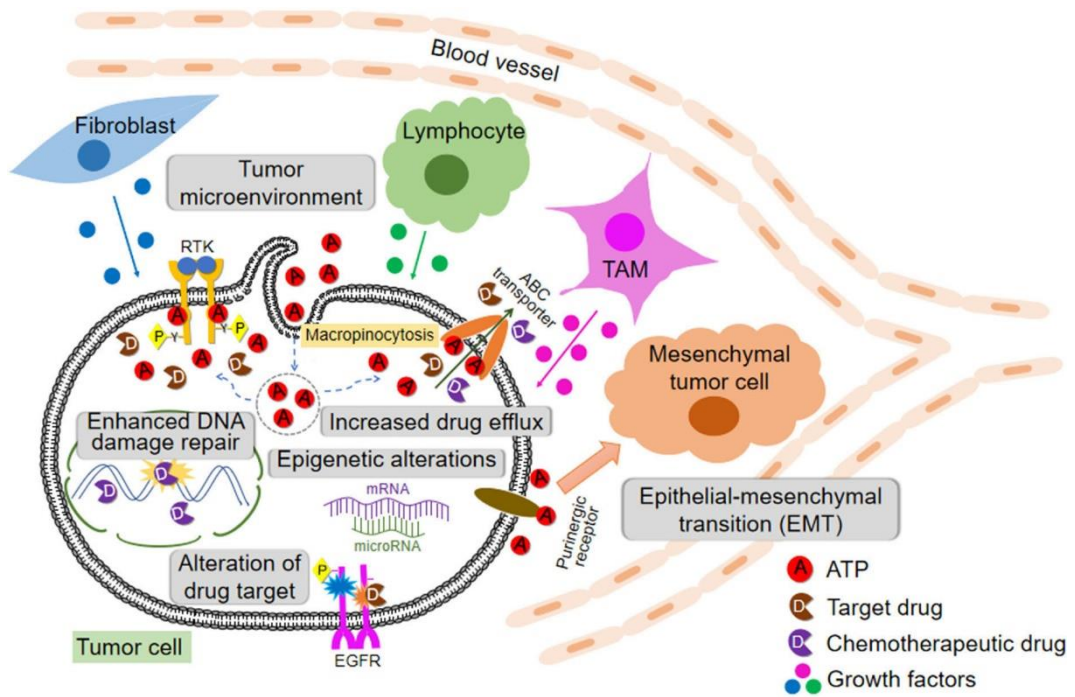


Figure 8 Cancer drug resistance³⁸

1.5 Multi target inhibitors

Drug design and discovery is a very dynamic process, necessary to counteract the global morbidity and mortality caused by incurable disease like cancer. Usually, the discovery of new therapies is based on the design of selective chemical compound that target a single enzyme or, more generally biological target. Most commonly they target a protein called “on-target”, the dominant or most relevant one in the pathology. By this approach the researchers aim to identify therapeutic agents devoid of side effects.^{65, 66} Unfortunately, the therapeutic agents directed towards one single target have shown low efficacy towards complex diseases; in particular this type of therapeutic agents have been associated with the increase of drug resistance.⁶⁷

Polypharmacology is a new approach to design and use compound that simultaneously act towards two or more targets, or multiple biochemical pathways involved in the disease; a single compound can recognize more than one biological target.⁶⁷

Multifactorial disease, such as cancer, are characterized by several intrinsic and/or environmental factors that contemporary act on the organism; with polypharmacology, multi-target compound show some benefit: a more predictive pharmacokinetic, better compliance of the patient and last but not list, the reduced risk of drug interaction.⁶⁸

The advantage of using selective inhibitors is the decrease chance to have side effects during the therapy; while multi-target inhibitors can act simultaneously towards different cell pathways or compensatory mechanisms, and this mechanism is more effective than selective inhibitions of one enzyme, principally in tumors in which are involved more pathway.⁶⁹

The first difficult for the development of multi-target compound, is the right combination of target for the disease: it is necessary to understand the target-disease associations, the pathway-target-drug-disease relationship and the side effects.⁷⁰ It is necessary to monitor the additive effects if the targets belong to the same pathway, and the synergism effects if the targets belong to complementary pathway: in both situation there is an effect with lower doses and therefore a better safe profile than the single-target compound.⁷¹

The design of multi-target compounds starts with combination of two distinct structures, take from inhibitors with activity towards the selected targets, into a single chemical entity.^{72, 73} Usually, multi-target compounds derive by assimilation of pharmacophores of

molecules like drugs or drug candidates, specific for the targets (**Fig. 9**). Pharmacophores can have similar scaffolds and, in this case, can be fused; if the pharmacophores have different structure for the target interaction, they can be combined through linkers.⁷⁴ To design multi-target compounds, it is necessary to consider a fundamental requisite: every framework must interact with its target; so, it became important to consider the structure-activity relationship between the interaction of starting molecules and their targets.⁷⁵

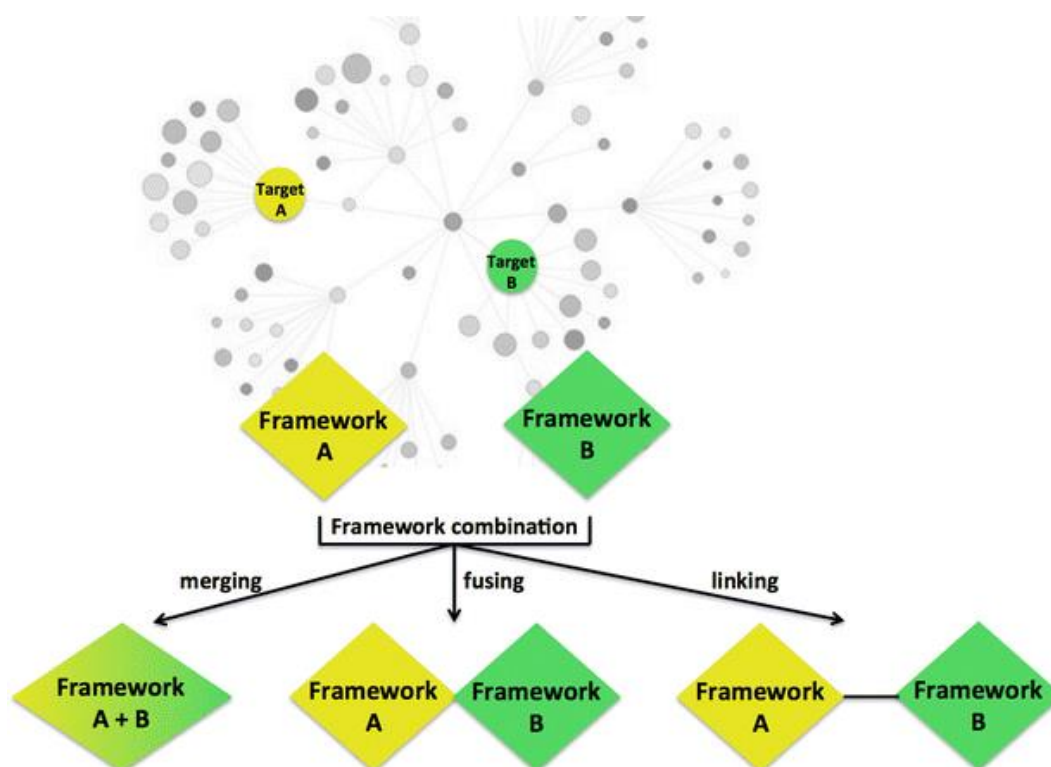


Figure 9 Design of multi-target compounds⁶⁶

One part of the molecule interacts with the target proposed, the other parts can impede the binding action. To solve the problem may be interesting working on the flexibility of the molecule, without exceeding to not interfere negatively in the binding affinity or in bioavailability of the compound.^{66, 75, 76}

Multi-target compounds represent a very promising strategy to cope problems of multifactorial disorders and particularly the drug resistance; they have more predictable pharmacokinetics respect to the combination therapies, guarantee higher patient compliance, and there are minus drug interactions.⁶⁸ Furthermore, with multi-target

agents toxicity and side effects decrease, respect to the single-target therapies, because require smaller doses.⁷²

Research of multi-target agents can be optimized by the use of computer-aided drug design (CADD)⁷⁶ the

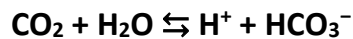
Therefore, with the aim of simplifying the screening of new multi-target molecules, in silico method have been studied, such as fragment-based and combinatorial approaches.⁷⁷

Combinatorial approaches execute parallel searches to determinate the hit molecules capability to interact with more than one target.⁷⁸ The use of in silico methods in drug design revealed to be very advantageous, often assuring better results with lower expenses and in a relatively shorter period of time. Moreover, as mentioned above can perform a screening on different targets permitting to only validate the activity of the most promising candidates.⁷⁶

CARBONIC ANHYDRASE

2.1 Carbonic Anhydrase: overview

Carbonic anhydrases (CAs) are a superfamily of ubiquitous zinc metalloenzyme, present in prokaryotes and eukaryotes, like animals, photosynthetic organisms and some bacteria.^{79,}
⁸⁰ They catalyze the reversible interconversion of carbon dioxide hydration to bicarbonate and protons.^{79, 81}



This reaction is essential for different physiological process: respiration and transport of CO₂/bicarbonate, pH and CO₂ homeostasis, metabolism, where they appear important for different pathways such as gluconeogenesis and ureagenesis, cell growth, calcification, photosynthesis, ionic, electrolyte secretion in tissue and organism.⁸⁰⁻⁸⁵

Five different and genetically unrelated gene families have been studied: α -, β -, γ -, δ - and ξ -CA.^{79, 81} α -CAs genes are principally expressed by vertebrates, but they are also found in algae, bacteria and cytoplasm of green plants, β -CAs genes are predominantly in bacteria, as well as expressed in algae, chloroplasts and both mono- dicotyledons. γ -CAs are found in in archaea and some bacteria; ζ - and ξ -CA are present in some marine diatoms.^{80, 81, 86-88}

CAs active form present one metal ion bound to the active site cavity; M(II) ion bound three amino acids residue and a water molecule/hydroxide ion, in a tetrahedral geometry.⁸⁹ α -, β - and δ -CAs use Zn(II) ion, ζ -CAs usually use Fe(II) but some study show that they can be active also with Zn(II) and Co(II) ions; γ -CAs use Cd(II) or Zn(II) ions.⁹⁰⁻⁹⁴

Each class of enzyme is found in different oligomerization state. α -CAs are usually monomers, and rarely they were found like dimers; β -CAs are oligomers, formed by 2-6 monomers, or octamers; γ -CAs are trimers, and δ -CAs are monomers; ζ -CAs are pseudo trimers, because of the presence of three active site present in the same protein backbone.⁸⁸

3.1.1 α -Carbonic Anhydrase

Sixteen mammalian α -CA isozymes, also called CA-related proteins (CARP), have been studied, each one with different subcellular localization and tissue distribution.^{80, 82, 83, 95} CA I-III, CA VII and CA XIII are cytosolic forms, CA IV, CA IX, CA XII, CA XIV and CA XV are membrane bound isozymes, CA VA and VB are found in mitochondria, and CA VI is a secreted isozyme in milk and saliva. Twelve isoforms (CA I-IV, VA-VB, VI-VII, IX, and

XII–XIV) present enzymatic activity, while three isoforms (VIII, X, and XI) do not present any catalytic activity. All human carbonic anhydrases belong to α -CAs class.

Physiological function of human CAs have been studied:⁹⁶⁻⁹⁸

- CA I, II and IV isoforms have a role in respiration and regulation of pH homeostasis, processes that involve transport of CO₂/bicarbonate between tissues and excretion sites, such as lungs and kidneys, and facilitated CO₂ secretion in capillary and lung, and the elimination of H⁺ ions in renes⁹⁸
- CA II is also involved in bone function and development, like differentiation of osteoclast and supply proton for bone resorption in osteoclasts⁹⁶
- CA II and VA supply bicarbonate for gluconeogenesis and fatty acids de novo biosynthesis
- CA V have a role in molecular signaling process, most of all the insulin secretion in pancreas β ⁹⁸
- CA IX, XII, CARP VIII are found in many tumors, and are involved in oncogenesis and tumor progression⁹⁸

In **Table 1** the subcellular localization, organ and tissue distribution, CO₂ hydrase activity with kinetic parameters (at 20°C and pH 7.5), and affinity for sulphonamides for all sixteen α -CA isozymes is represented.⁸⁸

Table 1 Subcellular localization, Organ/Tissue distribution, CO₂ hydrase activity with Kinetic Parameters and Affinity for Sulphonamides of α -CA⁸⁸

Isozymes	Subcellular localization	Organ/Tissue distribution	Catalytic Activity (CO ₂ Hydration)	<i>k_{cat}</i> /Km (M ⁻¹ s ⁻¹)	Affinity for Sulphonamides
<i>hCA I</i>	Cytosol	Erythrocytes, GI tract, eye	Low	5.0x10 ⁷	Medium
<i>hCA II</i>	Cytosol	Erythrocytes, GI tract, eye, bone osteoclasts, kidney, lung, testis, brain	High	1.5x10 ⁸	Very high
<i>hCA III</i>	Cytosol	Skeletal muscle, adipocytes	Very low	3.0x10 ⁵	Very Low
<i>hCA IV</i>	Membrane-bound	Kidney, lung, pancreas, brain capillaries, colon, heart muscles, GI	High	5.1x10 ⁷	High

tract

hCA VA	Mitochondria	Liver	Moderate-high	2.9×10^7	High
hCA VB	Mitochondria	Heart and skeletal muscle, pancreas. Kidney spinal cord, GI tract	High	9.8×10^7	High
hCA VI	Secreted in Saliva and Milk	Salivary and mammary glands	Moderate	4.9×10^7	Medium-low
hCA VII	Cytosol	CNS	High	8.3×10^7	Very high
CARP VIII	Cytosol	CNS	Acatalytic	/	*
hCA IX	Transmembrane	Tumors, GI mucosa	High	5.5×10^7	High
CARP X	Secreted	CNS	Acatalytic	/	*
CARP XI	Secreted	CNS	Acatalytic	/	*
hCA XII	Transmembrane	Kidney, intestine, reproductive epithelia, eye, tumors	Low	3.5×10^7	Very high
hCA XIII	Cytosol	Kidney, brain, lung, gut, reproductive tract	Moderate	1.1×10^7	High
hCA XIV	Transmembrane	Kidney, brain, liver, eye	Low	3.9×10^7	High
hCA XV	Membrane-bound	Kidney	Low	3.3×10^7	Unknown

*The native CARP isozymes do not contain Zn(II), so that their affinity for the sulfonamide inhibitors has not been measured. By site-directed mutagenesis it is possible to modify these proteins and transform them in enzymes with CA-like activity which probably are inhibited by sulfonamides, but no detailed studies on this subject are presently available

α -CAs catalyze several reactions represented in **Table 2**, not only the hydration of carbon dioxide (**2.A**) but also, the hydration of cyanate to carbamic acid, or of cyanamide to urea (**2.B** and **2.C**); the aldehyde hydration to gem-diols (**2.D**); the hydrolysis of carboxylic, or sulfonic (**2.E**, **2.F**), other hydrolytic processes, such as those described by equations **2.G-2.I**.⁸⁰

Table 2 Reaction catalyzed by α -CA⁹⁸

A	$\text{O}=\text{C}=\text{O} + \text{H}_2\text{O} \leftrightarrow \text{HCO}_3^- + \text{H}^+$
B	$\text{O}=\text{C}=\text{NH} + \text{H}_2\text{O} \leftrightarrow \text{H}_2\text{NCOOH}$
C	$\text{HN}=\text{C}=\text{NH} + \text{H}_2\text{O} \leftrightarrow \text{H}_2\text{NCONH}_2$
D	$\text{RCHO} + \text{H}_2\text{O} \leftrightarrow \text{RCH}(\text{OH})_2$
E	$\text{RCOOAr} + \text{H}_2\text{O} \leftrightarrow \text{RCOOH} + \text{ArOH}$
F	$\text{RSO}_3\text{Ar} + \text{H}_2\text{O} \leftrightarrow \text{RSO}_3\text{H} + \text{ArOH}$
G	$\text{ArF} + \text{H}_2\text{O} \leftrightarrow \text{HF} + \text{ArOH}$ (Ar = 2,4-dinitrophenyl)
H	$\text{PhCH}_2\text{OCOC}l + \text{H}_2\text{O} \leftrightarrow \text{PhCH}_2\text{OH} + \text{CO}_2 + \text{HCl}$
I	$\text{RSO}_2\text{Cl} + \text{H}_2\text{O} \leftrightarrow \text{RSO}_3\text{H} + \text{HCl}$ (R = Me; Ph)

X-ray crystallographic 3D structure data of all α -CA isozymes, except CA VB, have been studied.⁹⁹⁻¹⁰³ Cytosolic hCAs exhibit high sequence similarity and their secondary structure elements are preserved. Consequently, their 3D structure are very similar. Due to their relevant role in human metabolism several X-ray crystal structures of catalytically active isozyme of hCAs have been reported.^{89, 94, 99-103} By structural comparison of all crystallized hCAs, some structural differences can be observed in the region of residues 125-130 (using the hCA II amino acid numbering system), located in the surface, and residue 131 in the active site of the protein.^{86, 89, 94}

The cavity of the active site has a conical shape, with a 15 Å diameter entrance; it is divided in two distinct environments: the deepest part of the active site is formed by hydrophobic amino acids, in particular for hCA II, the most studied carbonic anhydrase, present Val-121, Val-143, Leu-198, Thr-199-CH3, Val-207, and Trp-209 (**Fig. 9** green surface); on the contrary, in the other side of the cavity, the surface, hydrophilic amino acids are prevailing (Tyr-7, Asn-62, His-64, Asn-67, Thr-199-O γ 1, and Thr-200-O γ 1) (**Fig. 9** magenta stick).⁸⁹

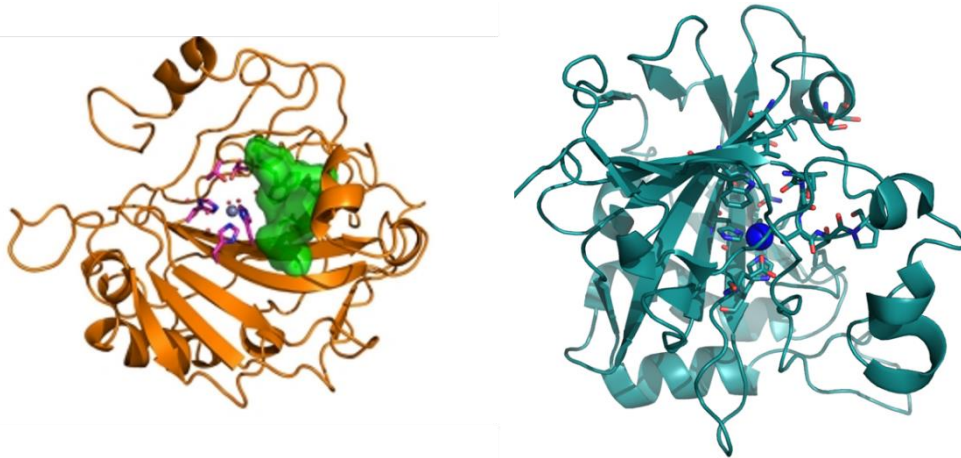


Figure 10 3D structure of hCAII and CA IX 5FL4.^{89, 104}

CA I, II, IX, and XII show interesting homologies between the residues of the active site. (Fig. 10). Very interesting the residue 131, different among the isoform: in CA II is a phenylalanine (F): its bulky side chain causes steric hindrance in the active site; while in CA IX there is a Valine in position 131 which permits a more favorable binding and greater isoform selectivity toward CA IX respect to CA II isoform.¹⁰⁵

```

CA-I      MSPDWGYDDKNGPEQWSKLYPIANGNNQSPVDIKTSETKHDTSLKPISVSY---NPATAK
CA-II     MSHHWGYGKHNHGFPEHWHKDFPIAKGERQSPVDIDHTAKYDPSLKPLSVSY---DQATSL
CA-IX     ---HWRY---GGDPPWPRVSPACAGRFQSPVDIRPQLAAFSPALRPLELSGFQLPPLPEL
CA-XII    -MSKWTFYFPGDGENSWSKKYPSCGGLLQSPIDLHSDILQYDASLTPLFQGYNLSANKQF
          . * * . * * : * . * * * : * : . . : * * : . . .

CA-I      EIINVGHSHFVNFEDNDRSVLKGGPFSDSYRLEFQHFHWGSTNE-HGSEHTVDGVKYSA
CA-II     RILNNGHAFNVEFDDSQDKAVLKGGPLDGTYRLEFQHFHWGSLDG-QGSEHTVDKKKYAA
CA-IX     RLRNNGHSVQLTLPGLEMK---L-GPGREYRALQLHLHWGAAGRP-GSEHTVEGHRFPA
CA-XII    LLTNNGHSVKLNLPSDMHIQ----GLQSRYSATQLHLHWGNPNDPHGSEHTVSGQHFAA
          : * * : . : : . . * * : * * * . . * * * * . : : *

CA-I      ELHVAHWNSAKYSSLAEAASKADGLAVIGVLMKVGE-ANPKLQKVLDAQAQIKTKGRAP
CA-II     ELHLVHWNT-KYGDFFGKAVQQPDGLAVLGIFLKVGS-AKPLQKVVLDLSIKTKGKSAD
CA-IX     EIHVHLSTK-YARVDEALGRPGGLAVLAAFLGEEPEENSAYEQLLSRLEEIAEEGSETQ
CA-XII    ELHIVHNSDLYPDASTASNKSEGLAVLAVLIEMGS-FNPSYDKIFSHLQHVYKYGQEAF
          * . * . * . : * * : * * * . : : * : : : . . * : : * . :

CA-I      FTNFDPSTLLPSSL-DFWYTPGSLTHPPLYESVTWIICKESISVSSEQLAQFRSLLSNVE
CA-II     FTNFDPRGLLPESL-DYWYTPGSLTTPPLLECVTWIVLKEPISVSSEQLKFRKLNFNGE
CA-IX     VPGLDISALLPSDFSRYFYEGSLTTPPCAQGVIIWTVFNQTVLSAKQLHTLSDTLWG--
CA-XII    VPGFNIEELLPERTAEYRYRGSLLTTPPCNPTVLWTVFRNPVQISQEQLLALETALYCTH
          . . : * * . : : * * * * * * * * : . : . : * * : :

CA-I      --GDNAVPMQHNNRPTQPLKGRTRASF-----
CA-II     --GEPEELMVDNWRPAQPLKNRQIKASF-----
CA-IX     ---PGDSRLQLNFRATQPLNGRVIEASFAGVDSRPR
CA-XII    MDDPSPREMINNFRQVQKFDERLVYTSFSQ-----
          : * * . * : . * : * *

```

Figure 11 Homologies between hCAI-II-IX and XII residues

The active site, approximately wide 12 Å and deep 15 Å, present the metal ion Zn(II) in a tetrahedral configuration, coordinated by three histidine residues, His94, His96 and His119, and a water molecule/hydroxide ion (Fig. 11); zinc-bound water binds by an

hydrogen bond the hydroxyl moiety of Thr199, that binds the carboxylate moiety of Glu 106.^{80, 82-85, 95} These interactions make the zinc-bound water molecule nucleophile, and facilitate the nucleophilic attack to the substrate CO₂ (**Fig. 12**).^{80, 82-84, 95}

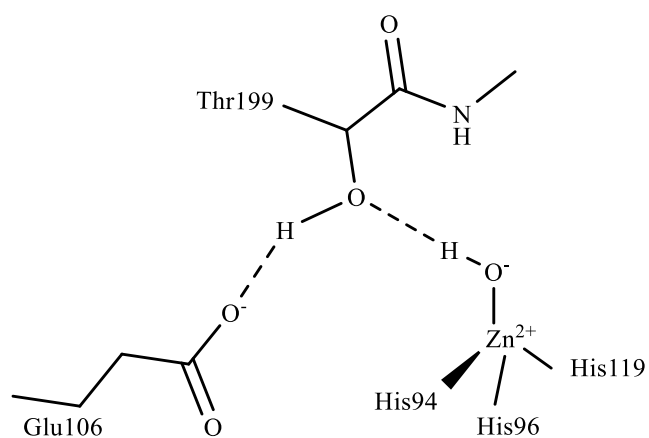


Figure 12 Zn²⁺ ion coordination⁸⁰

2.2 Carbonic Anhydrase IX E XII: physiological and pathological roles

Carbonic Anhydrase IX is a membrane-bound isozyme, in particular it is a glycoprotein that consists of an N-terminal proteoglycan domain, a CA domain, a single-pass transmembrane region, and a short intracellular tail.^{95, 101, 106-108} This enzyme forms a dimer, with an intermolecular disulfide bond between two Cys residues of the catalytic domains.¹⁰⁹ In normal conditions, the IX isoform is expressed in the epithelium of the stomach, bile duct, gallbladder duct, pancreatic duct, and in the rapidly-proliferating normal cells of small intestine^{107, 110} This isoform is strongly upregulated in different malignant and hypoxic tumor cells, such as breast, kidney, colon, ovarian, head-and-neck, pancreatic and lung tumor.^{95, 106, 107, 111}

Carbonic Anhydrase XII is also a membrane-bound isozyme, with a molecular mass of 40 kDa and a similar structure to CA IX: a N-terminal domain, a α -helical transmembrane region, and a C-terminal intracytoplasmic tail with two potential phosphorylation site, without the proteoglycan region domain present in CA IX.^{106, 108} This isoform form a dimer, with the active sites directed toward the extracellular environment. CA XII is expressed in different tissues in normal condition, like colon, kidney, prostate, endometrium, rectum, esophagus brain, pancreas, ovary, testis and sweat glands of skin.^{106, 112, 113} CA XII isozyme is overexpressed in several tumors like renal, breast, non-small cell lung cancer; both CA IX and XII are overexpressed in hypoxic tumor.^{32, 112, 113}

CA IX and XII are involved in pH homeostasis in tumor cells; they are potent biomarkers for patient prognosis and treatment resistance for different solid tumors.¹¹⁴⁻¹¹⁸ Both enzymes are essential for migration and invasion of tumor cells, and for metastases growth, but IX isoform have been studied more in depth with respect to the XII isoform.^{116, 119, 120} Indeed, several studies have shown that the pharmacological inhibition of both enzymes is related to the decrease of migration and invasion in different tumor cells. As a confirmation of that, the knockdown of CA IX in some breast cancer cells, with hypoxic condition, and other type of tumor, such as human fibrosarcomas, glioblastomas or ovarian cancer cells, reduce the migration and invasion of cells.^{121, 122} CA XI can generate invasive membrane retrusions and focal adhesion, necessary for tumor cell migration, thanks to interaction with integrins and ion exchange.^{119, 123} CA XII inhibits hedgehog pathway (Hh), involved in

tissue repair and homeostasis in healthy tissue, and in migration, survival and adaptation in tumor tissue with hypoxic environment and low pH.¹²⁴

The over-expression of CA IX and XII is connected to two different mechanisms: development of tumor phenotype that cause stress in microenvironment, and the loss of expression of *VHL* (von-Hippel Lindau) tumor suppressor gene.¹⁰⁸ Hypoxia caused by stress, is related to the expression of both CA IX and XII: the up-regulation of CA IX is directly connected to the transcriptional activation via HIF-1 complex; in normal condition ubiquitin-mediated proteolysis regulate the HIF-1, that afterwards is targeted by pVHL for destruction; *CA9* and *CA12* genes are induced by HIF-1.^{32, 125} *VHL* is a tumor suppressor gene with the role to stop the uncontrolled growth and proliferation of normal cells; if it is mutated or deleted, cells can grow uncontrolled, leading to defects in regulatory proteins and become cancerous.¹⁰⁸

Hypoxic tumor cells produce energy with glycolysis, but this process also generates pyruvate and lactate, two acidic byproducts. CA IX isoform is involved in pH regulation in tumor cells. It transfers protons from cytoplasm to extracellular environment, through the reversible hydration of CO₂, necessary for tumor cells survival.^{95, 107, 126, 127}

2.3 Inhibitors and activators of Carbonic Anhydrase

In the first step of the hydration, hydrophobic region, of the active site, sequesters the substrate, a carbon dioxide molecule, making available for the nucleophilic attack by Zn²⁺-bound hydroxide ion. This leads to the formation of bicarbonate, replaced from the active site, by a water molecule, positioned near the hydrophobic pocket, also known as “deep water”.^{89, 128, 129}



The rate limiting step consist in regeneration of catalytic active Zn²⁺ bound hydroxide ion: there is a proton transfer from Zn²⁺-bound water to a proton acceptor or to an active site residue.⁸⁶



For the α -CA class, in particular hCA II, the reaction occurs in presence of a solvent molecule with a pK_a =7, directly coordinated to Zn²⁺.⁷⁹

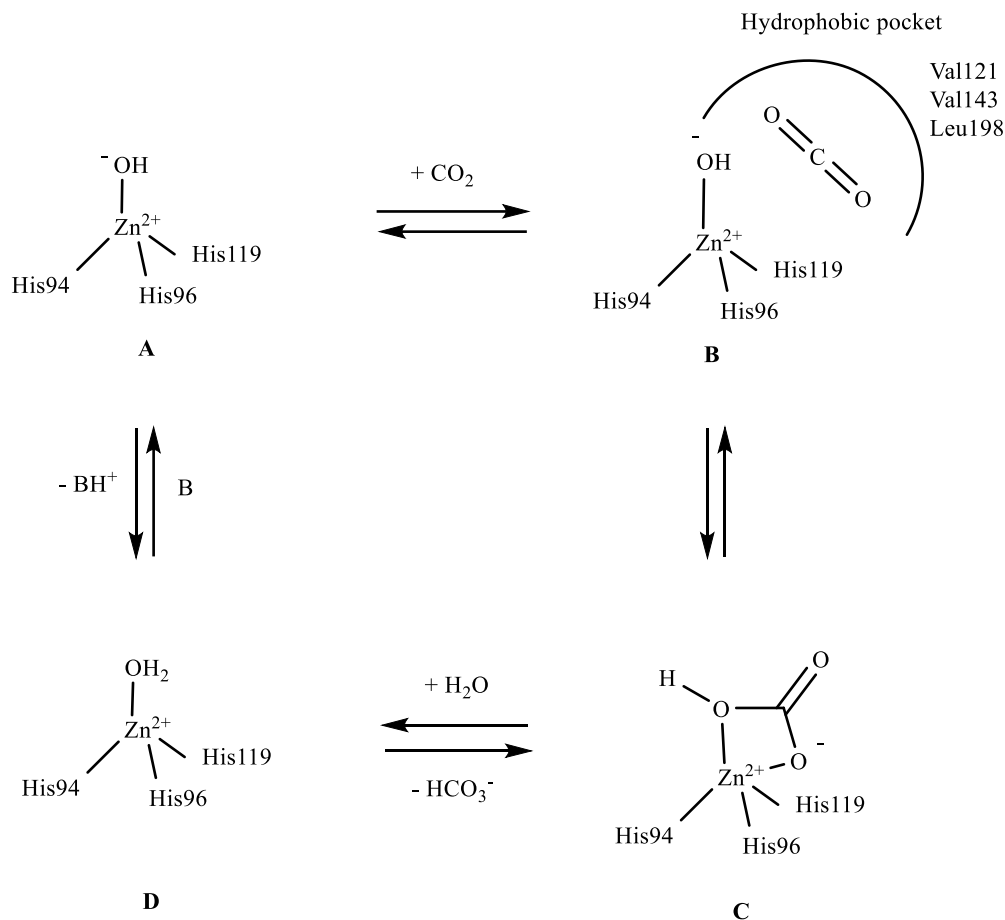


Figure 13 CO_2 hydration by α -CA II.⁸⁰

(13A) represented the active form of the enzyme, in which Zn(II) bound hydroxide; in this state, the enzyme attacks a CO_2 molecule bounding the hydrophobic pocket (in hCAII, the substrate binding site comprises Val121, Val143 and Leu198 residues) (13B), with the formation of bicarbonate coordinate to Zn(II), like shows in 13C. A water molecule replace the bicarbonate, inducing the formation of the acid and inactive form of the enzyme (Fig. 13D), in which a water molecule bound the Zn(II).^{80, 82-84, 95} The last reaction is a proton transfer from the active site, usually this reaction is assisted by an active site residues like His64 or buffers present in the environment; the regeneration of active form the enzyme occurs according to this mechanism.⁸⁸

Several compound can inhibit Carbonic Anhydrases. In particular three separate class of CAIs (CA inhibitors) can be distinguished:

- Compound that binds directly the metal ion, characterized by the presence of a typical zinc-binding group (ZBG);

- Molecules that incorporate into their structures, an anchoring group (AG), a hydrogen bonded to the metal ion coordinate nucleophile, maintaining the structural features and the variable tail as the zinc binders;
 - Compounds with a suicide inhibition mechanism.
- **CAIs with zinc-binding group**

The compound that directly binds the Zn(II) are divided in two separate classes: metal complexing anions, that substitute the water molecule binding Zn(II), and sulfonamide which can bind the Zn(II) ion; they can bind the metal in two different ways, addition to the metal coordination sphere, developing trigonal-bipyramidal species (**A**), or by substitution of non-protein zinc ligand (**B**).^{98, 130-132}

Anionic inhibitors, like thiocyanate, interact with CA in a very simple way, making a trigonal-bipyramidal adduct (**Fig. 14A**).⁹⁸

Fig. 14B shows the interaction between the enzyme and a sulfonamide: there are several hydrogen bonds that involve the NH₂ and OH groups of the Thr199 and Glu106. Furthermore, the skeleton of the inhibitor (R) interacts with hydrophilic and hydrophobic residues of the active site, leading to the formation of a tetrahedral geometry.^{96, 98}

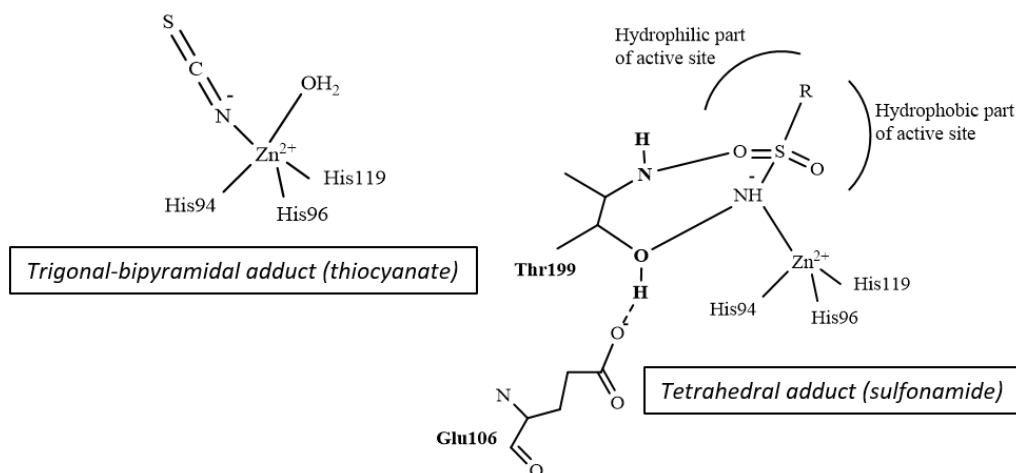


Figure 14 A: Trigonal-bipyramidal adduct; **B:** Tetrahedral adduct⁹⁸

This CAIs present a scaffold that interact with hydrophobic and/or hydrophilic region of the cavity, and a tail that can interact with other parts of the enzyme.⁸⁹

Sulfonamides are the most clinically used ZBG based inhibitors: acetazolamide, methazolamide, ethoxzolamide, sulthiamide, dichlorophenamide, dorzolamide,

brinzolamide, sulpiride, zonisamide, topiramate, saccharin, celecoxib, chlorothiazide derivatives, including hydrochlorothiazide, furosemide, bumethanide; they are used as diuretics, antiglaucoma agents, antiepileptic drugs in clinic since several years (**Fig. 16**).¹³³

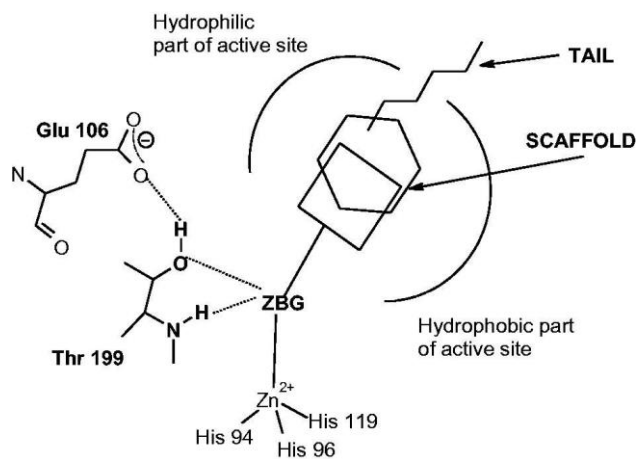


Figure 15 Example of Carbonic Anhydrase Inhibitor with Zinc-binding group¹³³

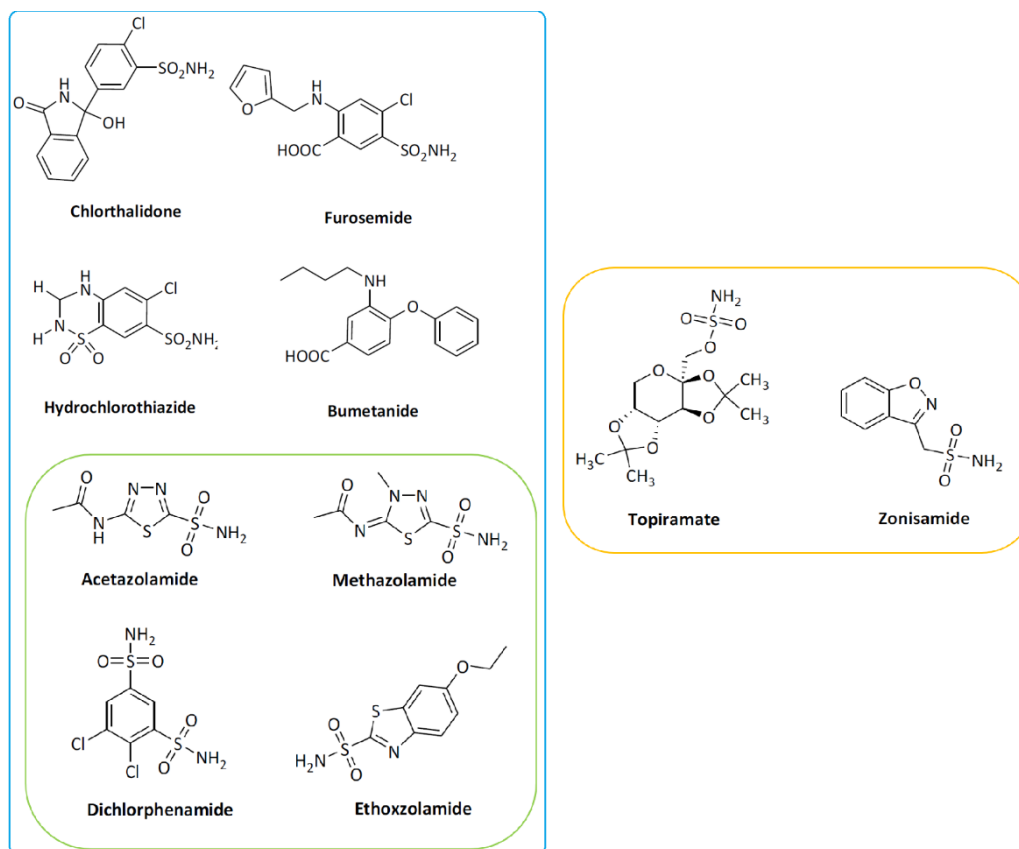


Figure 16 Sulphonamides: in the blue area the sulphonamides derivatives used as diuretics, in detail the green area contains sulfonamides that are used also like antiglaucoma drugs, and the orange are anticonvulsant

- **CAIs with an anchoring group**

CA inhibitors with the AG, anchor to the metal coordinated water molecule/hydroxide ion, with hydrogen bonds: one with zinc-bound water molecule/hydroxide ion, and the other with the OH of the “gate-keeping residues”.⁸⁹

This class of inhibitors contain chemical families like phenols, polyamines, esters and thioxocoumarins.¹³³

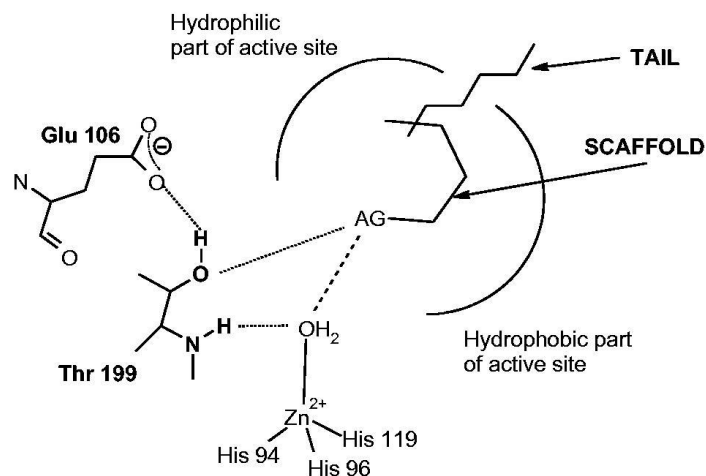


Figure 17 Example of Carbonic Anhydrase Inhibitor with anchoring-group¹³³

- **CAIs with suicide mechanism**

These molecules act with a suicide like inhibition mechanism: they partially occlude the entrance of the active site; most of CAIs that act in this way are coumarins.^{134, 135}

Coumarins act like prodrugs, moreover the real inhibitors are their hydrolysis products: esterase CA activity opens the lactone ring of the coumarin, creating these products, that remain bound to the entrance of cavity with many hydrophobic and polar interaction, occluding it (**Fig. 18**).¹³⁵

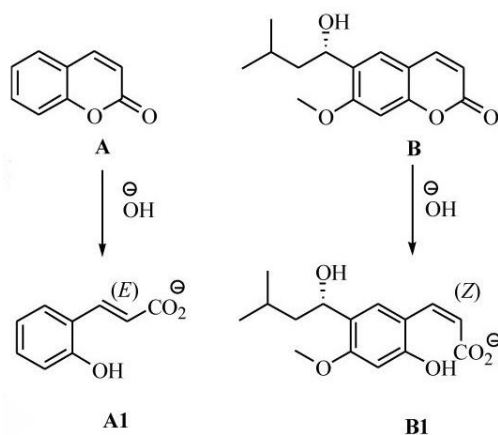


Figure 18 Hydrolysis product by esterase activity of CA enzyme¹³⁵

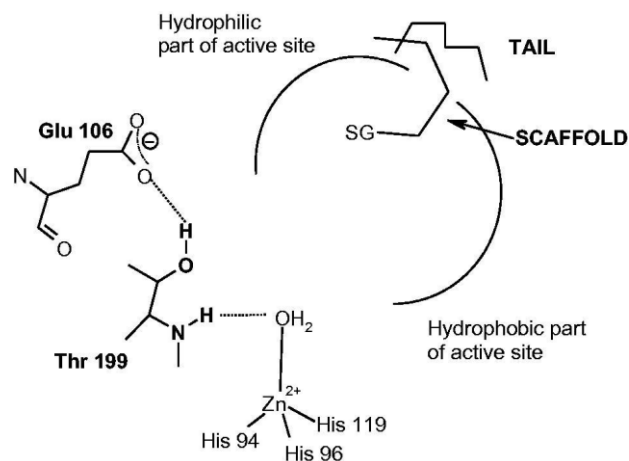


Figure 19 Example of Carbonic Anhydrase Inhibitor occluding active site entrance¹³³

- **CAIs with a sticky group**

This class of inhibitors has a sticky group (SG), such as OH, amino, COOH and other (**Fig. 20**).

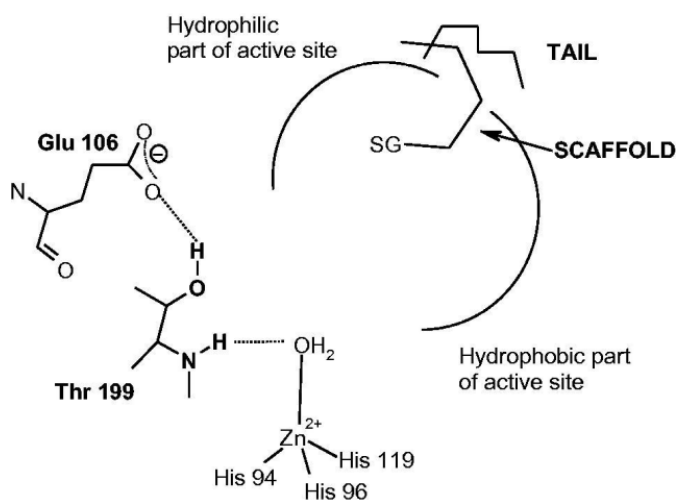


Figure 20 Example of CAI with SG¹³³

The last CA inhibitor class was recently discovered by means of X-ray crystallography: benzoic acid derivative can bind a hydrophobic pocket situated near and yet out the active site of the enzymes. They act blocking His64, the proton shuttle residue, in its out conformation.^{133, 136}

CYCLOXYGENASE

3.1 Cyclooxygenase: overview

Cyclooxygenases (COX), also known as prostaglandin-endoperoxide synthase (PTGS), are a family of enzymes present in two different isoforms: COX-1 and COX-2; lately COX-3, a splice variant of COX-1 usually known as COX1b or COX-1 variant, has been identified.¹³⁷⁻¹⁴⁰ They are membrane-bound heme-containing bifunctional glycoproteins with two different activities: peroxidase and prostaglandin synthase.¹⁴¹ They are involved in the conversion of arachidonic acid to prostanoids: prostaglandins (PGs) and thromboxanes (TxS).^{142, 143} More specifically they catalyze the double dioxygenation of arachidonic acid leading to prostaglandin G₂ (PGG₂), followed by the reduction of PGG₂ to prostaglandin H₂ (PGH₂).¹⁴⁴ Both isoform COX-1 and COX-2 have a cyclooxygenase active site, a hydrophobic channel with four amphipathic helices of the membrane binding domain in the entrance of the cavity where the conversion of arachidonic acid is performed.¹⁴⁵ These enzymes also contain a peroxidase active site, a globular catalytic domain with two intertwining lobes that create a fissure on the surface of the enzyme where heme is located.¹⁴⁵ For the first reaction, two molecules of O₂ are incorporated in arachidonic acid to obtain PGG₂ that move in the peroxidase active side, where it is reduced to PGH₂; subsequently, PGH₂ can be converted to different prostaglandins and thromboxane A₂ (TxA₂) by cell specific synthases (Fig. 21).¹⁴⁴

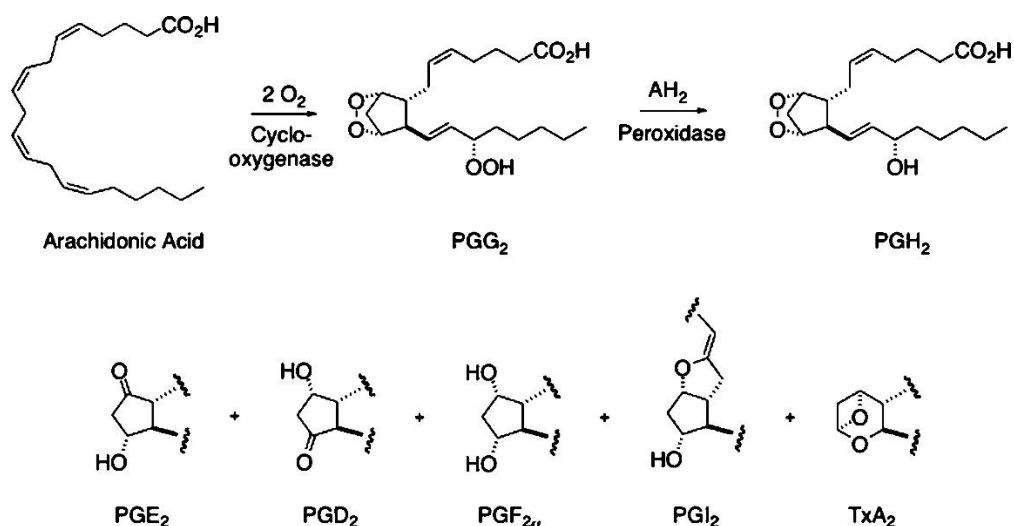


Figure 21 COX functions: peroxidase and prostaglandin synthase¹⁴⁴

COX-1 and COX-2 are encoded by two separate genes and have different amino acid sequences. However, both of the enzymes are homodimers, and need dimerization for their catalytic activity.

COX-1 isozyme is a housekeeping enzyme, usually expressed in several tissues like kidney, stomach, intestine, colon; it is important to preserve basal prostaglandin levels in tissues.³ COX-2 is expressed in normal cells at low levels, it has functions in brain, kidney and cardiovascular system; however it is mostly an inducible enzyme and its production is promoted by cytokines, mitogens, endotoxin, and tumor promoters; this isozyme produces prostaglandins during inflammatory and tumorigenesis (**Fig. 22**).^{3, 146-148}

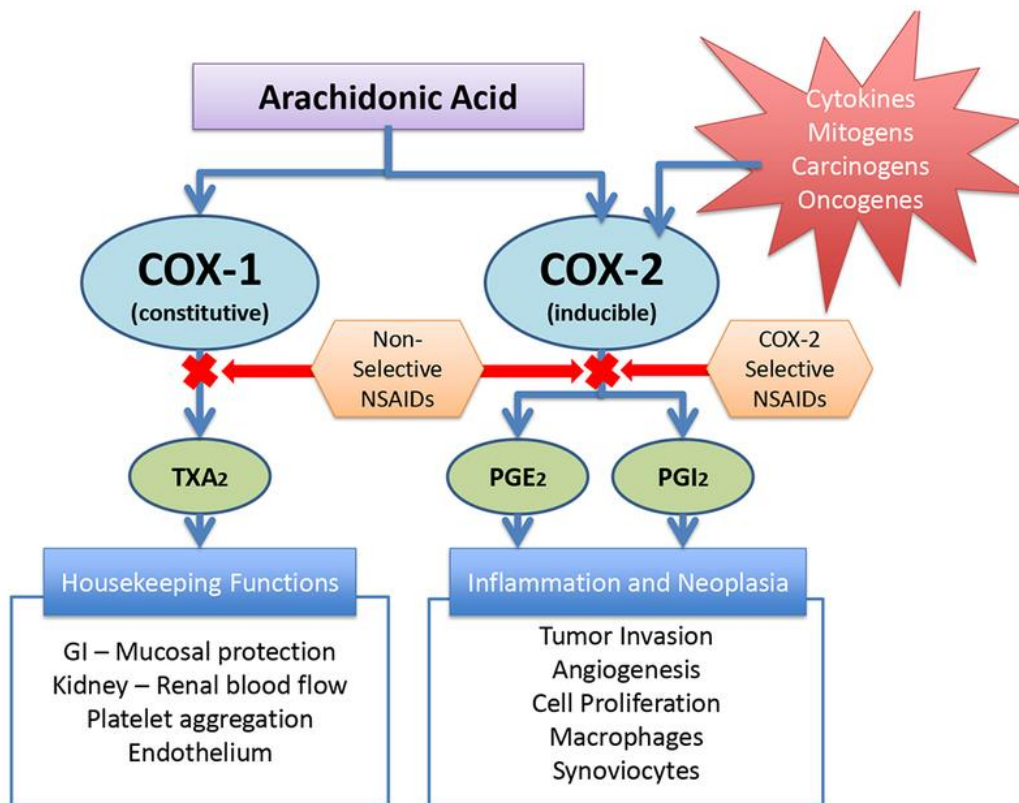


Figure 22 COX biosynthesis and function¹⁴⁸

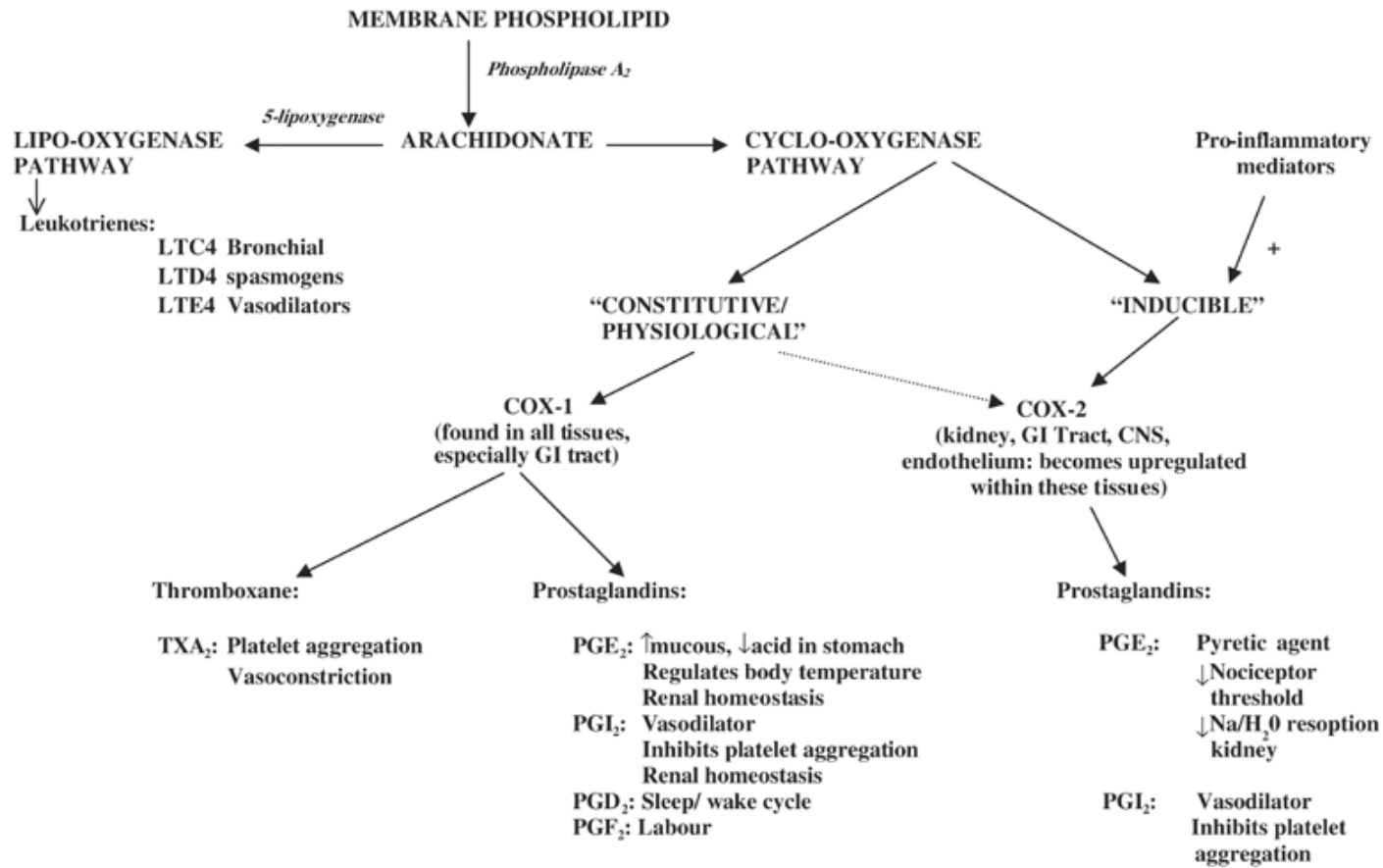


Figure 23 Role of COX-1 and COX-2¹⁴⁹

Prostaglandins are located in different human tissues; they are important for inflammation and regulate physiological response: blood clotting, ovulation, initiation of labor, bone metabolism, nerve growth and development, wound healing, kidney function, blood vessel tone, and immune responses.¹⁵⁰

COX-1 isozymes are necessary to supply precursors for thromboxane synthesis for platelet aggregation; in the vascular endothelium platelets release eicosanoids necessary for prostacyclin (PGI₂) production, molecules necessary for vasodilatation stimulation, to contrast the vasoconstrictor effects by thromboxanes. COX-1 is also present in kidney and stomach. After changes in blood flow, like lowered blood volume, angiotensin is released by the kidney to stimulate vasodilating PGs synthesis by kidney. Thus, COX-1 is necessary to PGs homeostasis and to PGs levels.¹⁵⁰

Fig. 24 shows the differences between the two enzymatic pockets of COX1 and COX2 enzyme. Position 522 of enzymatic pocket of COX-1, is occupied by a residue of isoleucine, in COX-2, this residue is displaced by a valine in position 523: this modify confers selectivity to COX-2 inhibitors.¹⁵¹

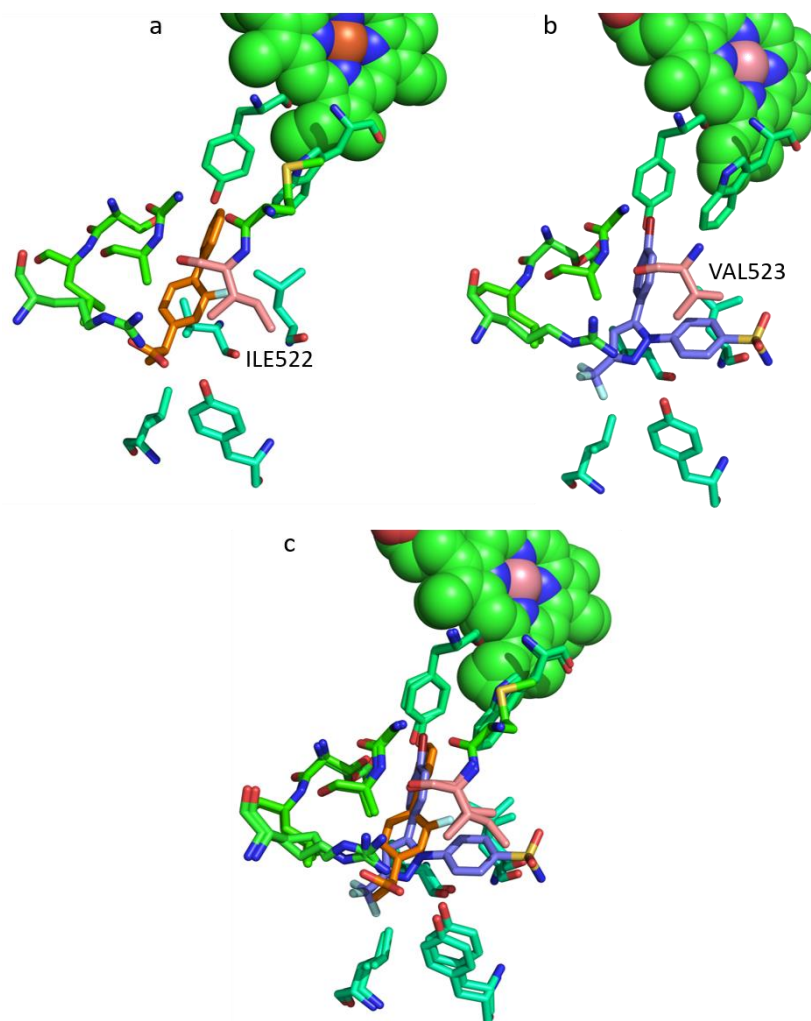


Figure 24 Differences on enzymatic pocket of COX-1 and COX-2. a) Enzymatic pocket of COX-1; with the inhibitor flurbiprofen b) Enzymatic pocket of COX-2 with co-crystallized compound S58 similar to Celecoxib; c) Superimposition of enzymatic task of both isoforms.

3.2 Cyclooxygenase-2: physiological and pathological roles

Cyclooxygenase-2 is overexpressed in many tumors and its expression can be induced by somatic mutations that continually activate stimuli: it can be also induced by cytokines and inflammatory mediators during an inflammation state; with increase of prostanoids synthesis tyrosine kinase, protein kinase C and several transcription factors can converge in MAPK pathway (mitogen activated protein kinase), involved in inflammatory genes transcription.¹⁴³ Its expression can be regulated during transcription, post-transcription, or post-translation. COX-2 contribute to get worse the inflammatory conditions, causing cancer, respiratory disorders, Alzheimer and other diseases.^{42, 143, 152}

Cyclooxygenase-2 concurs to tumorigenesis with prostaglandins synthesis, in particular PGE₂ have an important role in inflammation and in tumor progression.¹⁵³ PGE₂ act at different levels to induce tumorigenesis. It upregulates proto-oncogene Bcl-2, a suppressor of apoptosis, resulting in a longer life for tumor cells.¹⁵⁴ Moreover, prostaglandins E2 interact with MAPK-PI3K-AKT and NF-κB (Nuclear Factor kappa-light-chain-enhancer of activated B cells) pathways, that control DNA transcription, cytokine production, cell survival; they induce transcription of other factors that lead with tumorigenesis like vascular endothelial growth factor (VEGF), a protein that stimulate new blood vessels growth, responsible for angiogenesis.¹⁵⁵ PGE₂ is responsible of metastasis: by upregulation of two matrix metalloproteinases MMP2 and MMP9 and IL-11 (interleukin 11); they are also responsible of tumor growth by epidermal growth factor receptor (EGFR) upregulation.^{154, 156} PGE₂ can also regulate cancer cell invasion by ERK (extracellular signal-regulated kinase)¹⁵⁷

COX-2 induce Bcl-2 (B-cell lymphoma 2), an important member of a regulator proteins family that regulate cell death, inhibiting or inducing the apoptosis process, through the prostaglandin E₂; in this way, COX-2 protecting tumor cells from apoptosis.^{158, 159}

Lifestyle factors, like high-fat diet and tobacco, in association with genetic, and epigenetic alteration, supply to deregulation of COX pathway in chronic inflammation and subsequently in cancer.³³ The deregulation include the overexpression of receptor-mediated activity of prostaglandin E₂ respect to others PG (**Fig. 25**).³³

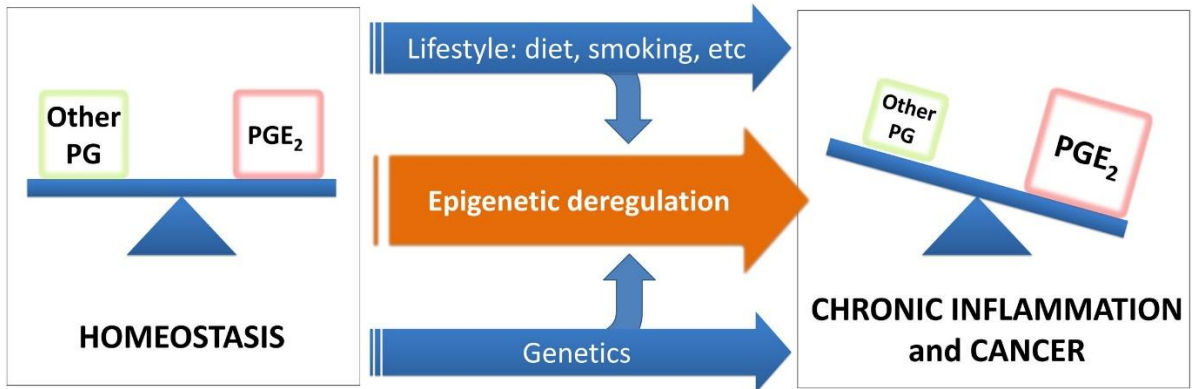


Figure 25 Deregulation of COX pathway³³

3.3 Inhibitors and activators of Cyclooxygenase-2

COX-2 isoform can be induced by several extracellular and intracellular factors, such as Lipopolysaccharide, interleukin-1, tumor necrosis factor, epidermal growth factor and transforming growth factor- α (TGF- α).¹⁶⁰ Furthermore, overexpression of COX-2 and PG due to growth factors is typically observed in tumors, promoting survival of cancer cells, and to tumor progression.¹⁶¹ Several carcinogenic agents induce the expression of COX-2 isoform, like tobacco smoke, UV radiation, polyunsaturated fatty acids, microbial agents and inflammatory cytokines.¹⁶²⁻¹⁶⁸

Overexpression of cyclooxygenase-2 and prostaglandins contribute to mutagenesis, mitogenesis, angiogenesis and metastasis, all important factors for the carcinogenesis; by inhibiting the enzyme, and arresting the prostaglandin cascade, it may be possible to reduce neoplastic growth and cancer development.¹⁶⁹⁻¹⁷³

COX inhibitors are subdivided in two major class, based to their selectivity toward the two isoforms: the nonsteroidal anti-inflammatory drugs (NSAIDs), and the selective COX-2 inhibitors (COXIBs).^{174, 175} NSAIDs are the most known inhibitors of both COX-1 and COX-2: they act by competitive binding to both the isozymes.¹⁷⁴ The smaller NSAIDs bind the pocket in the activation site of both enzymes, conversely, the bulkier COX-2 inhibitors are more specific toward the binding pocket of the COX-2 isozyme.¹⁷⁵ Different studies have demonstrated that the regular consumption of NSAIDs decrease the risk of cancer; however, their use leads to the emergence of gastrointestinal problems, mainly due to the inhibition of the constitutive COX-1 isoform.^{33, 176-178}

Celecoxib belongs to the class of COXIBs, it was developed for the treatment of rheumatoid arthritis and osteoarthritis, however it is currently used as an anti-inflammatory agent for different chronic inflammation, and has demonstrated to possess potential anticancer properties.¹⁷⁹⁻¹⁸¹ Celecoxib is a diaryl-substituted pyrazole compound (**Fig. 26**). COX-2 inhibition by celecoxib, is an efficient treatment for different type of tumor, including the lung and colorectal cancer, skin malignancy, mammary carcinoma breast cancer and hepatic carcinoma; several studies have demonstrated that the inhibitor decrease the incidence of colorectal cancer.¹⁸²⁻¹⁸⁴

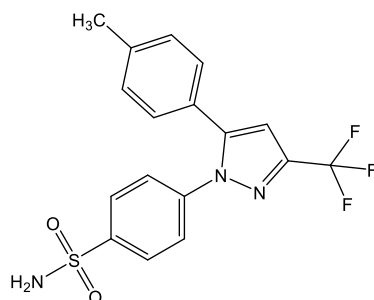


Figure 26 Celecoxib

Valdecoxib is also a COXIB selective COX-2 inhibitor, that reduce the production of prostaglandin E2 and I2; it was approved by FDA (Food and Drug Administration) in 2001.¹⁸⁵ It is a diaryl-substituted isoxazole, with a structure similar to celecoxib (**Fig. 27**).¹⁸⁶ This drug was discovered with the purpose to decrease the side effects of NSAIDs and maintaining the anti-inflammatory role; moreover it is used in the rheumatological practice for its gastrointestinal tolerability.¹⁸⁵ Valdecoxib acts entering in the hydrophobic channel of the enzyme, to block the entry of fatty acids.¹⁸⁵

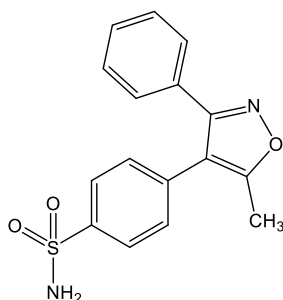


Figure 27 Valdecoxib

Rofecoxib belong to COXIB class, and, as its congeners, is a selective inhibitor of COX-2, developed for osteoarthritis and acute pain.¹⁸⁷ Rofecoxib is a methyl sulphonyl phenyl derivative (**Fig. 28**). This inhibitor can decrease the risk of colorectal cancer, but its use is associated with cardiovascular risk.¹⁸⁸

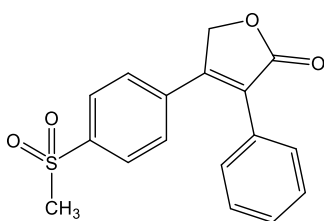


Figure 28 Rofecoxib

KINASES

4.1 Kinases: overview

Protein kinases are the major enzyme superfamily implicated in cell signal transduction.¹⁸⁹ They catalyze the protein phosphorylation; more specifically the transfer of the gamma-phosphoryl group of an ATP molecule, to a tyrosine, threonine or serine residues in the target protein. The activated protein could be deactivated through the reverse reaction performed by a protein phosphatases, these enzyme catalyze the protein dephosphorylation through the hydrolysis of the phosphate group from the substrate.¹⁸⁹ The phosphorylation/dephosphorylation process has an important role in the regulation of several biological function.¹⁹⁰

Protein kinase act as a template for the substrate, namely the molecule of ATP and the tyrosine/serine/threonine protein, inducing the transfer of a phosphoryl group from the first substrate (ATP), to the side chain hydroxyl of the protein.¹⁹¹ The transferring process can be divided in two different transition states, associative and dissociative (**Fig. 29**). In the associative transition state, the attacking oxygen create a bond with the reactive phosphorus atom while the bond between ADP and the phosphoryl group steel exist; in this state there is a tetrahedral intermediate.¹⁸⁹ In the dissociative transition state there is a nucleophilic attack from hydroxyl group followed by the detachment of the leaving group in a way similar to the SN1 reaction.^{189, 192}

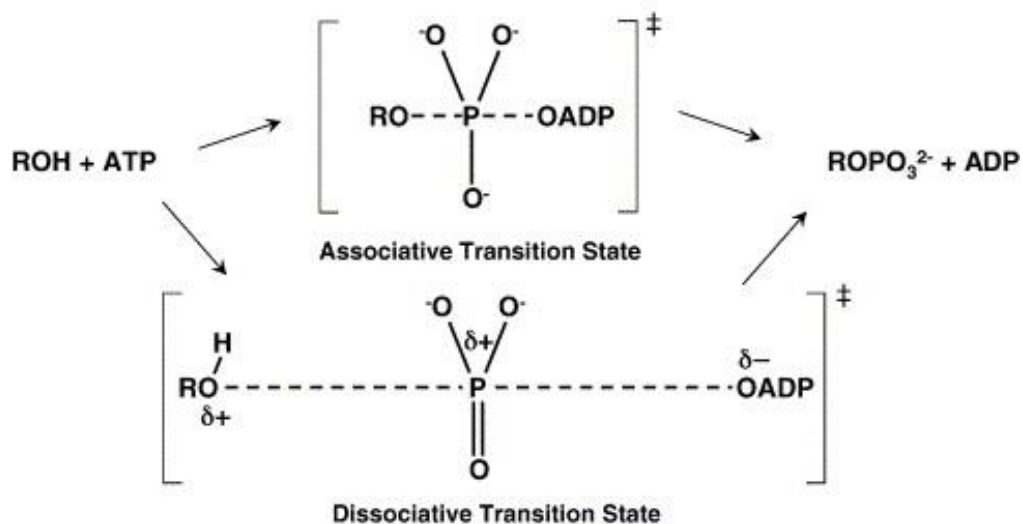


Figure 29 Associative and dissociative transfer of phosphoryl group, by protein kinase¹⁸⁹

The catalytic domain, also called kinase domain, is formed by two subdomains: the N-terminal lobe with five β -strands and one critical α -helix, and the C-terminal lobe,

constituted by α -helix; between these two subdomain, there is a peptide strand with a cleft that constitute the active site (**Fig. 30**).¹⁹⁰ The cleft has two pockets: the front pocket with the residues implicated in catalysis or ATP binding, and the back hydrophobic pocket for regulatory functions.^{193, 194}

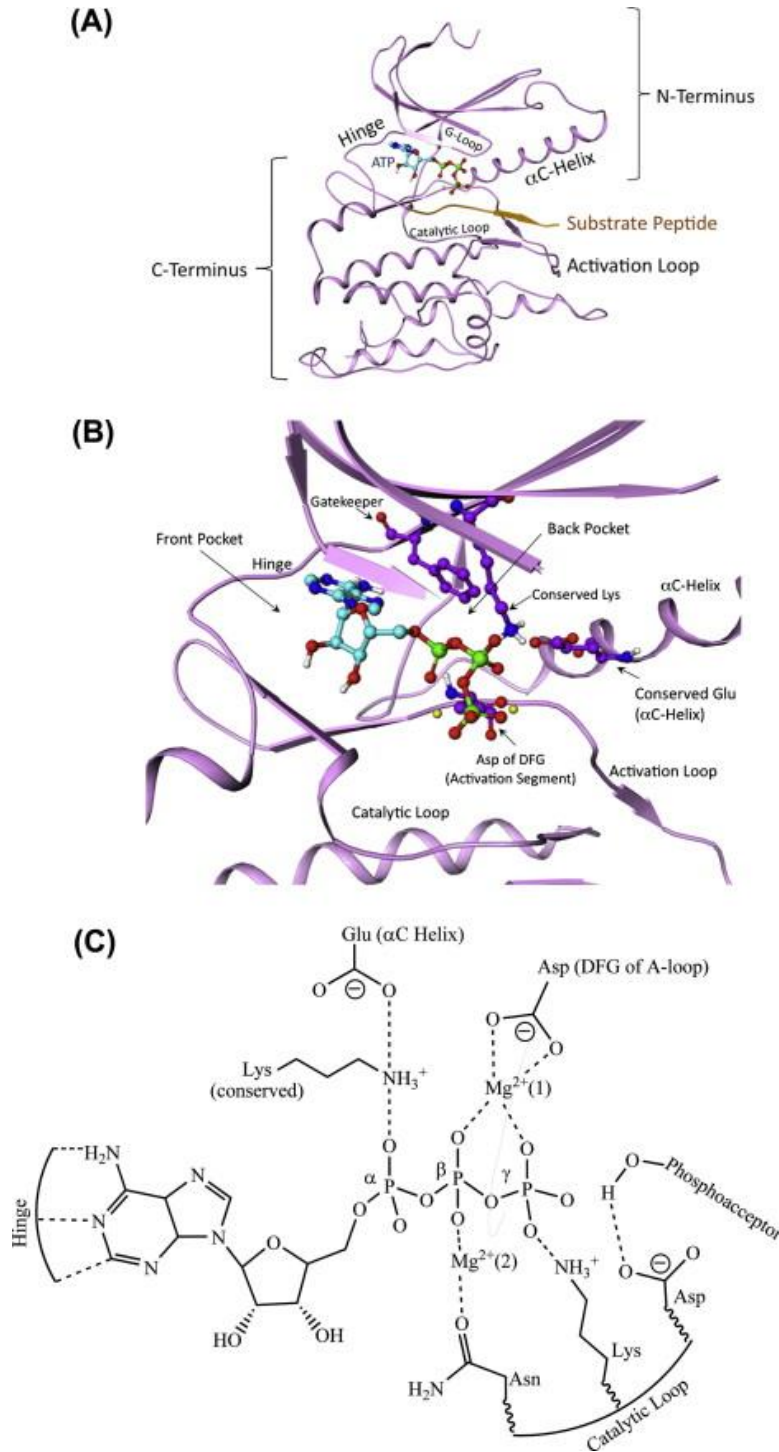


Figure 30 Protein kinase: A) Phosphorylase kinase bonding an ATP and a peptide substrate; B) Phosphorylase kinase catalytic region; C) Molecular contacts between substrates.¹⁹⁰

The superfamily of kinase, can be divided in two fundamental classes, based on the substrate specificity: the serine/threonine-specific, and the tyrosine-specific.¹⁹⁵

Protein tyrosine kinases (TKs) belong to the superfamily of protein kinases and have the role to transfer the γ -phosphate group from ATP to a tyrosine residue of other proteins, resulting in a conformational change, required for the protein functions. This reaction is cellular key strategy, to communicate between cells, regulate cellular specific activities such as the cell division and proliferation.

Receptor tyrosine kinases (RTKs) are transmembrane glycoproteins, that once activated by specific ligands, transduce the extracellular signal to cytoplasm through phosphorylation of tyrosine residues in receptors and on downstream signaling proteins. RTKs include different family.¹⁹⁶ The non-receptors tyrosine kinases (NRTKs) participate to the signaling cascades triggered by RTKs and other cell surface like G-proteins coupled receptors; Src and Abl belong to this big family.¹⁸⁹

Bcr-Abl and c-Src are two cytoplasmatic TKs, in particular Src belong to a Src family of kinases (SFKs); these enzymes show high structural homology within their catalytic domains⁶⁹

Src

Proteins belonging to SFKs family, have a N-terminal domain (SH4), a unique region, two Src homology domains (SH2 and SH3), a polyproline type II domain (SH1), responsible for TK activity, and a short C-terminal tail.⁶⁹ The regulation of SFKs activity is located in the SH2 and SH3 domains; SH2 have a β -sheet and two single helix packed to form two pockets.¹⁹⁷ The N-terminal lobe contain a glycine-rich G-loop, necessary for binding the γ -phosphate of ATP; C-terminal lobe contains the positive regulatory activation loop (A-loop) with Tyr-419, and The C.-terminal tail have the Tyr-530 residue, important for the negative regulation.¹⁹⁸ The two tyrosine residues present in the C-terminal lobe and tail, are responsible for the Src different conformations: the closed conformation, when the enzyme is in the inactive form, and the open conformation, when it is in the active form ; these two residues being phosphorylated in active state, and dephosphorylated while in the inactive state.⁶⁹

Src have two different regulatory tyrosine phosphorylation sites: one in the C-terminal tail, necessary to repress the activity. In fact, with the truncation of the C-terminal portion, the

enzyme is constitutively active, and the result is an uncontrolled growth of the cells. The second tyrosine is located in the activation loop and is an autophosphorylation site. The mutation of this tyrosine residue lead to an activation of the enzyme.^{199, 200}

c-Abl

c-Abl protein consists of a N-terminal, SH3 and SH2 domains, SH2-kinase linker, SH1 Catalytic domain, and a long C-terminal region.⁶⁹ SH1, SH2 and SH3 have high homology with those of Src. As observed in the case of Src, Abl can exist in two different conformations: the closed and inactive form, and the open, active form.⁶⁹ The N-terminal cap region is necessary for the formation of the inactive form of the enzyme: c-Abl proteins lacking this region, are mutated into a oncogenic, constitutively activated protein.²⁰¹ SH3 domain is necessary for the repression of the enzyme activity, a mutation of SH3 can constitutively activate the kinase, thus leading to cellular transformation.²⁰²

4.2 c-Src and Bcr-Abl: physiological and pathological roles

Bcr-Abl and c-Src are involved in the development of malignant tumor.⁶⁹ More specific, Bcr-Abl is responsible for the chronic myeloid leukemia (CML); Src is involved in the regulation of multiple signal transduction pathways for the cellular growth, proliferation, differentiation, migration, but also metabolism and apoptosis. Moreover, both proteins participate in different signaling processes like mitogenesis, T- and B- cells activation, and cytoskeleton restructuring.^{69, 196, 203}

Src is physiologically activated during several cellular events. Conversely, in solid tumor cells, it is overexpressed and hyper-activated. For this reason, it has an important role in the development of metastatic cancer phenotypes; Src is also implicated in several human carcinomas, such as breast, lung and colon cancer^{186, 204, 205}

SFKs are also involved in the proliferation of cells expressing Bcr-Abl.²⁰⁶

Src can be activated by several extracellular molecules, like growth factor receptors, integrins G-protein-coupled receptors (GPCRs), cytokine receptors, and many others. After its activation, the enzyme phosphorylates different targets to regulate multiple signal transduction pathways such as PI3K/Akt (Fig. 31).²⁰⁷

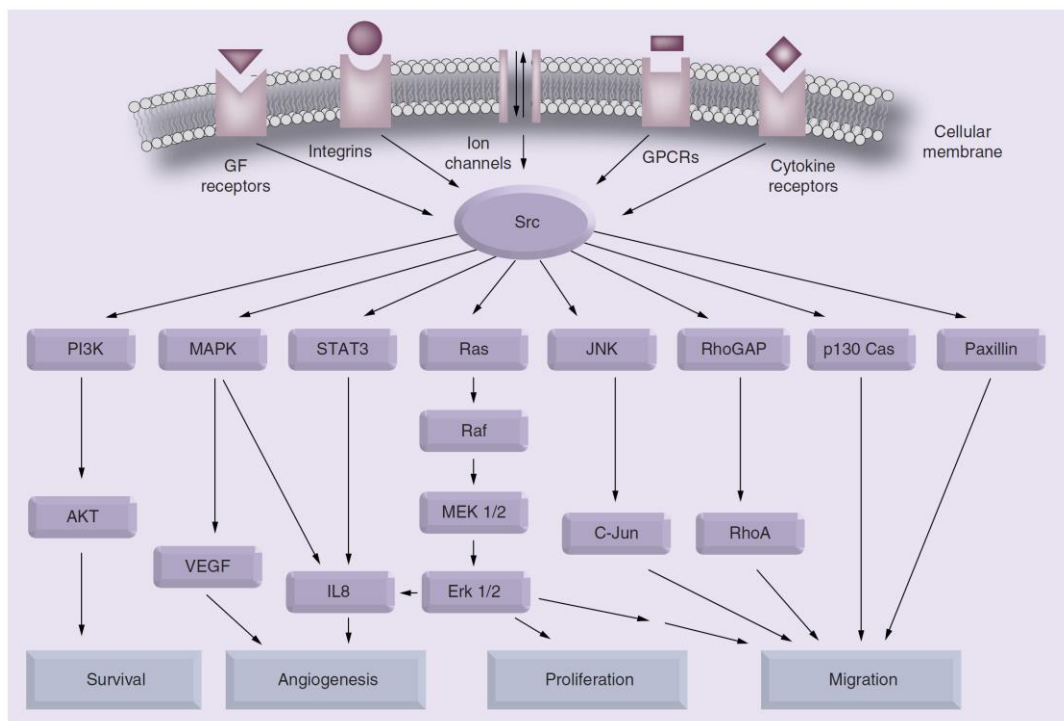


Figure 31 Src signaling pathways⁶⁹

Abl can be activated by phosphorylation of Tyr residue by PDGF and Src or by trans-phosphorylation.⁶⁹ With its activation, Abl can phosphorylate different substrates involved in signal transduction, like PI3K, Ras, paxillin and FAK (focal adhesion kinase).^{207, 208}

4.3 Inhibitors and activators of c-Src and Bcr-Abl

Having Abl and Src high structural homology, different inhibitors developed for Src exhibited inhibition also for Abl.⁶⁹

The most common dual Src/Abl inhibitors used in therapy are type I inhibitors targeting ATP-binding site in the active conformation mimicking the interaction of the adenine moiety of ATP.⁶⁹ The ATP-binding site is divided in subregions that are shown in **Fig. 32**: hydrophobic region I and II, ribose region, and phosphate-binding region.^{209, 210} The potency and selectivity of small molecules inhibitors mostly depends on the hydrophobic region I. In the entrance of the pocket there is a specific amino acid, called the gatekeeper, specific for Abl and for Src, Thr315 and Thr388 respectively: The mutation of the gatekeeper T315I in Abl is responsible for enzymatic resistance to inhibitors.²¹¹⁻²¹³ Dasatinib, a thiazole-carboxamide derivative, is one of this dual inhibitors Src/Abl, and it is used for the therapy of imatinib-resistant CML.⁶⁹ Bosutinib belonging to type I inhibitors is a 7-alkoxy-3-quinolinecarbonitrile derivative; with this inhibitors the proliferation of imatinib resistance tumor cells decreases with the exception of the T315I mutation.²¹⁴

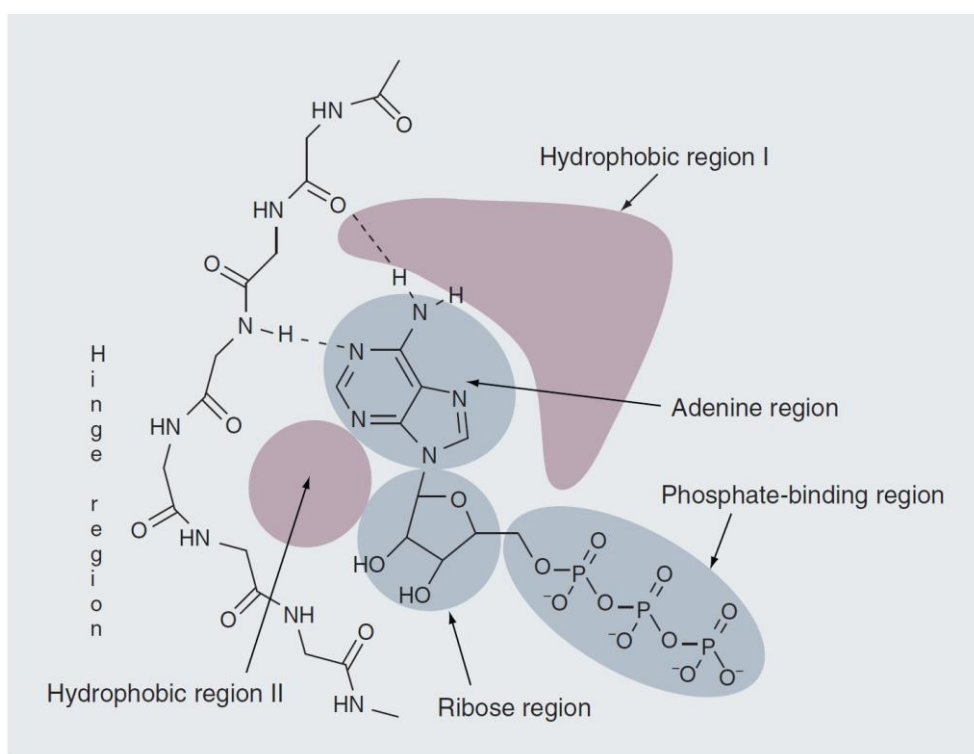


Figure 32 Details of ATP-binding site⁶⁹

Type II inhibitors were only used to target Abl. Imatinib, a milestone in the development history of kinase inhibitors, is a type II inhibitor. It is a Bcr-Abl ATP-competitive inhibitor approved for CML therapy, like nilotinib.⁶⁹ Both these inhibitors target the ATP-binding site when the enzyme is in the closed conformation. The new dual inhibitors of Bcr-Abl and Src, can bind both the ATP-binding site and the SH3 domain.⁶⁹

Type III inhibitors are allosteric, they inhibit the enzyme activity by binding a site remote from the active one. They are used in the presence of resistance mutation to the first generation ATP-competitive inhibitors.²¹⁵

PP1 and PP2 are pyrazolo[3,4-*d*]pyrimidines, they are the first dual inhibition, discovered as specific inhibitors for SFK members. Their activity towards Abl was later revealed.²¹⁶

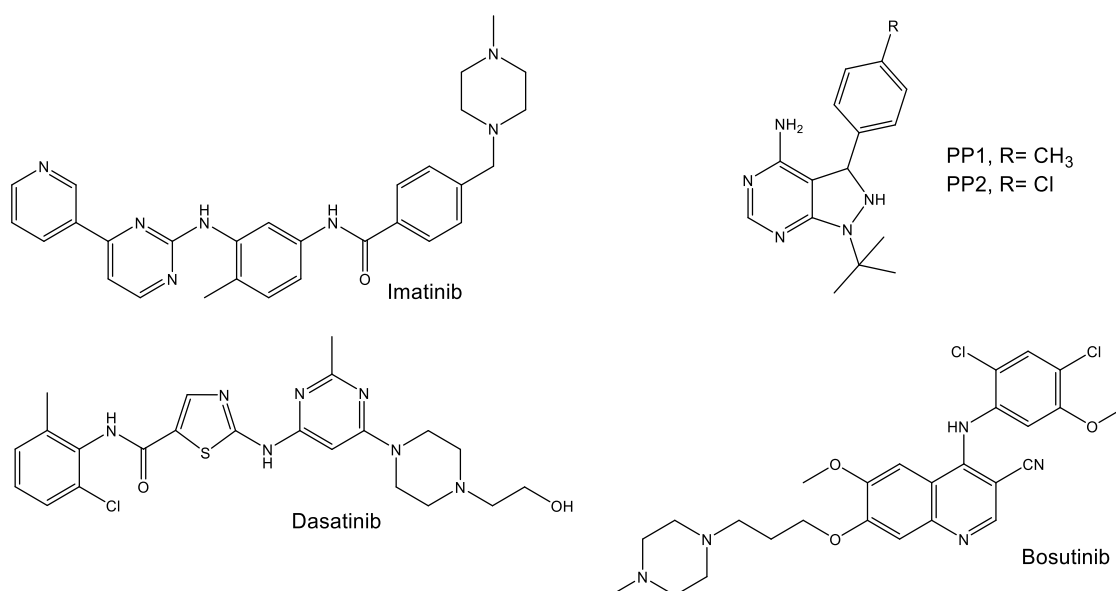


Figure 33 Abl inhibitor Imatinib, and dual Src/Abl inhibitors: Dasatinib, PP1 and PP2, and Bosutinib

Ponatinib is a specific inhibitor of Bcr-Abl T315I. More in detail it is an ATP-competitive inhibitor, and it has been recently approved for the treatment of resistant CML form, but it has several side effects (**Fig.45**).²¹⁷ Atixinib is another ATP-competitive inhibitor for Bcr-Abl T315I, developed by Pfizer and it is a promising candidate for the CML resistant form (**Fig.34**).²¹⁸

In the last few years have been discovered some classes of allosteric inhibitors active towards T315I mutant (**Fig.34**).^{218, 219} Among these drugs, DCC-2036 is a promising candidate that binds the motif used by Abl to switch from the inactive to the active conformation; Other candidates are GNF-2 and GNF-5 that are active towards T315I Bcr-

Abl mutant only in cooperation with I and II generation of ATP-competitive inhibitors (like Imatinib and Dasatinib) (**Fig.35**).^{220, 221}

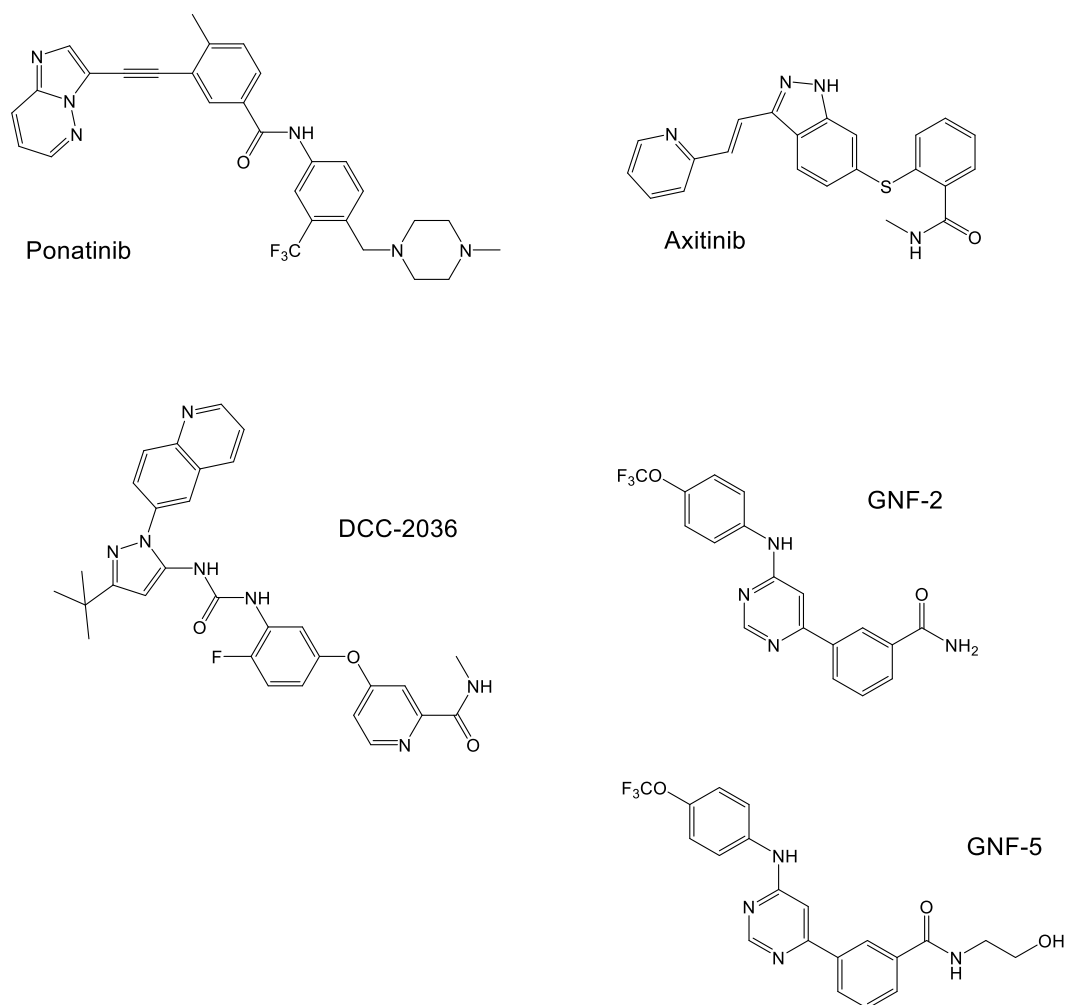


Figure 34 ATP-competitive and allosteric Bcr-Abl T315I inhibitors

PROJECTS

5.1 Selective inhibition of carbonic anhydrase IX and XII by coumarin and psoralen derivatives

5.1.1 Background

Carbonic anhydrases IX and XII allow the proliferation and invasion of cancer cells, they are necessary for the tumor survival and the malignancy.

Several studies demonstrated that synthetic and natural coumarin derivatives possess high selectivity and activity toward specific hCA isoforms, and they are also able to interact and inhibit others tumoral targets, such as CK2, EGFR, PI3K-AKT-mTOR pathway.²²²

With the purpose to further explore the influences of structural modifications on the coumarin and the psoralen core on the activity and selectivity towards tumoral CAs isoforms, we have designed and synthesized four different series of differently substituted coumarins and psoralenes derivatives (**Scheme 1**) (**Fig. 35**).

The **EMAC 10155 (a-m)** and **EMAC 10158 (a-m)** series present no substituent in the position 8 or 9 of the coumarin and psoralen nucleus respectively.

The **EMAC 10156 (a-m)** and **EMAC 10159 (a-m)** series are characterized by the presence of a methylene carboxyl group in the position 3 of the chromene, that, as already reported, might lead to the formation of a bidentate chelator of the Zn²⁺ ion in the catalytic pocket of the enzymes.²²³

The **EMAC 10157 (a-m)** and **EMAC 10160 (a-m)** series, namely methyl-2-[4-methyl-2-oxo-7-(2-oxo-2-arylethoxy)-8-propylchromen-3-yl]acetate and 2-(5-methyl-7-oxo-3-aryl-9-propyl-7H-furo[3,2-g]chromen-6-yl)acetic acid respectively, present a methylene carboxyl group in position 3 of the chromene, and a propyl substituent in the position 8 of the coumarin or in the position 9 of the psoralen nucleus.

Finally, the **EMAC 10161 (b-m)** and **EMAC 10162 (b-m)** series are characterized by the presence of ethylene carboxyl group in position 3 of the chromene.

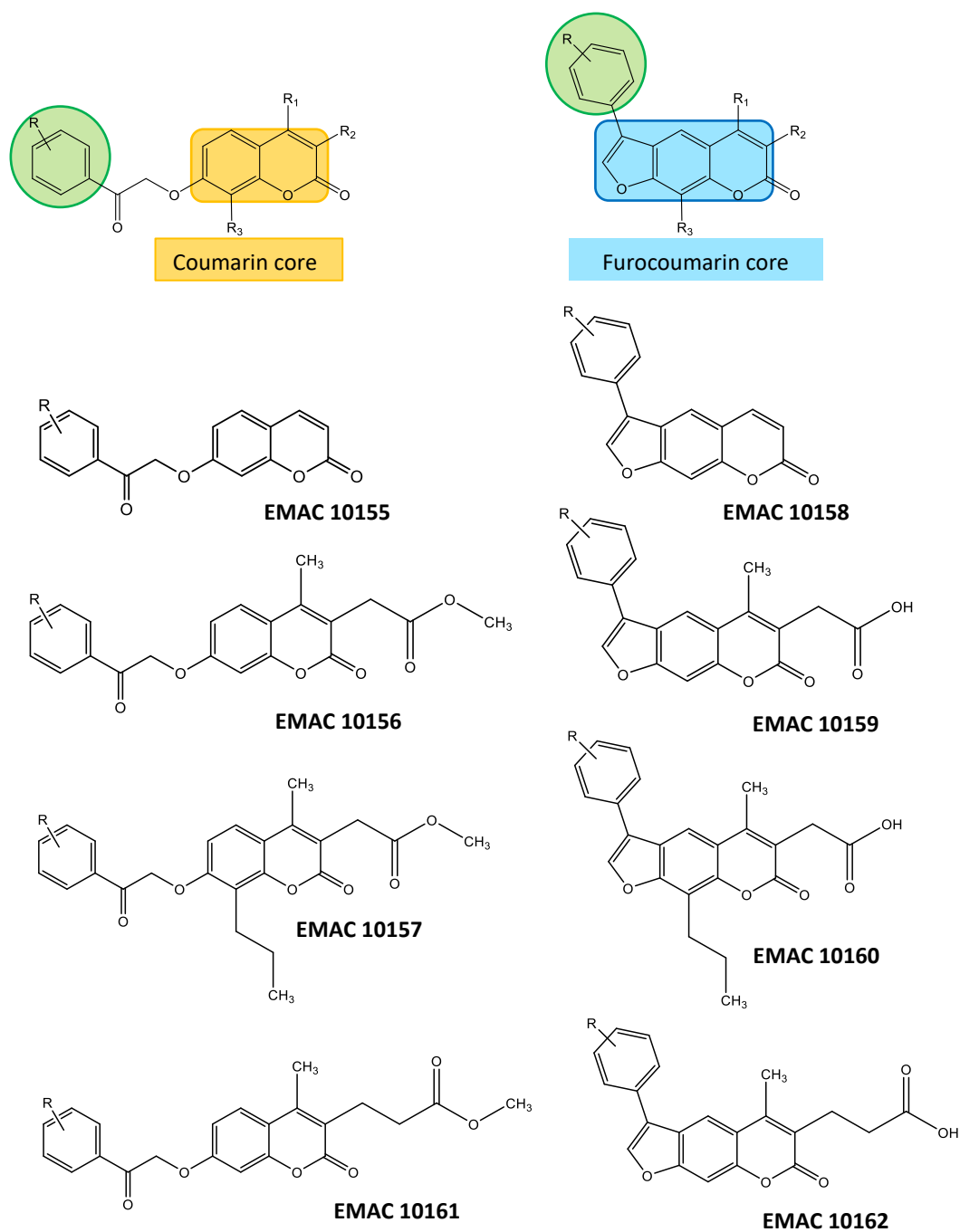


Figure 35 General structure of EMAC 10155, 10156, 10157, 10158, 10159, 10160, 10161, 10162

The synthesis of the series of EMAC 10156 (a-m), EMAC 10159 (a-m), EMAC 10157 (a-m), EMAC 10160 (a-m), EMAC 10161 (b-m) and EMAC 10162 (b-m) is divided in three steps: the first reaction is a Pechmann condensation performed in concentrated H₂SO₄ at room temperature. In this step dimethylacetylsuccinate and either resorcinol or 2-methylresorcinol were reacted; 96% H₂SO₄ was used as condensing agent and made unnecessary the use of the solvent (Fig. 36).

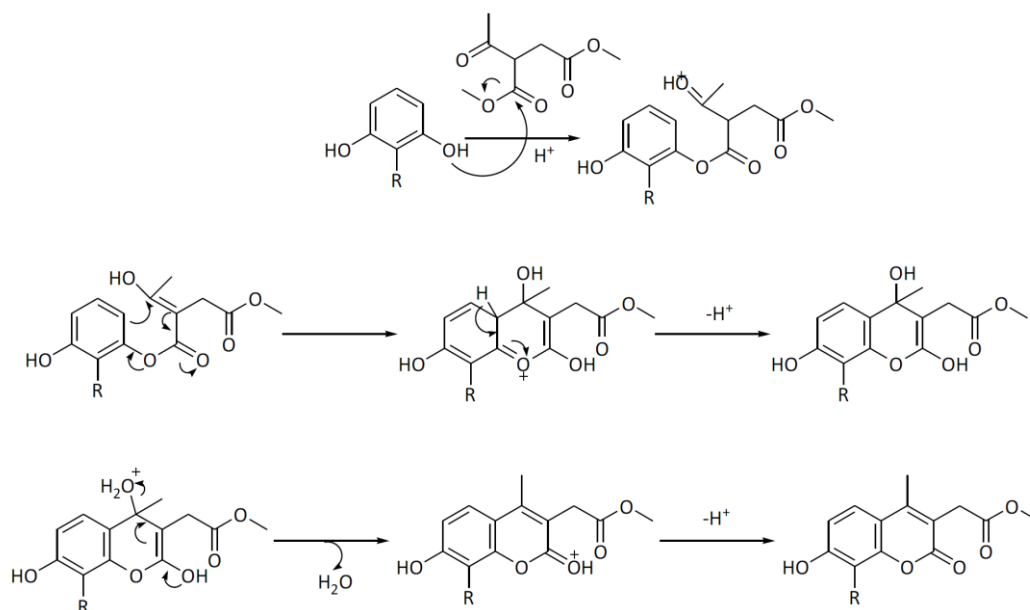
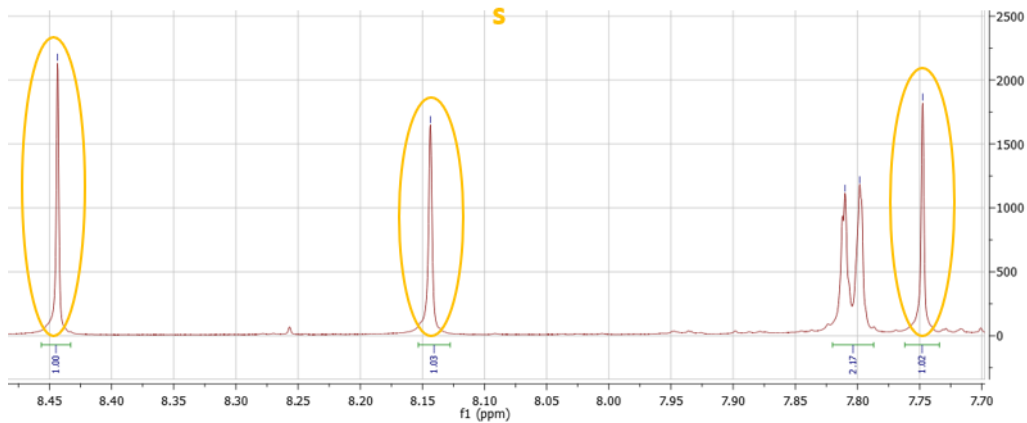
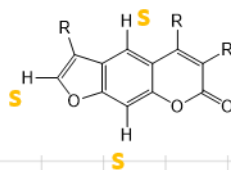


Figure 36 Example of Pechmann condensation mechanism

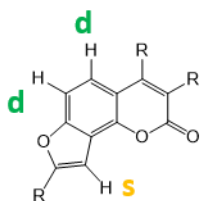
The second step of the synthetic pathway is a Williamson reaction between the phenolic group in the position 7 of the chromene ring and an appropriate α -haloketone. The reaction was performed in dry acetone and potassium carbonate as proton scavenger, to generate the corresponding substituted oxoethers which were purified and further reacted to give the formation of furocoumarins. More in detail, the asymmetric ethers were refluxed in NaOH 1N water solution to form the furan ring by intramolecular electrophilic substitution.

By heating in presence of NaOH (1M) the saponification of the ester groups in the position 3 of the chromene to the corresponding substituted 2-(5-methyl-7-oxo-7H-furo[3,2-g]chromen-6-yl)acetic acids was observed. The furan ring formation always led to linear furocoumarins as confirmed by $^1\text{H-NMR}$ spectra. The formation of the angular isomer was only observed for compound **10162 d**, as confirmed by $^1\text{H-NMR}$ spectra (**Fig.37**).

Linear furocoumarin



Angular furocoumarin



+

Linear furocoumarin

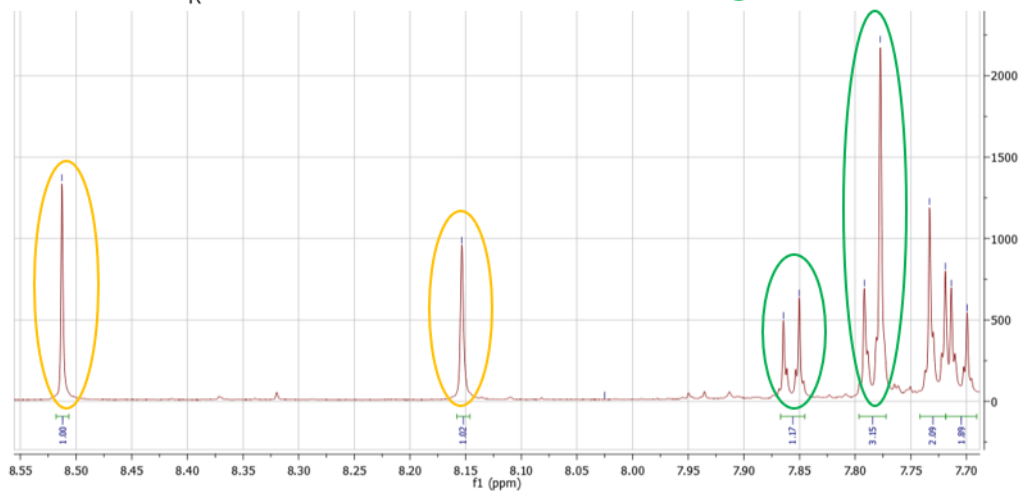
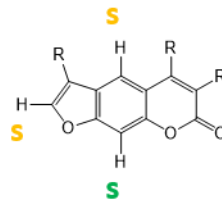
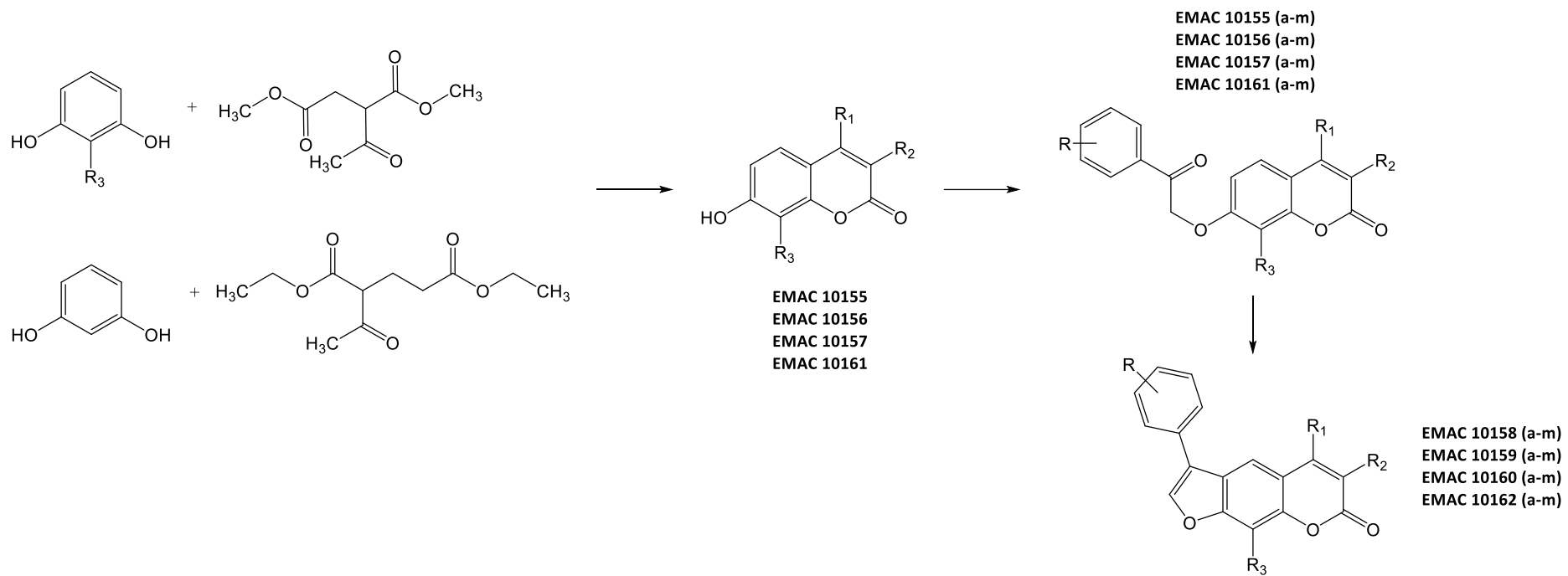


Figure 37 Angular and linear furocoumarins

The synthetic pathway to **EMAC 10155 (a-m)** and **EMAC 10158 (a-m)** series consists of only two steps as the Pechmann condensation step is no required.

All synthesized compounds were characterized by means of analytical and spectroscopic methods.



Scheme 1 General synthesis of compound **EMAC 10155 (a-m)**, **10156 (a-m)**, **10157(a-m)**, **10158 (a-m)**, **10159 (a-m)**, **10160 (a-m)**, **10161 (a-m)**, **10162 (b-m)**.

5.1.2 Biological results and discussion

Compounds **EMAC10155 (a-m)**, **EMAC10156 (a-m)**, **EMAC10157(a-m)**, **EMAC10158 (a-m)**, **EMAC10159 (a-m)**, **EMAC10160 (a-m)**, **EMAC10161 (a-m)** and **EMAC10162 (b-m)** were submitted to enzymatic evaluation towards hCA I, II, IX, and XII. The results are reported in **Table 3**. None of these compounds exhibited any inhibition activity towards hCA I and II isozymes. On the contrary, all of them are nanomolar inhibitors of the hCA tumor associated isoforms IX and XII. This behavior agrees with our previous findings and with the generally observed selectivity profile of coumarin derivatives.²²³

For what concerned hCA XII inhibition, derivatives **EMAC10159A**, **EMAC10159D**, **EMAC10159L** and **EMAC10159M**, that present a methyl group in position 4 of the furocoumarin core, and respectively a 4-methyl phenyl, 4-fluoro phenyl, phenyl and 4-chloro phenyl, as substituent in position 8 of the furocoumarin core, results as the most potent inhibitor with K_i value of 9.1 nM, 7.4 nM, 9.4 nM and 9.3 nM, respectively. Interestingly, this derivatives, exhibited selectivity towards the isoform XII.

For isoform hCA IX, derivate **EMAC10156M**, that presents a methyl group in position 4 of the coumarin core and a 4-chloro phenyl substituent bonded with the coumarin core, and derivatives **EMAC10159A**, **EMAC10159D** and **EMAC10159L**, are the most potent inhibitors, with K_i value of 23.6 nM, 23.0 nM, 17.7 nM and 17.5 nM respectively. More specific, the compound **EMAC10156M**, shows selectivity toward the tumor associate isoform IX.

The introduction of a methyl group in position 4 of the furocoumarin core, led to an increase of the activity and selectivity toward the CA tumoral associate isoforms.

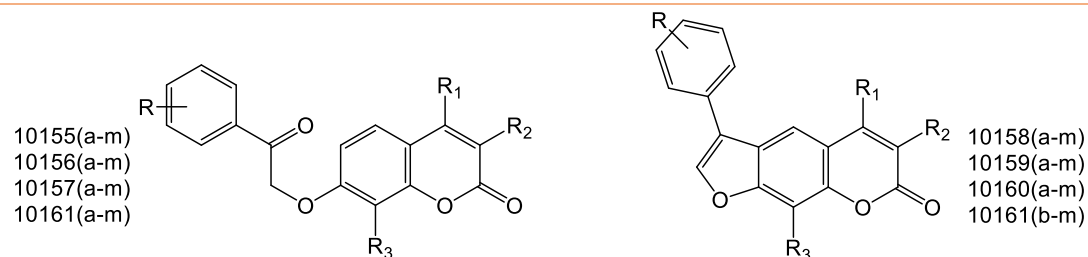
For what concern about the **EMAC10157** and **EMAC10160** derivatives, they are selective toward CA IX and XII, but the introduction of a methyl group in position four and a propyl group in position 9 of coumarin and furocoumarin core, led to a general decrease in the activity.

EMAC10160 derivatives with 4-methyl, 4-fluoro and 4-chloro as substituent of the phenyl ring bonded to the coumarin core, show increase of selectivity toward CA XII.

Unfortunately, COX inhibition evaluation for **EMAC10155 (a-m)**, **EMAC10156 (a-m)**, **EMAC10157(a-m)**, **EMAC10158 (a-m)**, **EMAC10159 (a-m)**, **EMAC10160 (a-m)**, **EMAC10161 (a-m)** and **EMAC10162 (b-m)** is still in progress.

The data are extremely encouraging and push our group toward further investigation and studies to better clarify and determine the structural determinant features for achieving the best activity and selectivity towards the CA tumoral isoforms.

Table 3 Inhibition data towards hCA I, II, IX, and XII of compounds **EMAC 10155(a-m)**, **10158 (a-m)**, **10156(a-m)**, **10159(a-m)**, **10157(a-m)**, **10160(a-m)**, **10161(a-m)** and **10162(b-m)**



K _i (nM)*								
Compound	R	R1	R2	R3	hCA I	hCAII	hCA IX	hCA XII
EMAC10155A	4-CH ₃	H	H	H	>10000	>10000	191.6	31.8
EMAC10155B	4-OCH ₃	H	H	H	>10000	>10000	107.3	44.2
EMAC10155C	4-Br	H	H	H	>10000	>10000	91.4	47.2
EMAC10155D	4-F	H	H	H	>10000	>10000	130.7	46.9
EMAC10155G	4-Phenyl	H	H	H	>10000	>10000	126.8	43.4
EMAC10155H	2,4-F	H	H	H	>10000	>10000	144.3	56.2
EMAC10155L	4-H	H	H	H	>10000	>10000	97.5	80.5
EMAC10155M	4-Cl	H	H	H	>10000	>10000	97.6	77.5
EMAC10158A	4-CH ₃	H	H	H	>10000	>10000	151.3	91.0
EMAC10158M	4-Cl	H	H	H	>10000	>10000	172.7	85.2

EMAC10156A**	4-CH ₃	CH ₃	CH ₂ COOCH ₃	H	>10000	>10000	122.8	56.6
EMAC10156B	4-OCH ₃	CH ₃	CH ₂ COOCH ₃	H	>10000	>10000	213.4	87.4
EMAC10156C	4-Br	CH ₃	CH ₂ COOCH ₃	H	>10000	>10000	213.4	381.2
EMAC10156D**	4-F	CH ₃	CH ₂ COOCH ₃	H	>10000	>10000	84.7	250.0
EMAC10156F	3-NO ₂	CH ₃	CH ₂ COOCH ₃	H	>10000	>10000	250.4	425.9
EMAC10156L**	4-H	CH ₃	CH ₂ COOCH ₃	H	>10000	>10000	89.7	72.5
EMAC10156M**	4-Cl	CH ₃	CH ₂ COOCH ₃	H	>10000	>10000	23.6	446.6
EMAC10159A**	4-CH ₃	CH ₃	CH ₂ COOH	H	>10000	>10000	23.0	9.1
EMAC10159B	4-OCH ₃	CH ₃	CH ₂ COOH	H	>10000	>10000	898.6	75.0
EMAC10159C	4-Br	CH ₃	CH ₂ COOH	H	>10000	>10000	291.2	83.9
EMAC10159D**	4-F	CH ₃	CH ₂ COOH	H	>10000	>10000	17.7	7.4
EMAC10159L**	4-H	CH ₃	CH ₂ COOH	H	>10000	>10000	17.5	9.4
EMAC10159M**	4-Cl	CH ₃	CH ₂ COOH	H	>10000	>10000	94.7	9.3
EMAC10157A***	4-CH ₃	CH ₃	CH ₂ COOCH ₃	CH ₂ CH ₂ CH ₃	>10,000	>10,000	247.7	350.3
EMAC10157B***	4-OCH ₃	CH ₃	CH ₂ COOCH ₃	CH ₂ CH ₂ CH ₃	>10,000	>10,000	352.7	324.2
EMAC10157D***	4-F	CH ₃	CH ₂ COOCH ₃	CH ₂ CH ₂ CH ₃	>10,000	>10,000	239.5	257.1
EMAC10157F	3-NO ₂	CH ₃	CH ₂ COOCH ₃	CH ₂ CH ₂ CH ₃	>10000	>10000	238.5	91.0
EMAC10157G***	4-Phenyl	CH ₃	CH ₂ COOCH ₃	CH ₂ CH ₂ CH ₃	>10,000	>10,000	135.2	283.1

EMAC10157H	2,4-F	CH ₃	CH ₂ COOCH ₃	CH ₂ CH ₂ CH ₃	>10000	>10000	154.2	86.7
EMAC10157L	4-H	CH ₃	CH ₂ COOCH ₃	CH ₂ CH ₂ CH ₃	>10000	>10000	957.0	79.8
EMAC10157M	4-Cl	CH ₃	CH ₂ COOCH ₃	CH ₂ CH ₂ CH ₃	>10000	>10000	239.2	344.1
EMAC10160A***	4-CH ₃	CH ₃	CH ₂ COOH	CH ₂ CH ₂ CH ₃	>10,000	>10,000	467.3	758.1
EMAC10160B***	4-OCH ₃	CH ₃	CH ₂ COOH	CH ₂ CH ₂ CH ₃	>10,000	>10,000	489.3	859.4
EMAC10160D***	4-F	CH ₃	CH ₂ COOH	CH ₂ CH ₂ CH ₃	>10,000	>10,000	379.7	460.0
EMAC10160G***	4-Phenyl	CH ₃	CH ₂ COOH	CH ₂ CH ₂ CH ₃	>10,000	>10,000	397.7	550.0
EMAC10160L	4-H	CH ₃	CH ₂ COOH	CH ₂ CH ₂ CH ₃	>10000	>10000	291.7	469.6
EMAC10160M	4-Cl	CH ₃	CH ₂ COOH	CH ₂ CH ₂ CH ₃	>10000	>10000	310.5	481.4
EMAC10161A	4-CH ₃	CH ₃	CH ₂ CH ₂ COOCH ₃	H	>10000	>10000	82.5	67.8
EMAC10161B	4-OCH ₃	CH ₃	CH ₂ CH ₂ COOCH ₃	H	>10000	>10000	278.8	226.7
EMAC10161D	4-F	CH ₃	CH ₂ CH ₂ COOCH ₃	H	>10000	>10000	238.4	64.8
EMAC10161G	4-Phenyl	CH ₃	CH ₂ CH ₂ COOCH ₃	H	>10000	>10000	126.7	92.6
EMAC10161H	2,4-F	CH ₃	CH ₂ CH ₂ COOCH ₃	H	>10000	>10000	80.9	92.4
EMAC10161L	4-H	CH ₃	CH ₂ CH ₂ COOCH ₃	H	>10000	>10000	278.1	480.0
EMAC10161M	4-Cl	CH ₃	CH ₂ CH ₂ COOCH ₃	H	>10000	>10000	87.1	36.1
EMAC10162B	4-OCH ₃	CH ₃	CH ₂ CH ₂ COOH	H	>10000	>10000	232.8	79.9
EMAC10162D	4-F	CH ₃	CH ₂ CH ₂ COOH	H	>10000	>10000	297.0	438.2

EMAC10162G	4-Phenyl	CH ₃	CH ₂ CH ₂ COOH	H	>10000	>10000	892.3	82.9
EMAC10162L	4-H	CH ₃	CH ₂ CH ₂ COOH	H	>10000	>10000	283.8	98.1
EMAC10162M	4-Cl	CH ₃	CH ₂ CH ₂ COOH	H	>10000	>10000	261.6	295.1
AAZ					250.0	12.1	25.8	5.7

*Mean from 3 different assays, by a stopped flow technique (errors were in the range of \pm 5-10 % of the reported values).

**Following previous work

***224

5.1.3 Conclusions

I have designed and synthesized four different series of coumarin derivatives and four series of psoralen derivatives: **EMAC10155 (a-m)**, **EMAC10156 (a-m)**, **EMAC10157(a-m)**, **EMAC10158 (a-m)**, **EMAC10159 (a-m)**, **EMAC10160 (a-m)**, **EMAC10161 (a-m)** and **EMAC10162 (b-m)**, to evaluate their activity and selectivity toward on hCA I, II, IX, and XII isozymes, and to obtain information on their structure-activity relationships. All compounds show selectivity toward the tumor associate isozymes IX and XII, in the nanomolar range, and none of them were able to inhibit the off-target isoforms I and II, confirming the literature reported chromene derivatives selectivity profile. According to these results, psoralen and coumarins derivatives could be considered as promising scaffolds for design of highly selective inhibitors of the hCAs IX-XII isoforms. These results are very encouraging and pushed us to further investigate these derivatives, in order to identify potential candidates for the treatment of hypoxic tumors.

5.2 New 4-((4-oxo-2-phenylthiazolidin-3-yl)amino)benzenesulfonamide synthesis and inhibitory activity toward carbonic anhydrase I, II, IX, XII and the potential dual CA/COX-2 inhibition

5.2.1 Background

Tumors are a multifactorial disease, characterized by extremal condition caused by different factors such as the deregulation of several enzymes' activity. In this respect hCAs IX and XII, and COX-2 were reported to be involved in the survival and progression of tumor cells. On these bases, the idea to design and synthesize multi-target inhibitors directed to both hCA and COX-2 is very attractive.

During my PhD, I have synthesized different series of potential multi-target agents to investigate on the structural requisites for the selective inhibition of tumor overexpressed hCAs and COX-2 enzymes. Identification of a common structural denominator between hCA and COX-2 inhibitors was the starting point to design multi-target compounds. Indeed, both inhibitors of the two enzyme families present a primary sulfonamide moiety in the majority of the most effective agents. Celecoxib and valdecoxib (**Fig. 24 e 25**) already demonstrated to have inhibitory activity towards both COX-2 and cancer related hCA enzymes.

Therefore, a structural model has been studied with the aim to satisfy both enzyme pharmacophoric requirements: the benzenesulphonamide group turned out to be not only efficient for the inhibition of COX-2 enzyme, but also capable to coordinate the hCAs zinc cofactor in the catalytic site. On these bases, we have designed potential dual inhibitors where the benzenesulphonamide moiety, binds a differently substituted central heterocyclic core through a linker. (**Fig.38**).

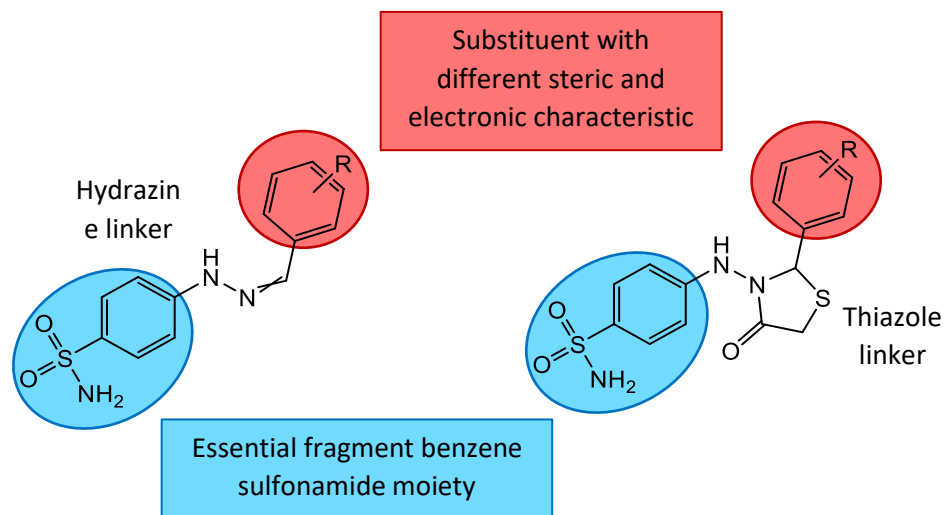
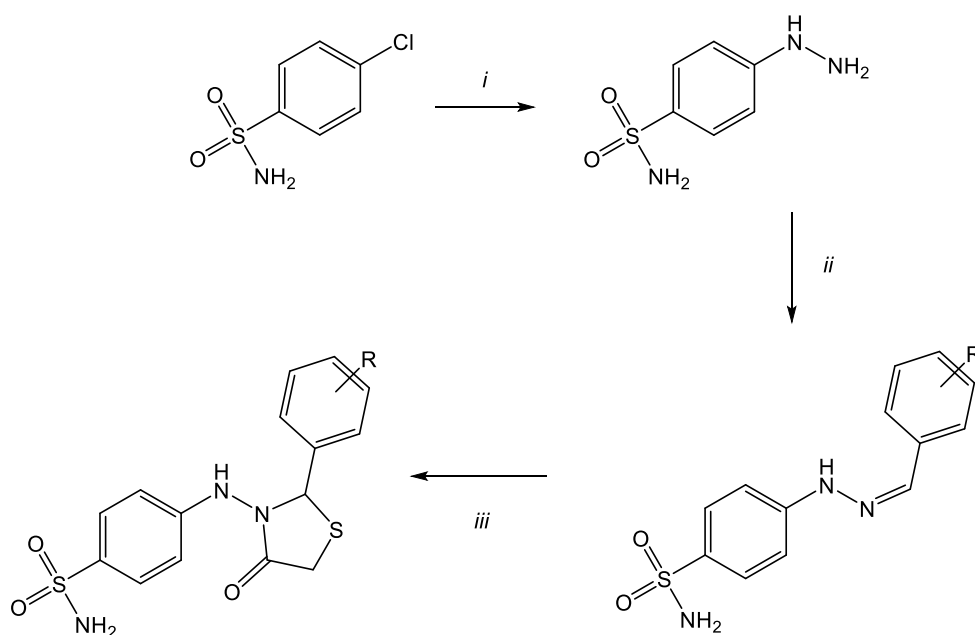


Figure 38 General structure of **EMAC 10190** and **EMAC 10191**

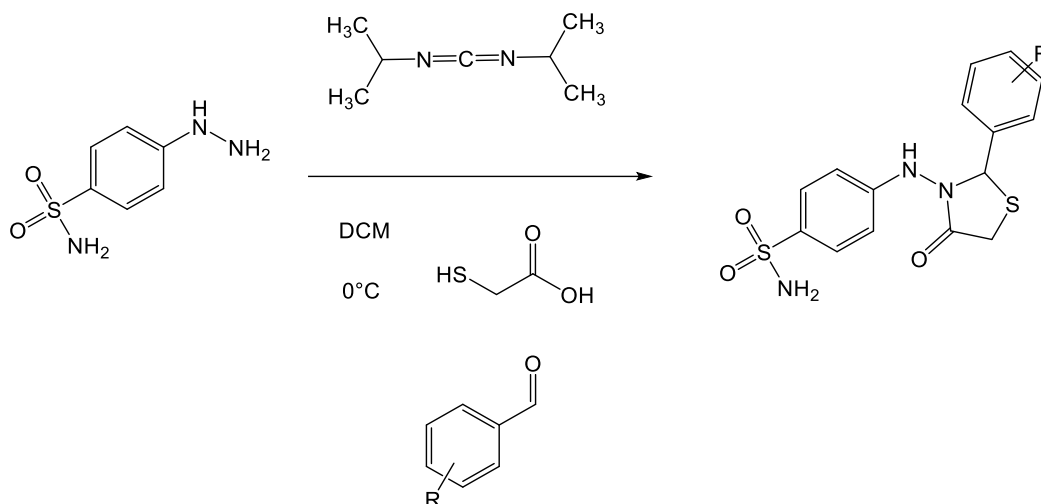
According to this model, different series of *4-((4-oxo-2-phenylthiazolidin-3-yl)amino)benzenesulphonamide* have been synthesized. All compounds are characterized by the presence of a thiazole core, substituted in the position 2 with various aromatic groups with different electronic and steric features.

The synthesis of **EMAC 10191 (b-I)** is subdivided in three steps (**Scheme 2**); the second step led to the formation of compounds, **EMAC 10190 (b-I)**, which can be further reacted to give derivatives **EMAC 10191**.



Scheme 2 Synthesis of derivatives **EMAC10190 (b-I)** and **EMAC10191 (b-I)**: (i.) Hydrazine, MW, 250 psi, 1h, H₂O, 80°C, 1h; (ii.) benzaldehyde, acetic acid, MeOH, Δ; (iii.) mercaptoacetic acid, 60°C.

To find the best synthetic pathway, trials were done by using different strategies. Among these, very interestingly, a one-pot two-step synthetic procedure was proposed for the preparation of the **EMAC 10191 (b-l)** derivatives.

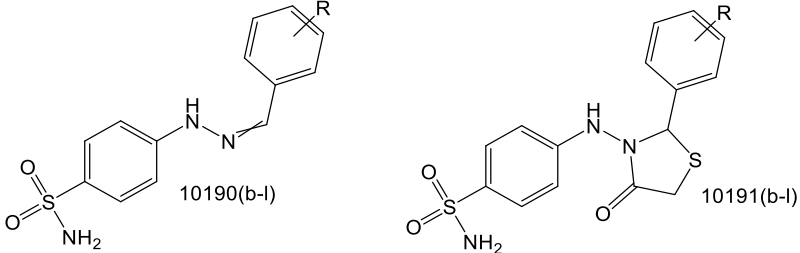


All synthesized compounds were characterized by means of analytical and spectroscopic methods.

5.2.2 Biological results and discussion

All the synthesized compounds **EMAC10190 (b-k)** and **EMAC10191 (b-k)** were submitted to enzymatic assay to evaluate their activity and selectivity towards human CA isozymes I, II, IX, XII. The results are illustrated in **Table 4**. Different activities towards CA isoforms were observed, with the majority of the compounds showing K_i values between the high to the low nanomolar range. In particular, most of the compounds exhibited interesting inhibition K_i values towards CA IX. **EMAC10190 D** and **EMAC10191 D**, that present 4-acethoxy-3-methoxy phenyl as substitution, are the most potent inhibitors towards the tumoral isoform CA IX, with K_i value 5.3 nM and 7.5 nM respectively. Most of **EMAC10191** derivatives (except for EMAC10191C and EMAC10191D) were selective against hCA II, suggesting that the introduction of a thiazole spacer led to inhibition of CA II; these derivatives can be used for a different therapeutic application.

Unfortunately, COX inhibition evaluation for **EMAC10190 (b-k)** and **EMAC10191 (b-k)** is still in progress.

Table 4 Inhibition data towards hCA I, II, IX, and XII of compounds **EMAC 10190 (b-I)** and **10191(b-I)**


K_i (nM)*					
Compound	R	hCA I	hCAII	hCA IX	hCA XII
EMAC10190B	4-CH ₃	792.4	43.3	41.0	78.1
EMAC10190C	3,4,5-OCH ₃	5093	621.7	66.4	40.0
EMAC10190D	4-Acethoxy-3-OCH ₃	727.2	26.5	5.3	80.7
EMAC10190F	2-Naphtal	5400	81.9	208.7	54.7
EMAC10190G	1-Naphtal	17.5	626.2	92.1	67.7
EMAC10190H	4-OCH ₂ CH ₃ -3-OCH ₃	3365	826.0	270.8	74.7
EMAC10190J	4-OCH ₃	2210	287.8	69.7	268.7
EMAC10190K	4-F	441.3	73.9	41.8	82.2
EMAC10190L	4-Cl	83.4	8.5	9.6	154.2
EMAC10191B	4-CH ₃	42.5	6.5	7.3	325.7
EMAC10191C	3,4,5-OCH ₃	403.1	8.8	8.3	63.5
EMAC10191D	4-Acethoxy-3-OCH ₃	87.9	22.6	7.5	83.6
EMAC10191F	2-Naphtal	72.4	6.8	23.6	91.2
EMAC10191G	1-Naphtal	63.8	5.1	8.3	158.7
EMAC10191H	4-OCH ₂ CH ₃ -3-OCH ₃	703.8	3.9	8.7	65.7
EMAC10191J	4-OCH ₃	51.5	5.1	8.6	83.8
EMAC10191K	4-F	16.7	4.5	5.7	39.5
EMAC10191L	4-Cl	26.8	3.2	5.3	42.2
AAZ		250.0	12.1	25.8	5.7

* Mean from 3 different assays, by a stopped flow technique (errors were in the range of $\pm 5-10$ % of the reported values).

5.2.3 Conclusions

Two series of potential dual inhibitors have been synthesized, in order to simultaneously obtain the block of a tumor associated inflammatory process and the mechanisms that the tumor cell activates to survive in hypoxic conditions.

The substitution of the phenyl ring bonded to the hydrazine spacer or to the thiazole spacer is determinant to the selectivity toward the CA tumoral isoform, in particular toward the isoform IX.

Hopefully, more data will be available in the next future and will guide us to the design and synthesis of new derivatives. For this reason, these compounds deserve further exploration and might constitute the basis for future development.

5.3 Evaluation of drug like properties

5.3.1 Background

It is well recognized that potential ADMET problems should be addressed at the early stages of drug discovery during the identification and optimization. This has been recognized as a significant cause of high rates of attrition in drug discovery.

Nearly 40% of drugs under development fail to pass clinical trials due to poor ADME. The ability to identify problematic candidates can dramatically reduce the amount of time and resources wasted and streamline the overall development process.

Among the properties analyzed, those described by Lipinsky's rule are the best known. Researcher Christopher Lipinsky in 1997 devised a simple algorithm that turns out to be very important for the design and development of orally absorbed drugs. The rule, properly called the "rule of 5 (Ro5)", is based on five simple foundations:

- Molecular weight < 500
- AlogP < 5, a measure of lipophilicity
- Hydrogen-bond donors < 5 bonds
- Hydrogen-bond acceptor < 10 bonds
- Rotatable bonds < 10

This criterion is very useful in the chemical-pharmaceutical field to simplify and favor the field of investigation, and thus drastically reduce the number of molecules among which a candidate molecule could be explored as a potential drug.²²⁵

There has been significant effort in developing more comprehensive and quantitative rules of drug-likeness.

To the properties described by Lipinsky, other properties have been added that define important molecular characteristics for the different phases of absorption, distribution, metabolism and excretion of drugs, such as: solubility,²²⁶ surface exposed to the solvent, molecular volume, overcoming of the blood-brain barrier, permeability of Caco cells -2 (colorectal Carcinoma) and MDCK (Madin – Darby Canine Kidney), binding to albumin, blocking the HERG K⁺ (Human-a-go-go- Related Gene) channel,²²⁷ are some examples.^{4, 228,}

229

Computational methods can help to predict, *in silico*, these properties and several programs suites implemented tools that help the researcher to evaluate the drug-likeness of compounds have been developed.

Qikprop predicts physically significant descriptors and pharmaceutically relevant properties of organic molecules.^{225, 226} It runs in normal mode predicting 44 properties (Tab. 5).

Table 5 QikProp properties and descriptors.

		RANGE OR RECOMMENDED VALUES
MOLECULE NAME	Molecule name taken from the title line in the input structure file. If the title line is blank, the input file name is used.	
#STARS	Number of property or descriptor values that fall outside the 95% range of similar values for known drugs. Outlying descriptors and predicted properties are denoted with asterisks (*) in the .out file. A large number of stars suggests that a molecule is less drug-like than molecules with few stars. The following properties and descriptors are included in the determination of #stars: MW, dipole, IP, EA, SASA, FOSA, FISA, PISA, WPSA, PSA, volume, #rotor, donorHB, accptHB, glob, QPpolrz, QplogPC16, QplogPoct, QplogPw, QplogPo/w, logS, QPLogKhsa, QplogBB, #metabol	0 – 5
#AMINE	Number of non-conjugated amine groups.	0 – 1
#AMIDINE	Number of amidine and guanidine groups.	0
#ACID	Number of carboxylic acid groups.	0 – 1
#AMIDE	Number of non-conjugated amide groups.	0 – 1
#ROTOR	Number of non-trivial (not CX3), non-hindered (not alkene, amide, small ring) rotatable bonds.	0 – 15
#RTVFG	Number of reactive functional groups; the specific groups are listed in the <i>jobname</i> .out file. The presence of these groups can lead to false positives in HTS assays and to decomposition, reactivity, or toxicity problems <i>in vivo</i> .	0 – 2
CNS	Predicted central nervous system activity on a –2 (inactive) to +2 (active) scale.	–2 to +2
MOL_MW	Molecular weight of the molecule.	130.0 – 725.0
DIPOLE†	Computed dipole moment of the molecule.	1.0 – 12.5
SASA	Total solvent accessible surface area (SASA) in square angstroms using a probe with a 1.4 Å radius.	300.0 – 1000.0
FOSA	Hydrophobic component of the SASA (saturated carbon and attached hydrogen).	0.0 – 750.0
FISA	Hydrophilic component of the SASA (SASA on N, O, and H on heteroatoms).	7.0 – 330.0

PISA	π (carbon and attached hydrogen) component of the SASA.	0.0 – 450.0
WPSA	Weakly polar component of the SASA (halogens, P, and S).	0.0 – 175.0
VOLUME	Total solvent-accessible volume in cubic angstroms using a probe with a 1.4 Å radius.	500.0 – 2000.0
DONORHB	Estimated number of hydrogen bonds that would be donated by the solute to water molecules in an aqueous solution. Values are averages taken over a number of configurations, so they can be non-integer.	0.0 – 6.0
ACCPHNB	Estimated number of hydrogen bonds that would be accepted by the solute from water molecules in an aqueous solution. Values are averages taken over a number of configurations, so they can be non-integer.	2.0 – 20.0
DIP²/V†	Square of the dipole moment divided by the molecular volume. This is the key term in the Kirkwood-Onsager equation for the free energy of solvation of a dipole with volume V.	0.0 – 0.13
ACXDN^{0.5}/SA	Index of cohesive interaction in solids. This term represents the relationship $(accptHB)(donorHB)/(SA)$.	0.0 – 0.05
GLOB	Globularity descriptor, $(4 \pi r^2)/(SASA)$, where r is the radius of a sphere with a volume equal to the molecular volume. Globularity is 1.0 for a spherical molecule.	0.75 – 0.95
QPPOLRZ	Predicted polarizability in cubic angstroms.	13.0 – 70.0
QPLOGPC16	Predicted hexadecane/gas partition coefficient.	4.0 – 18.0
QPLOGPOCT‡	Predicted octanol/gas partition coefficient.	8.0 – 35.0
QPLOGPW	Predicted water/gas partition coefficient.	4.0 – 45.0
QPLOGPO/W	Predicted octanol/water partition coefficient.	–2.0 – 6.5
QPLOGS	Predicted aqueous solubility, log S. S in mol dm ⁻³ is the concentration of the solute in a saturated solution that is in equilibrium with the crystalline solid.	–6.5 – 0.5
CIQPLOGS	Conformation-independent predicted aqueous solubility, log S. S in mol dm ⁻³ is the concentration of the solute in a saturated solution that is in equilibrium with the crystalline solid.	–6.5 – 0.5
QPLOGHERG	Predicted IC ₅₀ value for blockage of HERG K ⁺ channels.	Concern below –5
QPPCACO	Predicted apparent Caco-2 cell permeability in nm/sec. Caco-2 cells are a model for the gut blood barrier. QikProp predictions are for non-active transport.	<25 poor, >500 great
QPLOGBB	Predicted brain/blood partition coefficient. Note: QikProp predictions are for orally delivered drugs so, for example, dopamine and serotonin are CNS negative because they are too polar to cross the blood-brain barrier	–3.0 – 1.2
QPPMDCK	Predicted apparent MDCK cell permeability in nm/sec. MDCK cells are considered to be a good mimic for the blood-brain barrier. QikProp predictions are for non-active transport.	<25 poor, >500 great
QPLOGKP	Predicted skin permeability, log K _p .	–8.0 – –1.0

IP(EV)†	PM3 calculated ionization potential.	7.9 – 10.5
EA(EV)†	PM3 calculated electron affinity.	–0.9 – 1.7
#METAB‡	Number of likely metabolic reactions.	1 – 8
QPLOGK_{HSA}	Prediction of binding to human serum albumin.	–1.5 – 1.5
HUMANORAL ABSORPTION	Predicted qualitative human oral absorption: 1, 2, or 3 for low, medium, or high. The text version is reported in the output. The assessment uses a knowledge-based set of rules, including checking for suitable values of PercentHumanOralAbsorption, number of metabolites, number of rotatable bonds, logP, solubility and cell permeability.	
PERCENTHUMAN ORALABSORPTION	Predicted human oral absorption on 0 to 100% scale. The prediction is based on a quantitative multiple linear regression model. This property usually correlates well with HumanOralAbsorption, as both measure the same property.	80% is high <25% is poor
SAFLUORINE	Solvent-accessible surface area of fluorine atoms.	0.0 – 100.0
SAAMIDEO	Solvent-accessible surface area of amide oxygen atoms.	0.0 – 35.0
PSA	Van der Waals surface area of polar nitrogen and oxygen atoms.	7.0 – 200.0
#NANDO	Number of nitrogen and oxygen atoms.	2 – 15

The range is valid for 95% of known drugs.

Such an approach provides molecular properties employing QSAR calculation or similarity validated approaches.²³⁰ The comparison of the predicted value for the novel compounds with respect to the 95% of known drugs help to estimate their drug-likeness.

Compounds that fall within the defined ranges are described as ‘drug-like’.

5.3.1 Biological results and discussion

Hence, to estimate the drug-likeness of the compounds, we carried out *in silico* ADMET prediction.²³¹ In particular, here we report a selection of the predicted properties, the most significant investigated using the Qikprop²³² software for all the series synthesized.

The analysis of the predicted properties reveals the good drug-likeness of the compounds. However, the enormous quantity of data collected does not allow to enter all the properties values calculated.

For each series of compounds two tables are reported containing:

- Structural properties under Lipinski’s rule five (RO5) and other physicochemical properties;

- Other properties that could affect the pharmacokinetics and the safety of the compounds.

As it is shown in all the tables, most of the predicted properties are within the ranges specified with few exceptions.

Table 6 Predicted properties for the series **EMAC10155**

Molecule	#stars	MW	HBD	HBA	QplogPo/w	rot	PSA	QplogS
	0 – 5	130 – 725	0-6	2- 20	-2- 6.5	0 – 15	7 – 200	-6.5 – 0.5
EMAC10155A	0	294,3	0	4	2,6	4	75,8	-3,5
EMAC10155B	0	310,3	0	5	2,3	5	84,0	-3,1
EMAC10155C	0	359,2	0	4	2,8	4	75,8	-3,8
EMAC10155D	0	298,3	0	4	2,5	4	75,8	-3,3
EMAC10155E	1	325,3	0	5	1,5	5	120,8	-3,0
EMAC10155F	2	325,3	0	5	1,5	5	120,7	-3,0
EMAC10155G	1	356,4	0	4	3,9	5	75,8	-5,1
EMAC10155H	0	316,3	0	4	2,6	4	75,7	-3,5
EMAC10155I	0	349,2	0	4	3,1	4	74,5	-4,3
EMAC10155L	0	280,3	0	4	2,3	4	75,8	-2,9
EMAC10155M	0	314,7	0	4	2,8	4	75,8	-3,7

Table 7 Predicted properties for the series **EMAC10156**

Molecule	#stars	MW	HBD	HBA	QplogPo/w	#rotor	PSA	QplogS
	0 – 5	130 – 725	0-6	2- 20	-2- 6.5	0 – 15	7 – 200	-6.5 – 0.5
EMAC10156A	0	380,4	0	6	3,0	6	107,2	-4,8
EMAC10156B	0	396,4	0	7	2,8	7	115,5	-4,3
EMAC10156C	0	445,3	0	6	3,3	6	107,2	-5,0
EMAC10156D	0	384,4	0	6	3,0	6	107,2	-4,5
EMAC10156E	1	411,4	0	7	2,0	7	152,2	-4,2
EMAC10156F	2	411,4	0	7	2,0	7	152,1	-4,2
EMAC10156G	0	442,5	0	6	4,4	7	107,2	-6,3
EMAC10156H	0	402,4	0	6	3,1	6	107,1	-4,7
EMAC10156I	0	435,3	0	6	3,7	6	105,9	-5,5
EMAC10156L	0	366,4	0	6	2,7	6	107,2	-4,1

EMAC10156M	0	400,8	0	6	3,2	6	107,2	-4,9
-------------------	---	-------	---	---	-----	---	-------	------

Table 8 Predicted properties for the series **EMAC10157**

Molecule	#stars	MW	HBD	HBA	QplogPo/w	#rotor	PSA	QplogS
	0 – 5	130 – 725	0-6	2- 20	-2- 6.5	0 – 15	7 – 200	-6.5 – 0.5
EMAC10157A	0	422,5	0	6	4,4	8	104,3	-6,4
EMAC10157B	0	438,5	0	7	4,0	9	112,5	-5,5
EMAC10157C	0	487,3	0	6	4,5	8	104,2	-6,3
EMAC10157D	0	426,4	0	6	4,2	8	104,2	-5,8
EMAC10157E	1	453,4	0	7	3,2	9	149,2	-5,5
EMAC10157F	2	453,4	0	7	3,2	9	149,2	-5,4
EMAC10157G	2	484,5	0	6	5,6	9	104,3	-7,5
EMAC10157H	0	444,4	0	6	4,3	8	104,1	-5,9
EMAC10157I	0	477,3	0	6	4,3	8	102,0	-5,5
EMAC10157L	0	408,5	0	6	3,9	8	104,2	-5,4
EMAC10157M	0	442,9	0	6	4,4	8	104,2	-6,2

Table 9 Predicted properties for the series **EMAC10158**

Molecule	#stars	MW	HBD	HBA	QPlogPo/w	#rotor	PSA	QPlogS
	0 - 5	130 – 725	0-6	2- 20	-2- 6.5	0 - 15	7 - 200.0	-6.5 - 0.5
EMAC10158A	0	276,3	0	3	3,4	0	49,3	-4,2
EMAC10158B	0	292,3	0	4	3,1	1	57,6	-3,7
EMAC10158C	0	341,2	0	3	3,7	0	49,3	-4,5
EMAC10158D	0	280,3	0	3	3,3	0	49,3	-3,9
EMAC10158E	0	307,3	0	4	2,3	1	94,3	-3,6
EMAC10158F	0	307,3	0	4	2,3	1	94,3	-3,6
EMAC10158G	1	338,4	0	3	4,8	1	49,3	-5,7
EMAC10158H	0	298,2	0	3	3,5	0	49,3	-4,1
EMAC10158I	0	331,2	0	3	4,0	0	49,3	-4,7
EMAC10158L	0	262,3	0	3	3,1	0	49,3	-3,6
EMAC10158M	0	296,7	0	3	3,6	0	49,3	-4,3

Table 10 Predicted properties for the series **EMAC10159**

Molecule	#stars	MW	HBD	HBA	QPlogPo/w	#rotor	PSA	QPlogS
	0 - 5	130 – 725	0-6	2- 20	-2- 6.5	0 - 15	7 - 200.0	-6.5 - 0.5
EMAC10159A	0	348,4	1	5	3,6	2	94,8	-4,9
EMAC10159B	0	364,4	1	6	3,4	3	103,0	-4,6
EMAC10159C	0	413,2	1	5	3,8	2	94,8	-5,2
EMAC10159D	0	352,3	1	5	3,5	2	94,8	-4,7
EMAC10159E	0	379,3	1	6	2,6	3	139,8	-4,5
EMAC10159F	0	379,3	1	6	2,6	3	139,8	-4,5
EMAC10159G	0	410,4	1	5	4,9	3	94,8	-6,4
EMAC10159H	0	370,3	1	5	3,6	2	94,8	-4,9
EMAC10159I	0	403,2	1	5	4,2	2	94,8	-5,6
EMAC10159L	0	334,3	1	5	3,3	2	94,8	-4,4
EMAC10159M	0	368,8	1	5	3,8	2	94,8	-5,1

Table 11 Predicted properties for the series **EMAC10160**

Molecule	#stars	MW	HBD	HBA	QPlogPo/w	#rotor	PSA	QPlogS
	0 - 5	130 – 725	0-6	2- 20	-2- 6.5	0 - 15	7 - 200.0	-6.5 - 0.5
EMAC10160A	0	390,4	1	5	4,7	4	92,8	-6,3
EMAC10160B	0	406,4	1	6	4,5	5	101,1	-5,9
EMAC10160C	1	455,3	1	5	4,9	4	92,8	-6,6
EMAC10160D	0	394,4	1	5	4,6	4	92,8	-6,1
EMAC10160E	0	421,4	1	6	3,7	5	137,9	-5,9
EMAC10160F	0	421,4	1	6	3,7	5	137,8	-5,9
EMAC10160G	1	452,5	1	5	6,0	5	92,8	-7,8
EMAC10160H	0	412,4	1	5	4,7	4	92,8	-6,3
EMAC10160I	1	445,3	1	5	5,3	4	92,9	-7,0
EMAC10160L	0	376,4	1	5	4,4	4	92,8	-5,7
EMAC10160M	0	410,9	1	5	4,9	4	92,9	-6,5

Table 12 Predicted properties for the series EMAC10161

Molecule	#stars	MW	HBD	HBA	QPlogPo/w	#rotor	PSA	QPlogS
	0 - 5	130 – 725	0-6	2- 20	-2- 6.5	0 - 15	7 - 200.0	-6.5 - 0.5
EMAC10161A	0	408,5	0	6	3,8	8	108,1	-5,6
EMAC10161B	0	424,4	0	7	3,5	9	116,4	-5,2
EMAC10161C	2	473,3	0	6	4,2	8	108,1	-6,7
EMAC10161D	0	412,4	0	6	3,7	8	108,1	-5,4
EMAC10161E	1	439,4	0	7	2,7	9	153,1	-5,1
EMAC10161F	2	439,4	0	7	2,8	9	152,9	-5,8
EMAC10161G	2	470,5	0	6	5,1	9	108,1	-7,2
EMAC10161H	0	430,4	0	6	3,9	8	107,2	-5,7
EMAC10161I	0	463,3	0	6	4,4	8	106,8	-6,3
EMAC10161L	0	394,4	0	6	3,4	8	108,1	-5,0
EMAC10161M	0	428,9	0	6	4,0	8	108,1	-5,8

Table 13 Predicted properties for the series EMAC10162

Molecule	#stars	MW	HBD	HBA	QPlogPo/w	#rotor	PSA	QPlogS
	0 - 5	130 – 725	0-6	2- 20	-2- 6.5	0 - 15	7 - 200.0	-6.5 - 0.5
EMAC10162A	0	362,4	1	5	3,9	3	97,2	-5,3
EMAC10162B	0	378,4	1	6	3,6	4	105,5	-4,9
EMAC10162C	0	427,3	1	5	4,1	3	97,2	-5,6
EMAC10162D	0	366,3	1	5	3,8	3	97,2	-5,1
EMAC10162E	0	393,4	1	6	2,8	4	142,2	-4,9
EMAC10162F	0	393,4	1	6	2,8	4	142,2	-4,9
EMAC10162G	1	424,5	1	5	5,2	4	97,2	-6,7
EMAC10162H	0	384,3	1	5	3,9	3	97,2	-5,3
EMAC10162I	0	417,2	1	5	4,4	3	97,2	-6,0
EMAC10162L	0	348,4	1	5	3,5	3	97,2	-4,7
EMAC10162M	0	382,8	1	5	4,0	3	97,2	-5,5

Table 14 Predicted properties for the series EMAC10190

Molecule	#stars	MW	HBD	HBA	QPlogPo/w	#rotor	PSA	QPlogS
	0 - 5	130 – 725	0-6	2- 20	-2- 6.5	0 - 15	7 - 200.0	-6.5 - 0.5
EMAC10190aE	0	318,4	3	7	1,5	7	90,8	-3,5
EMAC10190aZ	1	318,4	3	7	1,5	7	89,7	-3,5
EMAC10190bZ	0	289,4	3	6	1,4	6	86,4	-3,2
EMAC10190bE	0	289,4	3	6	1,4	6	87,4	-3,2
EMAC10190cZ	0	365,4	3	8	1,3	9	109,8	-3,2
EMAC10190cE	0	365,4	3	8	1,4	9	110,7	-3,4
EMAC10190dZ	0	363,4	3	9	0,5	8	133,3	-3,0
EMAC10190dE	0	363,4	3	9	0,5	8	134,3	-3,2
EMAC10190eZ	0	341,4	4	7	1,3	7	104,2	-3,3
EMAC10190eE	0	341,4	4	7	1,3	7	105,0	-3,3
EMAC10190fZ	0	325,4	3	6	1,5	6	86,4	-3,8
EMAC10190fE	0	325,4	3	6	1,5	6	87,4	-3,8
EMAC10190gZ	0	325,4	3	6	1,6	6	86,7	-4,3
EMAC10190gE	0	325,4	3	6	1,5	6	87,0	-3,7
EMAC10190hZ	0	349,4	3	8	1,6	9	101,4	-3,5
EMAC10190hE	0	349,4	3	8	1,6	9	102,4	-3,8
EMAC10190iZ	0	311,3	3	6	1,5	6	86,3	-3,3
EMAC10190iE	0	311,3	3	6	1,5	6	87,4	-3,3
EMAC10190jZ	0	305,4	3	7	1,1	7	94,7	-2,9
EMAC10190jE	0	305,4	3	7	1,1	7	95,7	-3,0
EMAC10190kZ	0	293,3	3	6	1,3	6	86,4	-3,0
EMAC10190kE	0	293,3	3	6	1,3	6	87,4	-3,1
EMAC10190lZ	0	309,8	3	6	1,5	6	86,4	-3,4
EMAC10190lE	0	309,8	3	6	1,5	6	87,4	-3,4
EMAC10190mZ	0	265,3	3	7	0,5	6	93,5	-2,2
EMAC10190mE	0	265,3	3	7	0,5	6	97,1	-2,2

Table 15 Predicted properties for the series EMAC10191

Molecule	#stars	MW	HBD	HBA	QPlogPo/w	#rotor	PSA	QPlogS
-----------------	---------------	-----------	------------	------------	------------------	---------------	------------	---------------

	0 - 5	130 – 725	0-6	2- 20	-2- 6.5	0 - 15	7 - 200.0	-6.5 - 0.5
EMAC10191aR	0	392,5	3	9	1,6	5	108,1	-4,5
EMAC10191bS	0	363,4	3	8	1,5	4	104,7	-4,3
EMAC10191bR	0	363,4	3	8	1,5	4	104,6	-4,2
EMAC10191cS	0	439,5	3	10	1,3	7	128,8	-2,9
EMAC10191cR	0	439,5	3	10	1,3	7	129,1	-2,8
EMAC10191dS	0	437,5	3	11	0,4	6	152,1	-2,8
EMAC10191dR	0	437,5	3	11	0,4	6	152,1	-2,7
EMAC10191eS	0	415,5	4	8	1,5	5	119,9	-4,2
EMAC10191eR	0	415,5	4	8	1,5	5	119,9	-4,2
EMAC10191fS	0	399,5	3	8	2,1	4	104,6	-4,9
EMAC10191fR	0	399,5	3	8	2,1	4	104,7	-4,8
EMAC10191gS	0	399,5	3	8	2,0	4	104,4	-4,6
EMAC10191gR	0	399,5	3	8	2,0	4	104,2	-4,6
EMAC10191hS	0	423,5	3	9	1,8	7	119,8	-4,7
EMAC10191hR	0	423,5	3	9	1,8	7	119,7	-4,7
EMAC10191iS	0	385,4	3	8	1,6	4	104,7	-4,2
EMAC10191iR	0	385,4	3	8	1,6	4	104,7	-4,3
EMAC10191jS	0	379,4	3	8	1,3	5	112,9	-4,0
EMAC10191jR	0	379,4	3	8	1,3	5	112,9	-3,9
EMAC10191kS	0	367,4	3	8	1,4	4	104,6	-4,1
EMAC10191kR	0	367,4	3	8	1,4	4	104,6	-4,0
EMAC10191lS	0	383,9	3	8	1,7	4	104,7	-4,4
EMAC10191lR	0	383,9	3	8	1,7	4	104,7	-4,4
EMAC10191mS	0	339,4	3	8	0,7	4	113,3	-3,1
EMAC10191mR	0	339,4	3	8	0,7	4	113,3	-3,6

Table 16 Ranges of pharmacokinetics properties calculated considering 95% of drugs

QPPCaco	< 25 poor, >500 great
QPPMDCK	< 25 poor, >500 great
PercentHumanOralAbsorption	> 80 % is high < 25 % is
(%OA)	poor

QPlogHERG	>-5
CNS	- 2 (inactive) to +2 (active)
QPlogBB	-3.0 - 1.2
QPlogKhsa	-1.5 - 1.5

Table 17 Predicted pharmacokinetics properties for the series **EMAC10155**

Molecule	QPPCaco	QPPMDCK	%OA	QPlogHERG	CNS	QPlogBB	QPlogKhsa
	< 25 poor, >500 great	< 25 poor, >500 great	> 80 % is high, < 25 % is poor	>-5	- 2 (inactive) to +2 (active)	-3.0 - 1.2	-1.5 - 1.5
EMAC10155A	752,5	363,8	93,5	-5,9	-1	-0,8	-0,2
EMAC10155B	752,4	363,7	92,1	-5,8	-1	-0,9	-0,4
EMAC10155C	752,9	962,4	95,0	-5,9	0	-0,6	-0,2
EMAC10155D	753,2	653,8	93,0	-5,8	0	-0,7	-0,3
EMAC10155E	89,7	36,5	70,7	-5,9	-2	-1,8	-0,4
EMAC10155F	89,7	36,5	70,7	-5,9	-2	-1,8	-0,4
EMAC10155G	752,3	363,7	100,0	-7,2	-1	-1,0	0,3
EMAC10155H	758,6	878,0	93,9	-5,7	0	-0,6	-0,3
EMAC10155I	826,4	1928,2	100,0	-5,9	0	-0,5	-0,1
EMAC10155L	752,6	363,8	91,6	-5,9	-1	-0,8	-0,3
EMAC10155M	753,0	896,6	94,6	-5,8	0	-0,6	-0,2

Table 18 Predicted pharmacokinetics properties for the series **EMAC10156**

Molecule	QPPCaco	QPPMDCK	%OA	QPlogHERG	CNS	QPlogBB	QPlogKhsa
	< 25 poor, >500 great	< 25 poor, >500 great	> 80 % is high, < 25 % is poor	>-5	- 2 (inactive) to +2 (active)	-3.0 - 1.2	-1.5 - 1.5

EMAC10156A	439,1	203,2	92,1	-6,2	-2	-1,3	0,0
EMAC10156B	443,0	205,2	90,6	-6,1	-2	-1,4	-0,2
EMAC10156C	439,2	537,4	93,6	-6,2	-2	-1,1	-0,1
EMAC10156D	439,5	365,2	91,5	-6,1	-2	-1,2	-0,2
EMAC10156E	52,1	20,3	69,2	-6,2	-2	-2,5	-0,3
EMAC10156F	52,4	20,4	69,3	-6,2	-2	-2,5	-0,3
EMAC10156G	438,7	203,1	100,0	-7,4	-2	-1,5	0,4
EMAC10156H	446,2	494,9	92,4	-6,0	-2	-1,1	-0,1
EMAC10156I	483,1	1079,6	96,5	-6,1	-1	-1,0	0,0
EMAC10156L	443,2	205,3	90,2	-6,3	-2	-1,3	-0,2
EMAC10156M	439,2	500,6	93,1	-6,2	-2	-1,1	-0,1

Table 19 Predicted pharmacokinetics properties for the series **EMAC10157**

Molecule	QPPCaco	QPPMDCK	%OA	QPlogHERG	CNS	QPlogBB	QPlogKhsa
	< 25 poor, >500 great	< 25 poor, >500 great	> 80 % is high, < 25 % is poor	>-5	- 2 (inactive) to +2 (active)	-3.0 - 1.2	-1.5 - 1.5
EMAC10157A	631,9	301,2	100,0	-6,6	-2	-1,4	0,4
EMAC10157B	628,1	299,3	100,0	-6,2	-2	-1,4	0,2
EMAC10157C	627,7	790,6	100,0	-6,3	-2	-1,1	0,4
EMAC10157D	631,3	540,2	100,0	-6,2	-2	-1,2	0,3

EMAC10157E	74,9	30,1	79,1	-6,3	-2	-2,5	0,1
EMAC10157F	75,3	30,2	79,1	-6,3	-2	-2,5	0,1
EMAC10157G	631,9	301,2	96,9	-7,5	-2	-1,5	0,9
EMAC10157H	635,7	726,0	100,0	-6,1	-2	-1,1	0,3
EMAC10157I	518,3	967,0	100,0	-5,4	-2	-1,0	0,3
EMAC10157L	629,0	299,7	100,0	-6,4	-2	-1,3	0,2
EMAC10157M	631,4	741,1	100,0	-6,3	-2	-1,2	0,3

Table 20 Predicted pharmacokinetics properties for the series **EMAC10158**

Molecule	QPPCaco	QPPMDCK	%OA	QPlogHERG	CNS	QPlogBB	QPlogKhsa
	< 25 poor, >500 great	< 25 poor, >500 great	> 80 % is high, < 25 % is poor	>-5	- 2 (inactive) to +2 (active)	-3.0 - 1.2	-1.5 - 1.5
EMAC10158a	214,2	112,7	100,0	-5,2	0	-0,1	0,3
EMAC10158b	214,2	112,7	100,0	-5,2	0	-0,1	0,1
EMAC10158c	214,2	298,0	100,0	-5,3	1	0,1	0,3
EMAC10158d	214,2	202,4	100,0	-5,1	1	0,1	0,2
EMAC10158e	25,4	11,3	83,7	-5,3	-1	-1,0	0,1
EMAC10158f	26,2	11,6	83,9	-5,2	-1	-1,0	0,1
EMAC10158g	214,3	112,7	100,0	-6,7	0	-0,2	0,8
EMAC10158h	214,3	290,3	100,0	-5,0	1	0,2	0,2

EMAC10158i	214,3	545,9	100,0	-5,1	1	0,3	0,4
EMAC10158l	214,2	112,7	100,0	-5,2	0	0,0	0,2
EMAC10158m	214,2	277,1	100,0	-5,2	1	0,1	0,3

Table 21 Predicted pharmacokinetics properties for the series **EMAC10159**

Molecule	QPPCaco	QPPMDCK	%OA	QPlogHERG	CNS	QPlogBB	QPlogKhsa
	< 25 poor, >500 great	< 25 poor, >500 great	> 80 % is high, < 25 % is poor	>-5	- 2 (inactive) to +2 (active)	-3.0 - 1.2	-1.5 - 1.5
EMAC10159a	100,3	52,4	83,7	-3,5	-1	-0,9	0,3
EMAC10159b	100,3	52,4	82,4	-3,5	-1	-1,0	0,1
EMAC10159c	100,3	138,5	85,2	-3,5	-1	-0,7	0,2
EMAC10159d	100,3	94,0	83,2	-3,4	-1	-0,8	0,1
EMAC10159e	11,9	5,2	61,2	-3,5	-2	-1,9	0,1
EMAC10159f	11,9	5,2	61,2	-3,5	-2	-1,9	0,1
EMAC10159g	100,2	52,4	91,4	-4,9	-2	-1,1	0,7
EMAC10159h	100,3	129,2	84,0	-3,3	-1	-0,7	0,2
EMAC10159i	100,4	244,9	87,2	-3,4	-1	-0,6	0,3
EMAC10159l	100,3	52,4	81,9	-3,5	-1	-0,9	0,1
EMAC10159m	100,2	128,9	84,8	-3,5	-1	-0,8	0,2

Table 22 Predicted pharmacokinetics properties for the series **EMAC10160**

Molecule	QPPCaco	QPPMDCK	%OA	QPlogHERG	CNS	QPlogBB	QPlogKhsa
	< 25 poor, >500 great	< 25 poor, >500 great	> 80 % is high, < 25 % is poor	>-5	- 2 (inactive) to +2 (active)	-3.0 - 1.2	-1.5 - 1.5
EMAC10160a	111,7	58,9	91,1	-3,8	-2	-1,1	0,7
EMAC10160b	111,7	58,9	89,8	-3,8	-2	-1,2	0,5
EMAC10160c	111,7	155,6	92,5	-3,9	-1	-0,9	0,6
EMAC10160d	111,7	105,7	90,6	-3,8	-1	-1,0	0,5
EMAC10160e	13,3	5,9	68,5	-3,9	-2	-2,2	0,4
EMAC10160f	13,3	5,9	68,5	-3,9	-2	-2,2	0,4
EMAC10160g	111,7	58,9	85,9	-5,1	-2	-1,3	1,1
EMAC10160h	111,7	145,2	91,3	-3,7	-1	-0,9	0,6
EMAC10160i	111,5	277,1	81,6	-3,7	-1	-0,8	0,7
EMAC10160l	111,6	58,8	89,2	-3,9	-2	-1,1	0,5
EMAC10160m	111,6	144,8	92,1	-3,8	-1	-1,0	0,6

Table 23 Predicted pharmacokinetics properties for the series **EMAC10161**

Molecule	QPPCaco	QPPMDCK	%OA	QPlogHERG	CNS	QPlogBB	QPlogKhsa
	< 25 poor, >500 great	< 25 poor, >500 great	> 80 % is high, < 25 % is poor	>-5	- 2 (inactive) to +2 (active)	-3.0 - 1.2	-1.5 - 1.5

EMAC10161A	383,9	175,8	95,3	-6,5	-2,0	-1,6	0,2
EMAC10161B	380,9	174,3	93,6	-6,4	-2,0	-1,7	0,03
EMAC10161C	247,2	288,8	94,1	-6,9	-2,0	-1,8	0,3
EMAC10161D	383,6	315,3	94,7	-6,4	-2,0	-1,5	0,1
EMAC10161E	45,6	17,6	72,4	-6,5	-2,0	-2,8	-0,1
EMAC10161F	31,7	11,9	70,5	-6,8	-2,0	-3,1	0,1
EMAC10161G	383,3	175,5	90,3	-7,7	-2,0	-1,8	0,7
EMAC10161H	412,8	534,8	96,6	-6,3	-2,0	-1,3	0,1
EMAC10161I	404,4	860,9	100,0	-6,3	-2,0	-1,3	0,3
EMAC10161L	381,4	174,6	93,3	-6,6	-2,0	-1,6	0,1
EMAC10161M	381,2	429,5	96,3	-6,5	-2,0	-1,4	0,2

Table 24 Predicted pharmacokinetics properties for the series **EMAC10162**

Molecule	QPPCaco	QPPMDCK	%OA	QPlogHERG	CNS	QPlogBB	QPlogKhsa
	< 25 poor, >500 great	< 25 poor, >500 great	> 80 % is high, < 25 % is poor	>-5	- 2 (inactive) to +2 (active)	-3.0 - 1.2	-1.5 - 1.5
EMAC10162A	75,4	38,5	83,1	-3,7	-2,0	-1,2	0,4
EMAC10162B	75,4	38,5	81,8	-3,7	-2,0	-1,2	0,2
EMAC10162C	75,4	101,7	84,6	-3,7	-1,0	-0,9	0,3
EMAC10162D	75,4	69,1	82,6	-3,6	-2,0	-1,0	0,2

EMAC10162E	9,1	3,9	60,8	-3,7	-2,0	-2,2	0,2
EMAC10162F	9,0	3,9	60,6	-3,7	-2,0	-2,2	0,2
EMAC10162G	77,1	39,4	78,0	-5,0	-2,0	-1,3	0,8
EMAC10162H	75,4	104,6	83,5	-3,5	-1,0	-0,9	0,3
EMAC10162I	77,1	185,4	86,7	-3,6	-1,0	-0,8	0,4
EMAC10162L	77,1	39,4	81,5	-3,7	-2,0	-1,1	0,2
EMAC10162M	75,4	94,7	84,2	-3,7	-1,0	-0,9	0,3

Table 25 Predicted pharmacokinetics properties for the series **EMAC10190**

Molecule	QPPCaco	QPPMDCK	%OA	QPlogHERG	CNS	QPlogBB	QPlogKhsa
	< 25 poor, >500 great	< 25 poor, >500 great	> 80 % is high, < 25 % is poor	>-5	- 2 (inactive) to +2 (active)	-3.0 - 1.2	-1.5 - 1.5
EMAC10190aE	276,5	123,3	79,2	-5,9	-2	-1,5	-0,4
EMAC10190aZ	296,2	136,2	79,7	-5,9	-2	-1,5	-0,4
EMAC10190bZ	306,4	137,7	79,7	-5,7	-2	-1,4	-0,4
EMAC10190bE	286,4	128,0	79,2	-5,8	-2	-1,4	-0,4
EMAC10190cZ	303,6	139,6	79,2	-5,3	-2	-1,6	-0,5
EMAC10190cE	286,5	128,1	78,9	-5,6	-2	-1,6	-0,5
EMAC10190dZ	79,9	33,0	64,0	-5,5	-2	-2,1	-0,6
EMAC10190dE	75,1	30,1	63,7	-5,8	-2	-2,2	-0,6

EMAC10190eZ	162,1	70,8	74,1	-6,2	-2	-1,7	-0,4
EMAC10190eE	150,1	63,7	73,5	-6,3	-2	-1,8	-0,4
EMAC10190fZ	306,1	140,8	80,3	-6,5	-2	-1,4	-0,2
EMAC10190fE	286,3	128,0	79,8	-6,5	-2	-1,4	-0,2
EMAC10190gZ	193,2	85,6	77,0	-7,0	-2	-1,7	-0,2
EMAC10190gE	288,1	128,9	79,8	-6,5	-2	-1,4	-0,2
EMAC10190hZ	302,1	135,7	80,7	-5,8	-2	-1,6	-0,4
EMAC10190hE	286,1	127,9	80,5	-6,1	-2	-1,7	-0,4
EMAC10190iZ	303,6	395,2	80,0	-5,6	-2	-1,1	-0,5
EMAC10190iE	286,5	369,3	79,6	-5,6	-2	-1,2	-0,5
EMAC10190jZ	304,2	139,8	78,0	-5,7	-2	-1,4	-0,5
EMAC10190jE	285,7	130,7	77,6	-5,8	-2	-1,5	-0,5
EMAC10190kZ	306,0	246,9	78,8	-5,6	-2	-1,2	-0,5
EMAC10190kE	287,5	236,1	78,4	-5,8	-2	-1,3	-0,5
EMAC10190lZ	305,8	346,2	80,2	-5,8	-2	-1,2	-0,4
EMAC10190lE	285,4	314,0	79,7	-5,8	-2	-1,2	-0,4
EMAC10190mZ	290,4	133,0	74,0	-5,5	-2	-1,3	-0,7
EMAC10190mE	280,5	128,1	73,5	-5,4	-2	-1,3	-0,7

Table 26 Predicted pharmacokinetics properties for the series **EMAC10191**

Molecule	QPPCaco < 25 poor, >500 great	QPPMDCK < 25 poor, >500 great	%OA > 80 % is high, < 25 % is poor	QPlogHERG >-5	CNS - 2 (inactive) to +2 (active)	QPlogBB -3.0 - 1.2	QPlogKhsa -1.5 - 1.5
EMAC10191aR	155,2	115,2	75,5	-5,8	-2	-1,6	-0,2
EMAC10191bS	160,1	119,3	75,1	-5,7	-2	-1,5	-0,2
EMAC10191bR	160,3	116,8	75,1	-5,6	-2	-1,5	-0,2
EMAC10191cS	233,1	179,0	76,7	-3,7	-2	-1,2	-0,4
EMAC10191cR	225,1	168,3	76,4	-3,5	-2	-1,2	-0,4
EMAC10191dS	59,4	40,1	61,3	-3,9	-2	-1,6	-0,5
EMAC10191dR	59,4	39,1	61,2	-3,9	-2	-1,6	-0,5
EMAC10191eS	103,7	72,4	72,0	-6,0	-2	-1,7	-0,2
EMAC10191eR	103,9	72,6	72,0	-6,0	-2	-1,7	-0,2
EMAC10191fS	160,4	119,0	78,7	-6,4	-2	-1,5	-0,1
EMAC10191fR	160,3	116,7	78,6	-6,4	-2	-1,5	0,0
EMAC10191gS	163,2	111,7	78,3	-6,2	-2	-1,4	-0,1
EMAC10191gR	162,2	113,9	78,4	-6,3	-2	-1,5	-0,1
EMAC10191hS	160,1	116,5	76,9	-5,9	-2	-1,8	-0,2
EMAC10191hR	160,2	116,1	76,9	-5,9	-2	-1,8	-0,2
EMAC10191iS	160,4	324,9	75,9	-5,3	-2	-1,2	-0,3

EMAC10191iR	160,6	332,9	75,9	-5,4	-2	-1,2	-0,3
EMAC10191jS	161,2	120,0	74,1	-5,6	-2	-1,5	-0,3
EMAC10191jR	161,0	116,9	74,0	-5,5	-2	-1,5	-0,3
EMAC10191kS	161,6	215,9	74,9	-5,6	-2	-1,3	-0,3
EMAC10191kR	161,0	210,4	74,9	-5,6	-2	-1,3	-0,3
EMAC10191lS	160,3	287,4	76,2	-5,6	-2	-1,2	-0,3
EMAC10191lR	160,8	288,1	76,2	-5,6	-2	-1,3	-0,3
EMAC10191mS	160,2	106,0	70,3	-5,2	-2	-1,3	-0,5
EMAC10191mR	99,6	61,9	66,9	-5,8	-2	-1,7	-0,5

All compounds showed from 0 to 2 stars, which indicates that most of them did not exceed the ranges allowed for the following properties: MW, dipole, IP, EA, SASA, FOSA, FISA, PISA, WPSA, PSA, volume, #rotor, donorHB (HBD), accptHB (HBA), glob, QPpolrz, QPlogPC16, QPlogPoct, QPlogPw, QPlogPo/w, logS, QPlogKhsa, QPlogBB, #metabol.

Furthermore, we reported in the **Tables (17-26)** few more ADME properties such as: QPPCaco, QPPMDCK, %OA, QPlogHERG, that contribute to depict a more complete picture.

In fact, tissue distribution is an important element of a drug pharmacokinetic (PK) profile united with knowledge of the *in vitro* activity.

The Caco-2 cell monolayer resembles the human intestinal barrier also considering their characteristic in terms of morphology, the monolayer is used routinely to predict drug permeability in the intestine and the fraction of dose absorbed. QSAR models have been developed to predict bioactive compound's passive permeability of gut blood-barrier using data collected experimentally studying these cells, these data do not consider the Pgp efflux.

While QSAR models based on data of compounds able to cross the membrane of MDCK (Madin-Darby Canine Kidney) cells can help to understand the ability of the compounds to reach the CNS.

In general, all the synthesized compounds have a high predicted oral absorption, a good gut absorption, except for the nitro- derivatives. The permeability values are lower for the predicted MDCK cells crossing, which indicates a predicted difficulty by these compounds to reach the central nervous system (CNS).

The only worrying property is the predicted IC₅₀ for human Ether-à-go-go-Related Gene (HERG) K⁺ Channel Blockage in some reported series.

In certain cases, the value is borderline, in others, requires more attention and should be better investigated experimentally.

Finally, predicted binding to human serum albumin (QPlogKhsa) are within -0,5-0 ranges, while the reported drugs range is between -1,5-1,5. So we can be confident that, considering these data, all the synthesized compounds can bind the plasmatic proteins but not for a long time. This should be favorable for the duration and distribution process.

In conclusion, the prediction study of the physical-chemical and PK properties is encouraging and, albeit these data should be confirmed *in vitro*, according to the obtained data and considering to apply few optimization rounds, we are confident that the most of the PK problems can be solved.

Furthermore, other strategies like proper formulations or nanotechnology applications could ultimately help to overcome their limitation to reach the tumor localization.

5.4 Synthesis of new pyrazolo[3,4-*d*]pyrimidine compounds

5.4.1 Background

Src and Abl families are overexpressed in several tumors such as CML, colon and breast cancer, childhood neuroblastoma, osteosarcoma, prostate and stomach cancer.

CML therapies include the use of Imatinib, but over time, resistance have been observed; for this reason, second-generation drugs have been studied, like Dasatinib. With this new therapies, T315I mutation has appeared, which confers resistance to the second-generation drugs.

Compounds with pyrazolo[3,4-*d*]pyrimidine structure are able to inhibit the phosphorylation of tyrosine kinase Src, and consequentially the proliferation of tumor cells. Moreover, they are able to induce the apoptotic mechanism. Therefore, compounds owning the pyrazolo[3,4-*d*]pyrimidine structure turned out to be good inhibitors for T315I mutant cells.

With this purpose, during my stay at the Lead Discovery Siena (LDS) research company, we have designed and synthesized new pyrazolo[3,4-*d*]pyrimidine structure compounds substituted in position N-1, C-4 and C-6 (**Fig. 39**). According to what observed in a previous research, performed by the LDS team, we have identified a specific substitution pattern to be introduced in the pyrazolo[3,4-*d*]pyrimidine central core. In particular we have focused our attention on the introduction of different substituents in the positions 4 and 6 of the heterocycle. Therefore, the introduction of a chlorine atom in the position 4 was investigated to evaluate its impact on the biological activity. Moreover, we have investigated the effect on the biological properties of both a methylthio and an hydroxyethylamino substituent in the position 6 of the pyrazolo[3,4-*d*]pyrimidine nucleus. To prepare the desired compounds a synthetic pathway was devised (**Scheme 3**) based on the so called “pyrimidine approach” according to the starting point of the synthetic procedure.

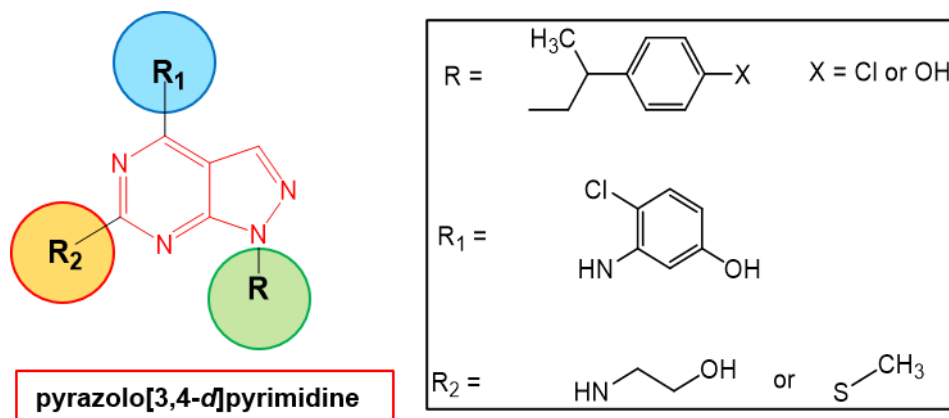
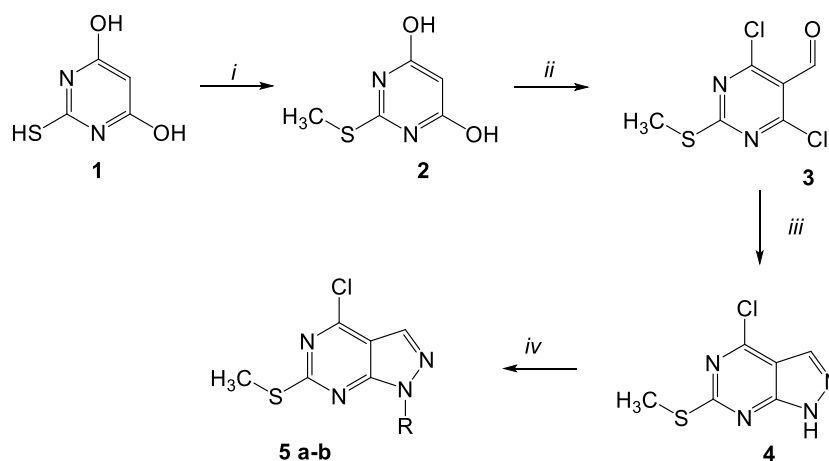


Figure 39 Scaffold pyrazolo[3,4-d]pyrimidine

PYRIMIDINE APPROACH

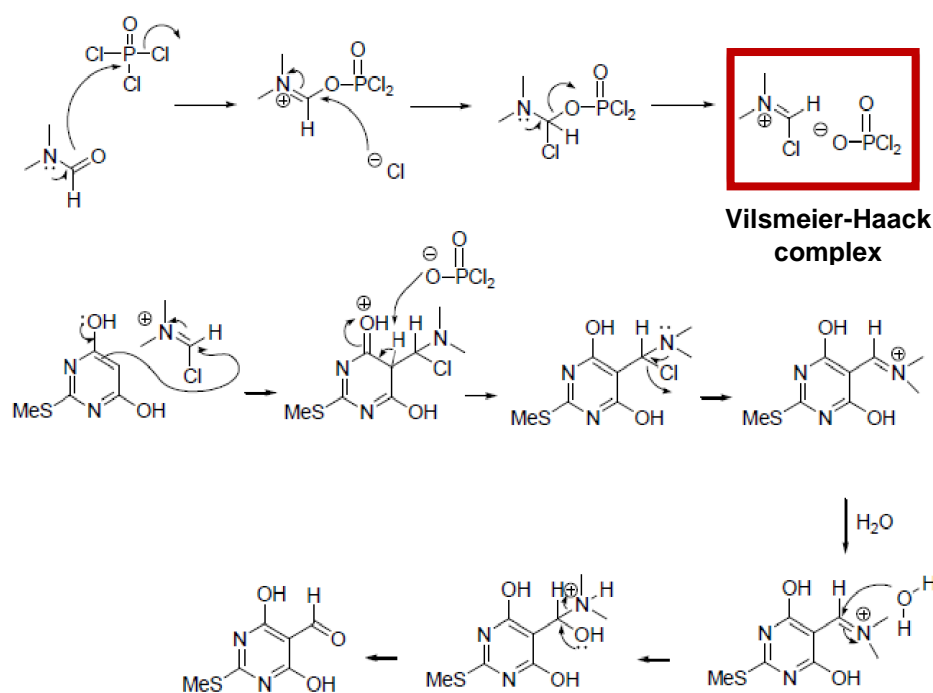
The recent pyrimidine approach provides the use of appropriately substituted pyrimidines as precursor of the pyrazolo-pyrimidine core. One of the classic procedures is described in

Scheme 3.



Scheme 3 Schematic synthetic pathway to pyrazolo-pyrimidine core .) Reagents and conditions: (i.) KOH, MeI, H₂O, reflux, 3 h; (ii). POCl₃, DMF, reflux, 12 h; (iii.) TEA, N₂H₄·H₂O, dioxane, rt, 5 h; (iv.) R₂OH, Ph₃P, DIAD, anhydrous THF, μW 100 °C, 3 min

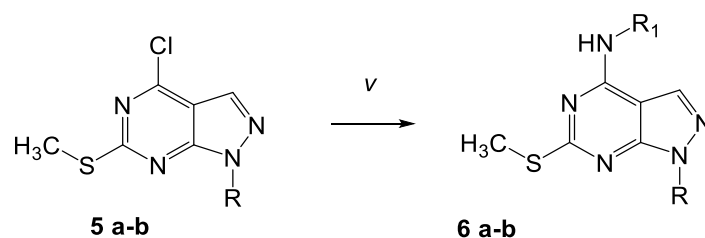
The alkylation of 2-thiobarbituric acid, under Vilsmeier-Haack conditions lead to the introduction of an aldehyde moiety in the 5 position of the methylthiobarbituric acid (Scheme 4).



Scheme 4 General mechanism of Vilsmeier-Haach formylation

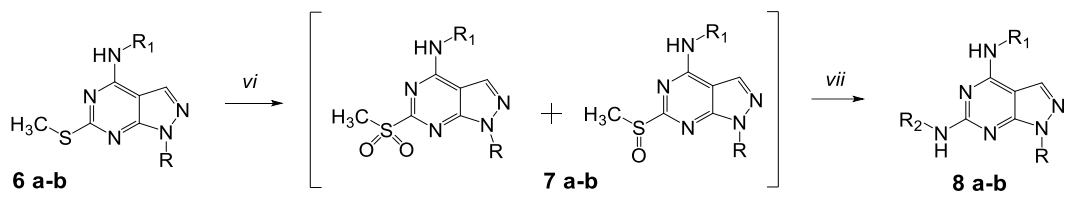
The obtained compound is cyclized to obtain the pyrazolo-pyrimidine core, which in turn is substituted in position N-1 with the opportune alcohol. To speed up the cyclization reaction, a procedure with the use of microwave have been studied. The substitution in position N-1 is obtained with a Mitsunobu reaction: recent studies have demonstrated that this reaction is regioselective and efficient.

To obtain the amino substitution in position C-4 of the pyrazolo-pyrimidine core, is necessary an aromatic nucleophilic substitution with alcohol solvent (**Scheme 5**).

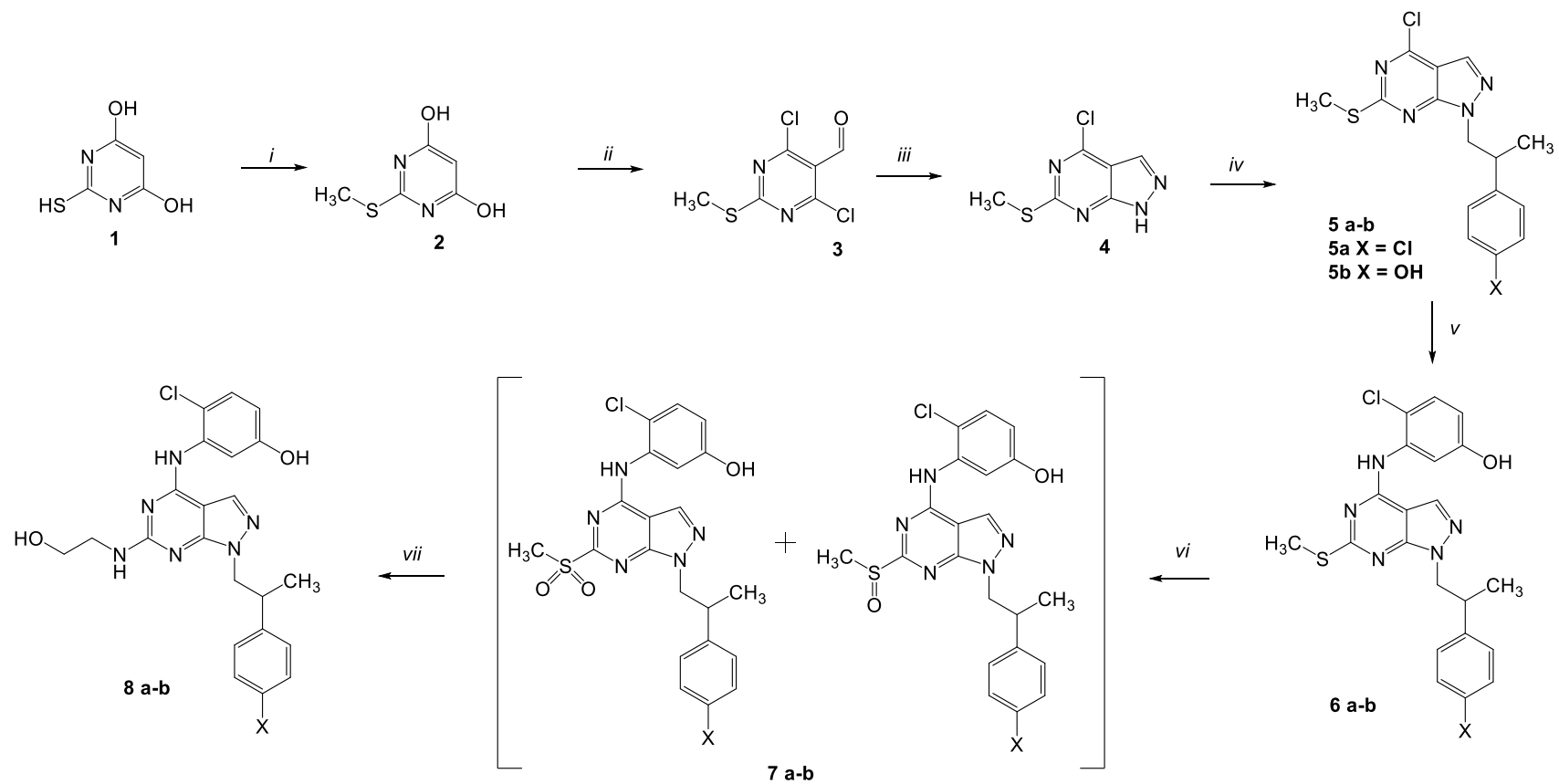


Scheme 5 Schematic procedure for the substitution in C-4 position. Reagents and conditions: (v.) amine, EtOH, reflux, 12 h

In literature different procedure have been studied for selective substitution in position C-6 of pyrazolo-pyrimidine core. The thiomethyl group, after reaction with oxidizing agent, take to formation of corresponding sulphone, which being replacing with the opportune nucleophile, in this case an aliphatic amine (**Scheme 7**).



Scheme 6 Schematic procedure for C-6 substitution. Reagents and conditions: (vi.) m-CPBA, DCM, rt, 2 h; (vii.) ETA, THF, 40 °C, overnight



Scheme 7 (i.) KOH, MeI, H₂O, reflux, 3 h; (ii.) POCl₃, DMF, reflux, 12 h; (iii.) TEA, N₂H₄·H₂O, dioxane, rt, 5 h; (iv.) R₂OH, Ph₃P, DIAD, anhydrous THF, μ W 100 °C, 3 min; (v.) amine, EtOH, reflux, 12 h; (vi.) m-CPBA, DCM, rt, 2 h; (vii.) ETA, THF, 40 °C, overnight.

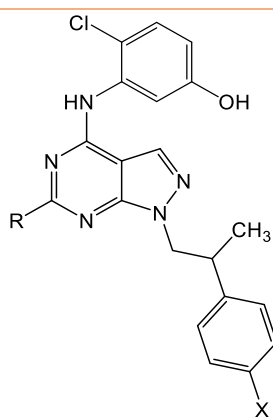
5.4.2 Biological results and discussion

The pyrazolo[3,4-*d*]pyrimidine derivatives were submitted to enzymatic assay to evaluate their activity and selectivity towards Abl and c-Src, and were submitted to cells assay to evaluate their activity toward K562 cells. The results are show in **Table 27**.

All of the compounds are micromolar inhibitors of Abl and c-Src. In particular, compound **8a** show good value of IC₅₀ in micromolar range against K562 cells, respect to compounds **6a** and **6b**, with a thiomethyl group in position C-6.

Compounds **6b** and **8a**, present high selectivity toward c-Src with a K_i value of 0.077 μM and 0.0198 μM respectively.

Table 27 Inhibition data towards Abl, c-Src and K652 cells of compounds 6a, 6b and 8a



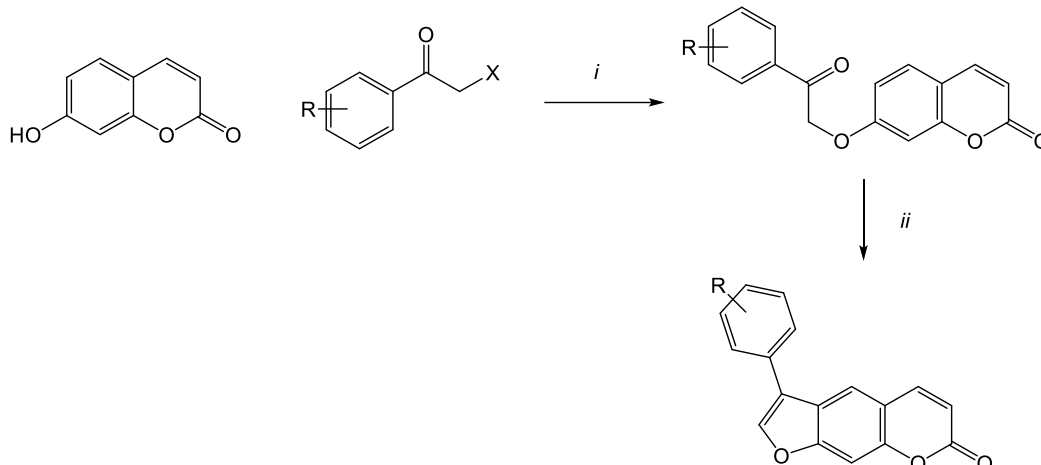
Compound	X	R	Abl K _i (μM)	c-Src K _i (μM)	K562 cells IC ₅₀ (μM)
6b	OH	SCH ₃	0.0225	0.077	7.76 ± 1.2
6a	Cl	SCH ₃	0.0192	0.1585	6.46 ± 0.5
8a	Cl	NHCH ₂ CH ₂ OH	0.0151	0.0198	0.59 ± 0.7
Imatinib			0.013	31.0	0.37±0.09

5.4.3 Conclusions

Three different pyrazolo[3,4-*d*]pyrimidines were synthesized and tested for their ability to inhibit proliferation of K562 cells, a Bcr-Abl-positive human leukemia cell lines, previously found to be dual c-Src-Abl inhibitors. These results corroborate the hypothesis that pyrazolo[3,4-*d*]pyrimidines could be advantageous for design of new dual c-Src-Abl inhibitors. In this context, further exploration and might constitute the basis for future development for the pathways involved in the proliferation of leukemia cell lines.

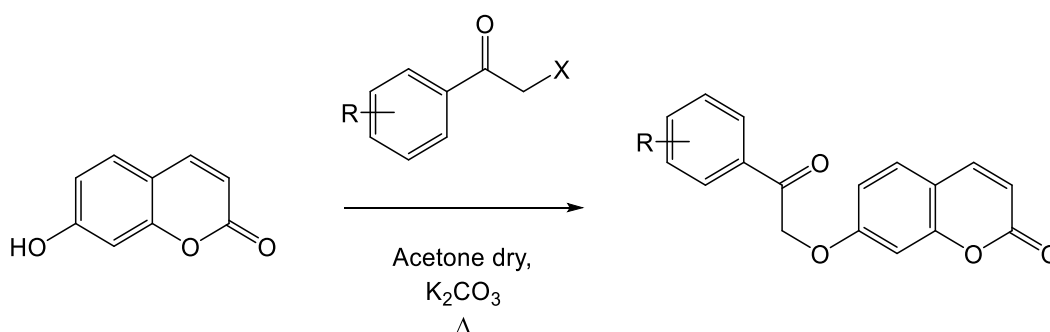
EXPERIMENTAL SECTION

EMAC 10155 (a-m) and EMAC 10158 (a-m)



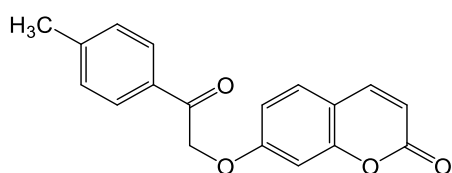
Scheme 8 Synthesis of derivatives **EMAC 10155 (a-m)** and **EMAC 10158 (a-m)**: (i.) 2-bromo/2-chloro-acetophenone, K₂CO₃, acetone, Δ; (ii.) NaOH 1N, Δ

General method for the synthesis of compounds EMAC 10155 (a-m)



Equimolar amounts of 7-hydroxycoumarin (1,8 mmol), and potassium carbonate (1,8 mmol) were stirred in dry acetone (5 mL), then the appropriate halogen-acetophenone (1,8 mmol) was added, and the reaction mixture was stirred at reflux until the end of the reaction. The reaction mixture was cooled to room temperature to obtain a solid which was dissolved in methanol and poured into crushed ice. The mixture was stirred until ice melting, then HCl 10% was added drop to drop to obtain the desired product, that was filtered.

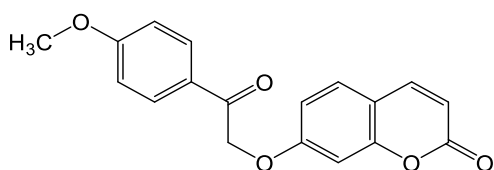
EMAC 10155 A: 7-(2-oxo-2-(p-tolyl)ethoxy)-2H-chromen-2-one



^1H NMR (400 MHz, DMSO) δ 7.99 (d, J = 9.5 Hz, 1H, CH-Ar), 7.94 (d, J = 8.2 Hz, 2H, CH-Ar), 7.63 (d, J = 8.6 Hz, 1H, CH-Ar), 7.39 (d, J = 8.0 Hz, 2H, CH-Ar), 7.07 (d, J = 2.4 Hz, 1H, CH-Ar), 7.01 (dd, J = 8.6, 2.5 Hz, 1H, CH-Ar), 6.29 (d, J = 9.5 Hz, 1H, CH-Ar), 5.70 (s, 2H, $-\text{OCH}_2-$), 2.41 (s, 3H, $-\text{CH}_3$).

^{13}C NMR (101 MHz, DMSO) δ 193.20 (1C), 161.18 (1C), 160.19 (1C), 155.23 (1C), 144.40 (1C), 144.40 (1C), 131.71 (1C), 129.39 (1C), 129.32 (2C), 127.98 (2C), 112.79 (1C), 112.64 (1C), 112.59 (1C), 101.57 (1C), 70.44 (1C), 21.22 (1C).

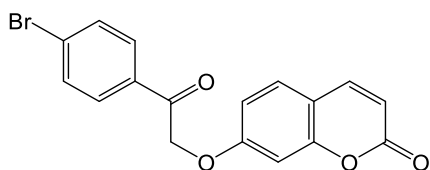
EMAC 10155 B: 7-(2-(4-methoxyphenyl)-2-oxoethoxy)-2H-chromen-2-one



^1H NMR (400 MHz, DMSO) δ 8.03 (s, 1H), 7.99 (d, J = 9.4 Hz, 2H, CH-Ar), 7.63 (d, J = 8.6 Hz, 1H, CH-Ar), 7.10 (d, J = 8.9 Hz, 2H, CH-Ar), 7.05 (d, J = 2.4 Hz, 1H, CH-Ar), 7.00 (dd, J = 8.6, 2.5 Hz, 1H, CH-Ar), 6.29 (d, J = 9.5 Hz, 1H, CH-Ar), 5.67 (s, 2H, $-\text{OCH}_2-$), 3.87 (s, 3H, $-\text{OCH}_3$).

^{13}C NMR (101 MHz, DMSO) δ 192.01 (1C), 163.64 (1C), 161.23 (1C), 160.20 (1C), 155.22 (1C), 144.23 (1C), 130.25 (2C), 129.39 (1C), 127.09 (1C), 114.04 (2C), 112.80 (1C), 112.61 (1C), 112.56 (1C), 101.55 (1C), 70.25 (1C), 55.62 (1C).

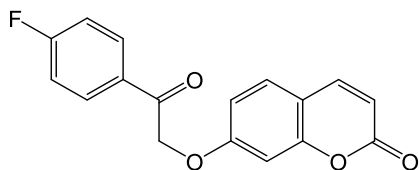
EMAC 10155 C: 7-(2-(4-bromophenyl)-2-oxoethoxy)-2H-chromen-2-one



^1H NMR (600 MHz, DMSO) δ 8.00 (d, J = 9.5 Hz, 1H, CH-Ar), 7.98 (d, J = 8.3 Hz, 2H, CH-Ar), 7.82 (d, J = 8.3 Hz, 2H, CH-Ar), 7.65 (d, J = 8.6 Hz, 1H, CH-Ar), 7.11 (d, J = 1.6 Hz, 1H, CH-Ar), 7.03 (dd, J = 8.6, 2.0 Hz, 1H, CH-Ar), 6.31 (d, J = 9.5 Hz, 1H, CH-Ar), 5.73 (s, 2H, $-\text{OCH}_2-$).

^{13}C NMR (151 MHz, DMSO) δ 193.57 (1C), 161.57 (1C), 160.69 (1C), 155.76 (1C), 144.72 (1C), 133.72 (1C), 132.37 (2C), 130.42 (2C), 129.92 (1C), 128.46 (1C), 113.32 (1C), 113.21 (1C), 113.16 (1C), 102.10 (1C), 71.04 (1C).

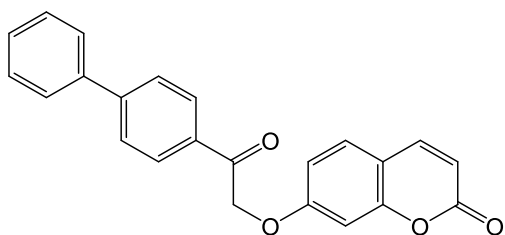
EMAC 10155 D: 7-(2-(4-fluorophenyl)-2-oxoethoxy)-2H-chromen-2-one



^1H NMR (600 MHz, DMSO) δ 8.13 (dd, $J = 8.7, 5.6$ Hz, 2H, CH-Ar), 8.00 (d, $J = 9.5$ Hz, 1H, CH-Ar Coum), 7.65 (d, $J = 8.6$ Hz, 1H, CH-Ar Coum), 7.43 (t, $J = 8.8$ Hz, 2H, CH-Ar), 7.10 (d, $J = 2.3$ Hz, 1H, CH-Ar), 7.03 (dd, $J = 8.6, 2.4$ Hz, 1H, CH-Ar), 6.31 (d, $J = 9.5$ Hz, 1H, CH-Ar), 5.74 (s, 2H, $-\text{OCH}_2-$).

^{13}C NMR (151 MHz, DMSO) δ 192.88 (1C), 166.71 (1C), 165.04 (1C), 161.62 (1C), 160.70 (1C), 155.75 (1C), 144.72 (1C), 131.49 (d, $J = 9.6$ Hz, 2C), 129.91 (1C), 116.38 (d, $J = 22.0$ Hz, 2C), 113.25 (d, $J = 19.6$ Hz), 113.14 (1C), 102.09 (1C), 70.99 (1C).

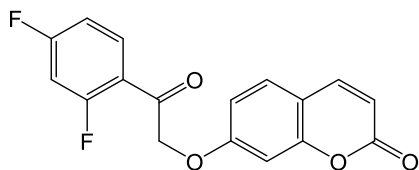
EMAC 10155 G: 7-(2-([1,1'-biphenyl]-4-yl)-2-oxoethoxy)-2H-chromen-2-one



^1H NMR (600 MHz, DMSO) δ 8.14 (d, $J = 8.4$ Hz, 2H, CH-Ar), 8.01 (d, $J = 9.5$ Hz, 1H, CH-Ar), 7.90 (d, $J = 8.4$ Hz, 2H, CH-Ar), 7.79 (d, $J = 7.5$ Hz, 2H, CH-Ar), 7.66 (d, $J = 8.6$ Hz, 1H, CH-Ar), 7.54 (t, $J = 7.6$ Hz, 2H), 7.46 (t, $J = 7.3$ Hz, 1H), 7.12 (d, $J = 2.4$ Hz, 1H, CH-Ar Coum), 7.05 (dd, $J = 8.6, 2.4$ Hz, 1H, CH-Ar Coum), 6.31 (d, $J = 9.5$ Hz, 1H, CH-Ar Coum), 5.79 (s, 2H, $-\text{OCH}_2-$).

^{13}C NMR (151 MHz, DMSO) δ 193.78 (1C), 161.69 (1C), 160.71 (1C), 155.77 (1C), 145.72 (1C), 144.74 (1C), 139.29 (1C), 133.51 (1C), 129.93 (s, 2C), 129.61 (2C), 129.15 (2C), 129.01 (2C), 127.54 (1C), 127.46 (1C), 113.33 (1C), 113.16 (d, $J = 5.1$ Hz, 1C), 102.13 (1C), 71.11 (1C).

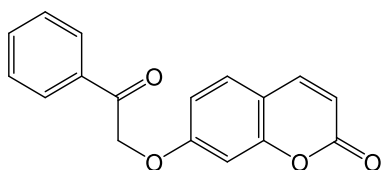
EMAC 10155 H: 7-(2-(2,4-difluorophenyl)-2-oxoethoxy)-2H-chromen-2-one



^1H NMR (600 MHz, DMSO) δ 8.04 (dd, $J = 15.3, 8.5$ Hz, 1H, CH-Ar), 8.00 (d, $J = 9.5$ Hz, 1H, CH-Ar), 7.64 (d, $J = 8.6$ Hz, 1H, CH-Ar), 7.52 – 7.49 (m, 1H, CH-Ar), 7.30 (td, $J = 8.5, 2.4$ Hz, 1H), 7.08 (d, $J = 2.4$ Hz, 1H, CH-Ar Coum), 7.02 (dd, $J = 8.6, 2.5$ Hz, 1H, CH-Ar Coum), 6.30 (d, $J = 9.5$ Hz, 1H, CH-Ar Coum), 5.54 (d, $J = 2.9$ Hz, 2H, $-\text{OCH}_2-$).

^{13}C NMR (151 MHz, DMSO) δ 191.14 (1C), 161.62 (1C), 160.70 (1C), 155.74 (s1C145.00 (1C), 144.72 (1C), 132.78 (1C), 130.18 (1C), 129.88 (1C), 113.60 (1C), 113.24 (2C), 113.16 (d, $J = 4.0$ Hz, 1C), 111.75 (1C), 105.67 (t, $J = 26.8$ Hz, 1C), 102.64 (2C), 102.03 (1C), 73.07 (d, $J = 11.2$ Hz, 1C).

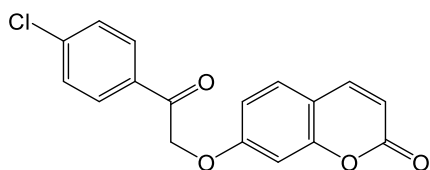
EMAC 10155 L: 7-(2-oxo-2-phenylethoxy)-2H-chromen-2-one



^1H NMR (600 MHz, DMSO) δ 8.05 (d, $J = 7.4$ Hz, 2H, CH-Ar), 8.01 (d, $J = 9.5$ Hz, 1H, CH-Ar Coum), 7.72 (t, $J = 7.0$ Hz, 1H, CH-Ar Coum), 7.65 (d, $J = 8.5$ Hz, 1H, CH-Ar Coum), 7.60 (t, $J = 7.3$ Hz, 2H, CH-Ar), 7.10 (s, 1H, Ar Coum), 7.04 (d, $J = 8.4$ Hz, 1H, Ar Coum), 6.31 (d, $J = 9.4$ Hz, 1H, Ar Coum), 5.76 (s, 2H, $-\text{OCH}_2-$).

^{13}C NMR (151 MHz, DMSO) δ 194.23 (1C), 161.67 (1C), 160.71 (1C), 155.75 (1C), 144.73 (1C), 134.71 (1C), 134.38 (1C), 129.91 (1C), 129.31 (2C), 128.39 (2C), 113.31 (1C), 113.15 (d, $J = 6.4$ Hz), 102.11 (1C), 71.07 (s1C)

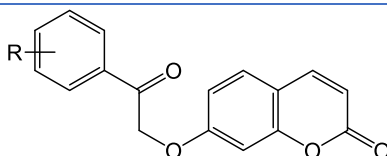
EMAC 10155 M: 7-(2-(4-chlorophenyl)-2-oxoethoxy)-2H-chromen-2-one



^1H NMR (400 MHz, DMSO) δ 8.04 (d, J = 7.0 Hz, 2H, CH-Ar), 7.99 (d, J = 9.2 Hz, 1H, CH-Ar Coum), 7.71 – 7.60 (m, J = 8.6 Hz, 3H, CH-Ar), 7.10 (s, 1H, CH-Ar Coum), 7.02 (d, J = 7.4 Hz, 1H, CH-Ar Coum), 6.30 (d, J = 9.0 Hz, 1H, CH-Ar Coum), 5.72 (s, 2H, $-\text{OCH}_2-$).

^{13}C NMR (101 MHz, DMSO) δ 192.84 (1C), 161.06 (1C), 160.20 (1C), 155.24 (1C), 144.21 (1C), 138.74 (1C), 132.87 (1C), 129.83 (2C), 129.41 (1C), 128.91 (2C), 112.81 (1C), 112.64 (1C), 112.64 (1C), 101.57 (1C), 70.54 (1C).

Table 28 Chemical, analytical, and physical data of derivatives **EMAC 10155 (a-m)**



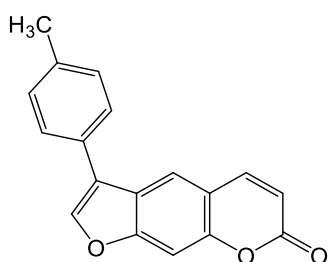
Compound	R	Aspect	MP °C	Yield %	RF AcOEt/Hex 5/1
10155 A	4-CH ₃	White solid	152-155	77	0.62
10155 B	4-OCH ₃	White solid	84-90	84	0.63
10155 C	4-Br	Dirty white solid	180-183	68	0.66
10155 D	4-F	White solid	202-204	90	0.61
10155 G	4-Phenyl	White solid	191-193	74	0.68
10155 H	2,4-F	Light orange solid	145-147	83	0.66
10155 L	4-H	White solid	168-171	74	0.61
10155 M	4-Cl	Dirty white solid	180-182		0.68

General method for the synthesis of compounds EMAC 10158 (a-m)



5 mL of 1 N sodium hydroxide were added to a suspension of the appropriate EMAC 10158 (a-m). The reaction mixture was stirred at reflux for 4 hours. Then, it was poured into crushed ice and water and it was stirred until ice melting. Hydrochloric acid was added dropwise to obtain a precipitate.

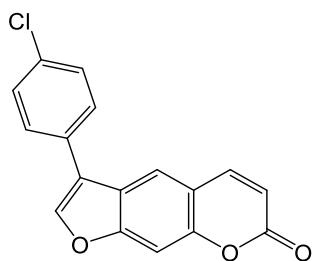
EMAC 10158 A: 3-(p-tolyl)-7H-furo[3,2-g]chromen-7-one



^1H NMR (600 MHz, DMSO) δ 8.45 (s, 1H, OCH-Ar Furoc), 8.32 (s, 1H, CH-Ar Furoc), 8.24 (d, J = 9.7 Hz, 1H, CH-Ar Furoc), 7.79 (s, 1H, CH-Ar Furoc), 7.68 (d, J = 7.5 Hz, 2H, CH-Ar), 7.35 (d, J = 7.5 Hz, 2H, CH-Ar), 6.47 (d, J = 9.5 Hz, 1H, CH-Ar Furoc), 2.38 (s, 3H, -CH₃).

^{13}C NMR (151 MHz, DMSO) δ 163.81 (1C), 160.33 (1C), 157.03 (1C), 145.57 (1C), 144.48 (1C), 137.75 (1C), 130.18 (2C), 129.84 (1C), 127.43 (2C), 123.67 (1C), 121.43 (1C), 120.71 (1C), 116.18 (1C), 114.73 (1C), 100.20 (1C), 21.31 (1C).

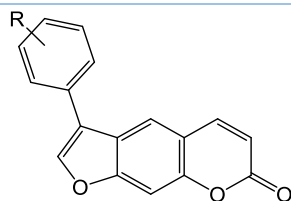
EMAC 10158 M: 3-(4-chlorophenyl)-7H-furo[3,2-g]chromen-7-one



^1H NMR (600 MHz, DMSO) δ 8.45 (s, 1H, OCH-Ar Furoc), 8.22 (s, 1H, CH-Ar Furoc), 8.12 (d, J = 9.0 Hz, 1H, CH-Ar Furoc), 7.76 – 7.67 (m, 3H, CH-Ar), 7.50 (d, J = 6.9 Hz, 2H, Ar), 6.39 (d, J = 9.1 Hz, 1H, Ar Furoc).

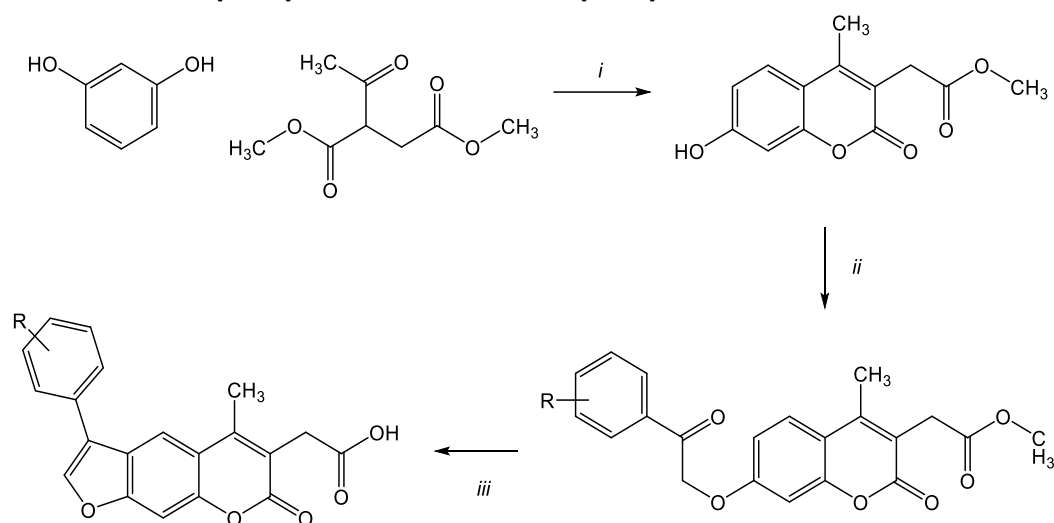
^{13}C NMR (151 MHz, DMSO) δ 160.54 (1C), 156.99 (1C), 152.20 (1C), 145.41 (1C), 145.26 (1C), 132.89 (1C), 130.06 (1C), 129.60 (2C), 129.21 (2C), 123.17 (1C), 120.58 (1C), 120.41 (1C), 116.27 (1C), 114.87 (1C), 100.27 (1C).

Table 29 Chemical, analytical, and physical data of derivatives **EMAC 10158 (a-m)**



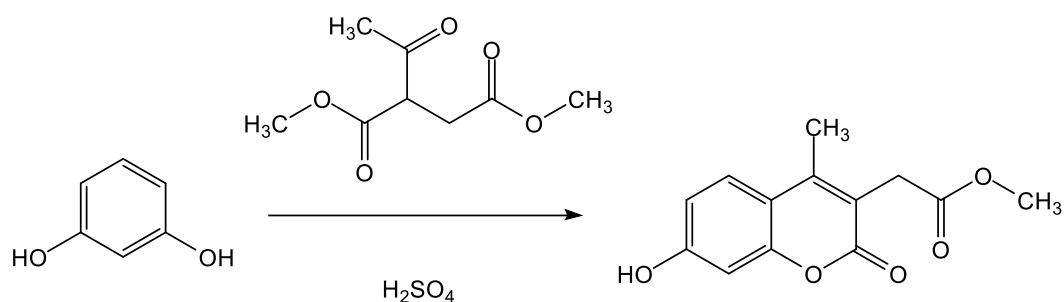
Compound	R	Aspect	MP °C	Yield %	RF AcOEt/Hex 5/1
10158 A	4-CH ₃	Light brown solid	130-133	69	0.73
10158 M	4-Cl	Yellow solid	197-198	92	0.76

EMAC 10156 (a-m) and EMAC 10159 (a-m)



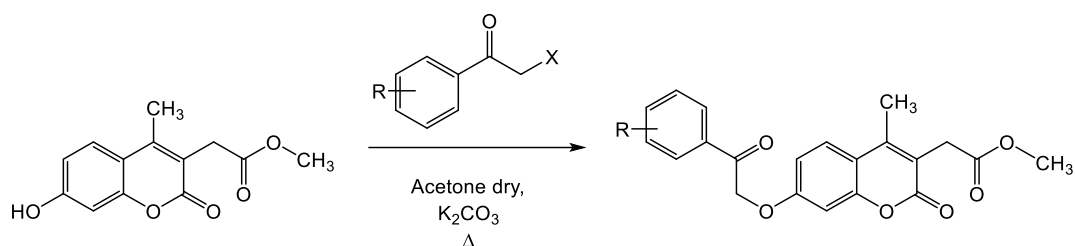
Scheme 9 Synthesis of derivatives **EMAC 10156(a-m)** and **EMAC 10159(a-m)**: (i.) dimethyl acetylsuccinate, H₂SO₄, rT, 30'; (ii.) 2-bromo/2-chloroacetophenone, acetone, K₂CO₃, Δ; (iii.) NaOH 1N, Δ

Synthesis of compound EMAC 10156



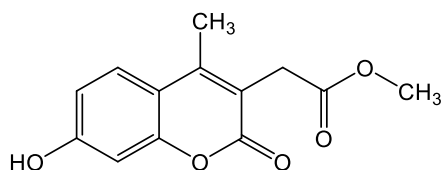
A mixture of resorcinol (4,5 mmol) and dimethyl acetylsuccinate (4,5 mmol) was stirred at room temperature. Sulfuric acid 98% (13,5 mmol) was added dropwise and the mixture was vigorously stirred until the end of the reaction. The reaction mixture was then poured into crushed ice to give a precipitate and stirred until ice melting. The formed precipitate was filtered off to obtain a white solid. The progression of the reaction was monitored by TLC (ethyl acetate/n-hexane 6/1).

General method for the synthesis of compounds EMAC 10156 (a-m)



Equimolar amounts of methyl 2-(7-hydroxy-4-methyl-2-oxo-2H-chromen-3-yl)acetate (1,8 mmol), and potassium carbonate (1,8 mmol) were stirred in dry acetone (5 mL), then the appropriate halogen-acetophenone (1,8 mmol) was added. The reaction mixture was stirred at reflux until the end of the reaction monitored by TLC. The mixture was then cooled to room temperature to obtain a solid which was dissolved in methanol and poured into crushed ice. The mixture was stirred until ice melting, then hydrochloric acid was added dropwise to give a precipitate.

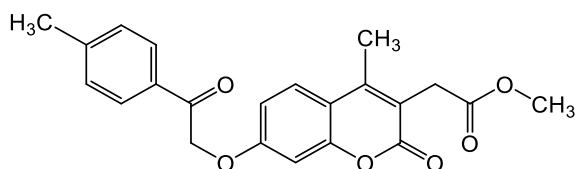
EMAC 10156: methyl 2-(7-hydroxy-4-methyl-2-oxo-2H-chromen-3-yl)acetate



^1H NMR (400 MHz, DMSO) δ 10.50 (s, 1H, -OH), 7.66 (d, J = 8.8 Hz, 1H, CH-Ar Coum), 6.82 (dd, J = 8.8, 2.4 Hz, 1H, CH-Ar Coum), 6.72 (d, J = 2.4 Hz, 1H, CH-Ar Coum), 3.65 (s, 2H, -CH₂-), 3.62 (s, 3H, -OCH₃), 2.35 (s, 3H, CH-Ar-CH₃).

^{13}C NMR (101 MHz, DMSO) δ 170.67 (1C), 160.93 (1C), 160.69 (1C), 153.43 (1C), 149.66 (1C), 126.92 (1C), 115.01 (1C), 113.06 (1C), 112.14 (1C), 101.96 (1C), 51.78 (1C), 32.30 (1C), 14.99 (1C).

EMAC 10156 A: methyl-2-oxo-7-(2-oxo-2-(p-tolyl)ethoxy)-2H-chromen-3-yl)acetate

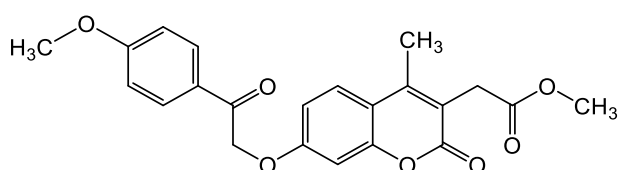


^1H NMR (400 MHz, DMSO) δ 7.94 (d, J = 8.2 Hz, 2H, CH-Ar), 7.76 (d, J = 8.9 Hz, 1H, CH-Ar Coum), 7.39 (d, J = 8.0 Hz, 2H, CH-Ar), 7.08 (d, J = 2.5 Hz, 1H, CH-Ar Coum), 7.04 (dd, J =

8.9, 2.5 Hz, 1H, CH-Ar Coum), 5.71 (s, 2H, -OCH₂-), 3.67 (s, 2H, Ar-CH₂), 3.62 (s, 3H, -OCH₃), 2.41 (s, 3H, CH-Ar-CH₃), 2.39 (s, 3H, CH-Ar-CH₃).

¹³C NMR (101 MHz, DMSO) δ 193.25 (1C), 170.56 (1C), 160.77 (1C), 160.69 (1C), 153.21 (1C), 149.45 (1C), 144.39 (1C), 131.73 (1C), 129.35 (2C), 127.90 (2C), 126.73 (1C), 116.11 (1C), 113.52 (1C), 112.72 (1C), 101.42 (1C), 70.44 (1C), 51.81 (1C), 32.36 (s1C21.22 (1C), 15.07 (1C).

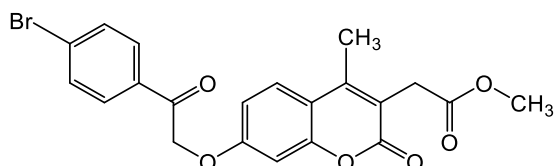
EMAC 10156 B: methyl 2-(7-(2-(4-methoxyphenyl)-2-oxoethoxy)-4-methyl-2-oxo-2H-chromen-3-yl)acetate



¹H NMR (400 MHz, DMSO) δ 8.02 (d, *J* = 8.8 Hz, 2H, CH-Ar), 7.75 (d, *J* = 8.9 Hz, 1H, CH-Ar Coum), 7.10 (d, *J* = 8.8 Hz, 2H, CH-Ar), 7.06 (d, *J* = 2.3 Hz, 1H, CH-Ar Coum), 7.03 (dd, *J* = 8.8 Hz, 1H, CH-Ar Coum), 5.67 (s, 2H, -OCH₂-), 3.87 (s, 3H, CH-Ar-OCH₃), 3.67 (s, 2H, Ar-CH₂-), 3.62 (s, 3H-OCH₃), 2.38 (s, 3H, CH-Ar-CH₃).

¹³C NMR (101 MHz, DMSO) δ 192.04 (1C), 170.56 (1C), 163.63 (1C), 160.77 (1C), 160.74 (1C), 153.20 (1C), 149.44 (1C), 130.24 (2C), 127.10 (1C), 126.71 (1C), 116.08 (1C), 114.05 (2C), 113.49 (1C), 112.71 (1C), 101.40 (1C), 70.24 (1C), 55.59 (1C), 51.81 (1C), 32.36 (1C), 15.05 (1C).

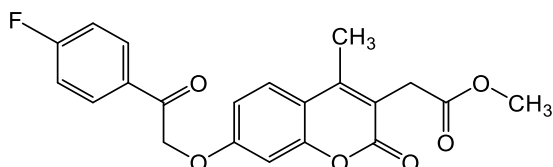
EMAC 10156 C: methyl 2-(7-(2-(4-bromophenyl)-2-oxoethoxy)-4-methyl-2-oxo-2H-chromen-3-yl)acetate



¹H NMR (400 MHz, DMSO) δ 7.97 (d, *J* = 8.7 Hz, 2H, CH-Ar), 7.81 (d, *J* = 8.7 Hz, 2H, CH-Ar), 7.76 (d, *J* = 8.9 Hz, 1H, CH-Ar Coum), 7.12 (d, *J* = 2.6 Hz, 1H, CH-Ar Coum), 7.05 (dd, *J* = 8.9, 2.6 Hz, 1H, CH-Ar Coum), 5.73 (s, 2H, -OCH₂-), 3.67 (s, 2H, Ar-CH₂-), 3.62 (s, 3H, -OCH₃), 2.39 (s, 3H, CH-Ar-CH₃).

^{13}C NMR (151 MHz, DMSO) δ 193.62 (1C), 171.04 (1C), 161.31 (1C), 161.08 (1C), 153.69 (1C), 149.94 (1C), 133.74 (1C), 132.37 (2C), 130.42 (2C), 128.44 (1C), 127.26 (1C), 116.67 (1C), 114.10 (1C), 113.25 (1C), 101.96 (1C), 71.04 (1C), 52.32 (1C), 32.88 (1C), 15.58 (1C).

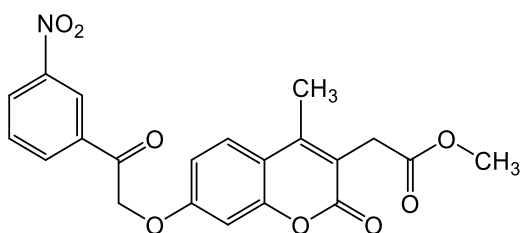
EMAC 10156 D: methyl 2-(7-(2-(4-bromophenyl)-2-oxoethoxy)-4-methyl-2-oxo-2H-chromen-3-yl)acetate



^1H NMR (400 MHz, DMSO) δ 8.15-8.10 (m, 2H, CH-Ar), 7.76 (d, $J = 9.0$ Hz, 1H, CH-Ar Coum), 7.42 (t, $J = 8.9$ Hz, 2H, CH-Ar), 7.11 (d, $J = 2.5$ Hz, 1H, CH-Ar Coum), 7.05 (dd, $J = 8.9, 2.5$ Hz, 1H, CH-Ar Coum), 5.73 (s, 2H, $-\text{OCH}_2-$), 3.67 (s, 2H, Ar- CH_2-), 3.62 (s, 3H, $-\text{OCH}_3$), 2.39 (s, 3H, CH-Ar- CH_3).

^{13}C NMR (101 MHz, DMSO) δ 192.57 (1C), 170.72 (1C), 166.63 (1C), 164.11 (1C), 160.91 (1C), 160.52 (1C), 153.11 (1C), 149.61 (1C), 130.95 (d, $J = 9.6$ Hz, 2C), 126.75 (1C), 116.06 (1C), 116.01 (1C), 115.79 (1C), 113.57 (1C), 112.78 (1C), 101.29 (1C), 70.33 (1C), 51.87 (1C), 32.30 (1C), 14.99 (1C).

EMAC 10156 F: methyl 2-(4-methyl-7-(2-(3-nitrophenyl)-2-oxoethoxy)-2-oxo-2H-chromen-3-yl)acetate

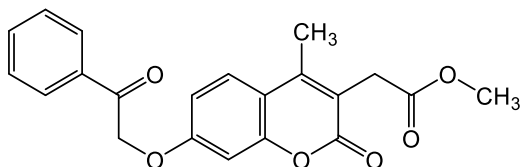


^1H NMR (400 MHz, DMSO) δ 8.75 (s, 1H, CH-Ar), 8.53 (d, $J = 6.6$ Hz, 1H, CH-Ar), 8.46 (d, $J = 6.5$ Hz, 1H, CH-Ar), 7.89 (s, 1H, CH-Ar), 7.77 (d, $J = 8.0$ Hz, 1H, CH-Ar Coum), 7.19 (s, 1H, CH-Ar Coum), 7.09 (d, $J = 7.2$ Hz, 1H, CH-Ar Coum), 5.85 (s, 2H, $-\text{OCH}_2-$), 3.68 (s, 2H, Ar- CH_2-), 3.62 (s, 3H, $-\text{OCH}_3$), 2.39 (s, 3H, CH-Ar- CH_3).

^{13}C NMR (151 MHz, DMSO) δ 193.06 (1C), 171.07 (1C), 161.27 (1C), 161.01 (1C), 153.77 (1C), 149.89 (1C), 148.52 (1C), 135.93 (1C), 134.66 (1C), 131.11 (1C), 128.44 (1C), 127.28

(1C), 122.91 (1C), 116.73 (1C), 114.17 (1C), 113.33 (1C), 101.98 (1C), 71.35 (1C), 52.33 (1C), 32.88 (1C), 15.59 (1C).

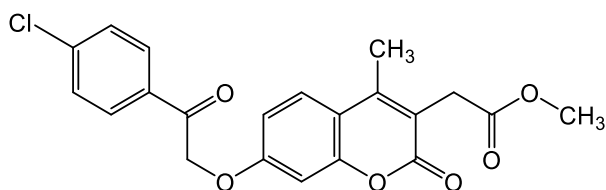
EMAC 10156 L: methyl 2-(4-methyl-2-oxo-7-(2-oxo-2-phenylethoxy)-2H-chromen-3-yl)acetate



^1H NMR (600 MHz, DMSO) δ 8.05 (d, J = 7.6 Hz, 2H, CH-Ar), 7.77 (d, J = 8.9 Hz, 1H, CH-Ar Coum), 7.72 (t, J = 7.4 Hz, 1H, CH-Ar), 7.60 (t, J = 7.6 Hz, 2H, CH-Ar), 7.11 (s, 1H, CH-Ar Coum), 7.07 (d, J = 8.8 Hz, 1H, CH-Ar Coum), 5.76 (s, 2H, -OCH₂-), 3.69 (s, 2H, Ar-CH₂-), 3.63 (s, 3H, -OCH₃), 2.40 (s, 3H, CH-Ar-CH₃).

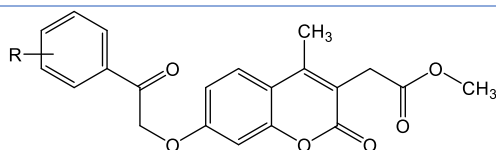
^{13}C NMR (151 MHz, DMSO) δ 194.27 (1C), 171.07 (1C), 161.29 (1C), 161.18 (1C), 153.73 (1C), 149.95 (1C), 134.73 (1C), 134.38 (1C), 129.32 (2C), 128.39 (2C), 127.24 (1C), 116.64 (1C), 114.06 (1C), 113.24 (1C), 101.96 (1C), 71.06 (1C), 52.32 (1C), 32.88 (1C), 5.58 (1C).

EMAC 10156 M: methyl 2-(7-(2-(4-chlorophenyl)-2-oxoethoxy)-4-methyl-2-oxo-2H-chromen-3-yl)acetate



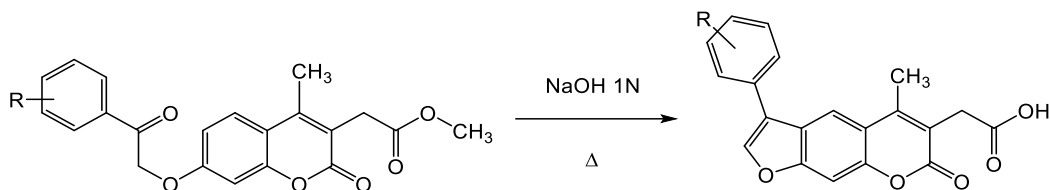
^1H NMR (600 MHz, DMSO) δ 8.07 (d, J = 8.4 Hz, 2H, CH-Ar), 7.78 (d, J = 8.9 Hz, 1H, CH-Ar Coum), 7.68 (d, J = 8.4 Hz, 2H, CH-Ar), 7.13 (d, J = 2.3 Hz, 1H, CH-Ar Coum), 7.07 (d, J = 8.9 Hz, 1H, CH-Ar Coum), 5.75 (s, 2H, -OCH₂-), 3.69 (s, 2H, Ar-CH₂-), 3.64 (s, 3H, -OCH₃), 2.41 (s, 3H, CH-Ar-CH₃).

^{13}C NMR (151 MHz, DMSO) δ 193.39 (1C), 170.90 (1C), 161.29 (1C), 161.10 (1C), 153.75 (1C), 149.93 (1C), 139.32 (1C), 133.32 (1C), 130.34 (2C), 129.42 (2C), 128.42 (1C), 127.17 (1C), 116.70 (1C), 113.25 (1C), 102.09 (1C), 71.07 (1C), 52.32 (1C), 32.88 (1C), 15.58 (1C).

Table 30 Chemical, analytical, and physical data of derivatives **EMAC 10156 (a-m)**

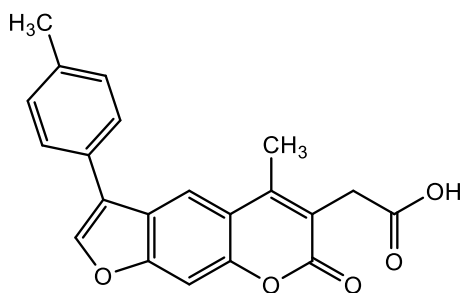
Compound	R	Aspect	MP °C	Yield %	RF AcOEt/Hex 5/1
10156 A	4-CH ₃	White solid	154-155	73	0.57
10156 B	4-OCH ₃	White solid	143-144	19	0.61
10156 C	4-Br	Light orange solid	155-157	68	0.60
10156 D	4-F	Light orange solid	90-93	80	0.61
10156 F	3-NO ₂	Yellow solid	150-153	59	0.58
10156 L	4-H	Light yellow solid	108-110	70	0.56
10156 M	4-Cl	Yellow solid	151-154	67	0.63

General method for the synthesis of compound EMAC 10159 (a-m)



EMAC 10156 (a-m) were stirred in a solution of 1N sodium hydroxide. The reaction mixture was stirred at reflux until the end of the reaction. Then, it was poured into crushed ice and water, and it was stirred until ice melting. Hydrochloric acid was added dropwise to obtain a precipitate. The precipitate was filtered to obtain the desired product. The reaction was monitored by TLC (ethyl acetate/n-hexane 5/1).

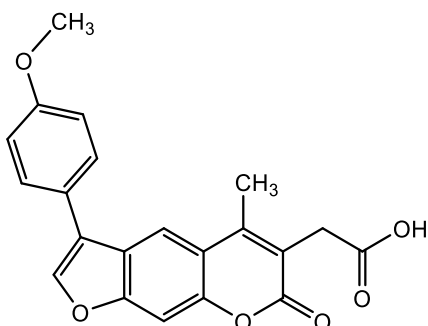
EMAC 10159 A: 2-(5-methyl-7-oxo-3-(p-tolyl)-7H-furo[3,2-g]chromen-6-yl)acetic acid



^1H NMR (400 MHz, DMSO) δ 12.48 (bs, 1H, -OH), 8.40 (s, 1H, CH-Ar Furoc), 8.14 (s, 1H, CH-Ar Furoc), 7.76 (s, 1H, CH-Ar Furoc), 7.69 (d, $J = 8.1$ Hz, 2H, CH-Ar), 7.34 (d, $J = 7.9$ Hz, 2H, CH-Ar), 3.65 (s, 2H, Ar-CH₂-), 2.51 (s, 3H, CH-Ar-CH₃), 2.37 (s, 3H, CH-Ar-CH₃).

^{13}C NMR (101 MHz, DMSO) δ 171.51 (1C), 160.78 (1C), 155.92 (1C), 149.74 (1C), 149.32 (1C), 137.23 (1C), 129.74 (2C), 127.54 (1C), 127.04 (2C), 123.03 (1C), 121.17 (1C), 118.07 (1C), 116.60 (1C), 116.60 (1C), 99.40 (1C), 32.85 (1C), 20.75 (1C), 15.45 (1C).

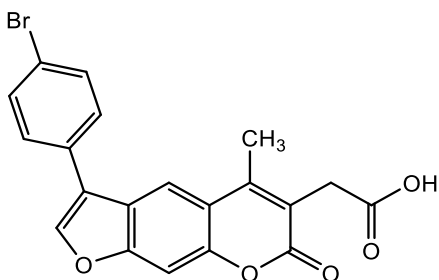
EMAC 10159 B: 2-(3-(4-methoxyphenyl)-5-methyl-7-oxo-7H-furo[3,2-g]chromen-6-yl)acetic acid



^1H NMR (400 MHz, DMSO) δ 12.47 (bs, 1H, -OH), 8.38 (s, 1H, CH-Ar Furoc), 8.17 (s, 1H, CH-Ar Furoc), 7.79 (s, 1H, CH-Ar Furoc), 7.75 (d, J = 8.7 Hz, 2H, CH-Ar), 7.11 (d, J = 8.8 Hz, 2H, CH-Ar), 3.83 (s, 3H, -OCH₃), 3.66 (s, 2H, Ar-CH₂-), 2.54 (s, 3H, CH-Ar-CH₃).

^{13}C NMR (101 MHz, DMSO) δ 171.45 (1C), 160.75 (1C), 158.97 (1C), 155.96 (1C), 149.83 (1C), 149.35 (1C), 128.51 (2C), 123.18 (1C), 122.85 (1C), 120.96 (1C), 118.15 (1C), 116.71 (1C), 116.65 (1C), 114.65 (2C), 99.47 (1C), 55.19 (1C), 32.90 (1C), 15.56 (1C).

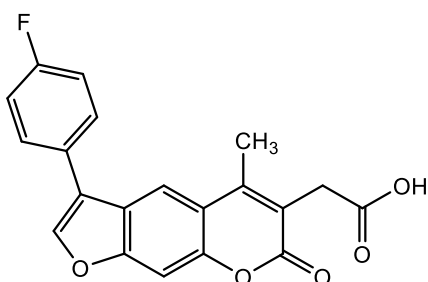
EMAC 10159 C: 2-(3-(4-bromophenyl)-5-methyl-7-oxo-7H-furo[3,2-g]chromen-6-yl)acetic acid



^1H NMR (400 MHz, DMSO) δ 12.46 (bs, 1H, -OH), 8.51 (s, 1H, CH-Ar Furoc), 8.17 (s, 1H, CH-Ar Furoc), 7.78 (d (d+s), J = 7.2 Hz, 3H, CH-Ar + CH-Ar Furoc), 7.72 (d, J = 8.6 Hz, 2H, CH-Ar), 3.65 (s, 2H, Ar-CH₂-), 2.53 (s, 3H, CH-Ar-CH₃).

^{13}C NMR (101 MHz, DMSO) δ 171.42 (1C), 160.67 (1C), 155.98 (1C), 149.92 (1C), 149.30 (1C), 132.06 (2C), 131.24 (1C), 129.90 (1C), 129.27 (2C), 122.53 (1C), 120.87 (1C), 120.26 (1C), 118.30 (1C), 116.84 (1C), 116.74 (1C), 99.58 (1C), 32.90 (1C), 15.57 (s).

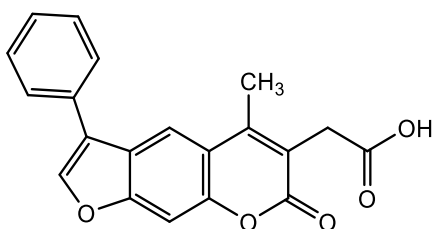
EMAC 10159 D: 2-(3-(4-fluorophenyl)-5-methyl-7-oxo-7H-furo[3,2-g]chromen-6-yl)acetic acid



^1H NMR (400 MHz, DMSO) δ 12.47 (bs, 1H, -OH), 8.46 (s, 1H, CH-Ar Furoc), 8.17 (s, 1H, CH-Ar Furoc), 7.87 (dd, J = 8.3, 5.6 Hz, 2H, CH-Ar), 7.79 (s, 1H, CH-Ar Furoc), 7.37 (t, J = 8.8 Hz, 2H, CH-Ar), 3.65 (s, 2H, Ar-CH₂-), 2.53 (s, 3H, CH-Ar-CH₃).

^{13}C NMR (101 MHz, DMSO) δ 171.42 (1C), 162.97 (1C), 160.68 (1C), 160.54 (1C), 155.94 (1C), 149.90 (1C), 149.31 (1C), 129.29 (d, J = 8.2 Hz, 2C), 127.07 (d, J = 3.2 Hz, 1C), 122.80 (1C), 120.35 (1C), 118.25 (1C), 116.78 (1C), 116.71 (1C), 116.17 (1C), 115.96 (1C), 99.54 (1C), 32.90 (1C), 15.58 (s).

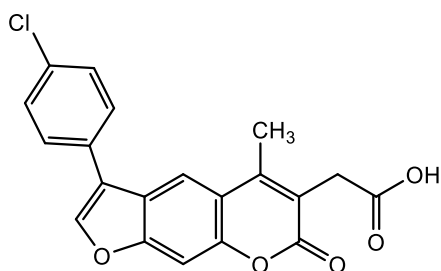
EMAC 10159 L: 2-(5-methyl-7-oxo-3-phenyl-7H-furo[3,2-g]chromen-6-yl)acetic acid



^1H NMR (600 MHz, DMSO) δ 12.48 (bs, 1H, -OH), 8.47 (s, 1H), 8.20 (s, 1H, CH-Ar Furoc), 7.82 (dd, J = 8.2, 1.1 Hz, 2H, CH-Ar), 7.80 (s, 1H, CH-Ar Furoc), 7.55 (t, J = 7.7 Hz, 2H, CH-Ar), 7.44 (t, J = 7.7 Hz, 1H, CH-Ar), 3.66 (s, 2H, CH-Ar-CH₂), 2.54 (s, 3H, CH-Ar-CH₃).

^{13}C NMR (151 MHz, DMSO) δ 171.95 (1C), 161.23 (1C), 156.53 (1C), 150.39 (1C), 149.83 (1C), 144.82 (1C), 131.14 (1C), 129.71 (2C), 128.34 (1C), 127.73 (2C), 123.41 (1C), 121.80 (1C), 118.74 (1C), 117.26 (2C), 100.05 (1C), 33.42 (1C), 16.08 (1C).

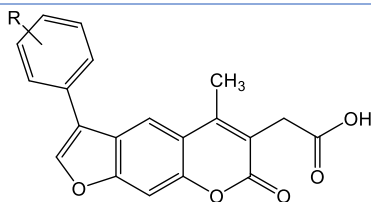
EMAC 10159 M: 2-(3-(4-chlorophenyl)-5-methyl-7-oxo-7H-furo[3,2-g]chromen-6-yl)acetic acid



^1H NMR (600 MHz, DMSO) δ 12.47 (bs, 1H, -OH), 8.50 (s, 1H, CH-Ar Furoc), 8.17 (s, 1H, CH-Ar Furoc), 7.84 (d, $J = 8.4$ Hz, 2H, CH-Ar), 7.79 (s, 1H, CH-Ar Furoc), 7.57 (d, $J = 8.4$ Hz, 2H, CH-Ar Furoc), 3.64 (s, 2H, CH-Ar-CH₂), 2.52 (s, 3H, CH-Ar-CH₃).

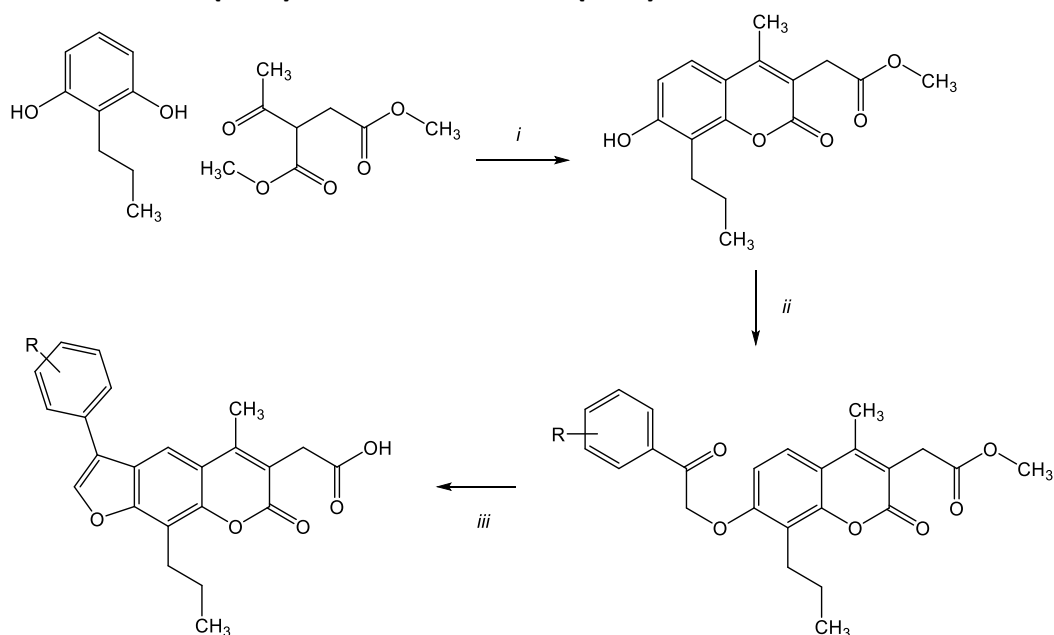
^{13}C NMR (151 MHz, DMSO) δ 171.92 (1C), 161.18 (1C), 156.50 (1C), 150.45 (1C), 149.82 (1C), 145.25 (1C), 132.89 (1C), 130.07 (1C), 129.66 (2C), 129.50 (2C), 123.11 (1C), 120.73 (1C), 118.82 (1C), 117.36 (1C), 117.28 (1C), 100.11 (1C), 33.42 (1C), 16.10 (1C).

Table 31 Chemical, analytical, and physical data of derivatives **EMAC 10159 (a-m)**



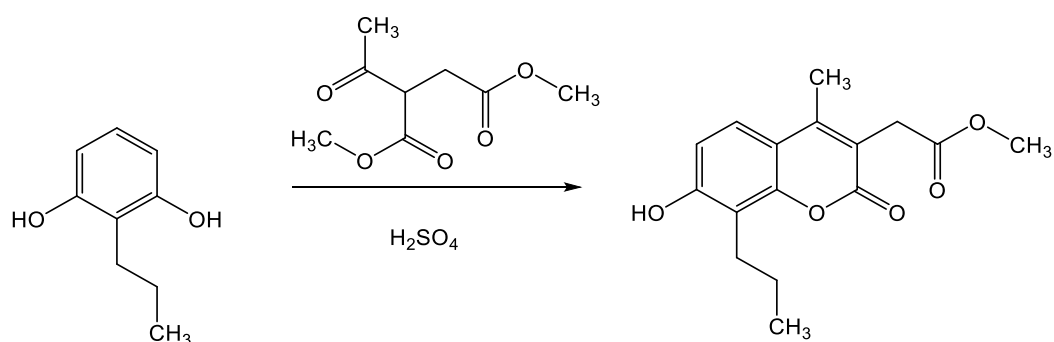
Compound	R	Aspect	MP °C	Yield %	RF AcOEt/Hex 5/1
10159 A	4-CH ₃	Dark green solid	194-196	94	0.65
10159 B	4-OCH ₃	Grey solid	187-190	83	0.61
10159 C	4-Br	Dark brown solid	75-78	76	0.67
10159 D	4-F	Light brown solid	140-143	73	0.61
10159 L	4-H	Light yellow solid	205-208	75	0.66
10159 M	4-Cl	Brown	172-175	87	0.73

EMAC 10157 (a-m) and EMAC 10160 (a-m)



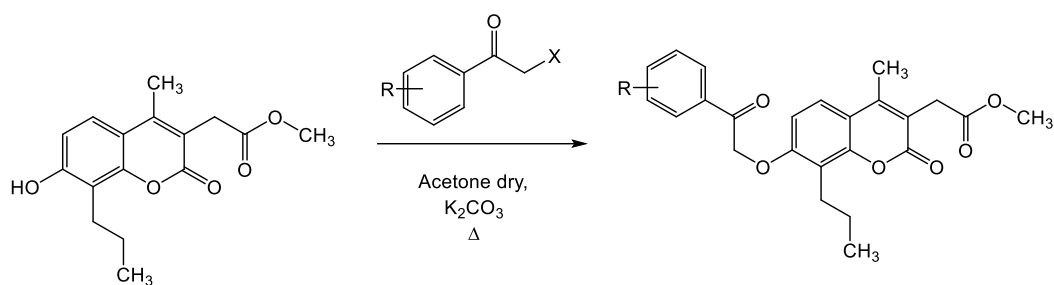
Scheme 10 Synthesis of derivatives **EMAC 10157(a-m)** and **EMAC 10160(a-m)**: (i.) dimethyl acetylsuccinate, H_2SO_4 , rT, 30'; (ii.) halogeno-acetophenone, acetone, K_2CO_3 , Δ ; (iii.) NaOH 1N, Δ

Synthesis of compound EMAC 10157



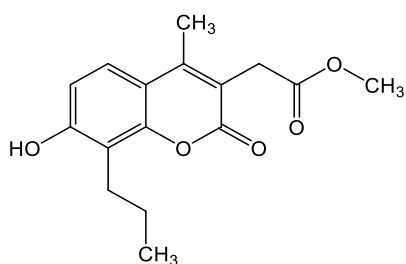
Equimolar amounts of 2-propyl resorcinol and dimethyl acetylsuccinate were stirred in sulfuric acid 98% at room temperature until the end of the reaction. A precipitate was formed, and it was the desired compound that was used for the next step without purification. The reaction was monitored by TLC (ethyl acetate/n-hexane 5/1).

General method for the synthesis of compounds EMAC 10157 (a-m)



Equimolar amounts of methyl 2-(7-hydroxy-4-methyl-2-oxo-8-propyl-2H-chromen-3-yl)acetate (1,8 mmol), and potassium carbonate (1,8 mmol) were stirred in dry acetone (5 mL), then the appropriate halogen-acetophenone (1,8 mmol) was added and the reaction mixture stirred at reflux until the end of the reaction. The reaction mixture was cooled to room temperature to obtain a precipitate.

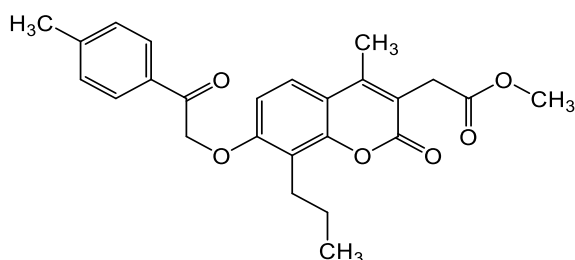
EMAC 10157: methyl 2-(7-hydroxy-4-methyl-2-oxo-8-propyl-2H-chromen-3-yl)acetate



¹H NMR (400 MHz, DMSO) δ 10.33 (s, 1H, -OH), 7.52 (d, J = 8.8 Hz, 1H, Coum), 6.88 (d, J = 8.8 Hz, 1H, Coum), 3.65 (s, 2H, Ar-CH₂-CO), 3.62 (s, 3H, -OCH₃), 2.69 (t, J = 7.2 Hz, 2H, Ar-CH₂-CH₂-), 2.34 (s, 3H, Ar-CH₃), 1.58 – 1.47 (m, 2H, -CH₂-CH₂-CH₃), 0.91 (t, J = 7.4 Hz, 3H, -CH₂-CH₂-CH₃).

¹³C NMR (101 MHz, DMSO) δ 170.76 (1C), 161.08 (1C), 158.42 (1C), 151.34 (1C), 149.95 (1C), 123.77 (1C), 115.01 (1C), 114.57 (1C), 112.16 (1C), 112.13 (1C), 51.77 (1C), 32.29 (1C), 24.22 (1C), 21.70 (1C), 15.05 (1C), 13.92 (1C).

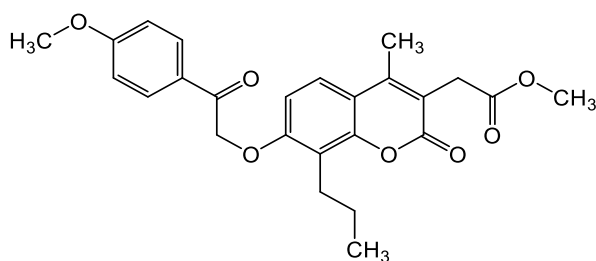
EMAC 10157 A: methyl 2-(4-methyl-2-oxo-7-(2-oxo-2-(p-tolyl)ethoxy)-8-propyl-2H-chromen-3-yl)acetate



^1H NMR (400 MHz, DMSO) δ 7.93 (d, J = 8, 2H, CH-Ar), 7.61 (d, J = 9.2, 1H, CH-Ar Coum), 7.39 (d, J = 8, 2H, CH-Ar), 7.00 (d, J = 8.8, 1H, CH-Ar Coum), 5.74 (s, 2H, $-\text{OCH}_2\text{-CO}-$), 3.68 (s, 2H, Ar- $\text{CH}_2\text{-CO}$), 3.62 (s, 3H, $-\text{OCH}_3$), 2.83–2.79 (m, 2H, Ar- $\text{CH}_2\text{-CH}_2-$), 2.41 (s, 3H, Ar- CH_3), 2.37 (s, 3H, Ar- CH_3), 1.64–1.55 (m, 2H, $-\text{CH}_2\text{-CH}_2\text{-CH}_3$), 0.95–0.91 (t, 3H, $-\text{CH}_2\text{-CH}_3$).

^{13}C NMR (101 MHz, DMSO) δ 193.70 (1C), 170.64 (1C), 160.88 (1C), 158.24 (1C), 150.61 (1C), 149.69 (1C), 144.37 (1C), 131.78 (1C), 129.34 (s, 2C), 127.96 (s, 2C), 123.92 (1C), 116.97 (1C), 115.87 (1C), 113.65 (1C), 108.77 (1C), 70.55 (1C), 51.82 (1C), 32.37 (1C), 24.34 (1C), 21.70 (1C), 21.22 (1C), 15.10 (1C), 13.96 (1C).

EMAC 10157 B: methyl 2-(7-(2-(4-methoxyphenyl)-2-oxoethoxy)-4-methyl-2-oxo-8-propyl-2H-chromen-3-yl)acetate

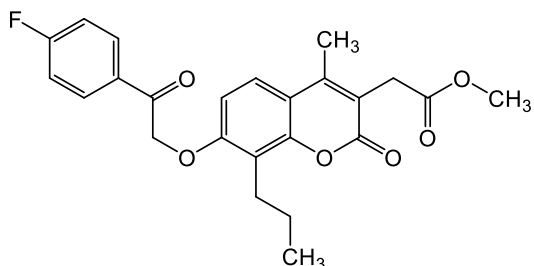


^1H NMR (400 MHz, DMSO) δ 8.01 (d, J = 8.8, 2H, CH-Ar), 7.61 (d, J = 8, 1H, CH-Ar Coum), 7.09 (d, J = 8, 2H, CH-Ar), 6.98 (d, J = 8, 1H, CH-Ar Coum), 5.70 (s, 2H, $-\text{OCH}_2\text{-CO}-$), 3.86 (s, 3H, CH-Ar- OCH_3), 3.68 (s, 2H, Ar- $\text{CH}_2\text{-CO}$), 3.62 (s, 3H, $-\text{OCH}_3$), 2.82–2.79 (m, 2H, Ar- $\text{CH}_2\text{-CH}_2-$), 2.36 (s, 3H, Ar- CH_3), 1.64–1.55 (m, 2H, $-\text{CH}_2\text{-CH}_2\text{-CH}_3$), 0.95–0.91 (t, 3H, $-\text{CH}_2\text{-CH}_3$)

^{13}C NMR (100 MHz, DMSO) δ 192.48 (1C), 170.64 (1C), 163.61 (1C), 160.89 (1C), 158.29 (1C), 150.60 (1C), 149.69 (1C), 130.23 (2C), 127.15 (1C), 123.90 (1C), 116.96v, 115.84 (1C),

114.05 (2C), 113.61 (1C), 108.76 (1C), 70.35 (1C), 55.60 (1C), 51.81 (1C), 32.36 (1C), 24.34 (1C), 21.70 (1C), 15.09 (1C), 13.96 (1C).

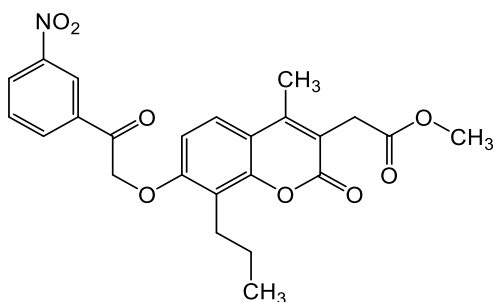
EMAC 10157 D: methyl 2-(7-(2-(4-fluorophenyl)-2-oxoethoxy)-4-methyl-2-oxo-8-propyl-2H-chromen-3-yl)acetate



^1H NMR (400 MHz, DMSO) δ 8.13–8.10 (m, 2H, CH-Ar), 7.62 (d, $J = 9.2$, 1H, CH-Ar Coum), 7.45–7.40 (m, 2H, CH-Ar), 7.03 (d, $J = 9.2$, 1H, CH-Ar Coum), 5.77 (s, 2H, $-\text{OCH}_2\text{-CO-}$), 3.68 (s, 2H, Ar- $\text{CH}_2\text{-CO-}$), 3.62 (s, 3H, $-\text{OCH}_3$), 2.83–2.79 (m, 2H, Ar- $\text{CH}_2\text{-CH}_2\text{-}$), 2.37 (s, 3H, Ar- CH_3), 1.64–1.55 (m, 2H, $-\text{CH}_2\text{-CH}_2\text{-CH}_3$), 0.95–0.91 (t, 3H, $-\text{CH}_2\text{-CH}_3$).

^{13}C NMR (100 MHz, DMSO) δ 192.90 (1C), 170.65 (1C), 166.59 (1C), 164.08 (1C), 160.89 (1C), 158.15 (1C), 150.60 (1C), 149.70 (1C), 131.01 (2C), 123.94 (1C), 116.98 (1C), 116.01 (1C), 115.91 (2C), 113.70 (1C), 108.79 (1C), 70.55 (1C), 51.82 (1C), 32.36 (1C), 24.33 (1C), 21.70 (1C), 15.10 (1C), 13.95 (1C).

EMAC 10157 F: methyl 2-(4-methyl-7-(2-(3-nitrophenyl)-2-oxoethoxy)-2-oxo-8-propyl-2H-chromen-3-yl)acetate

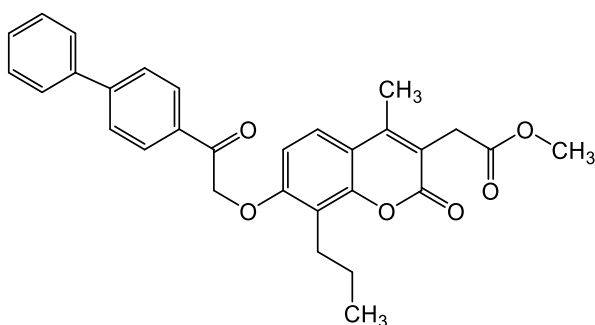


^1H NMR (400 MHz, DMSO) δ 8.75 (s, 1H, CH-Ar), 8.53 (d, $J = 7.2$ Hz, 1H, CH-Ar), 8.44 (d, $J = 7.2$ Hz, 1H, CH-Ar), 7.89 (t, $J = 7.6$ Hz, 1H, CH-Ar), 7.63 (d, $J = 8.6$ Hz, 1H, CH-Ar Coum), 7.11 (d, $J = 8.7$ Hz, 1H, CH-Ar Coum), 5.88 (s, 2H, $-\text{OCH}_2\text{-CO-}$), 3.68 (s, 2H, Ar- $\text{CH}_2\text{-CO-}$), 3.62 (s,

3H, -OCH₃), 2.81 (s, 2H, Ar-CH₂-CH₂-), 2.37 (s, 3H, Ar-CH₃), 1.59 (d, *J* = 6.6 Hz, 2H, -CH₂-CH₂-CH₃), 0.92 (t, *J* = 6.4 Hz, 3H, -CH₂-CH₃).

¹³C NMR (101 MHz, DMSO) δ 193.11 (1C), 170.62 (1C), 160.84 (1C), 158.00 (1C), 150.60 (1C), 149.65 (1C), 147.97 (1C), 135.47 (1C), 134.13 (1C), 130.62 (1C), 127.92 (1C), 123.95 (1C), 122.43 (1C), 117.01 (1C), 116.00 (1C), 113.81 (1C), 108.89 (1C), 70.97 (1C), 51.81 (1C), 32.37 (1C), 24.35 (1C), 21.72 (1C), 15.11 (1C), 13.95 (s).

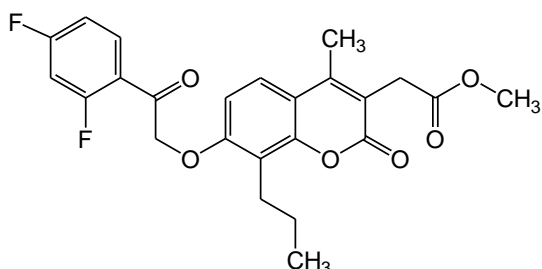
EMAC 10157 G: methyl 2-(7-(2-([1,1'-biphenyl]-4-yl)-2-oxoethoxy)-4-methyl-2-oxo-8-propyl-2H-chromen-3-yl)acetate



¹H NMR (400 MHz, DMSO) δ 8.12 (d, *J* = 8.4, 2H, CH-Ar), 7.88 (d, *J* = 8.4, 2H, CH-Ar), 7.78 (d, *J* = 7.2, 2H, CH-Ar), 7.65–7.61 (m, 1H, CH-Ar), 7.53 (t, *J* = 7.2, 2H, CH-Ar), 7.46 (d, *J* = 7.3, 1H, CH-Ar Coum), 7.05 (d, 1H, CH-Ar Coum), 5.82 (s, 2H, -OCH₂-CO-), 3.68 (s, 2H, Ar-CH₂-CO-), 3.62 (s, 3H, -OCH₃), 2.85–2.81 (m, 2H, Ar-CH₂-CH₂-), 2.37 (s, 3H, Ar-CH₃), 1.64–1.58 (m, 2H, -CH₂-CH₂-CH₃), 0.96–0.92 (t, 3H, -CH₂-CH₃).

¹³C NMR (100 MHz, DMSO) δ 193.78 (1C), 170.63 (1C), 160.88 (1C), 158.22 (1C), 150.62 (1C), 149.68 (1C), 145.17 (1C), 138.77 (1C), 133.07 (1C), 129.10 (2C), 128.61 (2C), 127.02 (2C), 126.96 (2C), 123.94 (1C), 116.99 (1C), 115.90 (1C), 113.68 (1C), 108.81 (1C), 73.94 (1C), 70.69 (1C), 51.81 (1C), 32.37 (1C), 24.37 (1C), 21.73 (1C), 15.11 (1C), 13.98 (1C).

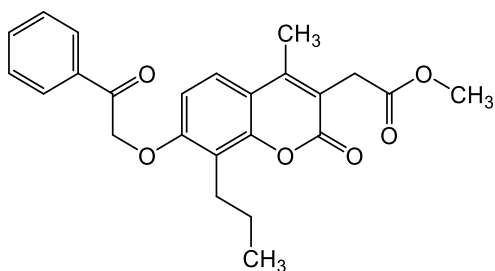
EMAC 10157 H: methyl 2-(7-(2-(2,4-difluorophenyl)-2-oxoethoxy)-4-methyl-2-oxo-8-propyl-2H-chromen-3-yl)acetate



^1H NMR (400 MHz, DMSO) δ 8.01 (td, $J = 8.6, 6.7$ Hz, 1H, CH-Ar), 7.60 (d, $J = 9.0$ Hz, 1H, CH-Ar Coum), 7.51 (ddd, $J = 11.5, 9.3, 2.4$ Hz, 1H, CH-Ar), 7.29 (td, $J = 8.5, 2.4$ Hz, 1H, CH-Ar), 7.02 (d, $J = 9.0$ Hz, 1H, CH-Ar Coum), 5.56 (d, $J = 2.7$ Hz, 2H, $-\text{OCH}_2\text{-CO}-$), 3.68 (s, 2H, Ar- $\text{CH}_2\text{-CO}-$), 3.62 (s, 3H, $-\text{OCH}_3$), 2.78 (t, 2H, Ar- $\text{CH}_2\text{-CH}_2-$), 2.37 (s, 3H, Ar- CH_3), 1.65 – 1.49 (m, 2H, $-\text{CH}_2\text{-CH}_2\text{-CH}_3$), 0.92 (t, $J = 7.4$ Hz, 3H, $-\text{CH}_2\text{-CH}_3$).

^{13}C NMR (101 MHz, DMSO) δ 191.23 (d, $J = 5.0$ Hz, 1C), 170.62 (1C), 160.86 (1C), 158.06 (1C), 150.59 (1C), 149.66 (1C), 123.91 (1C), 116.90 (1C), 115.94 (1C), 113.72 (1C), 108.73 (1C), 72.73 (d, $J = 10.5$ Hz, 1C), 51.81 (1C), 32.37 (1C), 24.34 (1C), 21.69 (1C), 15.11 (1C), 13.96 (1C).

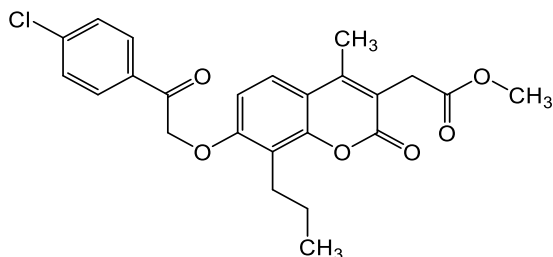
EMAC 10157 L: methyl 2-(4-methyl-2-oxo-7-(2-oxo-2-phenylethoxy)-8-propyl-2H-chromen-3-yl)acetate



^1H NMR (600 MHz, DMSO) δ 8.04 (d, $J = 7.7$ Hz, 2H, CH-Ar), 7.72 (t, $J = 7.4$ Hz, 1H, CH-Ar), 7.63 (d, $J = 9.0$ Hz, 1H, CH-Ar Coum), 7.60 (t, $J = 7.7$ Hz, 2H, CH-Ar), 7.04 (d, $J = 9.0$ Hz, 1H, CH-Ar Coum), 5.80 (s, 2H, $-\text{OCH}_2\text{-CO}-$), 3.70 (s, 2H, Ar- $\text{CH}_2\text{-CO}-$), 3.64 (s, 3H, $-\text{OCH}_3$), 2.87 – 2.80 (m, 2H, Ar- $\text{CH}_2\text{-CH}_2-$), 2.38 (s, 3H, Ar- CH_3), 1.62 (dq, $J = 14.7, 7.3$ Hz, 2H, $-\text{CH}_2\text{-CH}_2\text{-CH}_3$), 0.95 (t, $J = 7.3$ Hz, 3H, $-\text{CH}_2\text{-CH}_3$).

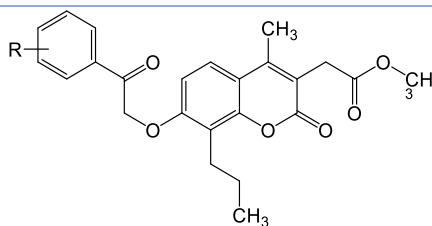
^{13}C NMR (151 MHz, DMSO) δ 194.76 (1C), 171.14 (1C), 161.38 (1C), 158.72 (1C), 151.13 (1C), 150.19 (1C), 134.80 (1C), 134.35 (1C), 129.32 (2C), 128.38 (2C), 124.44 (1C), 117.51 (1C), 116.41 (1C), 114.19 (1C), 109.30 (1C), 71.18 (1C), 52.32 (1C), 32.89 (1C), 24.86 (1C), 22.22 (1C), 15.62 (1C), 14.48 (1C).

EMAC 10157 M: methyl 2-(7-(2-(4-chlorophenyl)-2-oxoethoxy)-4-methyl-2-oxo-8-propyl-2H-chromen-3-yl)acetate



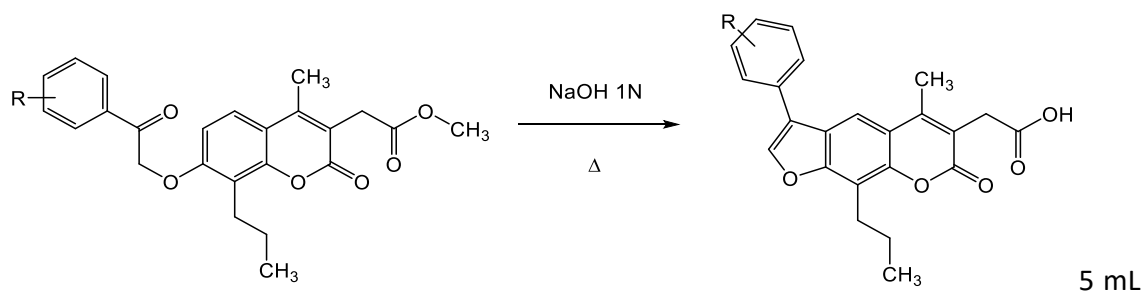
^1H NMR (600 MHz, DMSO) δ 8.05 (d, $J = 8.4$ Hz, 2H, CH-Ar), 7.67 (d, $J = 8.4$ Hz, 2H, CH-Ar), 7.63 (d, $J = 9.0$ Hz, 1H, CH-Ar Coum), 7.05 (d, $J = 9.0$ Hz, 1H, CH-Ar Coum), 5.78 (s, 2H, -OCH₂-CO-), 3.69 (s, 2H, Ar-CH₂-CO-), 3.63 (s, 3H, -OCH₃), 2.87 – 2.73 (m, 2H, Ar-CH₂-CH₂-), 2.38 (s, 3H, Ar-CH₃), 1.66 – 1.54 (m, 2H, -CH₂-CH₂-CH₃), 0.94 (t, $J = 7.4$ Hz, 3H, -CH₂-CH₃).

^{13}C NMR (151 MHz, DMSO) δ 193.87 (1C), 171.13 (1C), 161.37 (1C), 158.63 (1C), 151.12 (1C), 150.18 (1C), 139.22 (1C), 133.49 (1C), 130.33 (2C), 129.44 (2C), 124.45 (1C), 117.50 (1C), 116.45 (1C), 114.24 (1C), 109.32 (1C), 71.17 (1C), 52.32 (1C), 32.89 (1C), 24.86 (1C), 22.22 (1C), 15.62 (1C), 14.47 (s).

Table 32 Chemical, analytical, and physical data of derivatives **EMAC 10157 (a-m)**

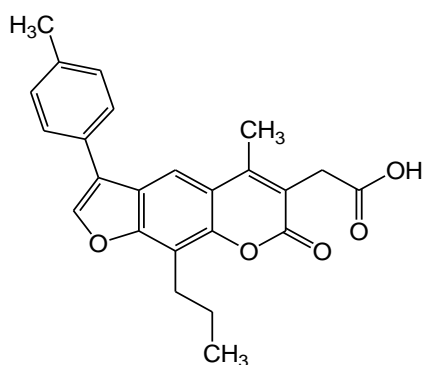
Compound	R	Aspect	MP °C	Yield %	RF DCM/MeOH 10/1
10157 A	4-CH ₃	White crystals	132-133	80	0.83
10157 B	4-OCH ₃	Pale brown solid	127-130	89	0.82
10157 D	4-F	White crystals	164-166	90	0.82
10157 F	3-NO ₂	Orange solid	135-141	36	0.86
10157 G	4-Phenyl	White crystals	138-140	71	0.83
10157 H	2,4-F	White solid	166-170	2	0.86
10157 L	4-H	White solid	147-150	90	0.84
10157 M	4-Cl	Beige solid	157-159	89	0.86

General method for the synthesis of compound EMAC 10160 (a-m)



of 1 N sodium hydroxide were added to a suspension of the appropriate EMAC 10161 (a-k), the reaction mixture was stirred at reflux for 4 hours. Then it was poured into crushed ice and water, and it was stirred until ice melting. Hydrochloric acid was added dropwise to obtain a precipitate.

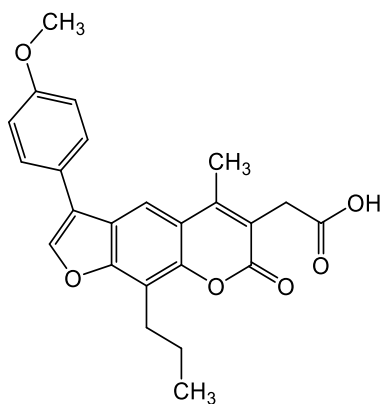
EMAC 10160 A: 2-(5-methyl-7-oxo-9-propyl-3-(p-tolyl)-7H-furo[3,2-g]chromen-6-yl)acetic acid



^1H NMR (400 MHz, DMSO) δ 12.47 (bs, 1H, -OH), 8.41 (s, 1H, -OCH-Ar Furoc), 8.03 (s, 1H, CH-Ar Furoc), 7.69 (d, $J = 8$, 2H, CH-Ar), 7.34 (d, $J = 7.9$, 2H, CH-Ar), 3.65 (s, 2H, Ar-CH₂-CO), 3.03 (t, $J = 7.5$, 2H, Ar-CH₂-CH₂-), 2.51 (s, 3H, Ar-CH₃), 2.38 (s, 3H, Ar-CH₃), 1.78–1.69 (m, 2H, -CH₂-CH₂-CH₃), 0.97–0.94 (t, 3H, -CH₂-CH₃).

^{13}C NMR (100 MHz, DMSO) δ 171.49 (1C), 160.72 (1C), 154.93 (1C), 149.65 (1C), 147.36 (1C), 143.62 (1C), 137.11 (1C), 129.72 (2C), 127.82 (1C), 127.11 (2C), 122.21 (1C), 121.45 (1C), 117.83 (1C), 116.71 (1C), 114.20 (1C), 112.93 (1C), 32.90 (1C), 24.85 (1C), 21.93 (1C), 20.79 (1C), 15.64 (1C), 13.83 (1C).

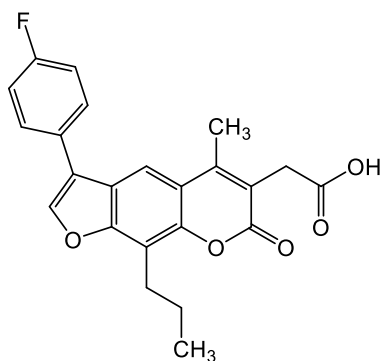
EMAC 10160 B: 2-(3-(4-methoxyphenyl)-5-methyl-7-oxo-9-propyl-7H-furo[3,2-g]chromen-6-yl)acetic acid



^1H NMR (400 MHz, DMSO) δ 12.47 (bs, 1H, -OH), 8.37 (s, 1H, OCH-Ar Furoc), 8.01 (s, 1H, CH-Ar Furoc), 7.73 (d, $J = 8.2$, 2H, CH-Ar), 7.10 (d, $J = 8.6$, 2H, CH-Ar), 3.82 (s, 3H, CH-Ar-OCH₃), 3.65 (s, 2H, Ar-CH₂-CO), 3.02 (t, $J = 6.8$, 2H, Ar-CH₂-CH₂-), 2.51 (s, 3H, Ar-CH₃), 1.71–1.68 (m, 2H, -CH₂-CH₂-CH₃), 0.97–0.94 (t, 3H, -CH₂-CH₃).

^{13}C NMR (100 MHz, DMSO) δ 171.50 (1C), 160.73 (1C), 158.92 (1C), 154.89 (1C), 149.66 (1C), 147.34 (1C), 143.17 (1C), 128.47 (2C), 123.00 (1C), 122.31 (1C), 121.18 (1C), 117.79 (1C), 116.66 (1C), 114.62 (2C), 114.16 (1C), 112.89 (1C), 55.17 (1C), 32.90 (1C), 24.84 (1C), 21.92 (1C), 15.65 (1C), 13.82 (1C).

EMAC 10160 D: 2-(3-(4-fluorophenyl)-5-methyl-7-oxo-9-propyl-7H-furo[3,2-g]chromen-6-yl)acetic acid

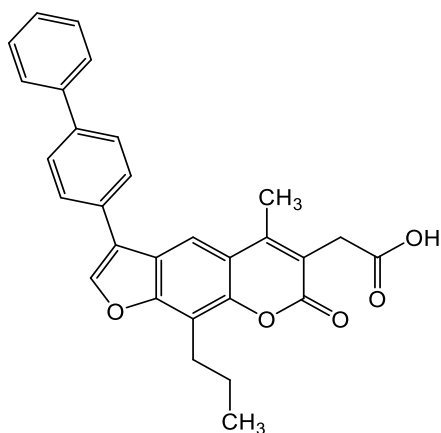


^1H NMR (400 MHz, DMSO) δ 12.47 (bs, 1H, -OH), 8.46 (s, 1H, -OCH-Ar Furoc), 8.03 (s, 1H, CH-Ar Furoc), 7.87–7.85 (m, 2H, CH-Ar), 7.37 (t, $J = 8.8$, 2H), 3.65 (s, 2H, Ar-CH₂-CO), 3.03

(t, $J = 7.5$, 2H, Ar-CH₂-CH₂-), 2.52 (s, 3H, Ar-CH₃), 1.78–1.69 (m, 2H, -CH₂-CH₂-CH₃), 0.97–0.94 (t, 3H, -CH₂-CH₃).

¹³C NMR (100 MHz, DMSO) δ 171.48 (1C), 162.91 (1C), 160.68 (1C), 160.51 (1C), 154.88 (1C), 149.67 (1C), 147.42 (1C), 129.23 (1C), 129.23 (1C), 127.21 (1C), 121.97 (1C), 120.59 (1C), 117.90 (1C), 116.81 (1C), 116.16 (1C), 115.94 (1C), 114.16 (1C), 112.98 (1C), 32.90 (1C), 27.45 (1C), 24.84 (1C), 21.92 (1C), 15.67 (1C), 13.82 (1C).

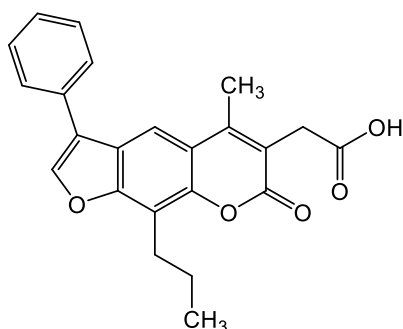
EMAC 10160 G: 2-(3-([1,1'-biphenyl]-4-yl)-5-methyl-7-oxo-9-propyl-7H-furo[3,2-g]chromen-6-yl)acetic acid



¹H NMR (400 MHz, DMSO) δ 12.49 (bs, 1H, -OH), 8.54 (s, 1H, -OCH-Ar Furoc), 8.13 (s, 1H, CH-Ar Furoc), 7.92 (d, 2H, $J = 8.4$, 2H, CH-Ar), 7.84 (d, $J = 8.4$, 2H, CH-Ar), 7.75 (d, $J = 7.2$, 2H, CH-Ar), 7.51 (t, $J = 7.2$, 2H, CH-Ar), 7.40 (t, $J = 7.2$, 1H, CH-Ar), 3.67 (s, 2H, Ar-CH₂-CO), 3.07–3.04 (m, 2H, Ar-CH₂-CH₂-), 2.55 (s, 3H, Ar-CH₃), 1.80–1.71 (m, 2H, -CH₂-CH₂-CH₃), 0.99–0.95 (t, 3H, -CH₂-CH₃).

¹³C NMR (100 MHz, DMSO) δ 171.49 (1C), 160.71 (1C), 155.01 (1C), 149.69 (1C), 147.44 (1C), 144.21 (1C), 139.56 (1C), 139.42 (1C), 129.93 (1C), 129.01 (2C), 127.73 (2C), 127.59 (1C), 127.37 (2C), 126.54 (2C), 122.04 (1C), 121.13 (1C), 117.92 (1C), 116.84 (1C), 114.35 (1C), 113.03 (1C), 32.92 (1C), 24.88 (1C), 21.94 (1C), 15.71 (1C), 13.85 (1C).

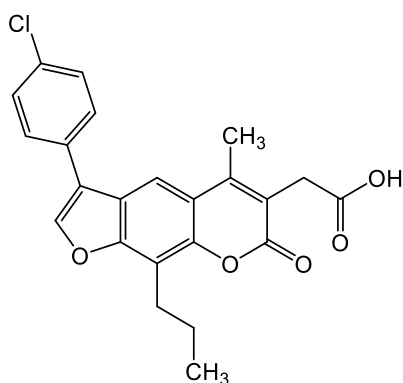
EMAC 10160 L: 2-(5-methyl-7-oxo-3-phenyl-9-propyl-7H-furo[3,2-g]chromen-6-yl)acetic acid



^1H NMR (400 MHz, DMSO) δ 12.49 (bs, 1H, OH), 8.45 (d, J = 1.6 Hz, 1H, -OCH-Ar Furoc), 8.05 (d, J = 3.6 Hz, 1H, CH-Ar Furoc), 7.80 (d, J = 7.6 Hz, 2H, CH-Ar), 7.54 (t, J = 7.5 Hz, 2H, CH-Ar), 7.43 (t, J = 7.3 Hz, 1H, CH-Ar), 3.65 (s, 2H, Ar-CH₂-CO), 2.97-3.06 (m, 2H, Ar-CH₂-CH₂-), 2.51 (s, 3H, Ar-CH₃) 1.68-1.78 (m, 2H, -CH₂-CH₂-CH₃), 0.96 (t, J = 7.2 Hz, 3H, -CH₂-CH₃).

^{13}C NMR (101 MHz, DMSO) δ 171.48 (1C), 160.69 (1C), 154.95 (1C), 149.64 (1C), 147.38 (1C), 130.77 (1C), 128.83 (2C), 127.75 (1C), 127.19 (2C), 122.04 (1C), 121.51 (1C), 117.87 (1C), 116.77 (1C), 114.20 (1C), 114.20 (1C), 112.97 (1C), 32.90 (1C), 24.85 (1C), 21.93 (1C), 15.65 (1C), 13.79 (1C).

EMAC 10160 M: 2-(3-(4-chlorophenyl)-5-methyl-7-oxo-9-propyl-7H-furo[3,2-g]chromen-6-yl)acetic acid



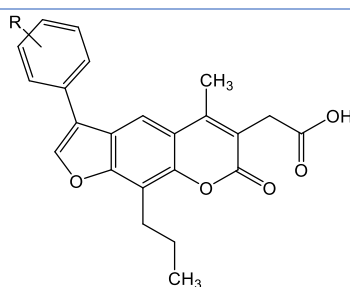
^1H NMR (400 MHz, DMSO) δ 8.48 (s, 1H, -OCH-Ar Furoc), 8.02 (s, 1H, CH-Ar Furoc), 7.82 (d, J = 8.6 Hz, 2H, CH-Ar), 7.57 (d, J = 8.6 Hz, 2H, CH-Ar), 3.64 (s, 2H, Ar-CH₂-CO), 3.03 – 2.96

(m, 2H, Ar-CH₂-CH₂-), 2.51 (s, 3H, Ar-CH₃) 1.75 – 1.66 (m, 2H, CH₂-CH₂-CH₃), 0.94 (t, *J* = 7.4 Hz, 3H, -CH₂-CH₃).

OH not detected.

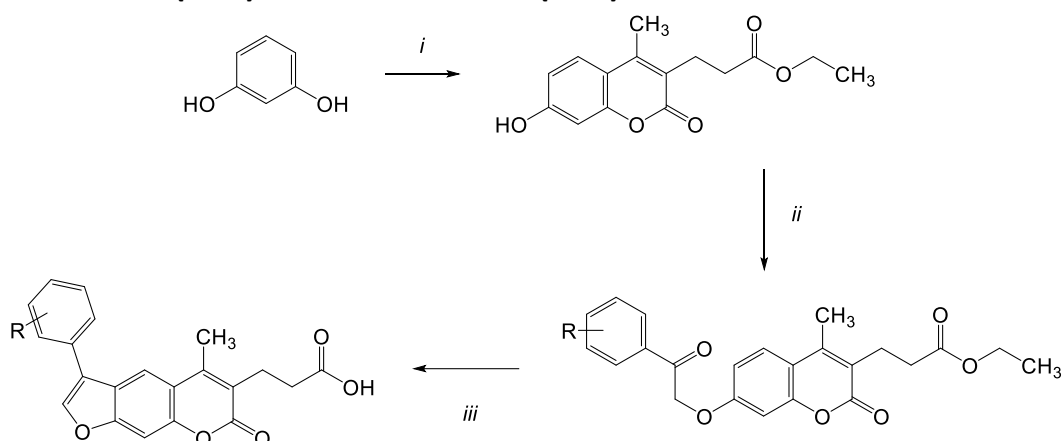
¹³C NMR (101 MHz, DMSO) δ 171.47 (1C), 160.65 (1C), 154.90 (1C), 149.63 (1C), 147.41 (1C), 142.82 (1C), 132.29 (1C), 129.66 (1C), 129.11 (2C), 128.90 (2C), 121.71 (1C), 120.40 (1C), 117.92 (1C), 116.83 (1C), 114.16 (1C), 113.01 (1C), 32.89 (1C), 24.82 (1C), 21.91 (1C), 15.65 (1C), 13.81 (s).

Table 33 Chemical, analytical, and physical data of derivatives **EMAC 10160 (a-m)**



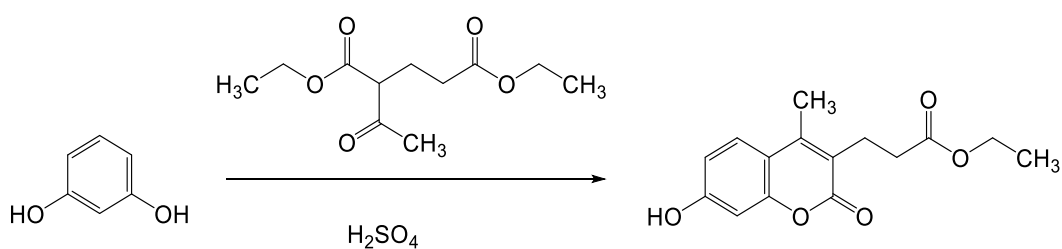
Compound	R	Aspect	MP °C	Yield %	RF DCM/MeOH 5/1
10160 A	4-CH ₃	Grey crystals	226-229	98	0.86
10160 B	4-OCH ₃	Green crystals	202-205	97	0.88
10160 D	4-F	Grey solid	135-139	92	0.87
10160 G	4-Phenyl	Pale brown crystals	248-250	97	0.91
10160 L	4-H	Blue solid	128-130	74	0.88
10160 M	4-Cl	Dark green solid	232-235	89	0.87

EMAC 10161 (a-m) and EMAC 10162 (a-m)



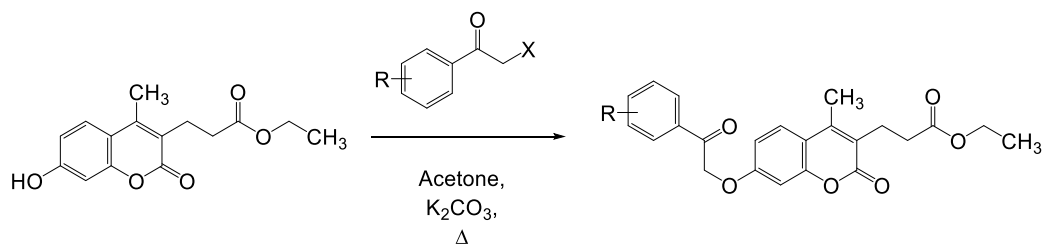
Scheme 11 Synthesis of derivatives **EMAC 10161 (a-m)** and **EMAC 10162 (a-m)**: (i.) diethyl 2-acetylglutarate, H_2SO_4 , RT, 30'; (ii.) 2-bromo/2-chloro-acetophenone, acetone, K_2CO_3 , Δ ; (iii.) NaOH 1N, Δ

Synthesis of compound EMAC 10161



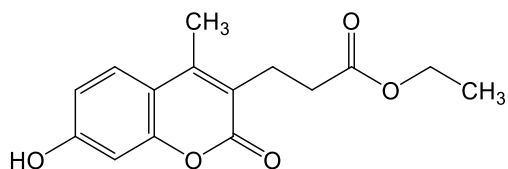
A mixture of resorcinol (4,5 mmol) and diethyl 2-acetylglutarate (4,5 mmol) was stirred at room temperature. Sulfuric acid 98% (13,5 mmol) was added dropwise to the reaction mixture which was vigorously stirred until the end of the reaction. After 30 minutes a homogeneous sticky solid was obtained which was dissolved in the minimum quantity of methanol and poured into crushed ice. The mixture was stirred until ice melting and then filtered off to obtain a light-yellow solid. The crude product was washed with ethyl ether giving a white powder which was recrystallized from methanol. The progression of the reaction was monitored by TLC (ethyl acetate/n-hexane 6/1).

General method for the synthesis of compounds EMAC 10161 (a-m)



Equimolar amounts of ethyl 3-(7-hydroxy-4-methyl-2-oxo-2H-chromen-3-yl)propanoate (1,8 mmol), and potassium carbonate (1,8 mmol) were stirred in dry acetone (5 mL). Then the appropriate 2-bromo-acetophenone or 2-chloro-acetophenone (1,8 mmol) was added, and the reaction mixture was stirred at reflux until the end of the reaction. The mixture was cooled to room temperature to obtain a solid which was dissolved in methanol and poured into crushed ice. The mixture was stirred until ice melting, then hydrochloric acid was added dropwise to obtain a precipitate. The crude product was filtered, washed with ethyl ether, and crystallized in ethanol to obtain the desired compound.

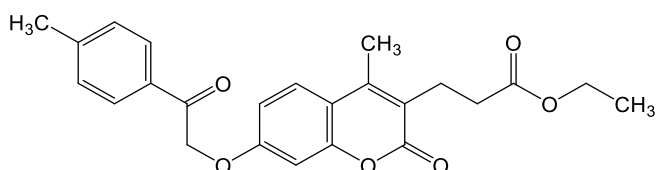
EMAC 10161: ethyl 3-(7-hydroxy-4-methyl-2-oxo-2H-chromen-3-yl)propanoate



¹H NMR (600 MHz, DMSO) δ 12.13 (bs, 1H, OH), 7.62 (d, *J* = 8.8 Hz, 1H, CH-Ar Coum), 6.79 (dd, *J* = 8.8, 2.4 Hz, 1H CH-Ar Coum), 6.68 (d, *J* = 2.4 Hz, 1H CH-Ar Coum), 2.80-2.73 (m, 2H, -OCH₂-CH₃), 2.50 (s, 3H, Ar-CH₃), 2.46 (m, 2H, OCH₂-CH₃), 2.40 – 2.36 (m, 5H, 2H+3H, -COCH₂-CH₂-CH-Ar, OCH₂-CH₃).

¹³C NMR (151 MHz, DMSO) δ 174.18 (1C), 161.30 (1C), 160.74 (1C), 153.78 (1C), 148.40 (1C), 127.14 (1C), 120.33 (1C), 113.34 (2C), 112.93 (1C), 102.36 (2C), 51.85 (1C), 32.83 (1C), 32.51 (1C), 23.23 (1C), 15.06 (1C).

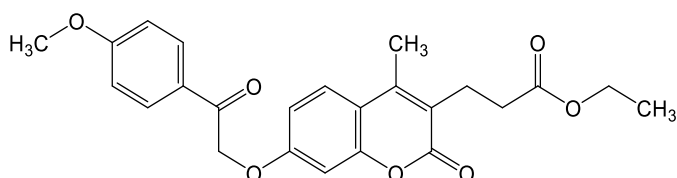
EMAC 10161 A: ethyl 3-(4-methyl-2-oxo-7-(2-oxo-2-(p-tolyl)ethoxy)-2H-chromen-3-yl)propanoate



^1H NMR (600 MHz, DMSO) δ 7.96 (d, J = 8.2 Hz, 2H, CH-Ar), 7.74 (d, J = 8.9 Hz, 1H, CH-Ar Coum), 7.41 (d, J = 8.0 Hz, 2H, CH-Ar), 7.06 (d, J = 2.5 Hz, 1H, CH-Ar Coum), 7.03 (dd, J = 8.8, 2.6 Hz, 1H, CH-Ar Coum), 5.71 (s, 2H, -OCH₂CO), 4.06 (q, J = 7.1 Hz, 2H, OCH₂-CH₃), 2.83 (t, J = 7.7 Hz, 2H, -COCH₂-CH₂-CH-Ar), 2.51-2.47 (m, 2H, -COCH₂-CH₂-CH-Ar), 2.43 (s, 6H, 3H+3H, Ar-CH₃, Ar-CH₃), 1.17 (t, J = 7.1 Hz, 3H, OCH₂-CH₃).

^{13}C NMR (151 MHz, DMSO) δ 193.80 (1C), 172.55 (1C), 161.14 (1C), 160.82 (1C), 153.57 (1C), 148.31 (1C), 144.88 (1C), 132.26 (1C), 129.83 (2C), 128.48 (2C), 126.99 (1C), 121.14 (1C), 114.28 (1C), 113.00 (1C), 101.82 (1C), 70.91 (1C), 60.42 (1C), 32.65 (1C), 23.22 (1C), 21.73 (1C), 15.15 (1C), 14.53 (1C).

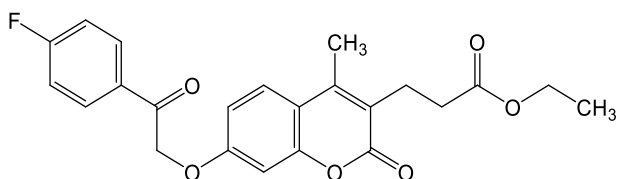
EMAC 10161 B: ethyl 3-(7-(2-(4-methoxyphenyl)-2-oxoethoxy)-4-methyl-2-oxo-2H-chromen-3-yl)propanoate



^1H NMR (600 MHz, DMSO) δ 8.01 (d, J = 8.9 Hz, 2H, CH-Ar), 7.72 (d, J = 8.8 Hz, 1H, CH-Ar Coum), 7.10 (d, J = 8.9 Hz, 2H, CH-Ar), 7.02 (d, J = 2.5 Hz, 1H, CH-Ar Coum), 7.00 (dd, J = 8.8, 2.6 Hz, 1H, CH-Ar Coum), 5.65 (s, 2H, -OCH₂CO), 3.87 (s, 3H, OCH₃), 3.59 (s, 3H, Ar-CH₃), 2.81 (t, J = 7.7 Hz, 2H, -COCH₂-CH₂-CH-Ar), 2.51 – 2.42 (m, 4H, 2H+2H, -COCH₂-CH₂-CH-Ar, OCH₂-CH₃), 2.41 (s, 3H, OCH₂-CH₃).

^{13}C NMR (151 MHz, DMSO) δ 192.61 (1C), 172.83 (1C), 164.14 (1C), 161.14 (1C), 160.88 (1C), 153.57 (1C), 148.37 (1C), 130.75 (2C), 127.64 (1C), 126.99 (1C), 121.08 (1C), 114.55 (2C), 114.25 (1C), 113.01 (1C), 101.81 (1C), 70.72 (1C), 56.13 (1C), 51.86 (1C), 40.55 (1C), 32.45 (1C), 23.20 (1C), 15.12 (s).

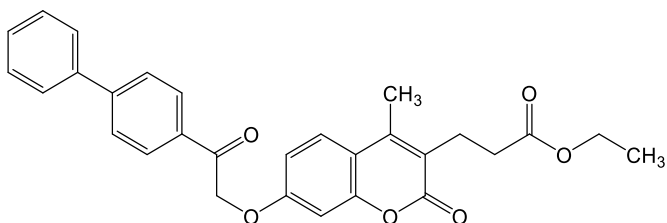
EMAC 10161 D: ethyl 3-(7-(2-(4-fluorophenyl)-2-oxoethoxy)-4-methyl-2-oxo-2H-chromen-3-yl)propanoate



^1H NMR (600 MHz, DMSO) δ 8.14 – 8.10 (m, 2H, CH-Ar), 7.72 (d, J = 8.9 Hz, 1H, CH-Ar Coum), 7.42 (m, J = 8.9 Hz, 2H, CH-Ar), 7.06 (d, J = 2.6 Hz, 1H, CH-Ar Coum), 7.02 (dd, J = 8.9, 2.6 Hz, 1H, CH-Ar Coum), 5.72 (s, 2H, -OCH₂CO), 3.59 (s, 3H, Ar-CH₃), 2.82 (t, J = 7.7 Hz, 2H, -COCH₂-CH₂-CH-Ar), 2.48 (s, 2H, OCH₂-CH₃), 2.43 – 2.39 (m, 5H, 3H+2H, OCH₂-CH₃, -COCH₂-CH₂-CH-Ar).

^{13}C NMR (151 MHz, DMSO) δ 192.98 (1C), 173.02 (1C), 166.67 (1C), 161.13 (1C), 160.76 (1C), 153.59 (1C), 148.36 (1C), 131.51 (2C), 131.48 (1C), 127.01 (1C), 121.14 (1C), 116.45 (1C), 116.31 (1C), 114.33 (1C), 113.03 (1C), 101.83 (1C), 70.95 (1C), 51.86 (1C), 40.55 (1C), 32.44 (1C), 23.21 (1C), 15.13 (s).

EMAC 10161 G: ethyl 3-(7-(2-([1,1'-biphenyl]-4-yl)-2-oxoethoxy)-4-methyl-2-oxo-2H-chromen-3-yl)propanoate

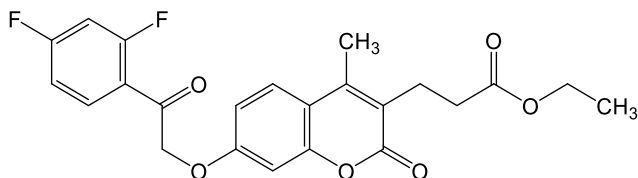


^1H NMR (600 MHz, DMSO) δ 8.12 (d, J = 8.3 Hz, 2H, CH-Ar), 7.89 (d, J = 8.3 Hz, 2H, CH-Ar), 7.78 (d, J = 7.4 Hz, 2H, CH-Ar), 7.73 (d, J = 8.9 Hz, 1H, CH-Ar Coum), 7.53 (t, J = 7.6 Hz, 2H, CH-Ar), 7.45 (t, J = 7.3 Hz, 1H, CH-Ar), 7.08 (d, J = 2.5 Hz, 1H, CH-Ar Coum), 7.04 (dd, J = 8.9, 2.5 Hz, 1H, CH-Ar Coum), 5.76 (s, 2H, -OCH₂CO), 3.59 (s, 3H, Ar-CH₃), 2.82 (t, J = 7.8 Hz, 2H, -COCH₂-CH₂-CH-Ar), 2.46 (m, 2H, OCH₂-CH₃), 2.48 – 2.34 (m, 5H, 3H+2H, OCH₂-CH₃, -COCH₂-CH₂-CH-Ar).

^{13}C NMR (151 MHz, DMSO) δ 193.88 (1C), 173.03 (1C), 161.15 (1C), 160.82 (1C), 153.60 (1C), 148.36 (1C), 145.70 (1C), 139.29 (1C), 133.55 (1C), 129.61 (2C), 129.14 (2C), 129.01

(1C), 127.50 (d, $J = 12.0$ Hz, 4H), 121.13 (1C), 114.32 (1C), 113.03 (1C), 101.86 (1C), 71.06 (1C), 51.87 (1C), 40.55 (1C), 32.45 (1C), 23.21 (1C), 15.13 (1C).

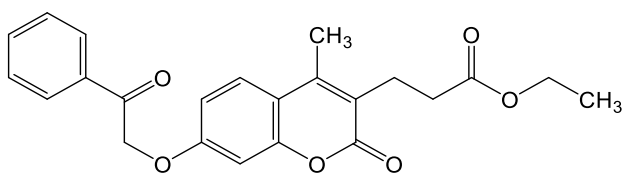
EMAC 10161 H: ethyl 3-(7-(2-(2,4-difluorophenyl)-2-oxoethoxy)-4-methyl-2-oxo-2H-chromen-3-yl)propanoate



^1H NMR (600 MHz, DMSO) δ 8.02 (dd, $J = 15.3, 8.5$ Hz, 1H, CH-Ar), 7.71 (d, $J = 8.9$ Hz, 1H, CH-Ar Coum), 7.51 (ddd, $J = 11.5, 9.4, 2.4$ Hz, 1H, CH-Ar), 7.29 (td, $J = 8.5, 2.4$ Hz, 1H, CH-Ar), 7.04 (d, $J = 2.6$ Hz, 1H, CH-Ar Coum), 7.01 (dd, $J = 8.9, 2.6$ Hz, 1H, CH-Ar Coum), 5.52 (d, $J = 2.9$ Hz, 2H, $-\text{OCH}_2\text{CO}$), 3.58 (s, 3H, Ar- CH_3), 2.81 (dd, $J = 14.0, 6.0$ Hz, 2H, $-\text{COCH}_2-\text{CH}_2-\text{CH-Ar}$), 2.76 (dd, $J = 13.5, 5.9$ Hz 2H, OCH_2-CH_3), 2.41 – 2.40 (m, 2H, $\text{COCH}_2-\text{CH}_2-\text{CH-Ar}$), 2.38 (t, $J = 11.8, 5.4$ Hz, 3H, OCH_2-CH_3).

^{13}C NMR (151 MHz, DMSO) δ 173.02 (1C), 161.14 (1C), 160.75 (1C), 153.58 (1C), 148.41 (1C), 148.34 (1C), 132.73 (1C), 127.14 (1C), 126.97 (1C), 120.33 (1C), 114.33 (1C), 113.34 (1C), 112.95 (2C), 105.68 (1C), 102.36 (1C), 101.76 (s, 2C), 73.06 (1C), 51.86 (1C), 32.83 (1C), 32.44 (1C), 23.20 (1C), 15.12 (1C).

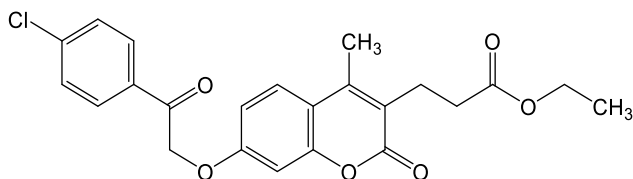
EMAC 10161 L: ethyl 3-(4-methyl-2-oxo-7-(2-oxo-2-phenylethoxy)-2H-chromen-3-yl)propanoate



^1H NMR (600 MHz, DMSO) δ 8.04 (d, $J = 7.7$ Hz, 2H, CH-Ar), 7.71 (t, $J = 9.3$ Hz, 2H, 1H+1H, CH-Ar, CH-Ar Coum), 7.59 (t, $J = 7.7$ Hz, 2H, CH-Ar), 7.06 (d, $J = 2.5$ Hz, 1H, CH-Ar Coum), 7.02 (dd, $J = 8.8, 2.6$ Hz, 1H, CH-Ar Coum), 5.74 (s, 2H, $-\text{OCH}_2\text{CO}$), 3.59 (s, 3H, Ar- CH_3), 2.82 (t, $J = 7.7$ Hz, 2H, $-\text{COCH}_2-\text{CH}_2-\text{CH-Ar}$), 2.49-2.46 (m, 2H, OCH_2-CH_3), 2.44 – 2.37 (m, 5H, 3H+2H, OCH_2-CH_3 , $-\text{COCH}_2-\text{CH}_2-\text{CH-Ar}$).

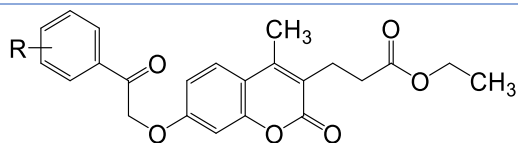
^{13}C NMR (151 MHz, DMSO) δ 194.32 (1C), 173.02 (1C), 161.14 (1C), 160.80 (1C), 153.58 (1C), 148.36 (1C), 134.74 (1C), 134.36 (1C), 129.31 (s, 2C), 128.38 (s, 2C), 127.00 (1C), 121.12 (1C), 114.31 (1C), 113.02 (1C), 101.84 (1C), 71.02 (1C), 51.86 (1C), 40.55 (1C), 32.44 (1C), 23.20 (1C), 15.13 (1C).

EMAC 10161 M: ethyl 3-(7-(2-(4-chlorophenyl)-2-oxoethoxy)-4-methyl-2-oxo-2H-chromen-3-yl)propanoate



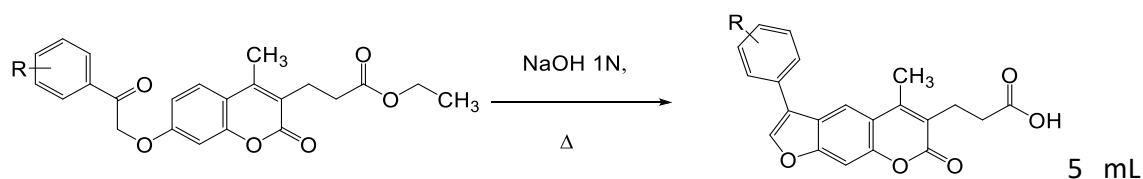
^1H NMR (600 MHz, DMSO) δ 8.05 (d, J = 8.6 Hz, 2H, CH-Ar), 7.72 (d, J = 8.9 Hz, 1H, CH-Ar Coum), 7.66 (d, J = 8.6 Hz, 2H, CH-Ar), 7.07 (d, J = 2.6 Hz, 1H, CH-Ar), 7.02 (dd, J = 8.9, 2.6 Hz, 1H, CH-Ar), 5.72 (s, 2H, -OCH₂CO), 4.04 (q, J = 7.1 Hz, 2H OCH₂-CH₃), 2.81 (t, J = 7.7 Hz, 2H-COCH₂-CH₂-CH-Ar), 2.49 – 2.42 (m, 2H-COCH₂-CH₂-CH-Ar), 2.41 (s, 3H, Ar-CH₃), 1.15 (t, J = 7.1 Hz, 3H, OCH₂-CH₃).

^{13}C NMR (151 MHz, DMSO) δ 193.45 (1C), 172.55 (1C), 161.13 (1C), 160.71 (1C), 153.58 (1C), 148.31 (1C), 139.23 (1C), 133.43 (1C), 130.34 (2C), 129.42 (2C), 127.01 (1C), 121.19 (1C), 114.34 (1C), 113.03 (1C), 101.83 (1C), 71.02 (1C), 60.42 (1C), 32.65 (1C), 23.22 (1C), 15.16 (1C), 14.53 (1C).

Table 34 Chemical, analytical, and physical data of derivatives **EMAC 10161 (a-m)**

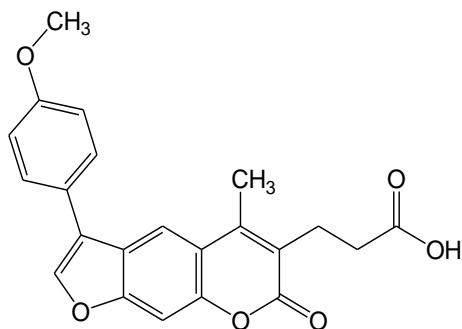
Compound	R	Aspect	MP °C	Yield %	RF AcOEt/Hex 2/1
10161 A	4-CH ₃	Pale yellow crystals	143-144	87	0.82
10161 B	4-OCH ₃	Pale yellow crystals	145-147	94	0.70
10161 D	4-F	Yellow crystals	144-145	83	0.76
10161 G	4-Phenyl	Pale yellow crystals	159-162	92	0.82
10161 H	2,4-F	Orange crystals	119-122	55	0.80
10161 L	4-H	Pale yellow crystals	134-136	96	0.76
10161 M	4-Cl	Yellow crystals	141-142	82	0.86

General method for the synthesis of compounds EMAC 10162 (b-m)



of 1 N sodium hydroxide were added to a suspension of the appropriate EMAC 10161 (a-m). The reaction mixture was stirred at reflux for 4 hours. Then, it was poured into crushed ice and water, and it was stirred until ice melting. Hydrochloric acid was added dropwise to obtain a precipitate. The product was filtered, and then recrystallized from isopropanol.

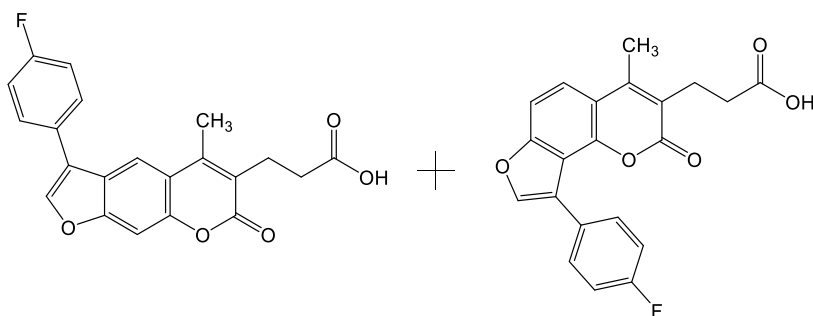
EMAC 10162 B: 3-(3-(4-methoxyphenyl)-5-methyl-7-oxo-7H-furo[3,2-g]chromen-6-yl)propanoic acid



^1H NMR (600 MHz, Acetone) δ 10.67 (bs, 1H, OH), 8.22 (s, 1H, OCH-Ar Furoc), 8.15 (s, 1H, CH-Ar Furoc), 7.74 (m, 2H, CH-Ar), 7.56 (s, 1H, CH-Ar Furoc), 7.10 (m, 2H, CH-Ar), 3.88 (s, 3H, -OCH₃), 3.01 – 2.97 (m, 2H, Ar-CH₂-CH₂-CO), 2.65 (s, 3H, Ar-CH₃), 2.60 (m, 2H, Ar-CH₂-CH₂-CO).

^{13}C NMR (151 MHz, Acetone) δ 173.08 (1C), 160.55 (1C), 159.55 (1C), 156.61 (1C), 150.55 (1C), 147.54 (1C), 142.76 (1C), 128.70 (2C), 123.64 (1C), 123.32 (1C), 122.95 (1C), 121.69 (1C), 117.32 (1C), 116.47 (1C), 114.58 (2C), 99.14 (1C), 54.78 (1C), 31.86 (1C), 23.25 (1C), 14.62 (1C).

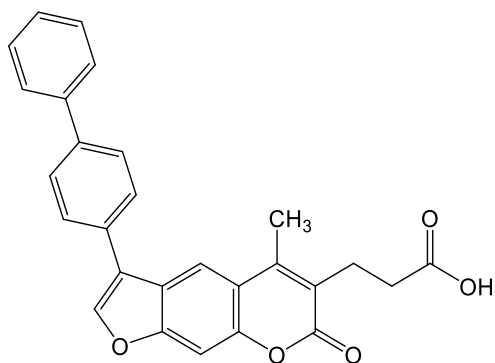
EMAC 10162 D: 3-(3-(4-fluorophenyl)-5-methyl-7-oxo-7H-furo[3,2-g]chromen-6-yl)propanoic acid



^1H NMR (600 MHz, DMSO) δ 12.24 (bs, 1H, OH), 8.51 (s, 1H, OCH-Ar Furoc), 8.15 (s, 1H, CH-Ar Furoc), 7.86 (d, J = 8.5 Hz, 1H, CH-Ar Furoc), 7.78 (d, J = 8.6 Hz, 3H, 1H+2H, CH-Ar Furoc, CH-Ar), 7.73 (d, J = 8.5 Hz, 1H, CH-Ar Furoc), 7.71 (d, J = 8.6 Hz, 1H, CH-Ar Furoc), 2.88 – 2.83 (m, 1H, Ar-CH₂-CH₂-CO), 2.57 (s, 3H, Ar-CH₃), 2.46 – 2.42 (m, 2H, Ar-CH₂-CH₂-CO).

^{13}C NMR (151 MHz, DMSO) δ 174.08 (2C), 163.06 (2C), 161.43 (2C), 160.96 (2C), 156.25 (2C), 150.34 (2C), 148.40 (2C), 144.73 (2C), 129.75 (d, J = 8.1 Hz, 4C), 127.60 (d, J = 3.0 Hz, 2C), 123.19 (2C), 122.98 (2C), 120.82 (2C), 117.48 (2C), 116.89 (2C), 116.64 (2C), 116.49 (2C), 99.91 (2C), 32.82 (2C), 23.51 (2C), 15.65 (2C).

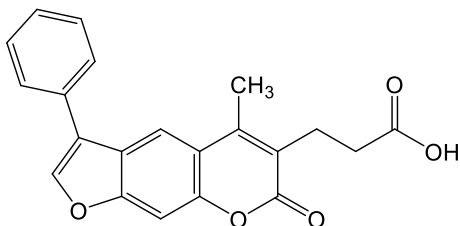
EMAC 10162 G: 3-(3-([1,1'-biphenyl]-4-yl)-5-methyl-7-oxo-7H-furo[3,2-g]chromen-6-yl)propanoic acid



^1H NMR (600 MHz, DMSO) δ 12.35 (bs, 1H, OH), 8.52 (s, 1H, OCH-Ar Furoc), 8.22 (s, 1H, CH-Ar Furoc), 7.92 (d, J = 8.1 Hz, 2H, CH-Ar), 7.84 (d, J = 8.2 Hz, 2H, CH-Ar), 7.78 (s, 1H, CH-Ar Furoc), 7.75 (d, J = 7.6 Hz, 2H, CH-Ar), 7.51 (t, J = 7.7 Hz, 2H, CH-Ar), 7.40 (t, J = 7.4 Hz, 1H, CH-Ar), 2.86 (t, J = 7.8, 8.4 Hz, 2H, Ar-CH₂-CH₂-CO), 2.59 (s, 3H, Ar-CH₃), 2.44 (t, J = 7.8, 8.4 Hz, 2H, Ar-CH₂-CH₂-CO).

^{13}C NMR (151 MHz, DMSO) δ 174.14 (1C), 161.00 (1C), 156.37 (1C), 150.36 (1C), 148.40 (1C), 144.91 (1C), 140.06 (1C), 139.95 (1C), 130.33 (1C), 129.52 (s, 2C), 128.21 (2C), 128.10 (1C), 127.89 (2C), 127.05 (1C), 123.26 (1C), 123.07 (s, 2C), 121.36 (1C), 117.53 (1C), 117.07 (1C), 99.96 (1C), 32.97 (1C), 23.59 (1C), 15.69 (s).

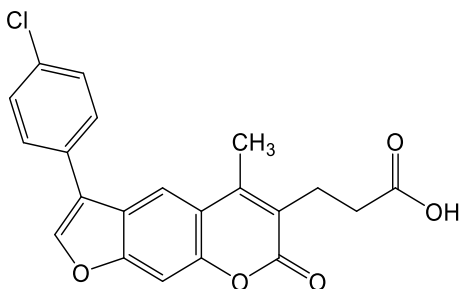
EMAC 10162 L: 3-(3-([1,1'-biphenyl]-4-yl)-5-methyl-7-oxo-7H-furo[3,2-g]chromen-6-yl)propanoic acid



^1H NMR (600 MHz, DMSO) δ 12.21 (bs, 1H, OH), 8.44 (s, 1H, OCH-Ar Furoc), 8.14 (s, 1H, CH-Ar Furoc), 7.80 (d, $J = 7.1$ Hz, 2H, CH-Ar), 7.75 (s, 1H, CH-Ar Furoc), 7.54 (t, $J = 7.7$ Hz, 2H, CH-Ar), 7.44 (t, $J = 7.4$ Hz, 1H, CH-Ar), 2.85 (t, $J = 7.8, 8.4$ Hz, 2H, Ar-CH₂-CH₂-CO), 2.56 (s, 3H, Ar-CH₃), 2.44 (t, $J = 7.8, 8.4$ Hz, 2H, Ar-CH₂-CH₂-CO).

^{13}C NMR (151 MHz, DMSO) δ 174.10 (1C), 160.99 (1C), 156.33 (1C), 150.31 (1C), 148.40 (1C), 144.73 (1C), 131.18 (1C), 129.69 (2C), 128.30 (1C), 127.69 (2C), 123.28 (1C), 122.96 (1C), 121.75 (1C), 117.46 (1C), 116.94 (1C), 99.91 (1C), 32.83 (1C), 23.51 (1C), 15.64 (s).

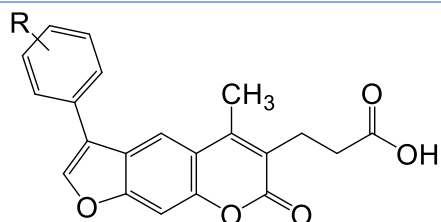
EMAC 10162 M: 3-(3-(4-chlorophenyl)-5-methyl-7-oxo-7H-furo[3,2-g]chromen-6-yl)propanoic acid



^1H NMR (600 MHz, DMSO) δ 12.21 (bs, 1H, OH), 8.51 (s, 1H, OCH-Ar Furoc), 8.15 (s, 1H, CH-Ar Furoc), 7.85 (d, $J = 8.5$ Hz, 2H, CH-Ar), 7.78 (s, 1H, CH-Ar Furoc), 7.59 (d, $J = 8.5$ Hz, 2H, CH-Ar), 2.86 (t, $J = 7.8, 8.4$ Hz, 2H, Ar-CH₂-CH₂-CO), 2.57 (s, 3H, Ar-CH₃), 2.44 (t, $J = 7.8, 8.4$ Hz, 2H, Ar-CH₂-CH₂-CO).

^{13}C NMR (151 MHz, DMSO) δ 174.09 (1C), 160.96 (1C), 156.31 (1C), 150.39 (1C), 148.43 (1C), 145.17 (1C), 132.85 (1C), 130.10 (1C), 129.67 (2C), 129.46 (2C), 123.05 (1C), 122.99 (1C), 120.69 (1C), 117.57 (1C), 116.99 (1C), 99.99 (1C), 32.82 (1C), 23.52 (1C), 15.68 (s).

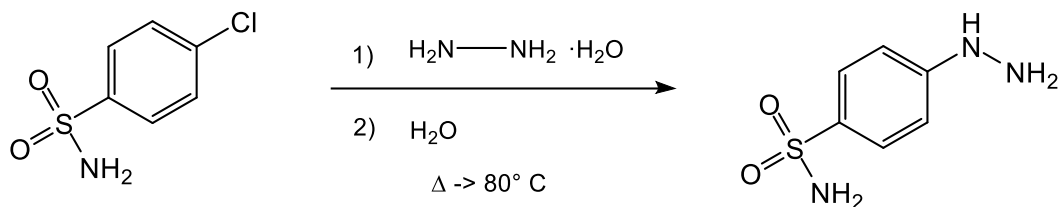
Table 35 Chemical, analytical, and physical data of derivatives **EMAC 10162 (a-m)**



Compound	R	Aspect	MP °C	Yield %	RF DCM/MeOH 3/1
10162 B	4-OCH ₃	Beige crystals	139-142	92	0.80
10162 D	4-F	Pale brown crystals	157-160	79	0.82
10162 G	4-Phenyl	Brown crystals	234-236	39	0.80
10162 L	4-H	Brown crystals	172-174	65	0.80
10162 M	4-Cl	Orange crystals	189-90	82	0.85

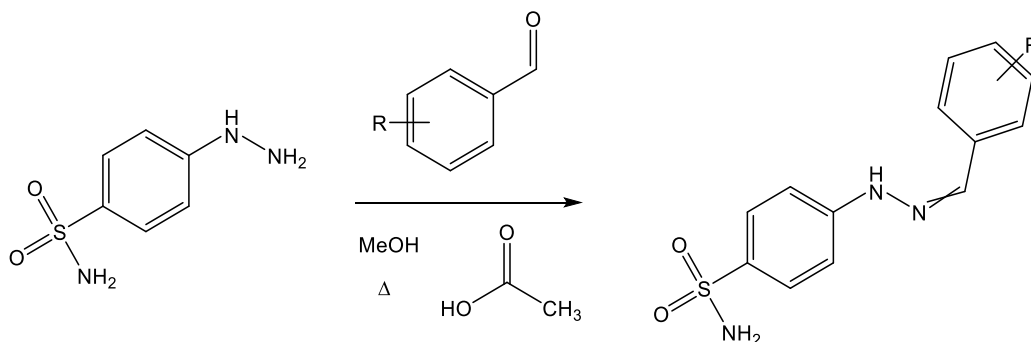
EMAC 10190 (b-I) and EMAC 10191 (b-I)

Synthesis of 4-hydrazineylbenzenesulfonamide



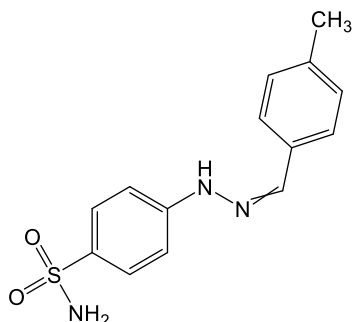
A solution of 4-chlorobenzenesulfonamide (1 mmol) and hydrazine monohydrate (1.0 mol) was irradiated under MW at 120°C with $p = 250$ psi. Then the mixture was poured into water (25 mL) and stirred for 30' at 80°C . After cooling at room temperature, a pearl white precipitate was formed. Then, the reaction mixture was put in the fridge overnight. The resulting precipitate was collected by filtration, washed thoroughly with water several times to eliminate the remaining hydrazine monohydrate, and with cold methanol, to eliminate the remaining 4-chlorobenzenesulfonamide. Then, the solid was dried under vacuum to give the title compound (95% yield) as a nacreous solid. The progression of the reaction was monitored by TLC (DCM/MeOH 20/1)

General method for the synthesis of derivatives EMAC 10190 (b-I) (ii)



To a solution of 4-hydrazineylbenzenesulfonamide (1 eq) and the opportune benzaldehyde (1 eq) in MeOH, acetic acid was added dropwise. The reaction mixture was stirred at reflux until the end of the reaction. A precipitate was formed, and it was filtered to obtain the desired compound, that was washed in H_2O to eliminate the remaining acid.

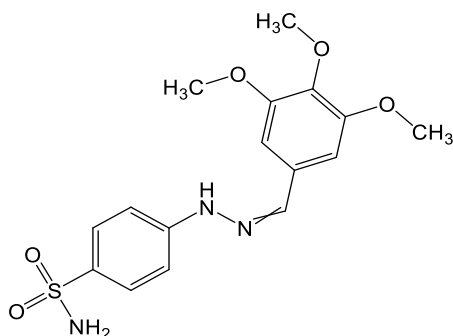
EMAC 10190 B: 4-(2-(4-methylbenzylidene)hydrazineyl)benzenesulfonamide



^1H NMR (600 MHz, DMSO) δ 10.69 (s, 1H, NH), 7.91 (s, 1H, -NCH), 7.65 (d, J = 8.8 Hz, 2H, CH-Ar Benz-Sulf), 7.58 (d, J = 8.0 Hz, 2H CH-Ar), 7.22 (d, J = 7.9 Hz, 2H CH-Ar), 7.13 (d, J = 8.7 Hz, 2H CH-Ar CH-Ar Benz-Sulf), 7.05 (s, 2H, SO_2NH_2), 2.33 (s, 3H, Ar- CH_3).

^{13}C NMR (151 MHz, DMSO) δ 148.32 (1C), 139.62 (1C), 138.64 (1C), 133.77 (1C), 133.01 (1C), 129.78 (s, 2C), 127.94 (s, 2C), 126.52 (2C), 111.54 (2C), 33.82 (s).

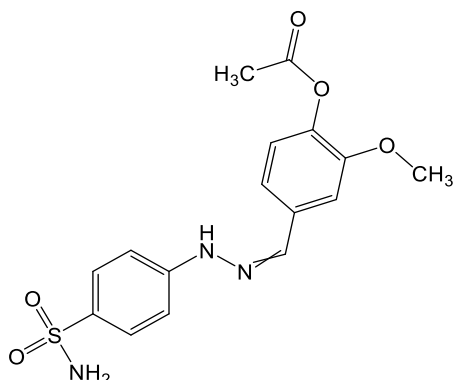
EMAC 10190 C: 4-(2-(3,4,5-trimethoxybenzylidene)hydrazineyl)benzenesulfonamide



^1H NMR (600 MHz, DMSO) δ 10.74 (s, 1H, NH), 7.88 (s, 1H, -NCH), 7.67 (d, J = 8.9 Hz, 2H, CH-Ar CH-Ar Benz-Sulf), 7.16 (d, J = 8.7 Hz, 2H, CH-Ar CH-Ar Benz-Sulf), 7.07 (s, 2H, CH-Ar), 7.00 (s, 2H, SO_2NH_2), 3.85 (s, 6H, 3H+3H, OCH_3 , OCH_3), 3.70 (s, 3H, OCH_3).

^{13}C NMR (151 MHz, DMSO) δ 153.66 (2C), 148.24 (1C), 139.48 (1C), 138.65 (1C), 133.87 (1C), 131.30 (1C), 127.91 (2C), 111.67 (2C), 103.86 (2C), 60.58 (1C), 56.42 (2C).

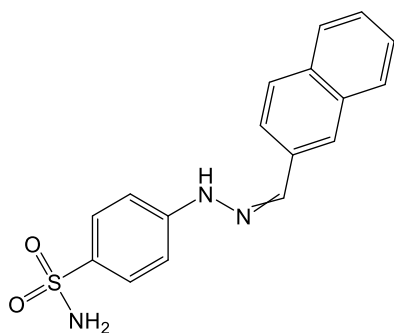
EMAC 10190 D: 2-methoxy-4-((2-(4-sulfamoylphenyl)hydrazineylidene)methyl)phenyl acetate



^1H NMR (600 MHz, DMSO) δ 10.82 (s, 1H, NH), 7.94 (s, 1H, -NCH), 7.67 (d, J = 8.9 Hz, 2H, CH-Ar Benz-Sulf), 7.44 (d, J = 1.7 Hz, 1H, CH-Ar), 7.27 (dd, J = 8.2, 1.7 Hz, 1H, CH-Ar), 7.17 (d, J = 8.8 Hz, 2H, CH-Ar CH-Ar Benz-Sulf), 7.12 (d, J = 8.1 Hz, 1H, CH-Ar), 7.08 (s, 2H, SO_2NH_2), 3.86 (s, 3H, OCH_3), 2.27 (s, 3H, $-\text{COCH}_3$).

^{13}C NMR (151 MHz, DMSO) δ 168.98 (1C), 151.61 (1C), 148.10 (1C), 140.09 (1C), 138.76 (1C), 134.68 (1C), 134.06 (1C), 127.93 (2C), 123.60 (1C), 119.25 (1C), 111.75 (2C), 110.02 (1C), 56.32 (1C), 20.89 (1C).

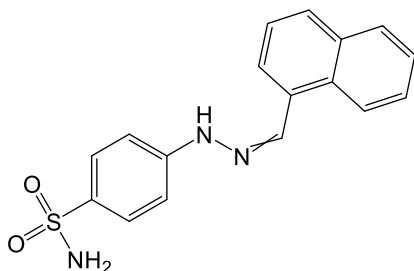
EMAC 10190 F: 4-(2-(naphthalen-2-ylmethylene)hydrazineyl)benzenesulfonamide



^1H NMR (600 MHz, DMSO) δ 10.81 (s, 1H, NH), 8.70 (d, J = 8.5 Hz, 1H, CH-Ar Napht), 8.50 (s, 1H, -NCH), 7.95-7.89 (m, 3H, 1H+2H, CH-Ar Napht, CH-Ar Napht), 7.70 (d, J = 8.9 Hz, 2H, CH-Ar Benz-Sulf) 7.66 – 7.56 (m, 3H, 2H+1H, CH-Ar Napht, CH-Ar Napht), 7.57 – 7.52 (m, 2H, CH-Ar Benz-Sulf), 7.06 (s, 2H, SONH_2).

^{13}C NMR (151 MHz, DMSO) δ 149.70 (1C), 138.16 (1C), 133.14 (1C), 132.90 (1C), 131.80 (1C), 130.15 (1C), 129.60 (1C), 129.10 (1C), 128.70 (2C), 127.59 (1C), 126.40 (1C), 126.10 (1C), 126.02 (1C), 123.90 (1C), 114.27 (2C).

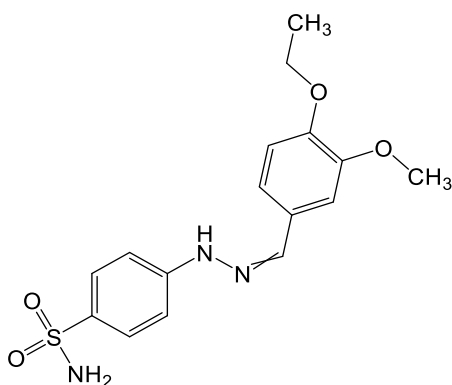
EMAC 10190 G: 4-(2-(naphthalen-1-ylmethylene)hydrazineyl)benzenesulfonamide



^1H NMR (600 MHz, DMSO) δ 10.92 (s, 1H, NH) 8.73 (d, J = 8.5 Hz, 1H, CH-Ar Napht), 8.64 (s, 1H, -NCH), 8.00 (d, J = 8.0 Hz, 1H, CH-Ar Napht), 7.95 (d, J = 7.6 Hz, 2H, CH-Ar Napht), 7.72 (d, J = 8.9 Hz, 2H, CH-Ar Benz-Sulf), 7.68 (ddd, J = 8.4, 6.8, 1.3 Hz, 1H, CH-Ar Napht), 7.59 (dd, J = 14.5, 6.8 Hz, 2H, CH-Ar Napht), 7.21 (d, J = 8.7 Hz, 2H, CH-Ar Napht), 7.10 (s, 2H, SO_2NH_2).

^{13}C NMR (151 MHz, DMSO) δ 148.16 (1C), 139.03 (1C), 134.14 (1C), 134.10 (1C), 130.91 (1C), 130.30 (1C), 129.47 (1C), 129.25 (1C), 128.06 (2C), 127.49 (1C), 126.56 (1C), 126.33 (1C), 126.12 (1C), 124.32 (1C), 111.74 (2C).

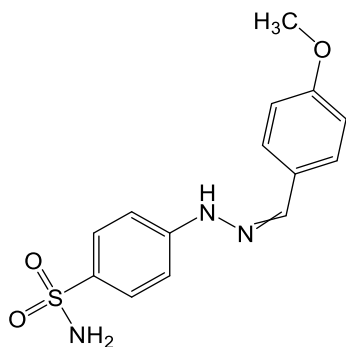
EMAC 10190 H: 4-(2-(4-ethoxy-3-methoxybenzylidene)hydrazineyl)benzenesulfonamide



^1H NMR (600 MHz, DMSO) δ 10.62 (s, 1H, NH), 7.88 (s, 1H, -NCH), 7.65 (d, J = 8.9 Hz, 2H, CH-Ar Benz-Sulf), 7.33 (d, J = 1.8 Hz, 1H, CH-Ar), 7.15 (d, J = 1.8 Hz, 1H, CH-Ar), 7.14-7.12 (m, 2H, CH-Ar Benz-Sulf), 7.05 (s, 2H, SO_2NH_2), 6.97 (d, J = 8.3 Hz, 1H, CH-Ar), 4.05 (q, J = 7.0 Hz, 2H, $\text{OCH}_2\text{-CH}_3$), 3.84 (s, 3H, $-\text{OCH}_3$), 1.35 (t, J = 7.0 Hz, 3H $\text{OCH}_2\text{-CH}_3$).

^{13}C NMR (151 MHz, DMSO) δ 149.64 (1C), 149.33 (1C), 148.42 (1C), 139.83 (1C), 133.52 (1C), 128.48 (1C), 127.92 (2C), 120.52 (1C), 113.07 (1C), 111.45 (2C), 108.80 (1C), 64.21 (1C), 55.94 (1C), 15.18 (1C).

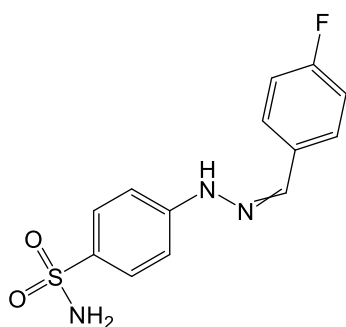
EMAC 10190 J: 4-(2-(4-methoxybenzylidene)hydrazineyl)benzenesulfonamide



^1H NMR (600 MHz, DMSO) δ 10.62 (s, 1H, NH), 7.91 (s, 1H, -NCH), 7.65 (dd, J = 10.4, 8.9 Hz, 4H, 2H+2H, CH-Ar, CH-Ar Benz-Sulf), 7.12 (d, J = 8.7 Hz, 2H CH-Ar Benz-Sulf), 7.05 (s, 2H, SO_2NH_2), 6.99 (d, J = 8.8 Hz, 2H, CH-Ar), 3.80 (s, 3H, OCH_3).

^{13}C NMR (151 MHz, DMSO) δ 160.25 (1C), 148.46 (1C), 139.55 (1C), 133.50 (1C), 128.37 (1C), 127.97 (d, J = 10.2 Hz, 4C), 114.70 (2C), 111.40 (2C), 55.71 (1C).

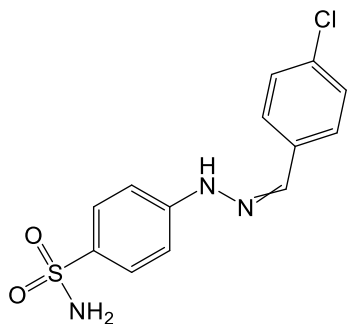
EMAC 10190 K: 4-(2-(4-fluorobenzylidene)hydrazineyl)benzenesulfonamide



^1H NMR (600 MHz, DMSO) δ 10.78 (s, 1H, NH), 7.95 (s, 1H, -NCH), 7.75 (dd, J = 8.5, 5.7 Hz, 2H, CH-Ar), 7.68 (d, J = 8.8 Hz, 2H, CH-Ar Benz-Sulf), 7.25 (t, J = 8.8 Hz, 2H, CH-Ar), 7.16 (d, J = 8.7 Hz, 2H CH-Ar Benz-Sulf), 7.08 (s, 2H, SO_2NH_2).

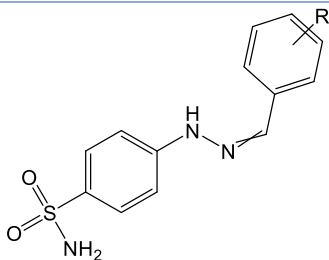
^{13}C NMR (151 MHz, DMSO) δ 163.53 (1C), 161.90 (1C), 148.24 (1C), 138.33 (1C), 133.99 (1C), 132.35 (d, J = 2.9 Hz, 1C), 128.49 (d, J = 8.2 Hz, 1C), 127.95 (2C), 116.17 (d, J = 21.8 Hz, 1C), 111.66 (2C).

EMAC 10190 L: 4-(2-(4-chlorobenzylidene)hydrazineyl)benzenesulfonamide



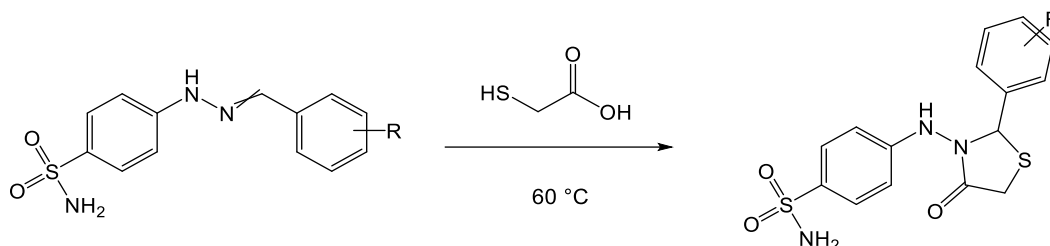
^1H NMR (600 MHz, DMSO) δ 10.87 (s, 1H, NH), 7.94 (s, 1H, -NCH), 7.72 (d, J = 8.5 Hz, 2H, CH-Ar Benz-Sulf), 7.67 (d, J = 8.9 Hz, 2H, CH-Ar), 7.47 (d, J = 8.5 Hz, 2H, CH-Ar Benz-Sulf), 7.16 (d, J = 8.8 Hz, 2H, CH-Ar), 7.08 (s, 2H, SO_2NH_2).

^{13}C NMR (151 MHz, DMSO) δ 157.08 (1C), 148.06 (1C), 138.05 (1C), 134.23 (1C), 133.27 (1C), 129.22 (2C), 128.02 (d, J = 21.6 Hz, 4C), 111.78 (2C).

Table 36 Chemical, analytical, and physical data of derivatives **EMAC 10190 (a-l)**

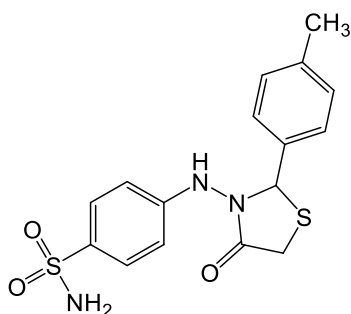
Compound	R	Aspect	MP °C	Yield %	RF DCM/MeOH 20/1
10190 B	4-CH ₃	Optic white crystals	220-221	65	0.29
10190 C	3,4,5-OCH ₃	Light yellow crystals	222-225	95	0.24
10190 D	4-Acethoxy-3-OCH ₃	Optic white crystals	185-188	93	0.25
10190 F	2-Naphtal	Light yellow crystals	230-233	71	0.26
10190 G	1-Naphtal	Green crystals	232-234	78	0.23
10190 H	4-OCH ₂ CH ₃ -3-OCH ₃	White crystals	183-185	84	0.26
10190 J	4-OCH ₃	Dirty white crystals	207-210	77	0.21
10190 K	4-F	White crystals	219-221	89	0.21
10190 L	4-Cl	White crystals	220-223	83	0.19

General method for the synthesis of derivates EMAC 10191 (b-I) (iii)



A solution of the opportune **EMAC10190 (b-I)** (1eq) in mercaptoacetic acid (15 eq), was stirred at 60°C until the end of the reaction. Then the solution was cooled at room temperature, and ethyl acetate was added; the organic layer was washed with NaHCO₃ (3 × 20 mL), and then with H₂O (3 × 20 mL), dried over Na₂SO₄ and then concentrated in vacuo to obtain a solid. It was purified with Isopropyl ether. The product was purified by flash chromatography (DCM/MeOH = 20/1). The progression of the reaction was monitored by TLC (DCM/MeOH 20/1).

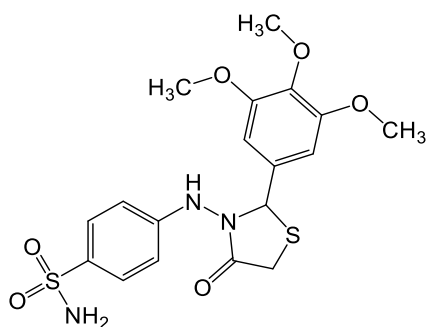
EMAC 10191 B: 4-((4-oxo-2-(p-tolyl)thiazolidin-3-yl)amino)benzenesulfonamide



¹H NMR (600 MHz, DMSO) δ 8.64 (s, 1H, NH), 7.58 (s, 2H, CH-Ar Benz-Sulf), 7.32 (s, 2H, CH-CH-Ar), 7.19 (d, *J* = 7.3 Hz, 2H, CH-Ar), 7.06 (s, 2H, SO₂NH₂), 6.74 (d, *J* = 8.1 Hz, 2H, CH-Ar Benz-Sulf), 5.85 (s, 1H, NCHS Thiaz), 4.38 (s, 3H, CH₃), 3.93 (d, *J* = 15.8 Hz, 1H, S-CH₂-thiaz), 3.81 (d, *J* = 15.7 Hz, 1H, S-CH₂-Thiaz).

¹³C NMR (151 MHz, DMSO) δ 198.63 (1C), 170.02 (1C), 149.98 (1C), 139.08 (1C), 135.10 (1C), 129.67 (2C), 127.68 (2C), 111.76 (4C), 48.26 (1C), 41.34 (1C), 25.80 (1C).

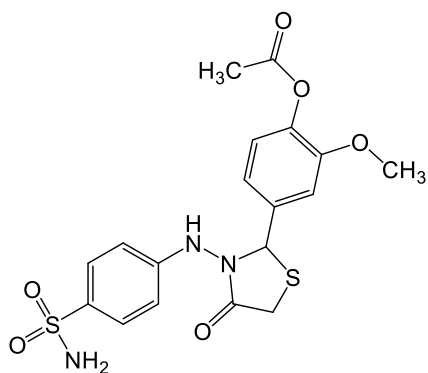
EMAC 10191 C: 4-((4-oxo-2-(3,4,5-trimethoxyphenyl)thiazolidin-3-yl)amino)benzenesulfonamide



^1H NMR (600 MHz, Acetone) δ 7.81 (s, 1H, NH), 7.68 (d, J = 8.7 Hz, 2H, CH-Ar Benz-Sulf), 6.85 (d, J = 8.8 Hz, 2H, CH-Ar Benz-Sulf), 6.80 (s, 2H, SO_2NH_2), 6.29 (s, 2H, CH-Ar), 5.89 (d, J = 1.2 Hz, 1H, NCHS Thiaz), 3.81 (s, 6H, 3H+3H, OCH_3 , OCH_3), 3.77-3.73 (m, 2H, SCH_2 -thiaz), 3.72 (s, 3H, OCH_3).

^{13}C NMR (151 MHz, Acetone) δ 196.54 (1C), 168.59 (1C), 153.74 (2C), 135.00 (1C), 127.68 (2C), 111.87 (2C), 104.79 (1C), 59.63 (1C), 55.60 (3C), 40.90 (1C).

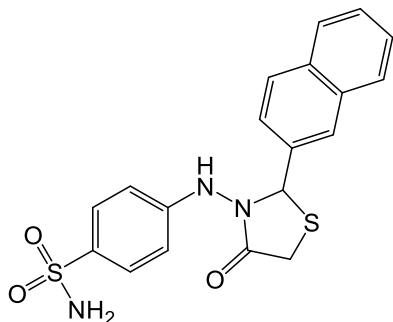
EMAC 10191 D: 2-methoxy-4-(4-oxo-3-((4-sulfamoylphenyl)amino)thiazolidin-2-yl)phenyl acetate



^1H NMR (600 MHz, Acetone) δ 7.92 (s, 1H, NH), 7.70 (d, J = 6.8 Hz, 2H, CH CH-Ar Benz-Sulf), 7.27 (s, 1H, CH-Ar), 7.07 (s, 2H, CH-Ar), 6.91 – 6.83 (m, 2H, CH-Ar Benz-Sulf), 6.31 (s, 2H, SO_2NH_2), 5.97 (s, 1H, NCHS Thiaz), 3.92 (dd, J = 15.8, 1.7 Hz, 1H, SCH_2 -thiaz), 3.83 (s, 3H, OCH_3), 3.78 (d, J = 15.8 Hz, 1H, SCH_2 -thiaz), 2.25 (s, 3H, COCH_3).

^{13}C NMR (151 MHz, DMSO) δ 169.05 (1C), 168.11 (1C), 151.72 (1C) 149.70 (1C), 140.48 (1C), 135.02 (1C), 127.72 (2C), 122.99 (2C), 119.62 (1C), 111.86 (2C), 111.55 (1C), 61.73 (1C), 55.48 (1C), 25.70 (1C), 19.60 (1C).

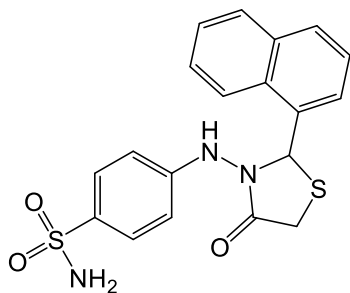
EMAC 10191 F: 4-((2-(naphthalen-2-yl)-4-oxothiazolidin-3-yl)amino)benzenesulfonamide



^1H NMR (600 MHz, DMSO) δ 8.73 (s, 1H, NH), 7.98 (d, J = 8.5 Hz, 1H, CH-Ar Napht), 7.93 (d, J = 5.2 Hz, 1H, CH-Ar Napht), 7.92 – 7.89 (m, 2H, CH-Ar Napht), 7.66 – 7.56 (m, 2H, CH-Ar Benz-Sulph), 7.57 – 7.52 (m, 3H CH-Ar Napht), 7.06 (s, 2H, NH_2), 6.77 (d, J = 8.4 Hz, 2H CH-Ar Benz-Sulf), 6.06 (s, 1H, NCHS thiaz), 4.04 (d, J = 15.8 Hz, 1H, SCH_2 -thiaz), 3.87 (d, J = 15.9 Hz, 1H, SCH_2 -thiaz).

^{13}C NMR (151 MHz, DMSO) δ 198.62 (1C), 169.47 (1C), 152.72 (1C), 134.71 (1C), 133.53 (1C), 132.99 (1C), 129.19 (1C), 128.43 (1C), 128.08 (1C), 127.71 (1C), 127.11 (1C), 127.03 (2C), 126.63 (1C) 125.78 (1C), 111.79 (2C), 41.34 (1C), 23.21 (1C).

EMAC 10191 G: 4-((2-(naphthalen-1-yl)-4-oxothiazolidin-3-yl)amino)benzenesulfonamide

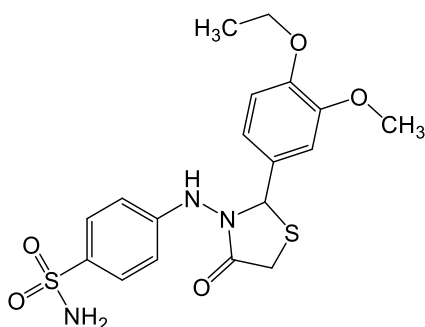


^1H NMR (600 MHz, Acetone) δ 8.13 (d, J = 7.1 Hz, 1H, NH), 8.07 (s, 1H CH-Ar Napht), 8.00 (d, J = 2.8 Hz, 1H CH-Ar Napht), 7.99 (d, J = 2.1 Hz, 1H CH-Ar Napht), 7.96 (d, J = 8.2 Hz, 1H CH-Ar Napht), 7.73 (d, J = 8.7 Hz, 2H CH-Ar Benz-Sulf), 7.64 – 7.54 (m, 4H, 2H+2H, CH-Ar

Napht, CH-Ar Benz-Sulf), 6.95 (d, $J = 8.7$ Hz, 2H, NH₂), 6.82 (s, 1H, , CH-Ar Napht), 6.32 (s, 1H, NCHS thiaz), 3.84 (q, $J = 16.1$ Hz, 2H, SCH₂-thiaz).

¹³C NMR (151 MHz, Acetone) δ 181.14 (1C), 169.67 (1C), 149.78 (1C), 135.25 (1C), 134.94 (1C), 134.22 (1C), 130.63 (1C), 129.12 (1C), 128.99 (1C), 127.76 (2C), 126.67 (1C), 126.10 (1C), 125.43 (1C), 122.59 (1C), 112.02 (2C), 58.72 (1C), 29.86 (1C).

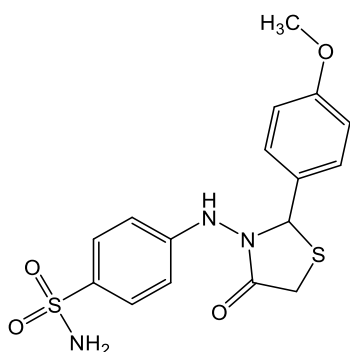
EMAC 10191 H: 4-((2-(4-ethoxy-3-methoxyphenyl)-4-oxothiazolidin-3-yl)amino)benzenesulfonamide



¹H NMR (600 MHz, DMSO) δ 7.90 (s, 1H, NH), 7.68 (d, $J = 6.8$ Hz, 2H, CH CH-Ar Benz-Sulf), 7.28 (s, 1H, CH-Ar), 7.04 (s, 2H, CH-Ar), 6.95 – 6.87 (m, 2H, CH-Ar Benz-Sulf), 6.28 (s, 2H, SO₂NH₂), 5.92 (s, 1H, NCHS Thiaz), 4.05 (q, $J = 7.0$ Hz, 2H, OCH₂-CH₃), 3.70 (s, 3H, OCH₃), 3.50 (d, $J = 15.8$ Hz, 1H, SCH₂-thiaz), 3.45 (d, $J = 15.8$ Hz, 1H, SCH₂-Thiaz), 2.25 (s, 3H, COCH₃).

¹³C NMR (151 MHz, DMSO) δ 169.98 (1C), 168.09 (1C), 151.60 (1C) 149.70 (1C), 141.60 (1C), 136.24 (1C), 128.92 (2C), 122.40 (2C), 118.67 (1C), 112.97 (2C), 111.40 (1C), 61.73 (1C), 55.48 (1C), 35.12 (1C), 19.60 (1C).

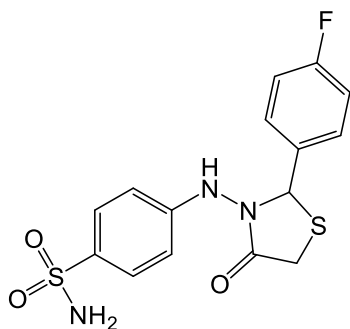
EMAC 10191 J: 4-((2-(4-methoxyphenyl)-4-oxothiazolidin-3-yl)amino)benzenesulfonamide



^1H NMR (600 MHz, Acetone) δ 7.74 (s, 1H, NH), 7.68 (d, J = 8.6 Hz, 2H, CH CH-Ar Benz-Sulf), 7.44 (d, J = 8.2 Hz, 2H, CH CH-Ar Benz-Sulf), 6.96 – 6.92 (m, 2H, CH CH-Ar), 6.86 – 6.82 (m, 2H, CH-Ar), 6.29 (s, 2H, NH₂), 5.90 (s, 1H, NCHS Thiaz), 3.87 (dd, J = 15.8, 1.7 Hz, 1H, SCH₂-Thiaz), 3.81 (s, 3H, OCH₃), 3.77 (d, J = 15.8 Hz, 1H, SCH₂-Thiaz).

^{13}C NMR (151 MHz, Acetone) δ 160.56 (1C), 135.33 (1C), 129.28 (1C), 129.22.16 (1C), 127.63 (2C), 113.97 (2C), 111.84 (4C), 54.75 (1C), 33- (1C), 29.43 (1C),

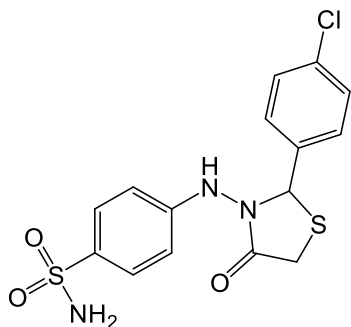
EMAC 10191 K: 4-((2-(4-fluorophenyl)-4-oxothiazolidin-3-yl)amino)benzenesulfonamide



^1H NMR (600 MHz, Acetone) δ 7.82 (s, 1H, NH), 7.69 (d, J = 8.6 Hz, 2H, CH CH-Ar Benz-Sulf), 7.62 – 7.55 (m, 2H, CH CH-Ar), 7.19 – 7.13 (m, 2H, CH CH-Ar), 6.85 (d, J = 8.8 Hz, 2H, CH CH-Ar Benz-Sulf), 6.31 (s, 2H, SO₂NH₂), 5.98 (s, 1H, NCHS Thiaz), 3.91 (dd, J = 15.9, 1.7 Hz, 1H, SCH₂-Thiaz), 3.79 (d, J = 15.9 Hz, 1H, SCH₂-Thiaz).

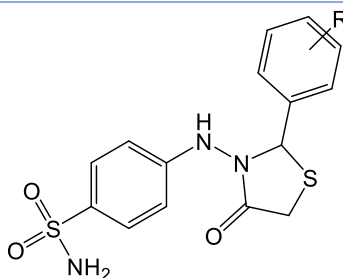
^{13}C NMR (151 MHz, Acetone) δ 169.20 – 168.48 (m), 163.76 (1C), 162.13 (1C), 149.74 (1C), 135.68 (1C), 135.09 (1C), 129.99 (1C), 127.66 (2C), 115.51 (1C), 115.37 (1C), 111.88 (2C), 61.37 (1C), 29.69 (1C).

EMAC 10191 L: 4-((2-(4-chlorophenyl)-4-oxothiazolidin-3-yl)amino)benzenesulfonamide



^1H NMR (600 MHz, DMSO) δ 8.69 (s, 1H, NH), 7.59 (d, J = 6.6 Hz, 2H, CH CH-Ar Benz-Sulf), 7.44 (d, J = 7.5 Hz, 4H, 2H+2H, CH-Ar, CH-Ar), 7.06 (s, 2H SO_2NH_2), 6.73 (d, J = 8.4 Hz, 2H, CH CH-Ar Benz-Sulf), 5.91 (s, 1H NCHS Thiaz), 3.96 (d, J = 15.7 Hz, 1H, SCH_2 -Thiaz), 3.81 (d, J = 15.8 Hz, 1H, SCH_2 -Thiaz).

^{13}C NMR (151 MHz, DMSO) δ 169.74 (1C) 149.69 (1C), 134.81 (1C), 133.77 (1C), 129.81 (1C), 129.13 (1C), 127.69 (2C), 127.69 (2C), 111.80 (2C), 60.47 (1C), 41.34 (1C).

Table 37 Chemical, analytical, and physical data of derivatives **EMAC 10191 (a-l)**

Compound	R	Aspect	MP °C	Yield %	RF DCM/MeOH 10/1
10191 B	4-CH ₃	White solid	146-148	21	0.59
10191 C	3,4,5-OCH ₃	Light yellow solid	151-153	27	0.53
10191 D	4-Acethoxy-3- OCH ₃	Light yellow solid	111-114	15	0.51
10191 F	2-Naphtal	White solid	219-221	23	0.58
10191 G	1-Naphtal	Light yellow solid	220-223	40	0.48
10191 H	4-OCH ₂ CH ₃ -3- OCH ₃	Yellow solid	110-113	20	0.47
10191 J	4-OCH ₃	White solid	144-147	19	0.47
10191 K	4-F	White solid	142-145	25	0.47
10191 L	4-Cl	Light yellow solid	146-148	40	0.47

General information

Starting materials and reagents were obtained from commercial suppliers and were used without purification. $^1\text{H-NMR}$ and $^{13}\text{C-NMR}$ spectra were registered on a Bruker AMX 400 MHz (chemical shifts in δ values) operating at 400 MHz and 100 MHz, respectively, or on a Bruker Avance III HD 600 operating at 600 MHz and 151 MHz, respectively. Chemical shifts are reported referenced to the solvent in which they were measured. Coupling constants J are expressed in hertz (Hz). Microanalytical data of the synthesized compounds are in agreement within $\pm 0.4\%$ of the theoretical values. TLC chromatography was performed using silica gel plates (Merck F 254), spots were visualized by UV light. Chromatographic purifications were performed on columns packed with Merk 60 silica gel, 23-400 mesh, for flash technique. All melting points were determined on a Stuart SMP11 melting points apparatus and are uncorrected.

Microwave Irradiation Experiments

Microwave irradiation experiments were conducted using a CEM Discover SP + Explorer Hybrid (CEM Corp., Matthews, NC). The machine consists of a continuous focused microwave power delivery system with operator-selectable power output from 0 to 300 W. The temperature of the contents of the vessels was monitored using a calibrated infrared temperature control mounted under the reaction vessel. All the experiments were performed using a stirring option whereby the contents of the vessel are stirred by means of a rotating magnetic plate located below the floor of the microwave cavity and a Teflon-coated magnetic stir bar in the vessel.

Carbonic anhydrase inhibition assay

The CA catalyzed CO_2 hydration/inhibition was measured by using a stopped-flow instrument (Applied Photophysics, Oxford, U.K.) as the method described earlier.²³³ Initial rates of the CA-catalyzed CO_2 hydration reaction were followed for 10–100 s. The CO_2 concentrations ranged from 1.7 to 17 mM for the determination of the inhibition constants. For each inhibitor, at least six traces of the initial 5–10% of the reaction were used for assessing the initial velocity. The uncatalyzed rates were subtracted from the total observed rates. Stock solutions of inhibitors (10 mM) and dilutions up to 0.01 nM were prepared in distilled-deionized water. Inhibitor and enzyme solutions were preincubated together for 15 min at room temperature prior to assay, in order to allow for the

formation of the E-I complex. The inhibition constants were obtained by non-linear least-squares methods using PRISM 3 as reported earlier and represent the mean from at least three different determinations^{46–48}. hCA I, hCA II, hCA IX (catalytic domain), and hCA XII (catalytic domain) were recombinant proteins produced in-house using our standardized protocol and their concentration in the assay system was in the range of 3–10 nM (and even lower for highly effective, sub-nanomolar inhibitors).^{234, 235}

Experimental part drug design

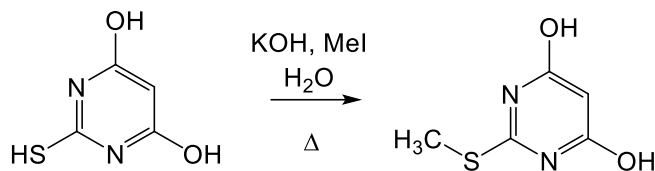
Theoretical 3D models of compounds were built by means of Maestro GUI or downloaded from the PDB.²³⁶ Ligands were docked in the global minimum energy conformation as determined by molecular mechanics conformational analysis performed with Macromodel software version 9.2.²³⁷ All parameters were left as default. The geometry was optimized by MMFFs (Merck molecular force fields)²³⁸ and GB/SA water implicit solvation model²³⁹ using Polak-Ribier Conjugate Gradient (PRCG) method, 5000 iterations and a convergence criterion of 0.05 kcal/(mol Å).

QikProp²³² results are not very sensitive to the conformation of the input structure.

However, the energy minimized ligands structures were evaluated for their drug-like properties.

Pyrazolo[3,4-*d*]pyrimidine

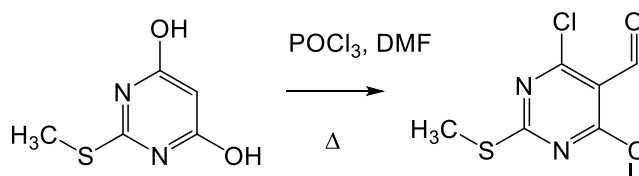
Synthesis of 2-(methylthio)pyrimidine-4,6-diol (2)



2-mercaptopyrimidine-4,6-diol

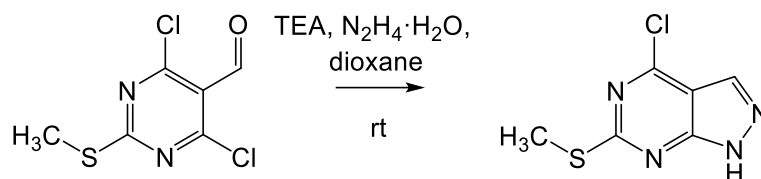
To a solution of 2-thiobarbituric acid (1) (5.00 g, 34.7 mmol, 1.00 eq.), KOH (5.84 g, 104.1 mmol, 3.00 eq.), and H₂O (50 mL), methyl iodide (2.4 mL, 38.2 mmol, 1.10 eq.) was added. The reaction mixture was heated for 3 hours under reflux. The transparent solution was cooled to room temperature and acidified with 3N HCl until pH 2. The product was obtained as a light-yellow precipitate and was recovered by filtration under vacuum.

Synthesis of 4,6-dichloro-2-(methylthio)pyrimidine-5-carbaldehyde (3)



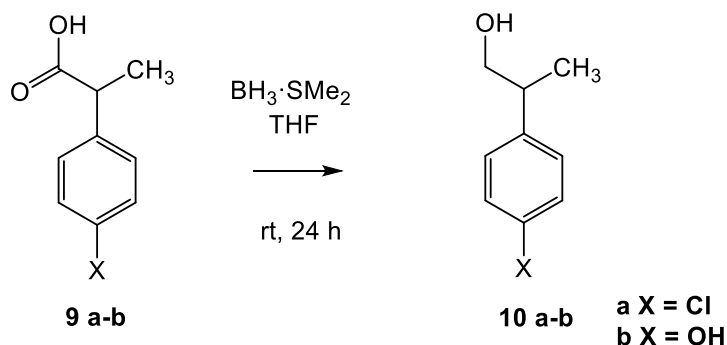
Anhydrous DMF (1.60 mL, 19.0 mmol, 3.00 eq.) was slowly added to an ice-cooled solution of distilled POCl₃ (4.40 mL, 47.5 mmol, 7.50 eq.), and the resulting solution was stirred for 1 hour at room temperature. 2-(methylthio)pyrimidine-4,6-diol (2) (1.00 g, 6.33 mmol, 1.00 eq.) was added in 3 portions within 30 minutes, and the resulting solution was stirred under reflux overnight. The reaction mixture was cooled to room temperature, diluted with H₂O (50 mL), and then stirred overnight at room temperature. The solution was neutralized with NaHCO₃ until pH 7. The product was extracted with EtOAc (3 x 50 mL), the organic layer was washed with brine, dried over Na₂SO₄, filtered and the solvent removed under reduced pressure. The obtained oil was added to the precipitate and was purified by flash chromatography (Hex/EtOAc = 99/1) to obtain the product as a white solid.

Synthesis of 4-chloro-6-(methylthio)1H-pyrazolo[3,4-d]pyrimidine (4)



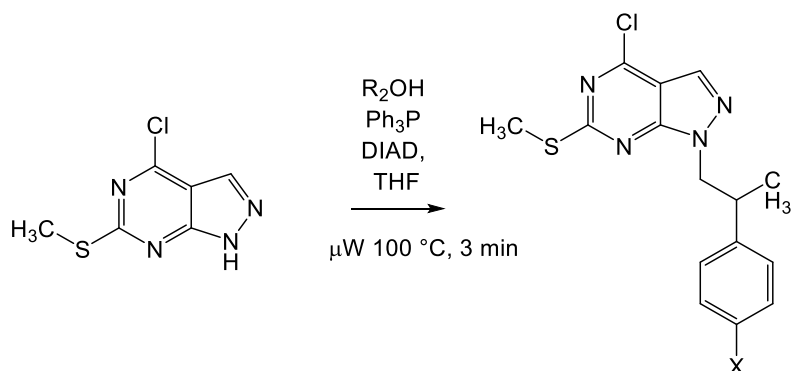
To an ice-cooled solution of 4,6-dichloro-2-(methylthio)pyrimidine-5-carbaldehyde (3) (100 mg, 0.45 mmol, 1.00 eq.) and TEA (0.06 mL, 0.45 mmol, 1.00 eq) in dioxane (1 mL), N₂H₄·H₂O (0.015 mL, 0.50 mmol, 1.10 eq) was added. After 5 minutes, the ice bath was removed, and the reaction was stirred at room temperature for 5 hours, until the completion of the reaction. To acidify the reaction, 10 mL of 0.5 N HCl were added. Then, an extraction with EtOAc (3 × 20 mL) was performed, and the organic phases were collected and dried over Na₂SO₄, filtered, and evaporated under reduced pressure to obtain a yellow solid. The product was purified by flash chromatography (DCM/MetOH = 99/1).

General Synthesis of 2-(4-arylphenyl)propan-1-ol



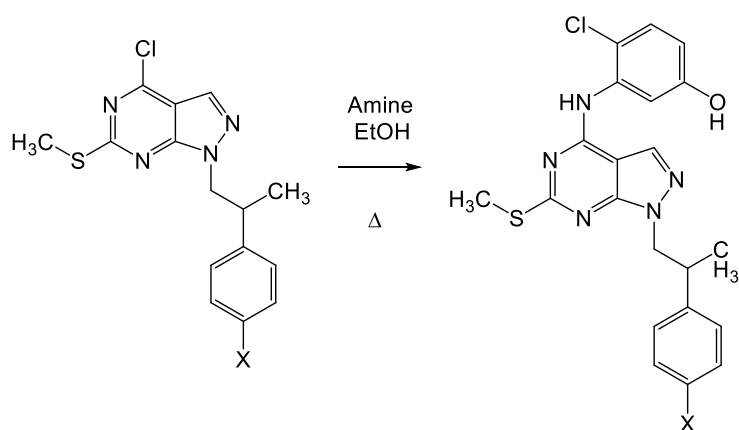
The appropriate 2-(4-arylphenyl)propanoic acid (6 mmol, 1 eq) was dissolved in dry THF (46 mL), and BH₃·SMe₂ (33.6 mmol, 5.6 eq) was added dropwise at 0° C. The reaction mixture was stirred for 2 hours at 0° C and then cooled to room temperature and stirred for 24 hours, till the completion of the reaction. The mixture was quenched with NaHCO₃, then the aqueous layer was extracted with Et₂O (3 x 20 mL). The combined organic layers were washed with brine and dried over Na₂SO₄, filtered and concentrated in vacuo. The product was purified by flash chromatography using DCM/MetOH 99/1

General synthesis of 4-chloro-1-(2-arylpropyl)-6-(methylthio)-1H-pyrazolo[3,4-d]pyrimidine (5a-b)



Ph_3P (40 mg, 0.15 mmol, 1.50 eq.) and 4-chloro-6-(methylthio)-1H-pyrazolo[3,4-d]pyrimidine (4) (20 mg, 0.10 mmol, 1.00 eq.) were dissolved in anhydrous THF while cooling with an ice bath. Then the corresponding alcohol (10 a-b) (0.15 mmol, 1.50 eq) was added. Immediately, DIAD (0.03 ml, 0.15 mmol, 1.50 eq.) was added dropwise over 1 minute. The reaction mixture was stirred at 4° C for 15 minutes, then allowed to warm to room temperature. The solution was irradiated under μW at 100° C for 3 minutes, $\lambda = 300$ Wmax and $p = 250$ psi. Then the reaction was taken to dryness to obtain a green oil, that was purified by flash chromatography using PE/AcOEt mixture as eluent.

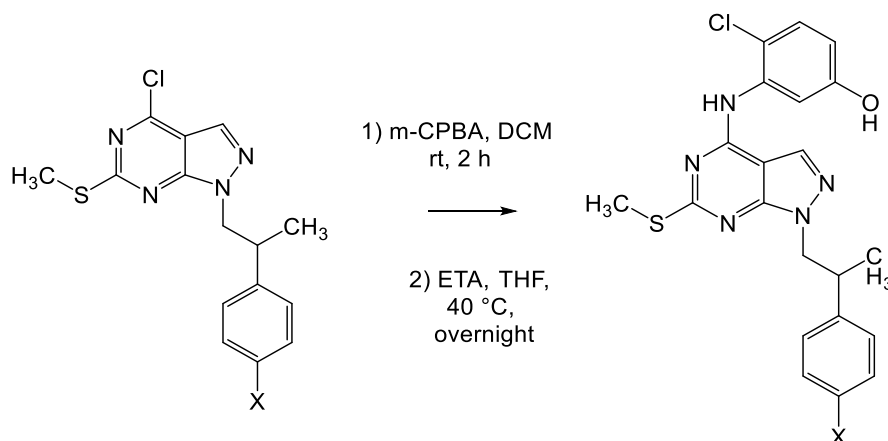
General synthesis of 4-chloro-3-(1-(2-arylpropyl)-6-(methylthio)-1H-pyrazolo[3,4-d]pyrimidin-4-ylamino)phenol (6a-b)



3-amino-4-chlorophenol (65 mg, 0.45 mmol, 3 eq.) was added to a solution of the appropriate 4-chloro-1-(2-arylpropyl)-6-(methylthio)-1H-pyrazolo[3,4-d]pyrimidine (5a-b) (53

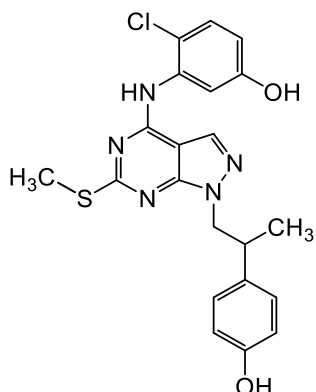
mg, 0.15 mmol, 1 eq.) in EtOH (2 mL). The reaction mixture was stirred under reflux overnight, until the completion of the reaction. The solvent was removed under reduced pressure, and the product was purified by flash chromatography using DCM/MeOH.

General synthesis of 4-chloro-3-(1-(2-arylpropyl)-6-(2-hydroxyethylamino)-1H-pyrazolo[3,4-d]pyrimidin-4-ylamino)phenol (8 a-b)



m-CPBA (22 mg, 0.13 mmol, 2.10 eq.) was added to a solution of the appropriate 4-chloro-3-(1-(2-arylpropyl)-6-(methylthio)-1H-pyrazolo[3,4-d]pyrimidin-4-ylamino)phenol (6 a-b) (28 mg, 0.06 mmol, 1.00 eq.) in DCM (3 mL) at 0°C. The reaction mixture was stirred overnight at room temperature. *m*-CPBA was neutralized with NaHCO₃, and an extraction with AcOEt (3 × 20 mL) was performed. The organic phase was washed with brine and dried over Na₂SO₄, filtered and the solvent removed under reduced pressure to obtain a yellow oily residue (7 a-b) (sulfone and sulfoxide). This compound (7 a-b) was solubilized in DMSO (1.5 mL) and Butan-1-ol (1.5 mL), then Ethanolamine (0.02 mL, 0.3 mmol, 5 eq.) was added. The reaction mixture was stirred at reflux overnight, till the completion of the reaction. Butan-1-ol was removed in vacuo and DMSO was removed through an extraction in AcOEt (3 × 20 mL), the organic phase was washed with brine and dried over Na₂SO₄, filtered and the solvent removed under reduced pressure. The product was purified by flash chromatography using DCM/MeOH as eluent.

7l: 4-chloro-3-((1-(2-(4-hydroxyphenyl)propyl)-6-(methylthio)-1H-pyrazolo[3,4-d]pyrimidin-4-yl)amino)phenol

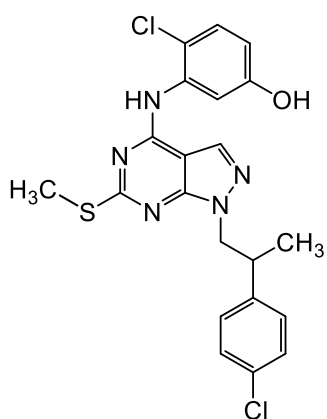


^1H NMR (400 MHz, Acetone): 8.70 (s, 1H, NH), 7.75 (s, 1H, CH-Pyraz), 7.61 (d, 1H, CH-Ar-CIOH), 7.47 (d, 1H, CH-Ar-CIOH), 7.30 (s, 1H, CH-Ar-CIOH), 6.89 (dd, 4H, 2H+2H, CH-Ar-Cl, CH-Ar-Cl), 4.69 (q, $J = 12.5, 7.5$ Hz, 1H, NPyraz-CH₂-CH-), 4.50 (q, $J = 12.5, 7.5$ Hz, 1H, NPyraz-CH₂-CH-), 3.75 – 3.57 (m, 1H, NPyraz-CH₂-CH(CH₃)-CH-Ar), 2.60 (s, 3H, SCH₃), 1.30 (d, $J = 6.8$ Hz, 3H, -CH-CH₃).

Ar-OH and Ar-OH not detected

^{13}C NMR (101 MHz, Acetone): 168.44 (1C), 156.72 (1C), 155.83 (1C), 154.50 (1C), 154.25 (1C), 136.46 (1C), 135.92 (1C), 130.93 (1C), 130.0 (1C)⁴, 129.91 (2C), 129.25(2C), 118.72 (1C), 114.91 (1C), 114.24 (1C), 98.64 (1C), 54.60 (1C), 41.14 (1C), 19.24 (1C), 13.17 (1C).

7m: 4-chloro-3-((1-(2-(4-chlorophenyl)propyl)-6-(methylthio)-1H-pyrazolo[3,4-d]pyrimidin-4-yl)amino)phenol



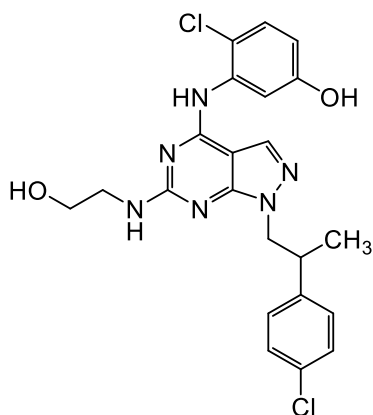
^1H NMR (400 MHz, Acetone): 8.76 (s, 1H, NH), 7.75 (s, 1H, CH-Pyraz), 7.59 (d, 1H, CH-Ar-CIOH), 7.45 (d, 1H, CH-Ar-CIOH), 7.36 (s, 1H, CH-Ar-CIOH), 6.91 (dd, 4H, 2H+2H, CH-Ar-Cl, CH-Ar-Cl), 4.75 (q, $J = 12.5, 7.5$ Hz, 1H, NPyraz-CH₂-CH-), 4.53 (q, $J = 12.5, 7.5$ Hz, 1H,

NPyras-CH₂-CH-), 3.72 – 3.55 (m, 1H, NPyras-CH₂-CH(CH₃)-CH-Ar), 2.61 (s, 3H, SCH₃), 1.37 (d, *J* = 6.8 Hz, 3H, -CH-CH₃).

Ar-OH not detected

¹³C NMR (101 MHz, Acetone): 168.95 (1C), 156.76 (1C), 154.74 (1C), 154.63 (1C), 142.63 (1C), 135.84 (1C), 131.72 (1C), 131.30 (1C), 130.07 (1C), 129.01 (1C), 128.30 (2C), 128.26 (2C), 118.85 (1C), 114.40 (1C), 98.39 (1C), 52.90 (1C), 39.39 (1C), 18.37 (1C), 13.20 (1C).

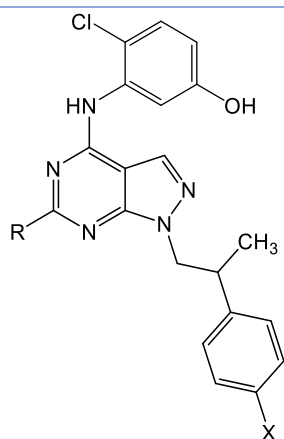
7n: 4-chloro-3-(1-(2-(4-chlorophenyl)propyl)-6-(2-hydroxyethylamino)-1H-pyrazolo[3,4-d]pyrimidin-4-ylamino)phenol



¹H NMR (400 MHz, Acetone) δ 7.89 (bs, 1H, Pyraz-NH-Ar), 7.73 (s, 1H, CH-Pyraz), 7.35-7.26 (m, 4H, CH-Ar-Cl), 7.20 (d, *J* = 7.5 Hz, 1H, CH-Ar(OH)(Cl)), 6.70 (dd, *J* = 7.5, 1.5 Hz, 1H, CH-Ar(OH)(Cl)), 6.20 (d, *J* = 1.5 Hz, 1H, CH-Ar(OH)(Cl)), 4.81 (q, *J* = 12.5, 7.5 Hz, 1H, NPyras-CH₂-CH-), 4.53 (q, *J* = 12.5, 7.5 Hz, 1H, NPyras-CH₂-CH-), 3.40-3.30 (m, 4H, -NH-CH₂-CH₂-OH), 2.96-2.90 (m, 1H, NPyras-CH₂-CH(CH₃)-CH-Ar), 1.26 (t, *J* = 6.8 Hz, 3H, -CH-CH₃).

Ar-OH, CH₂-OH and Pyraz-NH-CH₂ not detected.

¹³C NMR (101 MHz, Acetone) δ 161.54 (1C), 156.58 (2C), 155.21 (1C), 142.94 (2C), 136.39 (1C), 131.60 (1C), 131.08 (1C), 130.93 (1C), 129.77 (1C), 129.04 (1C), 128.27 (1C), 116.83 (1C), 113.08 (1C), 112.84 (1C), 96.10 (1C), 52.44 (1C), 44.18 (1C), 39.20 (1C), 18.44 (1C), 18.37 (1C).



Compound	X	R	Aspect	Yield %	MS (E/S) m/z
7l	OH	SCH ₃	White solid	25	441 [M - H] ⁻
7m	Cl	SCH ₃	White solid	24	459 [M - H] ⁻ .
7n	Cl	NHCH ₂ CH ₂ OH	White solid	20	472,12 [M - H] ⁻

General information

All commercially available chemicals were used as purchased. Anhydrous reactions were run under a positive pressure of dry N₂ or argon. TLC was carried out using Merck TLC plates silica gel 60 F254. Chromatographic purifications were performed on columns packed with Merck 60 silica gel, 23-400 mesh, for flash technique. ¹H NMR and ¹³C NMR spectra were recorded at 400 MHz on a Bruker Avance DPX400. Mass spectra (MS) data were obtained using an Agilent 1100 LC/MSD VL system (G1946C) with a 0.4 mL min⁻¹ flow rate using a binary solvent system of 95 : 5 = CH₃OH : H₂O. UV detection was monitored at 254 nm. MS were acquired in negative mode scanning over the mass range *m/z* 50-1500. The following ion source parameters were used: drying gas flow, 9 mL min⁻¹; nebulizer pressure, 40 psi; drying gas temperature, 350°C.

Microwave Irradiation Experiments

Microwave irradiation experiments were conducted using a CEM Discover Synthesis Unit (CEM Corp., Matthews, NC). The machine consists of a continuous focused microwave power delivery system with operator-selectable power output from 0 to 300 W. The temperature of the contents of the vessels was monitored using a calibrated infrared temperature control mounted under the reaction vessel. All the experiments were performed using a stirring option whereby the contents of the vessel are stirred by means of a rotating magnetic plate located below the floor of the microwave cavity and a Teflon-coated magnetic stir bar in the vessel.

Enzymatic Assay on Isolated Abl

Recombinant human Abl was purchased from Upstate. Activity was measured in a filter-binding assay using an Abl specific peptide substrate (Abtide, Upstate). Reaction conditions were as follows: 0.012 μM [γ -³²P]ATP, 50 μM peptide, and 0.022 μM c-Abl. The apparent affinity (*K_m*) values of the Abl preparation used for its peptide and ATP substrates were determined separately and found to be 1.5 μM and 10 μM, respectively. Kinetic analysis was performed as described for c-Src. Because of the noncompetitive mode of action and because of the fact that the enzyme concentration was higher than the ATP substrate concentration, ID₅₀ values were converted to *K_i* by eq 3: $K_i = ID_{50} / \{E_0 + [E_0(K_m(ATP)/S_0)]\}^{240} / E_0$, where *E₀* and *S₀* are the enzyme and the ATP concentrations,

respectively. Each experiment was done in triplicate, and mean values were used for the interpolation. Curve fitting was performed with the program GraphPad Prism.

Enzymatic Assay on Isolated Src

Recombinant human Src was purchased from Upstate (Lake Placid, NY). Activity was measured in a filter-binding assay using a commercial kit (Src Assay Kit, Upstate), according to the manufacturer's protocol, using 150 μM of the specific Src peptide substrate (KVEKIGEGTYGVVYK) and in the presence of 0.125 pmol of Src and 0.160 pmol of [γ - ^{32}P]-ATP. The apparent affinity (K_m) values of the Src preparation used for its peptide and ATP substrates were determined separately and found to be 30 μM and 5 μM , respectively.

Cell assay

Human CML K-562 cell lines in blast crisis were obtained from the American Type Culture Collection and were grown in RPMI 1640 medium (Euroclone, Devon, UK), containing 10% fetal bovine serum (FBS) and antibiotics (100 U/mL penicillin and 100 $\mu\text{g}/\text{mL}$ streptomycin).²⁴¹ The cultures were free of mycoplasma. Cells were cultured in normoxic conditions. For the experiments we used an incubator (KW Apparacchi Scientifici, Italy) set at 5% CO_2 , 20% O_2 (atmospheric oxygen ≈ 140 mmHg), and 37°C in a humidified environment. In our experiments, the O_2 tension was set and maintained constantly at 2% (≈ 14 mmHg) by injecting N_2 automatically in the chamber to bring the O_2 level to the set point. The compounds were dissolved in DMSO and used at the indicated concentrations. At the end of the experiments, cells were promptly analyzed.

BIBLIOGRAPHY

1. Ferlay J, E. M., Lam F, Colombet M, Mery L, Piñeros M, et al. , Global Cancer Observatory: Cancer Today. . Lyon: *International Agency for Research on Cancer* **2020**.
2. Sung, H.; Ferlay, J.; Siegel, R. L.; Laversanne, M.; Soerjomataram, I.; Jemal, A.; Bray, F., Global Cancer Statistics 2020: GLOBOCAN Estimates of Incidence and Mortality Worldwide for 36 Cancers in 185 Countries. *CA: a cancer journal for clinicians* **2021**, *71* (3), 209-249.
3. Greenhough, A.; Smartt, H. J.; Moore, A. E.; Roberts, H. R.; Williams, A. C.; Paraskeva, C.; Kaidi, A., The COX-2/PGE2 pathway: key roles in the hallmarks of cancer and adaptation to the tumour microenvironment. *Carcinogenesis* **2009**, *30* (3), 377-86.
4. Weinberg, R. A., Mechanisms of malignant progression. *Carcinogenesis* **2008**, *29* (6), 1092-5.
5. WHO (WORLD HEALTH ORGANIZATION). https://www.who.int/health-topics/cancer#tab=tab_1.
6. Liu, E., *Oncogenes and suppressor genes: genetic control of cancer*. Philadelphia: W.B. Saunders: 2004: 1108-1116.
7. Shord S, C. L., *Pharmacotherapy: a pathophysiologic approach*. 10th ed.; DiPiro J, Talbert R, Yee G et al: USA: McGraw-Hill, 2017; Vol. Cancer treatment and chemotherapy.
8. Siddiqui, I. A.; Sanna, V.; Ahmad, N.; Sechi, M.; Mukhtar, H., Resveratrol nanoformulation for cancer prevention and therapy. *Annals of the New York Academy of Sciences* **2015**, *1348* (1), 20-31.
9. Hennings, H.; Glick, A. B.; Greenhalgh, D. A.; Morgan, D. L.; Strickland, J. E.; Tennenbaum, T.; Yuspa, S. H., Critical aspects of initiation, promotion, and progression in multistage epidermal carcinogenesis. *Proceedings of the Society for Experimental Biology and Medicine. Society for Experimental Biology and Medicine (New York, N.Y.)* **1993**, *202* (1), 1-8.
10. Qian, B. Z.; Pollard, J. W., Macrophage diversity enhances tumor progression and metastasis. *Cell* **2010**, *141* (1), 39-51.
11. Meiliana, A.; Dewi, N.; Wijaya, A., Cancer Stem Cell Hypothesis: Implication for Cancer Prevention and Treatment. *The Indonesian Biomedical Journal* **2016**, *8*, 21.
12. Hanahan, D.; Weinberg, R. A., Hallmarks of cancer: the next generation. *Cell* **2011**, *144* (5), 646-74.
13. Chaffer, C. L.; Weinberg, R. A., How does multistep tumorigenesis really proceed? *Cancer discovery* **2015**, *5* (1), 22-4.
14. DeBerardinis, R. J.; Chandel, N. S., Fundamentals of cancer metabolism. *Science advances* **2016**, *2* (5), e1600200.
15. Moreno-Sánchez, R.; Rodríguez-Enríquez, S.; Marín-Hernández, A.; Saavedra, E., Energy metabolism in tumor cells. *The FEBS journal* **2007**, *274* (6), 1393-418.
16. Boroughs, L. K.; DeBerardinis, R. J., Metabolic pathways promoting cancer cell survival and growth. *Nature cell biology* **2015**, *17* (4), 351-9.
17. Akram, M., Mini-review on Glycolysis and Cancer. *Journal of Cancer Education* **2013**, *28* (3), 454-457.
18. Kroemer, G.; Pouyssegur, J., Tumor Cell Metabolism: Cancer's Achilles' Heel. *Cancer cell* **2008**, *13* (6), 472-482.
19. Warburg, O., The metabolism of tumours. *J Physiol Chem* **1910**, *56*:66–305.
20. Gatenby, R. A.; Gillies, R. J., Why do cancers have high aerobic glycolysis? *Nature reviews. Cancer* **2004**, *4* (11), 891-9.

21. Simabuco, F. M.; Morale, M. G.; Pavan, I. C. B.; Morelli, A. P.; Silva, F. R.; Tamura, R. E., p53 and metabolism: from mechanism to therapeutics. *Oncotarget* **2018**, *9* (34), 23780-23823.
 22. Cantor, J. R.; Sabatini, D. M., Cancer cell metabolism: one hallmark, many faces. *Cancer discovery* **2012**, *2* (10), 881-98.
 23. Dibble, C. C.; Manning, B. D., Signal integration by mTORC1 coordinates nutrient input with biosynthetic output. *Nature cell biology* **2013**, *15* (6), 555-64.
 24. Bryant, J. L.; Meredith, S. L.; Williams, K. J.; White, A., Targeting hypoxia in the treatment of small cell lung cancer. *Lung cancer (Amsterdam, Netherlands)* **2014**, *86* (2), 126-32.
 25. Semenza, G. L., HIF-1: mediator of physiological and pathophysiological responses to hypoxia. *Journal of applied physiology (Bethesda, Md. : 1985)* **2000**, *88* (4), 1474-80.
 26. Thomas, D. D.; Espey, M. G.; Ridnour, L. A.; Hofseth, L. J.; Mancardi, D.; Harris, C. C.; Wink, D. A., Hypoxic inducible factor 1alpha, extracellular signal-regulated kinase, and p53 are regulated by distinct threshold concentrations of nitric oxide. *Proceedings of the National Academy of Sciences of the United States of America* **2004**, *101* (24), 8894-9.
 27. Dang, C. V.; Kim, J. W.; Gao, P.; Yustein, J., The interplay between MYC and HIF in cancer. *Nature reviews. Cancer* **2008**, *8* (1), 51-6.
 28. Benej, M.; Pastorekova, S.; Pastorek, J., Carbonic anhydrase IX: regulation and role in cancer. *Sub-cellular biochemistry* **2014**, *75*, 199-219.
 29. McDonald, P. C.; Winum, J. Y.; Supuran, C. T.; Dedhar, S., Recent developments in targeting carbonic anhydrase IX for cancer therapeutics. *Oncotarget* **2012**, *3* (1), 84-97.
 30. Wilson, W. R.; Hay, M. P., Targeting hypoxia in cancer therapy. *Nature reviews. Cancer* **2011**, *11* (6), 393-410.
 31. Chiche, J.; Ilc, K.; Laferrière, J.; Trottier, E.; Dayan, F.; Mazure, N. M.; Brahimi-Horn, M. C.; Pouyssegur, J., Hypoxia-inducible carbonic anhydrase IX and XII promote tumor cell growth by counteracting acidosis through the regulation of the intracellular pH. *Cancer research* **2009**, *69* (1), 358-68.
 32. Wykoff, C. C.; Beasley, N. J.; Watson, P. H.; Turner, K. J.; Pastorek, J.; Sibtain, A.; Wilson, G. D.; Turley, H.; Talks, K. L.; Maxwell, P. H.; Pugh, C. W.; Ratcliffe, P. J.; Harris, A. L., Hypoxia-inducible expression of tumor-associated carbonic anhydrases. *Cancer research* **2000**, *60* (24), 7075-83.
 33. Cebola, I.; Peinado, M. A., Epigenetic deregulation of the COX pathway in cancer. *Progress in lipid research* **2012**, *51* (4), 301-13.
 34. Khan, M. O.; Deimling, M. J.; Philip, A., Medicinal chemistry and the pharmacy curriculum. *American journal of pharmaceutical education* **2011**, *75* (8), 161.
 35. Erhardt, P. W., Medicinal chemistry in the new millennium. A glance into the future. *Pure and Applied Chemistry* **2002**, *74* (5), 703-785.
 36. EF, P. J. a. G., *Rapid Review Biochemistry, 2nd ed.* 2nd ed.; Philadelphia, Mosby: 2007.
 37. Chen, I.; Lui, F., Physiology, Active Transport. In *StatPearls*, StatPearls Publishing
- Copyright © 2021, StatPearls Publishing LLC.: Treasure Island (FL), 2021.
38. Wang, X.; Zhang, H.; Chen, X., Drug resistance and combating drug resistance in cancer. *Cancer Drug Resist* **2019**, *2*, 141-160.
 39. Urruticoechea, A.; Alemany, R.; Balart, J.; Villanueva, A.; Viñals, F.; Capellá, G., Recent advances in cancer therapy: an overview. *Current pharmaceutical design* **2010**, *16* (1), 3-10.
 40. Baskar, R.; Lee, K. A.; Yeo, R.; Yeoh, K. W., Cancer and radiation therapy: current advances and future directions. *International journal of medical sciences* **2012**, *9* (3), 193-9.

41. Khalil, D. N.; Smith, E. L.; Brentjens, R. J.; Wolchok, J. D., The future of cancer treatment: immunomodulation, CARs and combination immunotherapy. *Nature reviews. Clinical oncology* **2016**, *13* (5), 273-90.
42. Wu, L.; Qu, X., Cancer biomarker detection: recent achievements and challenges. *Chemical Society reviews* **2015**, *44* (10), 2963-97.
43. Golubnitschaja, O.; Flammer, J., What are the biomarkers for glaucoma? *Survey of ophthalmology* **2007**, *52 Suppl 2*, S155-61.
44. Aronson, J. K.; Ferner, R. E., Biomarkers-A General Review. *Current protocols in pharmacology* **2017**, *76*, 9.23.1-9.23.17.
45. Prasad, V.; Fojo, T.; Brada, M., Precision oncology: origins, optimism, and potential. *The Lancet. Oncology* **2016**, *17* (2), e81-e86.
46. Schwartzberg, L.; Kim, E. S.; Liu, D.; Schrag, D., Precision Oncology: Who, How, What, When, and When Not? *American Society of Clinical Oncology educational book. American Society of Clinical Oncology. Annual Meeting* **2017**, *37*, 160-169.
47. Bao, J.; Qiao, L., New developments on targeted cancer therapy: Multi-faceted issues in targeted cancer therapy. *Cancer letters* **2017**, *387*, 1-2.
48. Rautio, J.; Kumpulainen, H.; Heimbach, T.; Oliyai, R.; Oh, D.; Järvinen, T.; Savolainen, J., Prodrugs: design and clinical applications. *Nature reviews. Drug discovery* **2008**, *7* (3), 255-70.
49. Walther, R.; Rautio, J.; Zelikin, A. N., Prodrugs in medicinal chemistry and enzyme prodrug therapies. *Advanced Drug Delivery Reviews* **2017**, *118*, 65-77.
50. Padma, V. V., An overview of targeted cancer therapy. *BioMedicine* **2015**, *5* (4), 19.
51. Conde-Estévez, D., Targeted cancer therapy: interactions with other medicines. *Clinical & translational oncology : official publication of the Federation of Spanish Oncology Societies and of the National Cancer Institute of Mexico* **2017**, *19* (1), 21-30.
52. Baudino, T. A., Targeted Cancer Therapy: The Next Generation of Cancer Treatment. *Current drug discovery technologies* **2015**, *12* (1), 3-20.
53. Kumar, M.; Ernani, V.; Owonikoko, T. K., Biomarkers and targeted systemic therapies in advanced non-small cell lung cancer. *Molecular aspects of medicine* **2015**, *45*, 55-66.
54. Farkona, S.; Diamandis, E. P.; Blasutig, I. M., Cancer immunotherapy: the beginning of the end of cancer? *BMC Medicine* **2016**, *14* (1), 73.
55. Anna, M.; Nurrani Mustika, D.; Andi, W., Cancer Immunotherapy: a Review. *Indonesian Biomedical Journal* **2016**, *8* (1), 1-20.
56. Mahoney, K. M.; Rennert, P. D.; Freeman, G. J., Combination cancer immunotherapy and new immunomodulatory targets. *Nature reviews. Drug discovery* **2015**, *14* (8), 561-84.
57. Sun, W.; Shi, Q.; Zhang, H.; Yang, K.; Ke, Y.; Wang, Y.; Qiao, L., Advances in the techniques and methodologies of cancer gene therapy. *Discovery medicine* **2019**, *27* (146), 45-55.
58. Santos, S. B.; Sousa Lobo, J. M.; Silva, A. C., Biosimilar medicines used for cancer therapy in Europe: a review. *Drug Discovery Today* **2019**, *24* (1), 293-299.
59. Rugo, H. S.; Linton, K. M.; Cervi, P.; Rosenberg, J. A.; Jacobs, I., A clinician's guide to biosimilars in oncology. *Cancer treatment reviews* **2016**, *46*, 73-9.
60. Walton, E. L., On the road to epigenetic therapy. *Biomedical journal* **2016**, *39* (3), 161-5.
61. Lippert, T. H.; Ruoff, H. J.; Volm, M., Intrinsic and acquired drug resistance in malignant tumors. The main reason for therapeutic failure. *Arzneimittel-Forschung* **2008**, *58* (6), 261-4.
62. Kelderman, S.; Schumacher, T. N.; Haanen, J. B., Acquired and intrinsic resistance in cancer immunotherapy. *Molecular oncology* **2014**, *8* (6), 1132-9.

63. Volm, M.; Koomagi, R.; Efferth, T., Prediction of Drug Sensitivity and Resistance of Cancer by Protein Expression Profiling. *Cancer genomics & proteomics* **2004**, *1* (2), 157-166.
64. Quintás-Cardama, A.; Kantarjian, H. M.; Cortes, J. E., Mechanisms of primary and secondary resistance to imatinib in chronic myeloid leukemia. *Cancer control : journal of the Moffitt Cancer Center* **2009**, *16* (2), 122-31.
65. Medina-Franco, J. L.; Giulianotti, M. A.; Welmaker, G. S.; Houghten, R. A., Shifting from the single to the multitarget paradigm in drug discovery. *Drug Discov Today* **2013**, *18* (9-10), 495-501.
66. Ramsay, R. R.; Popovic-Nikolic, M. R.; Nikolic, K.; Uliassi, E.; Bolognesi, M. L., A perspective on multi-target drug discovery and design for complex diseases. *Clinical and translational medicine* **2018**, *7* (1), 3.
67. Makhoba, X. H.; Viegas, C., Jr.; Mosa, R. A.; Viegas, F. P. D.; Poee, O. J., Potential Impact of the Multi-Target Drug Approach in the Treatment of Some Complex Diseases. *Drug Des Devel Ther* **2020**, *14*, 3235-3249.
68. Talevi, A., Multi-target pharmacology: possibilities and limitations of the "skeleton key approach" from a medicinal chemist perspective. *Frontiers in pharmacology* **2015**, *6*, 205.
69. Musumeci, F.; Schenone, S.; Brullo, C.; Botta, M., An update on dual Src/Abl inhibitors. *Future medicinal chemistry* **2012**, *4* (6), 799-822.
70. Hopkins, A. L., Network pharmacology: the next paradigm in drug discovery. *Nature chemical biology* **2008**, *4* (11), 682-690.
71. Bottegoni, G.; Favia, A. D.; Recanatini, M.; Cavalli, A., The role of fragment-based and computational methods in polypharmacology. *Drug Discov Today* **2012**, *17* (1-2), 23-34.
72. Morphy, R.; Rankovic, Z., Designing multiple ligands - medicinal chemistry strategies and challenges. *Current pharmaceutical design* **2009**, *15* (6), 587-600.
73. Morphy, R.; Rankovic, Z., Designed Multiple Ligands. An Emerging Drug Discovery Paradigm. *Journal of Medicinal Chemistry* **2005**, *48* (21), 6523-6543.
74. Morphy, R.; Rankovic, Z., The physicochemical challenges of designing multiple ligands. *J Med Chem* **2006**, *49* (16), 4961-70.
75. Decker, M. e., *Design of hybrid molecules for drug development*. 2017.
76. Jéssika de Oliveira Viana, M. B. F., Mayara dos Santos Maia, Vanessa de Lima Serafim, Luciana Scotti, Marcus Tullius Scotti, Drug discovery and computational strategies in the multitarget drugs era. *Brazilian Journal of Pharmaceutical Sciences* **2018**, *54*.
77. Ma, X. H.; Shi, Z.; Tan, C.; Jiang, Y.; Go, M. L.; Low, B. C.; Chen, Y. Z., In-silico approaches to multi-target drug discovery : computer aided multi-target drug design, multi-target virtual screening. *Pharmaceutical research* **2010**, *27* (5), 739-49.
78. Abdolmaleki, A.; Ghasemi, J. B.; Ghasemi, F., Computer Aided Drug Design for Multi-Target Drug Design: SAR /QSAR, Molecular Docking and Pharmacophore Methods. *Current drug targets* **2017**, *18* (5), 556-575.
79. Lindskog, S., Structure and mechanism of carbonic anhydrase. *Pharmacology & therapeutics* **1997**, *74* (1), 1-20.
80. Supuran, C. T., Carbonic anhydrases--an overview. *Current pharmaceutical design* **2008**, *14* (7), 603-14.
81. Gilmour, K. M., Perspectives on carbonic anhydrase. *Comparative biochemistry and physiology. Part A, Molecular & integrative physiology* **2010**, *157* (3), 193-7.
82. Hilvo, M.; Tolvanen, M.; Clark, A.; Shen, B.; Shah, G. N.; Waheed, A.; Halmi, P.; Hänninen, M.; Hämäläinen, J. M.; Vihinen, M.; Sly, W. S.; Parkkila, S., Characterization of CA XV, a new GPI-anchored form of carbonic anhydrase. *The Biochemical journal* **2005**, *392* (Pt 1), 83-92.
83. Supuran, C. T.; Scozzafava, A.; Casini, A., Carbonic anhydrase inhibitors. *Medicinal research reviews* **2003**, *23* (2), 146-89.

84. Nishimori, I.; Minakuchi, T.; Onishi, S.; Vullo, D.; Scozzafava, A.; Supuran, C. T., Carbonic anhydrase inhibitors. DNA cloning, characterization, and inhibition studies of the human secretory isoform VI, a new target for sulfonamide and sulfamate inhibitors. *J Med Chem* **2007**, *50* (2), 381-8.
85. Nishimori, I.; Vullo, D.; Innocenti, A.; Scozzafava, A.; Mastrolorenzo, A.; Supuran, C. T., Carbonic anhydrase inhibitors. The mitochondrial isozyme VB as a new target for sulfonamide and sulfamate inhibitors. *J Med Chem* **2005**, *48* (24), 7860-6.
86. Xu, Y.; Feng, L.; Jeffrey, P. D.; Shi, Y.; Morel, F. M., Structure and metal exchange in the cadmium carbonic anhydrase of marine diatoms. *Nature* **2008**, *452* (7183), 56-61.
87. Hewett-Emmett, D., Evolution and distribution of the carbonic anhydrase gene families. *Exs* **2000**, (90), 29-76.
88. Supuran, C. T., Carbonic Anhydrases as Drug Targets: General Presentation. *John Wiley & Sons* **2010**, 15-38.
89. Domsic, J. F.; Avvaru, B. S.; Kim, C. U.; Gruner, S. M.; Agbandje-McKenna, M.; Silverman, D. N.; McKenna, R., Entrapment of carbon dioxide in the active site of carbonic anhydrase II. *The Journal of biological chemistry* **2008**, *283* (45), 30766-71.
90. Supuran, C. T., Carbonic anhydrase inhibitors. *Bioorganic & medicinal chemistry letters* **2010**, *20* (12), 3467-74.
91. Alterio, V.; Di Fiore, A.; D'Ambrosio, K.; Supuran, C. T.; De Simone, G., Multiple binding modes of inhibitors to carbonic anhydrases: how to design specific drugs targeting 15 different isoforms? *Chemical reviews* **2012**, *112* (8), 4421-68.
92. Smith, K. S.; Jakubzick, C.; Whittam, T. S.; Ferry, J. G., Carbonic anhydrase is an ancient enzyme widespread in prokaryotes. *Proceedings of the National Academy of Sciences of the United States of America* **1999**, *96* (26), 15184-9.
93. Pilka, E. S.; Kochan, G.; Oppermann, U.; Yue, W. W., Crystal structure of the secretory isozyme of mammalian carbonic anhydrases CA VI: implications for biological assembly and inhibitor development. *Biochemical and biophysical research communications* **2012**, *419* (3), 485-9.
94. Supuran, C. T., Structure-based drug discovery of carbonic anhydrase inhibitors. *Journal of enzyme inhibition and medicinal chemistry* **2012**, *27* (6), 759-72.
95. Supuran, C. T., Carbonic anhydrases: novel therapeutic applications for inhibitors and activators. *Nature reviews. Drug discovery* **2008**, *7* (2), 168-81.
96. Supuran, C. T. S., A., Carbonic anhydrase - Its inhibitors and activators. Conway, J. E., Ed. CRC Press: Boca Raton (FL), USA, 2004; pp 1-363.
97. Chegwiddden, W. R.; Dodgson, S. J.; Spencer, I. M., The roles of carbonic anhydrase in metabolism, cell growth and cancer in animals. *Exs* **2000**, (90), 343-63.
98. Supuran, C. T., Carbonic anhydrases as drug targets--an overview. *Current topics in medicinal chemistry* **2007**, *7* (9), 825-33.
99. Di Fiore, A.; Truppo, E.; Supuran, C. T.; Alterio, V.; Dathan, N.; Botorabi, F.; Parkkila, S.; Monti, S. M.; De Simone, G., Crystal structure of the C183S/C217S mutant of human CA VII in complex with acetazolamide. *Bioorganic & medicinal chemistry letters* **2010**, *20* (17), 5023-6.
100. Duda, D. M.; Tu, C.; Fisher, S. Z.; An, H.; Yoshioka, C.; Govindasamy, L.; Laipis, P. J.; Agbandje-McKenna, M.; Silverman, D. N.; McKenna, R., Human Carbonic Anhydrase III: Structural and Kinetic Study of Catalysis and Proton Transfer. *Biochemistry* **2005**, *44* (30), 10046-10053.
101. Alterio, V.; Hilvo, M.; Di Fiore, A.; Supuran, C. T.; Pan, P.; Parkkila, S.; Scaloni, A.; Pastorek, J.; Pastorekova, S.; Pedone, C.; Scozzafava, A.; Monti, S. M.; De Simone, G., Crystal structure of the catalytic domain of the tumor-associated human carbonic anhydrase IX.

- Proceedings of the National Academy of Sciences of the United States of America* **2009**, *106* (38), 16233-8.
102. Kannan, K. K.; Ramanadham, M.; Jones, T. A., Structure, refinement, and function of carbonic anhydrase isozymes: refinement of human carbonic anhydrase I. *Annals of the New York Academy of Sciences* **1984**, *429*, 49-60.
103. Christianson, D. W.; Fierke, C. A., Carbonic Anhydrase: Evolution of the Zinc Binding Site by Nature and by Design. *Accounts of chemical research* **1996**, *29* (7), 331-339.
104. Leitans, J.; Kazaks, A.; Balode, A.; Ivanova, J.; Zalubovskis, R.; Supuran, C. T.; Tars, K., Efficient Expression and Crystallization System of Cancer-Associated Carbonic Anhydrase Isoform IX. *J Med Chem* **2015**, *58* (22), 9004-9.
105. Mboge, M. Y.; Chen, Z.; Wolff, A.; Mathias, J. V.; Tu, C.; Brown, K. D.; Bozdag, M.; Carta, F.; Supuran, C. T.; McKenna, R.; Frost, S. C., Selective inhibition of carbonic anhydrase IX over carbonic anhydrase XII in breast cancer cells using benzene sulfonamides: Disconnect between activity and growth inhibition. *PloS one* **2018**, *13* (11), e0207417.
106. Zamanova, S.; Shabana, A. M.; Mondal, U. K.; Ilies, M. A., Carbonic anhydrases as disease markers. *Expert opinion on therapeutic patents* **2019**, *29* (7), 509-533.
107. Pastorek, J.; Pastorekova, S., Hypoxia-induced carbonic anhydrase IX as a target for cancer therapy: from biology to clinical use. *Seminars in cancer biology* **2015**, *31*, 52-64.
108. Kivelä, A.-J.; Kivelä, J.; Saarnio, J.; Parkkila, S., Carbonic anhydrases in normal gastrointestinal tract and gastrointestinal tumours. *World J Gastroenterol* **2005**, *11* (2), 155-163.
109. Hilvo, M.; Baranauskienė, L.; Salzano, A. M.; Scaloni, A.; Matulis, D.; Innocenti, A.; Scozzafava, A.; Monti, S. M.; Di Fiore, A.; De Simone, G.; Lindfors, M.; Jänis, J.; Valjakka, J.; Pastoreková, S.; Pastorek, J.; Kulomaa, M. S.; Nordlund, H. R.; Supuran, C. T.; Parkkila, S., Biochemical characterization of CA IX, one of the most active carbonic anhydrase isozymes. *The Journal of biological chemistry* **2008**, *283* (41), 27799-27809.
110. Ivanov, S.; Liao, S. Y.; Ivanova, A.; Danilkovitch-Miagkova, A.; Tarasova, N.; Weirich, G.; Merrill, M. J.; Proescholdt, M. A.; Oldfield, E. H.; Lee, J.; Zavada, J.; Waheed, A.; Sly, W.; Lerman, M. I.; Stanbridge, E. J., Expression of hypoxia-inducible cell-surface transmembrane carbonic anhydrases in human cancer. *The American journal of pathology* **2001**, *158* (3), 905-19.
111. Svastová, E.; Hulíková, A.; Rafajová, M.; Zat'ovicová, M.; Gibadulinová, A.; Casini, A.; Cecchi, A.; Scozzafava, A.; Supuran, C. T.; Pastorek, J.; Pastoreková, S., Hypoxia activates the capacity of tumor-associated carbonic anhydrase IX to acidify extracellular pH. *FEBS letters* **2004**, *577* (3), 439-45.
112. Waheed, A.; Sly, W. S., Carbonic anhydrase XII functions in health and disease. *Gene* **2017**, *623*, 33-40.
113. Ivanov, S. V.; Kuzmin, I.; Wei, M. H.; Pack, S.; Geil, L.; Johnson, B. E.; Stanbridge, E. J.; Lerman, M. I., Down-regulation of transmembrane carbonic anhydrases in renal cell carcinoma cell lines by wild-type von Hippel-Lindau transgenes. *Proceedings of the National Academy of Sciences of the United States of America* **1998**, *95* (21), 12596-601.
114. Robertson, N.; Potter, C.; Harris, A. L., Role of carbonic anhydrase IX in human tumor cell growth, survival, and invasion. *Cancer research* **2004**, *64* (17), 6160-5.
115. Daunys, S.; Petrikaitė, V., The roles of carbonic anhydrases IX and XII in cancer cell adhesion, migration, invasion and metastasis. *Biology of the cell* **2020**, *112* (12), 383-397.
116. Chen, Z.; Ai, L.; Mboge, M. Y.; Tu, C.; McKenna, R.; Brown, K. D.; Heldermon, C. D.; Frost, S. C., Differential expression and function of CAIX and CAXII in breast cancer: A comparison between tumorgraft models and cells. *PloS one* **2018**, *13* (7), e0199476.
117. Parks, S. K.; Pouysségur, J., Targeting pH regulating proteins for cancer therapy- Progress and limitations. *Seminars in cancer biology* **2017**, *43*, 66-73.

118. Kaya, A. O.; Gunel, N.; Benekli, M.; Akyurek, N.; Buyukberber, S.; Tatli, H.; Coskun, U.; Yildiz, R.; Yaman, E.; Ozturk, B., Hypoxia inducible factor-1 alpha and carbonic anhydrase IX overexpression are associated with poor survival in breast cancer patients. *Journal of B.U.ON. : official journal of the Balkan Union of Oncology* **2012**, *17* (4), 663-8.
119. Swayampakula, M.; McDonald, P. C.; Vallejo, M.; Coyaud, E.; Chafe, S. C.; Westerback, A.; Venkateswaran, G.; Shankar, J.; Gao, G.; Laurent, E. M. N.; Lou, Y.; Bennewith, K. L.; Supuran, C. T.; Nabi, I. R.; Raught, B.; Dedhar, S., The interactome of metabolic enzyme carbonic anhydrase IX reveals novel roles in tumor cell migration and invadopodia/MMP14-mediated invasion. *Oncogene* **2017**, *36* (45), 6244-6261.
120. Guerrini, G.; Criscuoli, M.; Filippi, I.; Naldini, A.; Carraro, F., Inhibition of smoothed in breast cancer cells reduces CAXII expression and cell migration. *Journal of cellular physiology* **2018**, *233* (12), 9799-9811.
121. Amiri, A.; Le, P. U.; Moquin, A.; Machkalyan, G.; Petrecca, K.; Gillard, J. W.; Yoganathan, N.; Maysinger, D., Inhibition of carbonic anhydrase IX in glioblastoma multiforme. *European journal of pharmaceutics and biopharmaceutics : official journal of Arbeitsgemeinschaft fur Pharmazeutische Verfahrenstechnik e.V* **2016**, *109*, 81-92.
122. Ward, C.; Meehan, J.; Mullen, P.; Supuran, C.; Dixon, J. M.; Thomas, J. S.; Winum, J.-Y.; Lambin, P.; Dubois, L.; Pavathaneni, N.-K.; Jarman, E. J.; Renshaw, L.; Um, I. H.; Kay, C.; Harrison, D. J.; Kunkler, I. H.; Langdon, S. P., Evaluation of carbonic anhydrase IX as a therapeutic target for inhibition of breast cancer invasion and metastasis using a series of in vitro breast cancer models. *Oncotarget* **2015**, *6* (28), 24865-24870.
123. Svastova, E.; Pastorekova, S., Carbonic anhydrase IX: a hypoxia-controlled "catalyst" of cell migration. *Cell adhesion & migration* **2013**, *7* (2), 226-31.
124. Jia, J.; Martin, T. A.; Ye, L.; Meng, L.; Xia, N.; Jiang, W. G.; Zhang, X., Fibroblast activation protein- α promotes the growth and migration of lung cancer cells via the PI3K and sonic hedgehog pathways. *Int J Mol Med* **2018**, *41* (1), 275-283.
125. Maxwell, P. H.; Wiesener, M. S.; Chang, G. W.; Clifford, S. C.; Vaux, E. C.; Cockman, M. E.; Wykoff, C. C.; Pugh, C. W.; Maher, E. R.; Ratcliffe, P. J., The tumour suppressor protein VHL targets hypoxia-inducible factors for oxygen-dependent proteolysis. *Nature* **1999**, *399* (6733), 271-5.
126. Sneddon, D.; Niemans, R.; Bauwens, M.; Yaromina, A.; van Kuijk, S. J.; Liewes, N. G.; Biemans, R.; Pooters, I.; Pellegrini, P. A.; Lengkeek, N. A.; Greguric, I.; Tonissen, K. F.; Supuran, C. T.; Lambin, P.; Dubois, L.; Poulsen, S. A., Synthesis and in Vivo Biological Evaluation of (68)Ga-Labeled Carbonic Anhydrase IX Targeting Small Molecules for Positron Emission Tomography. *J Med Chem* **2016**, *59* (13), 6431-43.
127. Mboge, M. Y.; Mahon, B. P.; McKenna, R.; Frost, S. C., Carbonic Anhydrases: Role in pH Control and Cancer. *Metabolites* **2018**, *8* (1).
128. Liang, J. Y.; Lipscomb, W. N., Binding of substrate CO₂ to the active site of human carbonic anhydrase II: a molecular dynamics study. *Proceedings of the National Academy of Sciences of the United States of America* **1990**, *87* (10), 3675-9.
129. Merz, K. M., Carbon dioxide binding to human carbonic anhydrase II. *Journal of the American Chemical Society* **1991**, *113* (2), 406-411.
130. Mann, T.; Keilin, D., Sulphanilamide as a Specific Inhibitor of Carbonic Anhydrase. *Nature* **1940**, *146* (3692), 164-165.
131. Jonsson, B. H.; Liljas, A., Perspectives on the Classical Enzyme Carbonic Anhydrase and the Search for Inhibitors. *Biophysical journal* **2020**, *119* (7), 1275-1280.
132. Liljas, A.; Håkansson, K.; Jonsson, B. H.; Xue, Y., Inhibition and catalysis of carbonic anhydrase. Recent crystallographic analyses. *European journal of biochemistry* **1994**, *219* (1-2), 1-10.

133. Maresca, A.; Temperini, C.; Pochet, L.; Masereel, B.; Scozzafava, A.; Supuran, C. T., Deciphering the Mechanism of Carbonic Anhydrase Inhibition with Coumarins and Thiocoumarins. *Journal of Medicinal Chemistry* **2010**, *53* (1), 335-344.
134. Maresca, A.; Temperini, C.; Vu, H.; Pham, N. B.; Poulsen, S. A.; Scozzafava, A.; Quinn, R. J.; Supuran, C. T., Non-zinc mediated inhibition of carbonic anhydrases: coumarins are a new class of suicide inhibitors. *Journal of the American Chemical Society* **2009**, *131* (8), 3057-62.
135. Ferraroni, M.; Carta, F.; Scozzafava, A.; Supuran, C. T., Thioxocoumarins Show an Alternative Carbonic Anhydrase Inhibition Mechanism Compared to Coumarins. *J Med Chem* **2016**, *59* (1), 462-73.
136. De Simone, G.; Supuran, C. T., Carbonic anhydrase IX: Biochemical and crystallographic characterization of a novel antitumor target. *Biochimica et biophysica acta* **2010**, *1804* (2), 404-9.
137. Li, B.; Lu, Y.; Yu, L.; Han, X.; Wang, H.; Mao, J.; Shen, J.; Wang, B.; Tang, J.; Li, C.; Song, B., miR-221/222 promote cancer stem-like cell properties and tumor growth of breast cancer via targeting PTEN and sustained Akt/NF- κ B/COX-2 activation. *Chemico-biological interactions* **2017**, *277*, 33-42.
138. Hashemi Goradel, N.; Najafi, M.; Salehi, E.; Farhood, B.; Mortezaee, K., Cyclooxygenase-2 in cancer: A review. *Journal of cellular physiology* **2019**, *234* (5), 5683-5699.
139. Chandrasekharan, N. V.; Dai, H.; Roos, K. L.; Evanson, N. K.; Tomsik, J.; Elton, T. S.; Simmons, D. L., COX-3, a cyclooxygenase-1 variant inhibited by acetaminophen and other analgesic/antipyretic drugs: cloning, structure, and expression. *Proceedings of the National Academy of Sciences of the United States of America* **2002**, *99* (21), 13926-31.
140. Williams, C. S.; Mann, M.; DuBois, R. N., The role of cyclooxygenases in inflammation, cancer, and development. *Oncogene* **1999**, *18* (55), 7908-16.
141. Van der Ouderaa, F. J.; Buytenhek, M.; Nugteren, D. H.; Van Dorp, D. A., Purification and characterisation of prostaglandin endoperoxide synthetase from sheep vesicular glands. *Biochimica et biophysica acta* **1977**, *487* (2), 315-31.
142. Wang, M. T.; Honn, K. V.; Nie, D., Cyclooxygenases, prostanoids, and tumor progression. *Cancer metastasis reviews* **2007**, *26* (3-4), 525-34.
143. Fitzpatrick, F. A., Cyclooxygenase enzymes: regulation and function. *Current pharmaceutical design* **2004**, *10* (6), 577-88.
144. Blobaum, A. L.; Marnett, L. J., Structural and Functional Basis of Cyclooxygenase Inhibition. *Journal of Medicinal Chemistry* **2007**, *50* (7), 1425-1441.
145. Simmons, D. L.; Botting, R. M.; Hla, T., Cyclooxygenase isozymes: the biology of prostaglandin synthesis and inhibition. *Pharmacological reviews* **2004**, *56* (3), 387-437.
146. Svensson, C. I.; Yaksh, T. L., The spinal phospholipase-cyclooxygenase-prostanoid cascade in nociceptive processing. *Annual review of pharmacology and toxicology* **2002**, *42*, 553-83.
147. Kim, K. B.; Nam, Y. A.; Kim, H. S.; Hayes, A. W.; Lee, B. M., α -Linolenic acid: nutraceutical, pharmacological and toxicological evaluation. *Food and chemical toxicology : an international journal published for the British Industrial Biological Research Association* **2014**, *70*, 163-78.
148. Desai, S. J.; Prickril, B.; Rasooly, A., Mechanisms of Phytonutrient Modulation of Cyclooxygenase-2 (COX-2) and Inflammation Related to Cancer. *Nutrition and cancer* **2018**, *70* (3), 350-375.
149. Justice, E.; Carruthers, D. M., Cardiovascular risk and COX-2 inhibition in rheumatological practice. *Journal of human hypertension* **2005**, *19* (1), 1-5.

150. Dubois, R. N.; Abramson, S. B.; Crofford, L.; Gupta, R. A.; Simon, L. S.; Van De Putte, L. B.; Lipsky, P. E., Cyclooxygenase in biology and disease. *FASEB journal : official publication of the Federation of American Societies for Experimental Biology* **1998**, *12* (12), 1063-73.
151. Gierse, J. K.; McDonald, J. J.; Hauser, S. D.; Rangwala, S. H.; Koboldt, C. M.; Seibert, K., A Single Amino Acid Difference between Cyclooxygenase-1 (COX-1) and -2 (COX-2) Reverses the Selectivity of COX-2 Specific Inhibitors*. *Journal of Biological Chemistry* **1996**, *271* (26), 15810-15814.
152. Rumzhum, N. N.; Ammit, A. J., Cyclooxygenase 2: its regulation, role and impact in airway inflammation. *Clinical and experimental allergy : journal of the British Society for Allergy and Clinical Immunology* **2016**, *46* (3), 397-410.
153. Cui, Y.; Shu, X. O.; Li, H. L.; Yang, G.; Wen, W.; Gao, Y. T.; Cai, Q.; Rothman, N.; Yin, H. Y.; Lan, Q.; Xiang, Y. B.; Zheng, W., Prospective study of urinary prostaglandin E2 metabolite and pancreatic cancer risk. *International journal of cancer* **2017**, *141* (12), 2423-2429.
154. Hosseini, F.; Mahdian-Shakib, A.; Jadidi-Niaragh, F.; Enderami, S. E.; Mohammadi, H.; Hemmatzadeh, M.; Mohammed, H. A.; Anissian, A.; Kokhaei, P.; Mirshafiey, A.; Hassannia, H., Anti-inflammatory and anti-tumor effects of α -l-guluronic acid (G2013) on cancer-related inflammation in a murine breast cancer model. *Biomedicine & pharmacotherapy = Biomedecine & pharmacotherapie* **2018**, *98*, 793-800.
155. Todoric, J.; Antonucci, L.; Karin, M., Targeting Inflammation in Cancer Prevention and Therapy. *Cancer prevention research (Philadelphia, Pa.)* **2016**, *9* (12), 895-905.
156. Singh, B.; Berry, J. A.; Shoher, A.; Lucci, A., COX-2 induces IL-11 production in human breast cancer cells. *The Journal of surgical research* **2006**, *131* (2), 267-75.
157. Majumder, M.; Dunn, L.; Liu, L.; Hasan, A.; Vincent, K.; Brackstone, M.; Hess, D.; Lala, P. K., COX-2 induces oncogenic micro RNA miR655 in human breast cancer. *Sci Rep* **2018**, *8* (1), 327.
158. Saha, D.; Pyo, H.; Choy, H., COX-2 inhibitor as a radiation enhancer: new strategies for the treatment of lung cancer. *American journal of clinical oncology* **2003**, *26* (4), S70-4.
159. Sheng, H.; Shao, J.; Morrow, J. D.; Beauchamp, R. D.; DuBois, R. N., Modulation of apoptosis and Bcl-2 expression by prostaglandin E2 in human colon cancer cells. *Cancer research* **1998**, *58* (2), 362-6.
160. Williams, C. S.; DuBois, R. N., Prostaglandin endoperoxide synthase: why two isoforms? *The American journal of physiology* **1996**, *270* (3 Pt 1), G393-400.
161. Saha, D.; Datta, P. K.; Sheng, H.; Morrow, J. D.; Wada, M.; Moses, H. L.; Beauchamp, R. D., Synergistic induction of cyclooxygenase-2 by transforming growth factor-beta1 and epidermal growth factor inhibits apoptosis in epithelial cells. *Neoplasia (New York, N.Y.)* **1999**, *1* (6), 508-17.
162. Huang, R.-Y.; Chen, G. G., Cigarette smoking, cyclooxygenase-2 pathway and cancer. *Biochimica et Biophysica Acta (BBA) - Reviews on Cancer* **2011**, *1815* (2), 158-169.
163. Weylandt, K. H.; Krause, L. F.; Gomolka, B.; Chiu, C. Y.; Bilal, S.; Nadolny, A.; Waechter, S. F.; Fischer, A.; Rothe, M.; Kang, J. X., Suppressed liver tumorigenesis in fat-1 mice with elevated omega-3 fatty acids is associated with increased omega-3 derived lipid mediators and reduced TNF- α . *Carcinogenesis* **2011**, *32* (6), 897-903.
164. Funahashi, H.; Satake, M.; Hasan, S.; Sawai, H.; Newman, R. A.; Reber, H. A.; Hines, O. J.; Eibl, G., Opposing effects of n-6 and n-3 polyunsaturated fatty acids on pancreatic cancer growth. *Pancreas* **2008**, *36* (4), 353-62.
165. Reed, J. R.; Leon, R. P.; Hall, M. K.; Schwertfeger, K. L., Interleukin-1beta and fibroblast growth factor receptor 1 cooperate to induce cyclooxygenase-2 during early mammary tumourigenesis. *Breast cancer research : BCR* **2009**, *11* (2), R21.

166. Chang, K. Y.; Shen, M. R.; Lee, M. Y.; Wang, W. L.; Su, W. C.; Chang, W. C.; Chen, B. K., Epidermal growth factor-activated aryl hydrocarbon receptor nuclear translocator/HIF-1{beta} signal pathway up-regulates cyclooxygenase-2 gene expression associated with squamous cell carcinoma. *The Journal of biological chemistry* **2009**, *284* (15), 9908-16.
167. Liu, W.; Reinmuth, N.; Stoeltzing, O.; Parikh, A. A.; Tellez, C.; Williams, S.; Jung, Y. D.; Fan, F.; Takeda, A.; Akagi, M.; Bar-Eli, M.; Gallick, G. E.; Ellis, L. M., Cyclooxygenase-2 is up-regulated by interleukin-1 beta in human colorectal cancer cells via multiple signaling pathways. *Cancer research* **2003**, *63* (13), 3632-6.
168. Kaul, R.; Verma, S. C.; Murakami, M.; Lan, K.; Choudhuri, T.; Robertson, E. S., Epstein-Barr virus protein can upregulate cyclo-oxygenase-2 expression through association with the suppressor of metastasis Nm23-H1. *Journal of virology* **2006**, *80* (3), 1321-31.
169. Harris, R. E.; Beebe-Donk, J.; Alshafie, G. A., Cancer chemoprevention by cyclooxygenase 2 (COX-2) blockade: results of case control studies. *Sub-cellular biochemistry* **2007**, *42*, 193-212.
170. Schiff, S. J.; Rigas, B., The role of cyclooxygenase inhibition in the antineoplastic effects of nonsteroidal antiinflammatory drugs (NSAIDs). *The Journal of experimental medicine* **1999**, *190* (4), 445-50.
171. Howe, L. R.; Subbaramaiah, K.; Brown, A. M.; Dannenberg, A. J., Cyclooxygenase-2: a target for the prevention and treatment of breast cancer. *Endocrine-related cancer* **2001**, *8* (2), 97-114.
172. Singh, A.; Sharma, H.; Salhan, S.; Gupta, S. D.; Bhatla, N.; Jain, S. K.; Singh, N., Evaluation of expression of apoptosis-related proteins and their correlation with HPV, telomerase activity, and apoptotic index in cervical cancer. *Pathobiology : journal of immunopathology, molecular and cellular biology* **2004**, *71* (6), 314-22.
173. Harris, R. E.; Beebe, J.; Alshafie, G. A., Reduction in cancer risk by selective and nonselective cyclooxygenase-2 (COX-2) inhibitors. *Journal of experimental pharmacology* **2012**, *4*, 91-6.
174. Hippisley-Cox, J.; Coupland, C., Risk of myocardial infarction in patients taking cyclo-oxygenase-2 inhibitors or conventional non-steroidal anti-inflammatory drugs: population based nested case-control analysis. *BMJ (Clinical research ed.)* **2005**, *330* (7504), 1366.
175. Adelizzi, R. A., COX-1 and COX-2 in health and disease. *Journal of Osteopathic Medicine* **1999**, *99* (s11), 7-12.
176. Harris, R. E., Cyclooxygenase-2 (cox-2) blockade in the chemoprevention of cancers of the colon, breast, prostate, and lung. *Inflammopharmacology* **2009**, *17* (2), 55-67.
177. Chan, A. T.; Giovannucci, E. L., Primary prevention of colorectal cancer. *Gastroenterology* **2010**, *138* (6), 2029-2043.e10.
178. Arber, N.; Levin, B., Chemoprevention of colorectal neoplasia: the potential for personalized medicine. *Gastroenterology* **2008**, *134* (4), 1224-37.
179. Kismet, K.; Akay, M. T.; Abbasoglu, O.; Ercan, A., Celecoxib: a potent cyclooxygenase-2 inhibitor in cancer prevention. *Cancer detection and prevention* **2004**, *28* (2), 127-42.
180. Penning, T. D.; Talley, J. J.; Bertenshaw, S. R.; Carter, J. S.; Collins, P. W.; Docter, S.; Graneto, M. J.; Lee, L. F.; Malecha, J. W.; Miyashiro, J. M.; Rogers, R. S.; Rogier, D. J.; Yu, S. S.; AndersonGd; Burton, E. G.; Cogburn, J. N.; Gregory, S. A.; Koboldt, C. M.; Perkins, W. E.; Seibert, K.; Veenhuizen, A. W.; Zhang, Y. Y.; Isakson, P. C., Synthesis and biological evaluation of the 1,5-diarylpyrazole class of cyclooxygenase-2 inhibitors: identification of 4-[5-(4-methylphenyl)-3-(trifluoromethyl)-1H-pyrazol-1-yl]benzene nesulfonamide (SC-58635, celecoxib). *J Med Chem* **1997**, *40* (9), 1347-65.
181. Koki, A. T.; Masferrer, J. L., Celecoxib: a specific COX-2 inhibitor with anticancer properties. *Cancer control : journal of the Moffitt Cancer Center* **2002**, *9* (2 Suppl), 28-35.

182. Saxena, P.; Sharma, P. K.; Purohit, P., A journey of celecoxib from pain to cancer. *Prostaglandins & Other Lipid Mediators* **2020**, *147*, 106379.
183. Veetil, S. K.; Lim, K. G.; Ching, S. M.; Saokaew, S.; Phisalprapa, P.; Chaiyakunapruk, N., Effects of aspirin and non-aspirin nonsteroidal anti-inflammatory drugs on the incidence of recurrent colorectal adenomas: a systematic review with meta-analysis and trial sequential analysis of randomized clinical trials. *BMC cancer* **2017**, *17* (1), 763.
184. Sproviero, D.; Julien, S.; Burford, B.; Taylor-Papadimitriou, J.; Burchell, J. M., Cyclooxygenase-2 enzyme induces the expression of the α -2,3-sialyltransferase-3 (ST3Gal-I) in breast cancer. *The Journal of biological chemistry* **2012**, *287* (53), 44490-7.
185. Atukorala, I.; Hunter, D. J., Valdecoxib : the rise and fall of a COX-2 inhibitor. *Expert opinion on pharmacotherapy* **2013**, *14* (8), 1077-86.
186. Chavez, M. L.; DeKorte, C. J., Valdecoxib: a review. *Clinical therapeutics* **2003**, *25* (3), 817-51.
187. Scott, L. J.; Lamb, H. M., Rofecoxib. *Drugs* **1999**, *58* (3), 499-505; discussion 506-7.
188. Sada, O.; Ahmed, K.; Jeldo, A.; Shafi, M., Role of Anti-inflammatory Drugs in the Colorectal Cancer. *Hospital pharmacy* **2020**, *55* (3), 168-180.
189. Shen, K.; Hines, A. C.; Schwarzer, D.; Pickin, K. A.; Cole, P. A., Protein kinase structure and function analysis with chemical tools. *Biochimica et biophysica acta* **2005**, *1754* (1-2), 65-78.
190. Schwartz, P. A.; Murray, B. W., Protein kinase biochemistry and drug discovery. *Bioorganic chemistry* **2011**, *39* (5-6), 192-210.
191. M. Ho, H. N. B., D.E. Hansen, J.R. Knowles, E.T. Kaiser, Stereochemical course of the phospho group transfer catalyzed by cAMP-dependent protein kinase. *J. Am. Chem. Soc.* **1988**, *110*, 2680-2681.
192. Cohen, P., Protein kinases--the major drug targets of the twenty-first century? *Nature reviews. Drug discovery* **2002**, *1* (4), 309-15.
193. Huse, M.; Kuriyan, J., The conformational plasticity of protein kinases. *Cell* **2002**, *109* (3), 275-82.
194. Kornev, A. P.; Taylor, S. S., Defining the conserved internal architecture of a protein kinase. *Biochimica et biophysica acta* **2010**, *1804* (3), 440-4.
195. Hanks, S. K.; Quinn, A. M.; Hunter, T., The protein kinase family: conserved features and deduced phylogeny of the catalytic domains. *Science (New York, N.Y.)* **1988**, *241* (4861), 42-52.
196. Hubbard, S. R.; Till, J. H., Protein tyrosine kinase structure and function. *Annual review of biochemistry* **2000**, *69*, 373-98.
197. Waksman, G.; Shoelson, S. E.; Pant, N.; Cowburn, D.; Kuriyan, J., Binding of a high affinity phosphotyrosyl peptide to the Src SH2 domain: crystal structures of the complexed and peptide-free forms. *Cell* **1993**, *72* (5), 779-90.
198. Xu, W.; Doshi, A.; Lei, M.; Eck, M. J.; Harrison, S. C., Crystal structures of c-Src reveal features of its autoinhibitory mechanism. *Molecular cell* **1999**, *3* (5), 629-38.
199. Cooper, J. A.; Gould, K. L.; Cartwright, C. A.; Hunter, T., Tyr527 is phosphorylated in pp60c-src: implications for regulation. *Science (New York, N.Y.)* **1986**, *231* (4744), 1431-4.
200. Kmiecik, T. E.; Shalloway, D., Activation and suppression of pp60c-src transforming ability by mutation of its primary sites of tyrosine phosphorylation. *Cell* **1987**, *49* (1), 65-73.
201. Pluk, H.; Dorey, K.; Superti-Furga, G., Autoinhibition of c-Abl. *Cell* **2002**, *108* (2), 247-59.
202. Van Etten, R. A.; Debnath, J.; Zhou, H.; Casasnovas, J. M., Introduction of a loss-of-function point mutation from the SH3 region of the *Caenorhabditis elegans* sem-5 gene activates the transforming ability of c-abl in vivo and abolishes binding of proline-rich ligands in vitro. *Oncogene* **1995**, *10* (10), 1977-88.

203. Schenone, S.; Manetti, F.; Botta, M., Last findings on dual inhibitors of abl and SRC tyrosine-kinases. *Mini Rev Med Chem* **2007**, *7* (2), 191-201.
204. Biscardi, J. S.; Tice, D. A.; Parsons, S. J., c-Src, receptor tyrosine kinases, and human cancer. *Advances in cancer research* **1999**, *76*, 61-119.
205. Irby, R. B.; Yeatman, T. J., Role of Src expression and activation in human cancer. *Oncogene* **2000**, *19* (49), 5636-42.
206. Hu, Y.; Liu, Y.; Pelletier, S.; Buchdunger, E.; Warmuth, M.; Fabbro, D.; Hallek, M.; Van Etten, R. A.; Li, S., Requirement of Src kinases Lyn, Hck and Fgr for BCR-ABL1-induced B-lymphoblastic leukemia but not chronic myeloid leukemia. *Nature genetics* **2004**, *36* (5), 453-61.
207. Schenone, S.; Manetti, F.; Botta, M., SRC inhibitors and angiogenesis. *Current pharmaceutical design* **2007**, *13* (21), 2118-28.
208. Wisniewski, D.; Lambek, C. L.; Liu, C.; Strife, A.; Veach, D. R.; Nagar, B.; Young, M. A.; Schindler, T.; Bornmann, W. G.; Bertino, J. R.; Kuriyan, J.; Clarkson, B., Characterization of potent inhibitors of the Bcr-Abl and the c-kit receptor tyrosine kinases. *Cancer research* **2002**, *62* (15), 4244-55.
209. Zuccotto, F.; Ardini, E.; Casale, E.; Angiolini, M., Through the "gatekeeper door": exploiting the active kinase conformation. *J Med Chem* **2010**, *53* (7), 2681-94.
210. Liu, Y.; Gray, N. S., Rational design of inhibitors that bind to inactive kinase conformations. *Nature chemical biology* **2006**, *2* (7), 358-64.
211. Nagar, B.; Hantschel, O.; Young, M. A.; Scheffzek, K.; Veach, D.; Bornmann, W.; Clarkson, B.; Superti-Furga, G.; Kuriyan, J., Structural basis for the autoinhibition of c-Abl tyrosine kinase. *Cell* **2003**, *112* (6), 859-71.
212. Boggon, T. J.; Eck, M. J., Structure and regulation of Src family kinases. *Oncogene* **2004**, *23* (48), 7918-27.
213. Schenone, S.; Brullo, C.; Botta, M., New opportunities to treat the T315I-Bcr-Abl mutant in chronic myeloid leukaemia: tyrosine kinase inhibitors and molecules that act by alternative mechanisms. *Current medicinal chemistry* **2010**, *17* (13), 1220-45.
214. Thaimattam, R.; Daga, P. R.; Banerjee, R.; Iqbal, J., 3D-QSAR studies on c-Src kinase inhibitors and docking analyses of a potent dual kinase inhibitor of c-Src and c-Abl kinases. *Bioorg Med Chem* **2005**, *13* (15), 4704-12.
215. Hassan, A. Q.; Sharma, S. V.; Warmuth, M., Allosteric inhibition of BCR-ABL. *Cell cycle (Georgetown, Tex.)* **2010**, *9* (18), 3710-4.
216. Tatton, L.; Morley, G. M.; Chopra, R.; Khwaja, A., The Src-selective kinase inhibitor PP1 also inhibits Kit and Bcr-Abl tyrosine kinases. *The Journal of biological chemistry* **2003**, *278* (7), 4847-53.
217. Prasad, V.; Mailankody, S., The accelerated approval of oncologic drugs: lessons from ponatinib. *Jama* **2014**, *311* (4), 353-4.
218. Pemovska, T.; Johnson, E.; Kontro, M.; Repasky, G. A.; Chen, J.; Wells, P.; Cronin, C. N.; McTigue, M.; Kallioniemi, O.; Porkka, K.; Murray, B. W.; Wennerberg, K., Axitinib effectively inhibits BCR-ABL1(T315I) with a distinct binding conformation. *Nature* **2015**, *519* (7541), 102-5.
219. Huang, W. S.; Metcalf, C. A.; Sundaramoorthi, R.; Wang, Y.; Zou, D.; Thomas, R. M.; Zhu, X.; Cai, L.; Wen, D.; Liu, S.; Romero, J.; Qi, J.; Chen, I.; Banda, G.; Lentini, S. P.; Das, S.; Xu, Q.; Keats, J.; Wang, F.; Wardwell, S.; Ning, Y.; Snodgrass, J. T.; Broudy, M. I.; Russian, K.; Zhou, T.; Commodore, L.; Narasimhan, N. I.; Mohemmad, Q. K.; Iulucci, J.; Rivera, V. M.; Dalgarno, D. C.; Sawyer, T. K.; Clackson, T.; Shakespeare, W. C., Discovery of 3-[2-(imidazo[1,2-b]pyridazin-3-yl)ethynyl]-4-methyl-N-{4-[(4-methylpiperazin-1-yl)methyl]-3-(trifluoromethyl)phenyl}benzamide (AP24534), a potent, orally active pan-inhibitor of

- breakpoint cluster region-abelson (BCR-ABL) kinase including the T315I gatekeeper mutant. *J Med Chem* **2010**, *53* (12), 4701-19.
220. Choi, H. G.; Zhang, J.; Weisberg, E.; Griffin, J. D.; Sim, T.; Gray, N. S., Development of 'DFG-out' inhibitors of gatekeeper mutant kinases. *Bioorganic & medicinal chemistry letters* **2012**, *22* (16), 5297-5302.
221. Zhang, J.; Adrián, F. J.; Jahnke, W.; Cowan-Jacob, S. W.; Li, A. G.; Iacob, R. E.; Sim, T.; Powers, J.; Dierks, C.; Sun, F.; Guo, G. R.; Ding, Q.; Okram, B.; Choi, Y.; Wojciechowski, A.; Deng, X.; Liu, G.; Fendrich, G.; Strauss, A.; Vajpai, N.; Grzesiek, S.; Tuntland, T.; Liu, Y.; Bursulaya, B.; Azam, M.; Manley, P. W.; Engen, J. R.; Daley, G. Q.; Warmuth, M.; Gray, N. S., Targeting Bcr-Abl by combining allosteric with ATP-binding-site inhibitors. *Nature* **2010**, *463* (7280), 501-6.
222. Wu, Y.; Xu, J.; Liu, Y.; Zeng, Y.; Wu, G., A Review on Anti-Tumor Mechanisms of Coumarins. *Front Oncol* **2020**, *10*, 592853-592853.
223. Melis, C.; Distinto, S.; Bianco, G.; Meleddu, R.; Cottiglia, F.; Fois, B.; Taverna, D.; Angius, R.; Alcaro, S.; Ortuso, F.; Gaspari, M.; Angeli, A.; Del Prete, S.; Capasso, C.; Supuran, C. T.; Maccioni, E., Targeting Tumor Associated Carbonic Anhydrases IX and XII: Highly Isozyme Selective Coumarin and Psoralen Inhibitors. *ACS medicinal chemistry letters* **2018**, *9* (7), 725-729.
224. Meleddu, R.; Deplano, S.; Maccioni, E.; Ortuso, F.; Cottiglia, F.; Secci, D.; Onali, A.; Sanna, E.; Angeli, A.; Angius, R.; Alcaro, S.; Supuran, C. T.; Distinto, S., Selective inhibition of carbonic anhydrase IX and XII by coumarin and psoralen derivatives. *Journal of enzyme inhibition and medicinal chemistry* **2021**, *36* (1), 685-692.
225. Lipinski, C. A.; Lombardo, F.; Dominy, B. W.; Feeney, P. J., Experimental and computational approaches to estimate solubility and permeability in drug discovery and development settings. *Advanced Drug Delivery Reviews* **2001**, *46* (1-3), 3-26.
226. Jorgensen, W. L.; Duffy, E. M., Prediction of drug solubility from structure. *Advanced Drug Delivery Reviews* **2002**, *54* (3), 355-366.
227. Cavalli, A.; Poluzzi, E.; De Ponti, F.; Recanatini, M., Toward a pharmacophore for drugs inducing the long QT syndrome: insights from a CoMFA study of HERG K(+) channel blockers. *J Med Chem* **2002**, *45* (18), 3844-53.
228. Lipinski, C. A.; Lombardo, F.; Dominy, B. W.; Feeney, P. J., Experimental and computational approaches to estimate solubility and permeability in drug discovery and development settings. *Adv Drug Deliv Rev* **2001**, *46* (1-3), 3-26.
229. Bickerton, G. R.; Paolini, G. V.; Besnard, J.; Muresan, S.; Hopkins, A. L., Quantifying the chemical beauty of drugs. *Nature Chemistry* **2012**, *4* (2), 90-98.
230. Hoekman, D., Exploring QSAR Fundamentals and Applications in Chemistry and Biology, Volume 1. Hydrophobic, Electronic and Steric Constants, Volume 2 *J. Am. Chem. Soc.* **1995**, *117*, 9782. *Journal of the American Chemical Society* **1996**, *118* (43), 10678-10678.
231. Lagorce, D.; Reynes, C.; Camproux, A.-C.; Miteva, M. A.; Sperandio, O.; Villoutreix, B. O., In silico ADME/Tox predictions. In *ADMET for Medicinal Chemists*, John Wiley & Sons, Inc.: 2011; pp 29-124.
232. Walker, N.; Stuart, D., An empirical method for correcting diffractometer data for absorption effects. *Acta Crystallographica, Section A* **1983**, *39* (1), 158-166.
233. Khalifah, R. G., The carbon dioxide hydration activity of carbonic anhydrase. I. Stop-flow kinetic studies on the native human isoenzymes B and C. *The Journal of biological chemistry* **1971**, *246* (8), 2561-73.
234. Berrino, E.; Angeli, A.; Zhdanov, D. D.; Kiryukhina, A. P.; Milaneschi, A.; De Luca, A.; Bozdag, M.; Carradori, S.; Selleri, S.; Bartolucci, G.; Peat, T. S.; Ferraroni, M.; Supuran, C. T.; Carta, F., Azidothymidine "Clicked" into 1,2,3-Triazoles: First Report on Carbonic Anhydrase-Telomerase Dual-Hybrid Inhibitors. *Journal of medicinal chemistry* **2020**, *63* (13), 7392-7409.

235. Pacchiano, F.; Carta, F.; McDonald, P. C.; Lou, Y.; Vullo, D.; Scozzafava, A.; Dedhar, S.; Supuran, C. T., Ureido-substituted benzenesulfonamides potently inhibit carbonic anhydrase IX and show antimetastatic activity in a model of breast cancer metastasis. *J Med Chem* **2011**, *54* (6), 1896-902.
236. Berman, H. M.; Westbrook, J.; Feng, Z.; Gilliland, G.; Bhat, T. N.; Weissig, H.; Shindyalov, I. N.; Bourne, P. E., The Protein Data Bank. *Nucleic Acids Research* **2000**, *28* (1), 235-242.
237. Mohamadi, F.; Richards, N. G.; Guida, W. C.; Liskamp, R.; Lipton, M.; Caufield, C.; Chang, G.; Hendrickson, T.; Still, W. C., MacroModel—an integrated software system for modeling organic and bioorganic molecules using molecular mechanics. *Journal of Computational Chemistry* **1990**, *11* (4), 440-467.
238. Halgren, T. A., Merck molecular force field. II. MMFF94 van der Waals and electrostatic parameters for intermolecular interactions. *Journal of Computational Chemistry* **1996**, *17* (5-6), 520-552.
239. Kollman, P. A.; Massova, I.; Reyes, C.; Kuhn, B.; Huo, S.; Chong, L.; Lee, M.; Lee, T.; Duan, Y.; Wang, W.; Donini, O.; Cieplak, P.; Srinivasan, J.; Case, D. A.; Cheatham, T. E., Calculating structures and free energies of complex molecules: combining molecular mechanics and continuum models. *Accounts of Chemical Research* **2000**, *33* (12), 889-897.
240. Chilin, A.; Battistutta, R.; Bortolato, A.; Cozza, G.; Zanatta, S.; Poletto, G.; Mazzorana, M.; Zagotto, G.; Uriarte, E.; Guiotto, A.; Pinna, L. A.; Meggio, F.; Moro, S., Coumarin as attractive casein kinase 2 (CK2) inhibitor scaffold: an integrate approach to elucidate the putative binding motif and explain structure-activity relationships. *J Med Chem* **2008**, *51* (4), 752-9.
241. Ogura, M.; Morishima, Y.; Ohno, R.; Kato, Y.; Hirabayashi, N.; Nagura, H.; Saito, H., Establishment of a novel human megakaryoblastic leukemia cell line, MEG-01, with positive Philadelphia chromosome. *Blood* **1985**, *66* (6), 1384-92.

APPENDIX

Oral Communications in Scientific Meetings

- “Multi-enzyme inhibitors for the treatment of cancer”
Serenella Deplano^a, Rita Meleddu,^a Simona Distinto^a, Lisa Sequeira^a, Benedetta Fois^a, Filippo Cottiglia^a, Claudiu T. Supuran^b, and Elias Maccioni^a
^a*Department of Life and Environmental Sciences, University of Cagliari, Via Ospedale 72, 09124-Cagliari, Italy*
^b*Department of NEUROFARBA, Sezione di Scienze Farmaceutiche, Università degli Studi di Firenze, Sesto Fiorentino, Florence, Italy*
4th Annual meeting – MuTaLig Cost Action – Catanzaro (Italy), June 13-15th 2019

Poster Communications in Scientific Meetings

- “Exploring new scaffolds for the dual inhibition of HIV-1 rt polymerase and ribonuclease associated functions”
Serenella Deplano^a, Rita Meleddu^a, Angela Corona^a, Simona Distinto^a, Filippo Cottiglia^a, Lisa Sequeira^a, Daniela Secci^a, Alessia Onali^a, Erica Sanna^a, Francesca Esposito^a, Italo Cirone^a, Francesco Ortuso^b, Stefano Alcaro^b, Enzo Tramontano^a, Peter Matyus^c and Elias Maccioni^a
^a *Department of Life and Environmental Sciences, University of Cagliari, Cittadella Universitaria di Monserrato, S.P. 8 km 0.700, 09042 Monserrato Cagliari (CA), Italy*
^b *Dipartimento di Scienze della Salute, Università Magna Graecia di Catanzaro, Campus ‘S. Venuta’, Viale Europa, 88100 Catanzaro, Italy*
^c *Institute of Digital Health Sciences, Faculty of Health and Public Services, Semmelweis University, Ferenc tér 15, Budapest, 1094, Hungary*
Paul Ehrlich MedChem Euro PhD Network - Virtual Meeting, July 26-28th 2021
- “Benzenesulfonamide-n-ethylidihydrothiazole hybrids as inhibitors of human carbonic anhydrase isozymes”
Serenella Deplano^a, Claudiu T. Supuran,^b Rita Meleddu,^a Simona Distinto,^a Filippo Cottiglia,^a Rossella Angius,^c and Elias Maccioni ^a
^a *Department of Life and Environmental Sciences, University of Cagliari, Via Ospedale 72, 09124 Cagliari, Italy*
^b *Dipartimento NEUROFARBA, Sezione di Scienze Farmaceutiche, Università degli Studi di Firenze, Sesto Fiorentino, Florence, Italy*

^c Laboratorio NMR e Tecnologie Bioanalitiche, Sardegna Ricerche, 09010 Pula (CA), Italy
4th Satellite Meeting on Carbonic Anhydrase - Parma (Italy), November 14-17th 2019

- “From (z)-4-(2-(2-(2-oxoindolin-3-ylidene)hydrazinyl)thiazol-4-yl)aryl to 3'-acetyl-5'-aryl-1h-spiro[indole-3,2'-[1,3,4]oxadiazole]-2-one derivatives: structural evolution of HIV-1 rt dual function inhibitors”

Rita. Meleddu¹, **Serenella Deplano**¹, Angela Corona¹, Francesca Esposito¹, Enzo Tramontano¹, Simona Distinto¹ and Elias Maccioni¹

¹Department of Life and Environmental Sciences, University of Cagliari, Cagliari, Italy
4th IAAASS Innovative Approaches for Identification of Antiviral Agents Summer School – September 24-29th 2018

Manuscripts in International Journals

- Rita Meleddu, Angela Corona, Simona Distinto, Filippo Cottiglia, **Serenella Deplano**, Lisa Sequeira, Daniela Secci, Alessia Onali, Erica Sanna, Francesca Esposito, Italo Cirone, Francesco Ortuso, Stefano Alcaro, Enzo Tramontano, Péter Mátyus and Elias Maccioni. *Exploring New Scaffolds for the Dual Inhibition of HIV-1 RT Polymerase and Ribonuclease Associated Functions*. *Molecules*. 2021 Jun 23;26(13):3821. doi: 10.3390/molecules26133821
- Rita Meleddu, **Serenella Deplano**, Elias Maccioni, Francesco Ortuso, Filippo Cottiglia, Daniela Secci, Alessia Onali, Erica Sanna, Andrea Angeli, Rossella Angius 4, Stefano Alcaro, Claudiu T Supuran, Simona Distinto. *Selective inhibition of carbonic anhydrase IX and XII by coumarin and psoralen derivatives*. *J Enzyme Inhib Med Chem*. 2021 Dec;36(1):685-692. doi: 10.1080/14756366.2021.1887171.
- Rita Meleddu, Simona Distinto, Filippo Cottiglia, Rossella Angius, Pierluigi Caboni, Andrea Angeli, Claudia Melis, **Serenella Deplano**, Stefano Alcaro, Francesco Ortuso, Claudiu T Supuran, Elias Maccioni. *New Dihydrothiazole Benzensulfonamides: Looking for Selectivity toward Carbonic Anhydrase Isoforms I, II, IX, and XII*. *ACS Med Chem Lett*. 2020 Feb 13;11(5):852-856. doi: 10.1021/acsmchemlett.9b00644. eCollection 2020 May 14.
- Benedetta Fois, Simona Distinto, Rita Meleddu, **Serenella Deplano**, Elias Maccioni, Costantino Floris, Antonella Rosa, Mariella Nieddu, Pierluigi Caboni, Claudia Sissi, Andrea Angeli, Claudiu T Supuran, Filippo Cottiglia. *Coumarins from Magydaris*

- pastinacea* as inhibitors of the tumour-associated carbonic anhydrases IX and XII: isolation, biological studies and in silico evaluation. *J Enzyme Inhib Med Chem.* 2020 Dec;35(1):539-548. doi: 10.1080/14756366.2020.1713114.
- Rita Meleddu, Vilma Petrikaite, Simona Distinto, Antonella Arridu, Rossella Angius, Lorenzo Serusi, Laura Škarnulytė, Ugnė Endriulaitytė, Miglė Paškevičiūtė, Filippo Cottiglia, Marco Gaspari, Domenico Taverna, **Serenella Deplano**, Benedetta Fois, and Elias Maccioni. *Investigating the Anticancer Activity of Isatin/Dihydropyrazole Hybrids.* *ACS Med. Chem. Lett.* 2019, 10, 4, 571–576 doi: 10.1021/acsmchemlett.8b00596
 - Simona Distinto, Rita Meleddu, Francesco Ortuso, Filippo Cottiglia, **Serenella Deplano**, Lisa Sequeira, Claudia Melis, Benedetta Fois, Andrea Angeli, Clemente Capasso, Rossella Angius, Stefano Alcaro, Claudiu T Supuran, Elias Maccioni. *Exploring new structural features of the 4-[(3-methyl-4-aryl-2,3-dihydro-1,3-thiazol-2-ylidene)amino]benzenesulphonamide scaffold for the inhibition of human carbonic anhydrases.* *J Enzyme Inhib Med Chem.* 2019 Dec;34(1):1526-1533. doi: 10.1080/14756366.2019.1654470.
 - Rita Meleddu, Simona Distinto, Filippo Cottiglia, Rossella Angius, Marco Gaspari, Domenico Taverna, Claudia Melis, Andrea Angeli, Giulia Bianco, **Serenella Deplano**, Benedetta Fois, Sonia Del Prete, Clemente Capasso, Stefano Alcaro, Francesco Ortuso, Matilde Yanez, Claudiu T Supuran, Elias Maccioni. *Tuning the Dual Inhibition of Carbonic Anhydrase and Cyclooxygenase by Dihydrothiazole Benzensulfonamides.* *ACS Med Chem Lett.* 2018 Sep 17;9(10):1045-1050. doi: 10.1021/acsmchemlett.8b00352. eCollection 2018 Oct 11.

La borsa di dottorato è stata cofinanziata con risorse del
Programma Operativo Nazionale Ricerca e Innovazione 2014-2020 (CCI 2014IT16M2OP005),
Fondo Sociale Europeo, Azione I.1 "Dottorati Innovativi con caratterizzazione Industriale"



UNIONE EUROPEA
Fondo Sociale Europeo

